

Università degli Studi di Milano
Scuola di Dottorato di Ricerca in Innovazione Tecnologica per le Scienze Agro-
Alimentari e Ambientali; XXIII ciclo.

**HERBICIDE TRANSPORT FROM LAND TO SURFACE WATER IN AN
ARTIFICIALLY DRAINED CATCHMENT**

Alice Tediosi; *Matr. n. R07675*

Tutor: Prof. Claudio Gandolfi

Dipartimento di Ingegneria Agraria, Sez. di Idraulica, Università degli Studi di Milano

Co-tutor: Dr. Mick Whelan

Natural Resources Department, Cranfield University

Anno Accademico 2009 – 2010

EXECUTIVE SUMMARY

Purpose of the study and context

The study presented in this thesis deals with the analysis of herbicide transport from land to surface waters in heavy underdrained soils. The main aim of the work described in this thesis is to test the hypothesis that drain flow is a most significant pathway for agricultural herbicide contamination in the catchment. The work focuses on the Upper Cherwell catchment (England, UK), which is predominantly clay based. This catchment is defined by a drinking water reservoir abstraction point at Banbury (Oxfordshire), where water quality is monitored regularly by Thames Water Limited. The monitoring of raw waters has revealed that concentrations of a number of commonly used herbicides significantly exceed the Drinking Water Directive (98/83/EC) Maximum Admissible Concentration (MAC, $0.1 \mu\text{g l}^{-1}$) at the reservoir, each year. Pesticides at such levels do not necessarily cause harm to ecosystems or pose risks to human health. However, if water is to be used for potable supply it will require expensive treatment to ensure that it meets EU standards. Such treatment has high initial capital expenditure, high operating costs, and needs large amounts of energy to operate. In addition, it cannot always cope with high peak pesticide concentrations. Such breaches are often difficult to control because of the diffuse nature of contamination sources and pathways, which are difficult to identify or understand properly.

Summary of the work done

The processes contributing to herbicide transport from land to surface water in the Upper Cherwell catchment were examined, with specific emphasis on propyzamide and carbetamide, two key herbicides for black grass control in oilseed rape. A combination of existing data analysis, monitoring, and modelling was used.

Historical data (for the period 1996-2008) on herbicide concentrations was carried out to provide a framework to herbicide issues in the catchment. Some simple descriptive statistics were calculated in order to summarise the extent and timing of herbicide problems in the catchment. The degree of correlation between herbicide concentration and rainfall and river discharge was also investigated.

Field investigations were conducted on an artificially drained field dominated by heavy clay soil (Denchworth soil association), in order to ascertain the role played by tile drains as conduits for herbicide transport. Field work included environmental variable monitoring and water sampling. The main field drain was monitored over five months during November 2009 to March 2010, when the field was in oilseed rape (OSR, widely grown in the catchment) and was treated with propyzamide and carbetamide. Drain flow was measured continuously over the whole monitoring period; water was sampled (a) in the autumn during the period of soil moisture recovery, before and after the application of propyzamide, and (b) in late winter, before and after the application of carbetamide. Samples were taken every 8 hours. Additional information about weather and soil conditions were obtained monitoring soil moisture and temperature, air temperature, and rainfall.

Some modelling was carried out in order to understand more about the processes involved in herbicide transport that were observed at the experimental field. The pesticide fate model used is MACRO, as it accounts explicitly for preferential flow, which is typical in heavy clay soils. The model was calibrated in order to achieve a satisfactory representation of field observations. Both drain flow and herbicide leaching were described.

The information and understanding acquired from working on the experimental field were used to estimate flows and herbicide behaviour at the catchment scale. A model of catchment-scale pesticide transfers was developed as a preliminary analysis of the processes affecting herbicide losses and flows at the catchment outlet. The model is based on the concept of distribution of the areas contributing to the point of analysis at the catchment outlet - as expressed by the area function - and integrates hillslope responses, which are simulated using the MACRO model, through the river network.

Results and findings

The statistical analysis of existing data showed that the Upper Cherwell catchment has got a long history of herbicide problem, with a peak in 2006 and 2007, when the number of days in which measured concentrations exceeded the DWD MAC varied between 8 and 14. Moreover the results of the correlation analysis show that herbicide

concentrations are more significantly correlated with discharge than with precipitation. These results indicate that rapid pathways such as overland flow and runoff from hard surfaces (e.g. farm yards) are probably not major contamination pathways, because they would be expected to generate short lived peak concentrations on the same day as the storm event.

The monitoring conducted at the Experimental Field provided insights into the processes controlling herbicide transfers from land to water in the catchment. The results suggest that artificial drainage systems serving the heavy clay soils in the catchment transport significant quantities of herbicide to the channel network. Both chemicals were detected at very high concentrations (up to 55.7 $\mu\text{g l}^{-1}$ and 694 $\mu\text{g l}^{-1}$ for propyzamide and carbetamide, respectively). The concentration pattern clearly followed drain discharge, with rapid increase on the rising hydrograph limb and a quasi-exponential decline on the recession limb. Pulses of herbicide concentration and drain flow occurred concurrently, suggesting that transport to drains occurs via rapid pathways (i.e. preferential flow).

This hypothesis is supported by the application of the MACRO model (nearly 100% of solute leaching to drains occurs via macropore flow). MACRO appeared to be a valid approach for representing the most important processes observed at the field scale, despite it is a monodimensional model. However it should be noted that calibration seemed to be a key step in order to obtain satisfactory results.

Catchment-wide results provided interesting insights about the catchment. Simulation of flows suggested that the hydrologically active catchment may vary over the year, depending on weather conditions (i.e. precipitation). In fact, a relevant part of the catchment drains into the Oxford Canal instead of draining into the river Cherwell. However river and canal interact (by means of overflow weirs and locks); as a consequence the area effectively draining in the river may change. Application dates appeared to be another key issue, especially affecting herbicide peak timing significantly.

Despite these uncertainties, the catchment-scale results suggest that drain flow is likely to be a major source of contamination: widespread herbicide losses (via artificial drainage system) in the catchment may result in high peaks at the outlet.

Limitations of the study and reliability of the results

This study has a number of limitations, by far the main one is the relatively poor knowledge of herbicide application timing, rates, and areas treated. Another key issue is represented by the catchment hydrology, which is complicated by the interaction between river and canal. A number of assumptions and idealisations, therefore, had to be made in order to develop a model of the system, which limits the degree of certainty we can attach to the results. Moreover the MACRO modelling, used to represent field-scale observations, tended to underestimate herbicide leaching (mainly because of the failure to represent some of the discharges). However, when considering catchment-scale conditions, herbicide loads are not always underestimated. These results suggest that another important factor affecting herbicide losses might be connected to chemical properties (i.e. mobility), which were considered to be uniform in the whole catchment but may vary from field to field.

Conclusions

This study suggests that artificial drainage systems serving the heavy clay soils in the Upper Cherwell catchment transport significant quantities of herbicide to the river. Drain flow seems to be the dominant process driving herbicide contamination in the catchment. If this is correct, then measures to reduce herbicide transfers from point sources (such as farm yards) and in surface runoff (e.g. via the establishment of grassed filter strips) will be relatively ineffective. Where field drains are extensive, as they are in the Upper Cherwell, buffer zones are likely to provide relatively poor mitigation because they are effectively bypassed by the drains. Furthermore, whilst losses from hard standings can have local and short term impacts on concentrations, they are unlikely to be important at the catchment outlet because they take place from very limited areas. Concentrations are, therefore, likely to be reduced significantly by dilution and hydrodynamic dispersion (e.g. Gandolfi *et al.*, 2001).

Management of diffuse-source herbicide contamination in this catchment, and others, should focus on adjusting the magnitude (and possibly the timing) of herbicide inputs. Short of banning the use of certain herbicides, there are some options which could be examined. One could be to restrict the area of the catchment in OSR by extending the

length of crop rotations. Other options include the development and installation of wetland- or pond-based treatment systems between drain outlets and the stream network (subject to proven performance and the provision of sufficient space) as well as potentially changing the means of OSR establishment. Drain blocking could also be possible, although this is likely to have an impact on crop production because it will increase the area of land which is seasonally waterlogged. Possibly a combination of different actions would be more effective than taking a single approach.

In this context, pesticide fate modelling at the catchment scale could become an important tool for providing information, analysing alternative scenarios, and supporting pesticide management. It is important to note that field investigations and field data collection appeared to be a prerequisite for the modelling.

Suggestions for further work

Further work could be done to corroborate and extend the findings presented in this thesis. It would be useful to continue monitoring field drains in order to gain a better understanding of herbicide transport in the catchment. This monitoring should be extended to other chemicals and to other drains and soil associations to ascertain if the observations reported here are relevant more widely. This could also provide additional insights, which could be helpful in defining management strategies to reduce herbicide losses to surface waters, such as optimising application timing or limiting the spatial extent of applications. In addition, it would be interesting to explore the impact of different cultural practices on herbicide transport via artificial drainage: i.e. the role of different tillage practices, the effects of no tillage and the role of subsoiling in encouraging or mitigating pesticide transport from land to water. Such experimental work should be conducted on a systematic (and well replicated) basis in the laboratory and or in the field in order to establish scientific credibility. Field investigation should also be extended to other possible contamination processes (e.g. overland flow) in order to ascertain their importance and their effect on pesticide contamination at the field- and catchment-scale.

With respect to the catchment-scale modelling, it would be helpful to obtain more detailed and precise information about herbicide usage from farmers, farm staff, and or

agronomists. More data would be needed also for a better-understanding and a better knowledge of the catchment (e.g. hydrologically active catchment area, artificial drainage extent, land use distribution).

TABLE OF CONTENTS

EXECUTIVE SUMMARY	i
TABLE OF CONTENTS.....	vii
LIST OF FIGURES	xi
LIST OF TABLES.....	xix
ACRONYMS.....	xxiii
ACKNOWLEDGEMENTS.....	xxv
Chapter 1 – INTRODUCTION.....	1
1.1 Pesticides in the environment	1
1.2 Legislative background.....	2
1.3 Pesticide usage in the UK	3
1.4 Aims and objectives.....	4
1.4 Thesis structure	5
Chapter 2 – HERBICIDE TRANSPORT FROM LAND TO SURFACE WATER.....	7
2.1 The introduction of herbicides into the water cycle.....	7
2.2 Transport mechanisms	8
2.3 Subsurface agricultural drainage.....	11
2.3.1 Drain flow versus overland flow.....	12
2.3.2 Pesticide transport to subsurface drains.....	13
2.3.3 Drain flow and transport pathways to subsurface drains.....	15
2.4 Pesticide movement in soils.....	18
2.4.1 Solute movement in soils.....	18
2.5 Pesticide characteristics	20
2.6 Pesticide fate modelling.....	23
2.6.1 MACRO – mono-dimensional pesticide leaching model	25
Chapter 3 – THE UPPER CHERWELL CATCHMENT	29
3.1 Pesticides in the Upper Cherwell.....	29
3.2 The Voluntary Initiative.....	29
3.3 The Upper Cherwell catchment	31
3.3.1 Catchment characteristics	31

3.3.2 Pesticide usage in the catchment.....	43
Chapter 4 – ANALYSIS OF EXISTING DATA	47
4.1 Data sources	47
4.1.1 Rainfall data	47
4.1.2 Discharge data.....	48
4.1.3 Herbicide concentration data	48
4.2 Methodology	50
4.2.1 Statistical analysis of historical data (1996 – 2008)	50
4.2.2 Qualitative analysis of daily carbetamide and propyzamide concentrations in 2009 measured using SAMOS.....	51
4.3 Results.....	51
4.3.1 Statistical analysis of historical data (1996-2008)	51
4.3.2 Analysis of carbetamide and propyzamide peaks in 2009 using the SAMOS data.....	58
Chapter 5 – FIELD INVESTIGATIONS	65
5.1 Site description.....	65
5.2 Methodology	69
5.2.1 Drain flow characterisation at the Experimental Field	69
5.2.2 Herbicide concentrations in the Experimental Field.....	75
5.2.3 Manual grab samples	78
5.3 Results.....	80
5.3.1 Drain flow	80
5.3.2 Herbicide concentrations and drain flow	83
5.3.3 Manual grab samples	97
Chapter 6 – FIELD-SCALE MODELLING.....	101
6.1 Data sources	101
6.1.1 Meteorological data	101
6.1.2 Soil data	102
6.2 Methodology	103
6.2.1 The MACRO model.....	105
6.2.2 MACRO calibration.....	110

6.2.3 Simulation characteristics	112
6.3 Evaluation of MACRO performance	115
6.4 Results.....	116
6.4.1 Calibrated parameter values.....	116
6.4.2 Hydrology	118
6.4.2 Herbicide leaching	127
6.5 Conclusions: is MACRO a valid approach?	132
Chapter 7 – CATCHMENT-SCALE MODELLING	135
7.1 Data sources	136
7.1.1 Meteorological data	136
7.1.2 Soil map	137
7.1.3 Land use and herbicide usage data.....	137
7.2 Methodology	138
7.2.1 Conceptual model	139
7.2.2 Model description	142
7.3 Simulation characteristics	153
7.3.1 Hillslope responses	153
7.3.2 Transport to the catchment outlet	155
7.4 Results.....	158
7.4.1 Water flow	158
7.4.2 Herbicide leaching	166
Chapter 8 – CONCLUSIONS.....	179
REFERENCES	189
Appendix 1 – Development of a digital river network map	201
Appendix 2 – Redefinition of the catchment boundary	205
Appendix 3 – Land use	211
Appendix 4 – MACRO application: parameter values	213
Appendix 5 – Temperature data series reconstruction.....	227

LIST OF FIGURES

Figure 1 – Pesticide use in Great Britain (Source: FERA, accessed online at http://pusstats.csl.gov.uk/).....	3
Figure 2 - Different hydrological pathways that water can take after precipitation (Source: personal communication Whelan, 2008).....	9
Figure 3 – Partitioning of rainfall into infiltration, overland flow (surface runoff), soil storage, groundwater flow (often called base or subsurface flow), and deep percolation (Source: Kladivko et al., 2001).	13
Figure 4 – Diagram illustrating the effect of macropores on the relationship between leaching of dissolved pesticides and the adsorption coefficient (Jacobsen and Kjær, 2007).....	15
Figure 5 – Soil profile showing the various water pathways from the surface to drains and groundwater (solid lines with arrows) for three water table levels. The location of the drainage trench and water table are indicated by thick grey and dotted lines respectively. An open circle indicates a drain at 1 m depth. The soil profile consists of a plough layer, a layer dominated by biopores, and a deeper calcareous layer mainly dominated by tectonic fractures (Jacobsen and Kjær, 2007).....	17
Figure 6 - GUS (Groundwater Ubiquity Score) index, which expresses pesticide leaching potential (Source: Mick Whelan, personal communication, constructed using Equation (2)).....	22
Figure 7 – Fractures and microtopography are triggers for preferential infiltration (top). Diverse structure/matrix interfaces stained by dye tracer visualise different preferential transport paths; these interfaces may affect lateral diffusion, sorption and degradation (middle). Soil matrix and macropore characteristics and resulting transport patterns; actual patterns also depend on the characteristics of rainfall and of overlaying soil horizons (simplified after Weiler and Flühler, 2004) (bottom) (Source: Köhne et al., 2009b).	26

Figure 8 – River Cherwell at Edgcote (approximately 10 km Northeast of Banbury) (http://www.geograph.org.uk/ [accessed on 12 th October 2010]). © Copyright Stephen McKay and licensed for reuse under the Creative Commons Attribution-ShareAlike 2.0 Licence.	31
Figure 9 – Catchment of the upper River Cherwell above Banbury. Note that some areas shown here drain to the Oxford Canal and are not strictly part of the catchment draining to Grimsbury reservoir (see Appendix 2).	32
Figure 10 – Vector land use map of the Upper Cherwell catchment (Intellectual property rights IMAGE2000 of JRC, based on Landsat 7 ETM+ © ESA, distributed by Eurimage; ortho-correction EU15 © Metria, ortho-correction other countries GISAT; mosaic production GISAT).	34
Figure 11 – (a) Soil map of the catchment (Source: Natmap, NSRI) and (b) description of the main soil associations (Source: Jarvis et al., 1984).	36
Figure 12 – Monthly average rainfall from 1996 to 2008, Grimsbury gauging station (Error bars show the mean ± one standard deviation) (Source: EA [Thames West]).	39
Figure 13 – Discharge from 1966 to 2006 at Banbury (Source: www.nwl.ac.uk [accessed 8 th December 2009]).	39
Figure 14 – Integrated River Monitoring Map of the Upper Cherwell catchment (Source: Thames Water, personal communication). Flow direction is shown (black arrow).	40
Figure 15 – Map of the River Cherwell and the Oxford Canal between Banbury and Cropredy. The insets show Cropredy and the Cropredy Lock (GEOProjects, 2004).	42
Figure 16 – Maximum concentrations of carbetamide and propyzamide observed in the Upper Cherwell at Banbury between 1996 and 2008.	44
Figure 17 – Number of days with observed herbicide concentration above the MAC.	52
Figure 18 – Fraction of measurements above the MAC over the total number of concentration measurements (%).	52
Figure 19 - Average concentration of carbetamide for each month of the year over the period 1996-2008. Error bars show the mean ± one standard deviation.	54
Figure 20 - Average concentration of propyzamide for each month of the year over the period 1996-2008. Error bars show the mean ± one standard deviation.	55

Figure 21 – Correlation coefficients between carbetamide concentration and precipitation and discharge for different lag periods (days).....	56
Figure 22 – Correlation coefficients between propyzamide concentration and precipitation and discharge for different lags (days).....	56
Figure 23 – Daily rainfall totals measured at Grimsbury (columns), river discharge in the Cherwell at Banbury (grey line), and carbetamide (carb) and propyzamide (prop) concentrations measured using SAMOS (black solid and dashed lines) at the catchment outlet in March 2009.	60
Figure 24 - Daily rainfall totals measured at Grimsbury (columns), river discharge in the Cherwell at Banbury (grey line), and carbetamide (carb) and propyzamide (prop) concentrations measured using SAMOS (black solid and dashed lines) at the catchment outlet in November 2009.....	62
Figure 25 – Experimental Field (black line; the yellow marker shows the outlet of the main field drain).	67
Figure 26 – Photograph of the Experimental Field which was monitored. The apparatus visible was installed by ADAS to measure in-field overland flow and was not connected with the project described in this thesis.	67
Figure 27 – Experimental Field (black thick line): 1:25,000 map (Ordnance Survey) with geology map (British Geological Survey; 1:50,000) superimposed. ULi = Upper Lias; NS = Northampton Sands; MLi = Middle Lias; MRB = Marlstone Rock Bed. A cross-section is also shown (Ken Rushton, personal communication, 2010).....	68
Figure 28 – (a) The Delta-T datalogger installed at the Experimental Field, and (b) SM200 soil moisture sensors installed in the field.....	70
Figure 29 – A WSC flume (photo from M.G. Kay).....	71
Figure 30 – Calibration curve for the WSC flume installed at the drain monitored at the Experimental Field.	72
Figure 31 – The WSC flume installed at the outlet of the main field drain in the Experimental Field.....	73
Figure 32 – Linear equation for calculating the actual water head in the stilling well.	74
Figure 33 – Linear equation for calculating the water head measured in the WSC flume.	75

Figure 34 – (a)Lange Xian 1000 Automatic Water Sampler set up at the WSC flume. (b) Sampling module, and (c) the container module.....	76
Figure 35 - Sampling areas (numbers 1 to 3 refer to sampling point locations: 1. Experimental Site; 2. upstream Woodford Halse; 3. Ashby Brook between Eydon and Moreton Pinkney).....	79
Figure 36 – Drain flow ($l\ s^{-1}$) measured in the WSC flume installed at the main field drain. Also shown are daily rainfall totals (primary axis [$mm\ d^{-1}$]), and daily soil moisture content (secondary axis [% total volume]) (average at 5 cm to 25 cm depth). The period 15 th October 2009 to 31 st March 2010 is shown.....	82
Figure 37 – Drain flow ($l\ s^{-1}$) and propyzamide concentrations (black points [$\mu g\ l^{-1}$]) at the main field drain.	85
Figure 38 – Solute rating curve: propyzamide concentration with respect to discharge for the period 5 th to 16 th November 2009 is shown.	87
Figure 39 - Solute rating curve: propyzamide concentration with respect to discharge for the period 16 th to 18 th November 2009 is shown.	88
Figure 40 - Solute rating curve: propyzamide concentration with respect to discharge for the period 21 st to 23 rd November 2009 is shown.....	88
Figure 41 - Solute rating curve: propyzamide concentration with respect to discharge for the period 6 th to 7 th December 2009 is shown.....	89
Figure 42 - Drain flow ($l\ s^{-1}$) and carbetamide concentrations (black points [$\mu g\ l^{-1}$]) at the main field drain.	91
Figure 43 – Solute rating curve: carbetamide concentration with respect to discharge for the period 15 th to 17 th February 2010 is shown.....	93
Figure 44 – Solute rating curve: carbetamide concentration with respect to discharge for the period 17 th to 18 th February 2010 is shown.....	94
Figure 45 - Solute rating curve: carbetamide concentration with respect to discharge for the period 24 th to 25 th February 2010 is shown.....	94
Figure 46 - Solute rating curve: carbetamide concentration with respect to discharge for the period 27 th February to 1 st March 2010 is shown.....	95
Figure 47 – National Soil Map, scale 1:250,000 (NATMAP vector © Cranfield University and for the Controller of HMSO, 2009).....	102

Figure 48 - Photograph of the surface of a Denchworth soil taken on the 27 th of July 2009, illustrating the formation of significant cracks at the surface. The mobile telephone is placed for scale and measures approximately 7 cm long by 4 cm wide.	104
Figure 49 – Predicted (black line) and measured (grey line) hourly drain flow (mm h^{-1}), and measured rainfall (black line, secondary axis); 6 th October to 27 th December 2009.	119
Figure 50 – Predicted (black line) and measured (grey line) hourly drain flow (mm/h), and measured rainfall (black line, secondary axis); 11 th February to 4 th March 2010.	120
Figure 51 – Predicted (black line) and measured (black symbols) soil moisture ($\text{m}^3 \text{m}^{-3}$) along the soil profile (0-25 cm) for autumn 2009.	121
Figure 52 - Predicted (black line) and measured (black symbols) soil moisture ($\text{m}^3 \text{m}^{-3}$) along the soil profile (0-25 cm) for winter 2010 (daily average values).	122
Figure 53 – Cross-section of the Experimental Field: geological strata are shown (British Geological Survey; 1:50,000). ULi = Upper Lias; NS = Northampton Sands; MLi = Middle Lias; MRB = Marlstone Rock Bed. (Ken Rushton, personal communication, 2010) (see Figure 26).	124
Figure 54 – Seepage observed at the top of Experimental Field on 30 th March 2010 (photograph taken by Ken Rushton).	124
Figure 55 - Measured (grey solid line) hourly drain flow (mm h^{-1}), base flow (black dotted line [mm h^{-1}]), and predicted drain flow plus base flow (black solid line [mm h^{-1}]). Measured rainfall is also shown (black line, secondary axis); 6 th October to 27 th December 2009.	125
Figure 56 - Measured (grey solid line) hourly drain flow (mm h^{-1}), base flow (black dotted line [mm h^{-1}]), and predicted drain flow plus base flow (black solid line [mm h^{-1}]). Measured rainfall is also shown (black line, secondary axis); 11 th February to 4 th March 2010.	126
Figure 57 – Predicted (grey line) and measured (black symbols) propyzamide flux ($\mu\text{g h}^{-1} \text{m}^{-2}$); 3 rd November 2009 to 14 th December 2009. K_{OC} used in the model parameterisation is $250 \text{ dm}^3 \text{ kg}^{-1}$	128

Figure 58 – Accumulated propyzamide loss to drain: total flow (macropore and micropore flows; black solid line), and micropore flow (grey line).....	129
Figure 59 - Predicted (grey line) and measured (black symbols) hourly carbetamide flux ($\mu\text{g h}^{-1} \text{ m}^{-2}$); 11 th February 2010 to 4 th March 2010. K_{OC} used in the model parameterisation is $89 \text{ dm}^3 \text{ kg}^{-1}$	130
Figure 60 - Accumulated carbetamide loss to drain: total flow (macropore and micropore flows; black solid line), and micropore flow (grey line).....	131
Figure 61 – Conceptual model of pesticide transport from the soil surface to the catchment outlet: a) vertical movement from the soil surface down the soil profile; b) Lateral movement in the saturated zone to field drains; c) movement along the field drains to reach the surface water network; d) movement along the surface water network to the catchment outlet (grey areas do not contribute to pesticide leaching as they are not artificially drained).	140
Figure 62 – Water flow: movement along the surface water network to the catchment outlet: the whole catchment contributes to total flow.....	141
Figure 63 – Catchment area function: distance from the outlet (x axis) is along the river network; the area function is expressed as a frequency distribution.	145
Figure 64 – Discharge measured at the catchment outlet (primary axis [$\text{m}^3 \text{ s}^{-1}$], and drain flow (secondary axis [$\text{m}^3 \text{ s}^{-1}$]) monitored at the Experimental Field.....	146
Figure 65 – Discharge at the catchment outlet ($\text{m}^3 \text{ s}^{-1}$)(primary axis), and drain flow measured at the Experimental Field ($10^{-3} \text{ m}^3 \text{ s}^{-1}$) with respect to the observed lag (hours). Only peaks with similar magnitude are shown ($\alpha < 0.15$).	148
Figure 66 – Discharge at the catchment outlet ($\text{m}^3 \text{ s}^{-1}$) on the x axis, and time delay (hours). All the peaks are shown: the ones with similar magnitude ($\alpha < 0.15$) are marked with a circle.	149
Figure 67 – Area function: X is the distance from the outlet and it is divided in n equal distances (x). At each distance from the outlet X_i corresponds an area F_i	150
Figure 68 – Area function for all the clay soil areas in the Upper Cherwell catchment.	151
Figure 69 – Area function for Banbury soil areas in the Upper Cherwell catchment.....	152

Figure 70 – Probability density function for propyzamide application in November - December 2008.....	157
Figure 71 – Probability density function for carbetamide application in January - February 2009.....	157
Figure 72 – Mean daily discharge ($\text{m}^3 \text{s}^{-1}$) at Banbury: measured (red line), and modelled (blue line). Catchment area used in this simulation is 129 km^2	160
Figure 73 - Mean daily discharge ($\text{m}^3 \text{s}^{-1}$) at Banbury: measured (red line), and modelled (blue solid line refers to 129 km^2 catchment area; blue dotted line refers to 199 km^2 catchment area).....	161
Figure 74 - Mean daily discharge ($\text{m}^3 \text{s}^{-1}$) at Banbury: measured (red line) and modelled (blue line). Catchment area used in this simulation is 129 km^2	163
Figure 75 - Mean daily discharge ($\text{m}^3 \text{s}^{-1}$) at Banbury: measured (red line), and modelled (blue solid line refers to 129 km^2 catchment area; blue dotted line refers to 199 km^2 catchment area). Day 1 is 1 st October 2009.....	165
Figure 76 – Daily mean propyzamide loads (g h^{-1}) at Banbury: measured (red line), and modelled (blue solid line refers to sim1; blue dotted line refers to sim2). Period 1 st October 2008 to 31 st March 2009. Also shown are daily rainfall totals (columns [mm d^{-1}]).....	168
Figure 77 – Daily mean propyzamide loads (g h^{-1}) at Banbury: measured (red line), and modelled (blue solid line refers to sim1; blue dotted line refers to sim2). Period 1 st November 2009 to 31 st March 2010. Also shown are daily rainfall totals (columns [mm d^{-1}]).....	170
Figure 78 – Daily mean carbetamide loads (g h^{-1}) at Banbury: measured (red line), and modelled (blue solid line refers to sim1; blue dotted line refers to sim2). Period 8 th January 2009 to 31 st March 2009. Also shown are daily rainfall totals (columns [mm d^{-1}]).....	173
Figure 79 – Daily mean carbetamide loads (g h^{-1}) at Banbury: measured (red line), and modelled (blue solid line refers to sim1; blue dotted line refers to sim2). Period 1 st November 2009 to 31 st March 2010. Also shown are daily rainfall totals (columns [mm d^{-1}]).....	175

Figure 80 – Propyzamide concentrations monitored at the main drain of the Experimental Field (primary axis, grey symbols), and at the catchment outlet (SAMOS) (secondary axis, black symbols) in November 2009..... 183

Figure 81 – Carbetamide concentrations monitored at the main drain of the Experimental Field (primary axis, grey symbols), and at the catchment outlet (SAMOS) (secondary axis, black symbols) in the period 22nd February to 3rd March 2010. 184

LIST OF TABLES

Table 1 – Agricultural land use for the Local Authority ‘Cherwell’ (DEFRA statistics, 2007).....	34
Table 2 – HOST classification and SPR coefficients of the Upper Cherwell catchment (Source: Boorman et al., 1995).....	37
Table 3 – Banbury gauging station characteristics (Source: www.nwl.ac.uk [accessed 8 th December 2009]).	38
Table 4 – Key properties of propyzamide and carbetamide pertinent to the potential for leaching loss (www.eu-footprint.org [accessed 7 th December 2009]). DT ₅₀ is the median dissipation time, K _{OC} is the organic carbon to water partition coefficient and GUS is the Groundwater Ubiquity Score (Gustafson, 1989).....	44
Table 5 – Physico-chemical properties of propyzamide and carbetamide (www.eu-footprint.org [accessed 7 th December 2009]).	45
Table 6 – Grimsbury weather station location and details.....	47
Table 7 – Banbury gauging station details.....	48
Table 8 – Available carbetamide and propyzamide concentration data sets examined in this project.	49
Table 9 – Maximum concentrations measured every year (1996-2008), for carbetamide and propyzamide.....	53
Table 10 – Characteristics of the WSC flume used for the monitoring conducted at the Experimental Field.....	71
Table 11 – Characteristics of the Barologger and Levelogger used for recording the head of water in the stilling well installed at the main drain monitored at the Experimental Field.....	74
Table 12 – Sampling points monitored during spring and autumn 2009.....	79
Table 13 – Monthly rainfall and drain flow at the Experimental Field.	80
Table 14 – Concentrations of carbetamide ($\mu\text{g l}^{-1}$) observed in grab samples collected from the River Cherwell at Woodford Halse (site 2).	97
Table 15 – Concentrations of propyzamide ($\mu\text{g l}^{-1}$) observed in the grab samples.	99

Table 16 – Description of the soil associations represented in Figure 47 (NATMAP data set).....	103
Table 17 –Parameters which were used for the model calibration.	111
Table 18 – Soil properties (NATMAP, www.landis.org.uk [accessed 15 th December 2009]) used in simulations performed with MACRO (Denchworth soil series).	113
Table 19 – Crop information (oilseed rape) used in simulations performed with MACRO.	113
Table 20 - Weather data and site characteristics used in simulations performed with MACRO.....	113
Table 21 – Key properties and application details of the herbicides considered in this thesis.	114
Table 22 – Soil physical parameter values.	117
Table 23 - K_{OC} values used in the model calibration and Nash-Sutcliffe efficiency index.	118
Table 24 – Location of Radcliffe Meteorological Observatory, Oxford (http://www.geog.ox.ac.uk/research/climate/rms/).....	136
Table 25 – Agricultural land use (DEFRA agricultural census 2007).....	137
Table 26 – Drain flow peaks recorded at the Experimental Field (Q_{field} [$m^3 s^{-1}$]), flow peaks at the catchment outlet (Q_{outlet} [$m^3 s^{-1}$]), and observed lag (hours).....	147
Table 27 – Soil properties (NATMAP, www.landis.org.uk [accessed 15 th December 2009]) used in simulations performed with MACRO (Banbury soil series). ...	154
Table 28 – Crop information (permanent grassland) used in simulations performed with MACRO.....	154
Table 29 – Nash-Sutcliffe efficiency index for 2008 – 09 season (A is the catchment area used in the simulation).....	161
Table 30 – Predicted and measured runoff considering a catchment area of 199 km^2 for the first season (2008 – 09) (in brackets values referred to 129- km^2 area).	161
Table 31 – Measured and predicted total runoff in relation to total rainfall (2008 – 09).	162

Table 32 – Nash-Sutcliffe efficiency index for 2009 – 10 season (A is the catchment area used in the simulation).....	165
Table 33 – Predicted and measured runoff considering a catchment area of 199 km ² for the second season (2009 – 10) (in brackets values referred to 129-km ² area).	165
Table 34 – Propyzamide losses for the period October 2008 to March 2009.....	168
Table 35 – Propyzamide losses for the period October 2009 to March 2010.....	170
Table 36 – Comparison between measured and predicted propyzamide concentrations (µg l ⁻¹): mean values and range of variation, and number of days exceeding the DWD MAC (0.1 µg l ⁻¹).	171
Table 37 – Carbetamide losses for the period October 2008 to March 2009.	172
Table 38 – Carbetamide losses for the period October 2009 to March 2010.	174
Table 39 – Comparison between measured and predicted carbetamide concentrations (µg l ⁻¹): mean values and range of variation, and number of days exceeding the DWD MAC (0.1 µg l ⁻¹).	176

ACRONYMS

ADAS	Agricultural Development and Advisory Service
ASCE	American Society of Civil Engineers
BTC	Breakthrough Curve
CDE	Convection-Dispersion Equation
CPA	Crop Protection Association
CTU	Chlortoluron
DEFRA	Department for Environment Food and Rural Affairs
DEM	Digital Elevation Model
DSM	Digital Surface Model
DTM	Digital Terrain Model
DWD	Drinking Water Directive
EA	Environment Agency
EEC	European Economic Community
EC	European Commission
EPIC	Erosion Productivity Impact Calculator
EQS	Environmental Quality Standard
EU	European Union
FC	Field Capacity
FERA	Food and Environment Research Agency
FOCUS	FORum for the Co-ordination of pesticide fate models and their USE
GC	Gas Chromatography
GIS	Geographical Information System
GRP	Glass-Reinforced Plastic
GUS	Groundwater Ubiquity Score
HOST	Hydrology Of Soil Types
IPU	Isoproturon
IWRM	Integrated Water Resources Management
JRC	Joint Research Centre (European Commission)

LG	Liquid Chromatography
LOD	Limit Of Detection
MAC	Maximum Admissible Concentration
MCPA	2-methyl-4-chlorophenoxyacetic acid
MCPP	2-(2-Methyl-4-chlorophenoxy) propionic acid
NATMAP	National Soil Map
NSE	Nash-Sutcliffe Efficiency index
NSRI	National Soil Resources Institute
OC	Organic Carbon
OLF	Overland Flow
OS	Ordnance Survey
OSR	Oilseed Rape
PET	Potential Evapotranspiration
PNEC	Predicted No Effect Concentration
PTF	PedoTransfer Function
RMSE	Root Mean Square Error
SAMOS	System for the Automated Monitoring of Organic Substances
SMD	Soil Moisture Deficit
SPE	Solid-Phase Extraction
SPR	Standard Percentage Runoff
SWAT	Soil and Water Assessment Tool
SWATCATCH	Surface Water Attenuation Catchment model
TFM	Transfer Function Model
UN	United Nations
USDA	United States Department of Agriculture
UK	United Kingdom
VI	Voluntary Initiative
WFD	Water Framework Directive
WSC	Washington State College

ACKNOWLEDGEMENTS

I am very grateful to my supervisor, Claudio Gandolfi, for his advice and for having given me many opportunities to study and learn during these years.

Many thanks to Mick Whelan, my supervisor at Cranfield University, for his advice, patience, and continuous encouragement.

My acknowledgements also go to Michele Rienzner for his help with the modelling and for his perceptive comments on my work.

I would like to thank Colin Brown for having provided information and advice for the field-scale modelling, Pat Bellamy for her help with the statistical analysis, and Ian Seymour for his invaluable support with my field equipment.

My thanks also go to Jon Bellamy, a TAG agronomist operating in the Cherwell catchment, for his suggestions and advice about farming operations and to the farmers and staff of the main farm used for the field investigations for allowing access to their land and for providing invaluable information about their operations during my field work.

I would like to express my most sincere gratitude to Ken Rushton for having shared his knowledge and experience, and for his continuous help and moral support.

Chapter 1 – INTRODUCTION

1.1 Pesticides in the environment

Pesticides are chemicals which control a range of pests and diseases in agriculture, amenity management (e.g. weed control on roads and railways) and in domestic activities. In agriculture, pesticides increase crop yields by combating insect pests, fungal diseases and weeds and are used to help maintain health livestock (e.g. by controlling parasites such as sheep ticks). If pesticides were to be banned, Gavrilescu (2005) estimates that the pre-harvest crop could be reduced by as much as 40%. In addition to helping to increase (and reduce the variability of) yields, low food and agricultural commodity prices have also been attributed, in part, to pesticide use. Despite these benefits, pesticide use is often associated with a number of negative impacts on the environment and on water quality. Many agricultural chemicals are toxic to some degree to non-target organisms (animals or plants). Toxicity may pose risks on site (e.g. to birds, beneficial insects or to the crop itself) or in environments away from the fields to which the chemicals are applied (e.g. in adjacent aquatic or terrestrial ecosystems which can be exposed via spray drift contamination or via the transfer of contaminated runoff). The extent of any impact will be determined by the level of exposure, relative to the toxic effect threshold (which will be different for different chemicals and to different organisms). Other undesirable environmental risks include long range transport potential to remote ecosystems (e.g. via volatilisation and atmospheric transport to high latitudes), direct atmospheric impacts (e.g. the impact of methyl bromide on stratospheric ozone depletion: UN, 2002) and bioaccumulation in food webs (a feature of many of the older generation of persistent and hydrophobic chemicals). In addition, there are a number of legal thresholds for environmental quality and drinking water provision which should be respected.

1.2 Legislative background

Water protection has a high priority in European Legislation. Pesticide use is restricted via legislation on registration (e.g. 91/414/EC). The registration process consists of an extensive series of laboratory tests, field studies and numerical modelling which manufacturers need to perform in order to demonstrate acceptable risks associated with a given use of a pesticide to the environment and to human health. The philosophy behind registration is simple: once a chemical has undergone the risk assessment it is allowed to be used in a given set of situations, at a given rate.

In 1998 the European Union revamped the Drinking Water Directive (DWD), Council Directive 98/83/EC, which concerns the quality of water intended for human consumption. The objective of the Drinking Water Directive is to protect the health of consumers in the European Union and to make sure the water is wholesome and clean, setting standards for the most common substances (named parameters) that can be found in drinking water (<http://ec.europa.eu/> [accessed 7th December 2009]). As far as pesticides are concerned, the principle upon which the drinking water legislation is based is zero presence. When an earlier version of the DWD was drafted (80/778/EEC), a typical limit of detection for pesticides in water was $0.1 \mu\text{g l}^{-1}$. This was, thus, adopted as the drinking water standard (Maximum Admissible Concentration: MAC), despite the fact that the toxic effect threshold for different pesticides varies significantly and the adoption of a single threshold for all chemicals is, therefore, not risk-based.

In 2000 the Water Framework Directive (WFD, 2000/60/EC) was adopted, as a response to the increasing demand by citizens and environmental organisations for cleaner waters. The WFD establishes a legal framework to protect and restore surface and ground water bodies from both a quantity and a quality perspective by defining new objectives (e.g. achieving *good ecological status* of all water bodies by 2015), new principles (like the use of pricing policies and the polluter pays principle in order to promote water use efficiency and reduce water pollution) and new paradigms (Integrated Water Resources Management [IWRM]). Under the WFD, environmental quality standards (EQSs) have been set for many pesticides (EC, 2009) – usually based on

predicted no effect concentrations (PNECs) derived from laboratory ecotoxicological studies (EC, 2009).

Both the directives require improvements in the quality of many surface waters. In cases where concentrations of agrochemicals are high, new management strategies will be needed.

1.3 Pesticide usage in the UK

Data on the use of pesticides in Great Britain over the last 20 years suggest that the area treated with pesticides increased between the early 1990s and the last eight years (pesticide data accessed online at <http://pusstats.csl.gov.uk/> [7th December 2009]) (Figure 1). In parallel, recent pesticide contamination of ground and surface waters in the UK has been well documented (Brown *et al.*, 2001; Holman *et al.*, 2004; Edwards *et al.*, 2008). In many cases this contamination results in exceedances of legislative thresholds such as the MAC defined by the DWD or EQS values defined under the WFD. Such breaches are often difficult to control because of the diffuse nature of contamination sources and pathways, which are difficult to identify or understand properly.

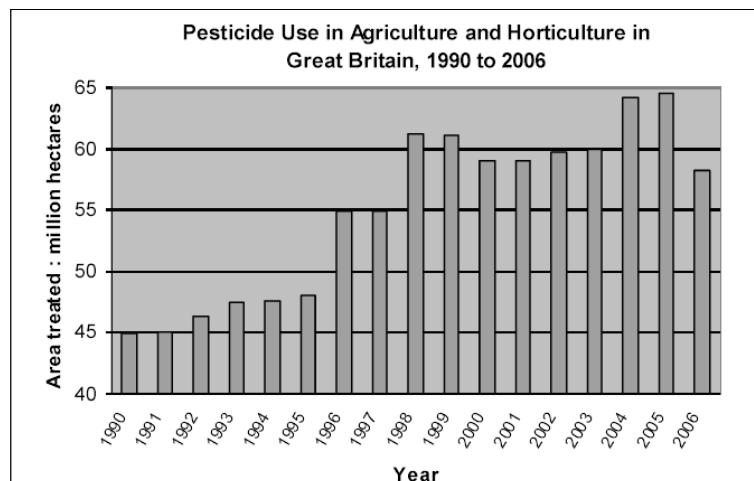


Figure 1 – Pesticide use in Great Britain (Source: FERA, accessed online at <http://pusstats.csl.gov.uk/>).

Herbicides (used to control weeds) are the most widely used pesticides in agricultural practice (Leonard, 1990). Herbicides are more efficient and cost-effective means of weed control than mechanical methods (Carlile, 2006). Although they are used in both rural and urban contexts, their usage in agriculture (including horticulture) represents about 80% of all herbicide use in England and Wales (<http://www.environment-agency.gov.uk> [accessed 16th December 2009]). Due to a combination of their widespread use and their physico-chemical properties (modern herbicides are often relatively water soluble, poorly hydrophobic and moderately persistent), herbicides are frequent contaminators of surface and ground waters in agricultural catchments in the UK (Holman *et al.*, 2004).

1.4 Aims and objectives

This thesis deals with the analysis of herbicide transport from land to surface water at field and catchment scale. The work presented here focuses on the Upper Cherwell catchment, where herbicide transport processes were analysed via monitoring and modelling. This catchment is defined by a drinking water reservoir abstraction point at Banbury in Oxfordshire, where water quality is monitored regularly by Thames Water Limited. A number of herbicides frequently exceed the DWD MAC at the reservoir. The main aim of the work described in this thesis is to test the hypothesis that drain flow is a most significant pathway for agricultural herbicide contamination in the catchment, with specific emphasis on propyzamide and carbetamide.

The thesis has three specific objectives which can be summarised as follows:

- Review the processes that could contribute to herbicide contamination of surface waters.
- Quantify the contribution of agricultural drain flow to herbicide transport in the Upper Cherwell via a combination of measurement of stream water and drain water concentrations and mathematical modelling.

- Make relevant recommendations for further investigations.

The above objectives were achieved via

- A review of key processes which could contribute to elevated concentrations of herbicides in the Upper Cherwell and similar catchments;
- Analysis of existing data on stream flow, rainfall, air temperature and herbicide concentrations;
- Monitoring soil moisture, air and soil temperature, rainfall, drain flow, and drain water quality (analysis for key herbicides);
- Modelling of hydrological and contaminant transport processes in the catchment, both at field and catchment scale.

1.4 Thesis structure

In addition to this introductory chapter, this thesis contains seven chapters:

- Chapter 2 provides a review of the processes which can contribute to herbicide transport from land to water;
- Chapter 3 provides a description of the Upper Cherwell catchment and some background on the pesticide problem;
- Chapter 4 describes the statistical analysis of existing data, which aimed at a better-understanding of herbicide issue in the catchment and at providing useful insights to plan the following steps of this work;
- Chapter 5 includes the field investigations carried out in a clay field in the catchment;
- Chapter 6 presents the modelling of hydrological and contaminant transport processes at the field scale; together with the previous chapters it provides the bases for the development of a model of catchment-scale pesticide transfers in the Upper Cherwell catchment (reported in Chapter 7).

- Chapter 8 presents the conclusions.

Chapter 2 – HERBICIDE TRANSPORT FROM LAND TO SURFACE WATER

2.1 The introduction of herbicides into the water cycle

The river catchment is a fundamental unit of landscape organisation and process integration. Climatic, hydrological, ecological, edaphic and biogeochemical processes interact within the catchment boundary and contribute to the magnitude and temporal patterns of material fluxes to the catchment outlet (Whelan *et al.*, 2009). The influences of land management, industrial activity and other human interventions are also integrated at the catchment scale. Catchments are usually defined topographically, with water and material fluxes accounted for within its boundary.

The catchment concept is important for understanding diffuse pollution because it links a specified land area to a given point in the channel network. Within this area, contamination sources can be divided into two groups: *point sources* such as discharges from industrial or municipal waste treatment plants and *diffuse sources* such as eroded soil, nutrients or pesticides which might be transported in agricultural runoff. It should be noted that for some contaminants, there is not always a clear distinction between these two different kinds of contamination.

In agricultural areas, there are three main sources for pesticides in surface waters:

- (1) Farmyards can act as pseudo point sources (spillages, tank filling and hard standing runoff);
- (2) Spray drift during application can contaminate streams and ditches;
- (3) Diffuse source transfer of pesticides by hydrological processes from fields to the surface water network (Müller *et al.*, 2002; Gerecke *et al.*, 2002).

The role of point sources, such as runoff from contaminated hard standings, in affecting pesticide concentrations in medium sized and large catchments is somewhat

controversial. It is clear that bad agronomic practices (e.g. spilling zones, washing, and tank filling) can result in local pesticide contamination of receiving surface waters (Mason *et al.*, 1999; Fait *et al.*, 2007; Neumann *et al.*, 2002; Edwards *et al.*, 2008; Kreuger, 1998; Ramwell *et al.*, 2004). According to Leu *et al.* (2004), farmyard losses can result in high concentrations, but may not contribute significantly to total loads. However, local concentration peaks resulting from short duration “spills” or washoff during storm events are likely to diminish significantly due to hydrodynamic dispersion in the channel network (*cf.* Gandolfi *et al.*, 2001). Furthermore, once identified, point sources can be controlled by improving farmyard practices or by technical measures, such as bunding and “biobeds” or other treatment systems. Similarly, spray drift can be controlled by implementing no-spray zones adjacent to water courses or via changes in spray technology (such as using low-drift directed nozzles, changing boom height and tractor forward speed). Diffuse sources, on the other hand, are more difficult to handle since they are influenced by numerous interacting factors including soil properties (fixed and variable), weather, pesticide properties, and agricultural management practices (Leonard, 1990; Kladvko *et al.*, 2001; Leu *et al.*, 2004). The remainder of this thesis will focus on diffuse source pesticide contamination.

2.2 Transport mechanisms

In order to understand herbicide transfer mechanisms, it is necessary, first, to focus on the hydrological pathways that water can take after precipitation (see Figure 2).

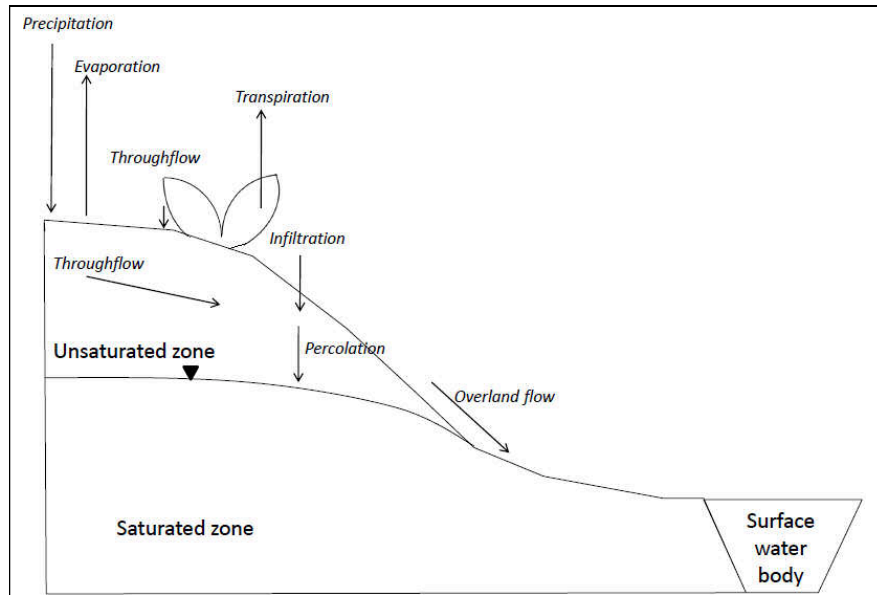


Figure 2 - Different hydrological pathways that water can take after precipitation (Source: personal communication Whelan, 2008).

Precipitated water can be intercepted by the plant foliage and then evaporate or it may fall through the canopy or drip off it to reach the ground (in throughfall). The amount of water that reaches the ground (directly or after throughfall) can be transported via a number of mechanisms:

- **Infiltration:** Water (rainfall or melting snow) infiltrates the soil surface. Infiltration is controlled by the intensity and duration of precipitation relative to the product of hydraulic conductivity (which varies with soil water content) and the potential energy gradient (which is also related to water content via the soil water release curve). Hydraulic conductivity and the water release curve are both related to soil texture and structure (e.g. Marshall and Holmes, 1980);
- **Percolation:** Water transfer in the unsaturated zone towards the water table. The percolation rate will also be a function of permeability and potential energy gradient. Water which reaches the water table is called groundwater recharge. Groundwater may contribute to stream flow via springs, seeps or direct discharge to the channel through bed and banks;

- Overland flow: Water can flow over the soil surface if it cannot infiltrate (either because the near surface soil is saturated or because the infiltration rate is exceeded by the rainfall or snowmelt rate). Significant water movement over the surface requires a gradient and an exceedance of depression storage (the depth of water which can be stored in microtopographic cavities on the soil surface). Infiltration excess overland flow can be enhanced by reduced permeability due to the presence of a cap or by soil compaction by animals or machinery. Both infiltration excess and saturation overland flow can occur across small or large areas, depending on the amount and intensity of precipitation and the soil type, soil moisture status and vegetative cover and topography (particularly local slope angle and area drained per unit contour width). Surface saturation is most likely to occur in areas with low topographic gradient and high contributing area (e.g. Anderson and Burt, 1978; Beven and Kirkby, 1979);
- Throughflow (sub-surface lateral flow): If infiltrated water encounters a permeability discontinuity (for example a clay layer) or a saturated layer at depth, it can be diverted laterally along the line of maximum hydraulic gradient. The flow line is often in a downslope direction but may also be affected by the presence of soil macropores or artificial drains (if the land is artificially drained - this process is called drain flow) until it reaches the surface water network;
- Evapotranspiration: Plants take up water through their roots and transfer it to their leaves where it re-enters the air by transpiration via their stomata. In addition water can evaporate directly from the soil (and from plant foliage). These processes together are called evapotranspiration (e.g. Ward and Robinson, 1990).

Any water flowing across or through the landscape can carry dissolved and particle-associated materials with to the channel network (Whitford, 2002). Although sediment transport is often associated with surface transport (e.g. overland flow), it is now

recognised that colloids and sediments can also be transported through macropores in the subsurface to field drains (e.g. Levin *et al.*, 2006).

As far as herbicide transport is concerned, the predominant hydrological routes by which pollutants can reach surface waters include leaching to field drains and overland flow. Groundwater seepage, throughflow and wet or dry deposition following transport in air are generally considered to be less significant routes of entry (Brown *et al.*, 2004).

2.3 Subsurface agricultural drainage

Subsurface drainage is a common water management practice in badly drained soils. Excess water is removed from the soil surface and/or soil profile by artificial means in order to increase crop production and reduce soil erosion. Excess water is removed from the plant root zone by artificially lowering the water table through a series of drainage pipes (made of clay or concrete or corrugated plastic), installed below the soil surface usually just below the root zone. Drains are typically installed at depths of 0.7 to 1.3 m, and horizontal spacings of 5 to 30 m. The subsurface-drain network generally outlets directly to an open ditch, stream, or in some cases a large collector main pipe that then outlets to a ditch or stream (Kladivko *et al.*, 2001). Different factors can contribute to excess water problems in agricultural soils including excess precipitation (including snow), soil characteristics (fine texture, massive structure, and low permeability), soil compaction, topography and restrictive geologic layers underlying the soil profile.

Soil texture affects water-holding capacity (i.e. the water filled pore space at field capacity) and hydraulic conductivity (often referred to as permeability). In general, fine-textured soils retain water well, but they often have drainage problems as a consequence. Coarse-textured soils, on the other hand, are often better drained, but their water-holding capacity is limited, which means that plant-available water may be low. Soil structure also affects permeability, easing or limiting water movement.

Human activities can cause or exacerbate soil water problems. For example, in the context of agricultural activities, operating farm equipment under wet soil conditions may compact the soil, damage its structure, and, as a consequence, reduce its permeability.

2.3.1 Drain flow versus overland flow

Drain flow and overland flow are both induced by precipitation and irrigation. The relative importance of each process depends on soil type, topography, antecedent soil water content, the depth of the water table and the intensity, and duration of precipitation (or the volume of snow and the rate of snowmelt, where relevant). Subsurface drain spacings and depth are also important. Other hydrological factors which could be important include the rate of evapotranspiration (which will influence the soil water content for the next event), the existence of throughflow (promoted by impermeable layers, for example), and percolation to deep groundwater (Kladivko *et al.*, 2001).

According to Bengtson *et al.* (1984) and Schwab *et al.* (1985) the introduction of subsurface drainage can reduce overland flow by 29 to 65%, due to an enhanced capacity of the soil to absorb rainfall (see Figure 3).

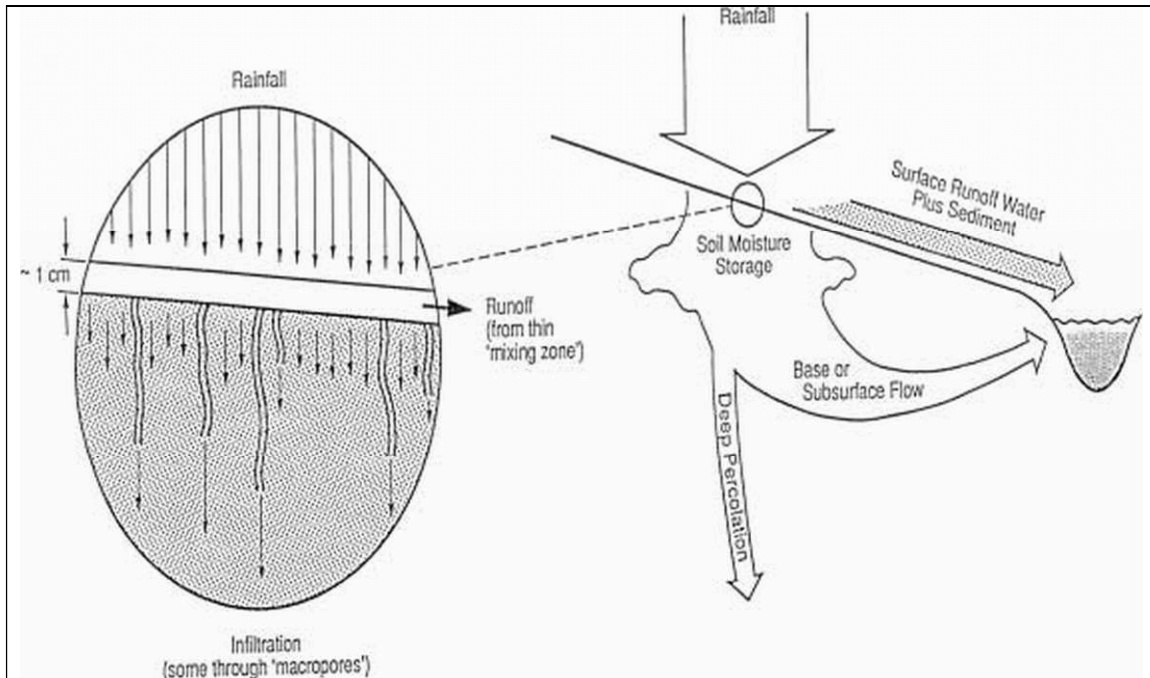


Figure 3 – Partitioning of rainfall into infiltration, overland flow (surface runoff), soil storage, groundwater flow (often called base or subsurface flow), and deep percolation (Source: Kladivko *et al.*, 2001).

2.3.2 Pesticide transport to subsurface drains

The presence of artificial drainage can have a significant impact on pesticide transport by increasing infiltration and decreasing overland flow, along with the transport of sorbed compounds (Kladivko *et al.*, 2001). However, this does not necessarily mean that pesticide transport to surface waters is reduced. There is considerable evidence that pesticides have the potential to move very quickly to field drains and then to the surface water network. According to Johnson *et al.* (1996) the vast majority (75-90%) of isoproturon losses in a small drained clay catchment occurred via the artificial drainage network; volumes of water moved by overland flow were low, although concentrations in overland flow and in drain flow were similar. Harris and Catt (1999) also concluded that rapid movement to sub-surface drains was a major pathway for pesticide transport to surface waters in heavy clay soils (see also Haria *et al.*, 1994).

The relationship between rainfall intensity and pesticide concentration is complex. Intense rainfall in the period following pesticide application is likely to result in pesticide transfers to surface waters. Although there is likely to be a positive relationship between rainfall intensity in this post application period and the pesticide flux, the relationship between concentration and intensity may be more complex because high rainfall over an area including non-treated areas is likely to reduce the concentration, due to dilution (Whitford, 2002). The relationship will also be affected by pesticide-specific properties (principally DT_{50} and K_{OC}), the amount and timing of application, soil texture and structure, soil organic carbon content and distribution and antecedent soil moisture content. Soils with high organic carbon contents are, in principle, likely to retain hydrophobic pesticides via absorption into the organic matrix. However, in practice, preferential flow may result in a significant fraction of matrix “bypass” (Stone and Wilson, 2006).

Leaching of sorbing pesticides in tile-drained loamy and clayey soils mainly occurs via macropores (Kladivko *et al.*, 1991; Kladivko *et al.*, 2001). If the water containing them is flowing in the soil matrix, the residence time and the sorption capacity will prevent most pesticides from leaching. In macropores, in contrast, pesticides can be transported very quickly to tile drains either in solution via chemical non-equilibrium transport or absorbed to mobile particles (Jacobsen and Kjær, 2007).

Pesticide sorption properties affect the type of transport (solute or particle-bound) and pathways (Figure 4). At very low adsorption coefficients, leaching will be lower in macroporous soils, because water without pesticide will bypass most of the soil matrix where the pesticide has diffused. At higher sorption (i.e. particle-bound pesticides), leaching is higher in macroporous soils, as macropore transport will become the dominant mechanism (Jacobsen and Kjær, 2007).

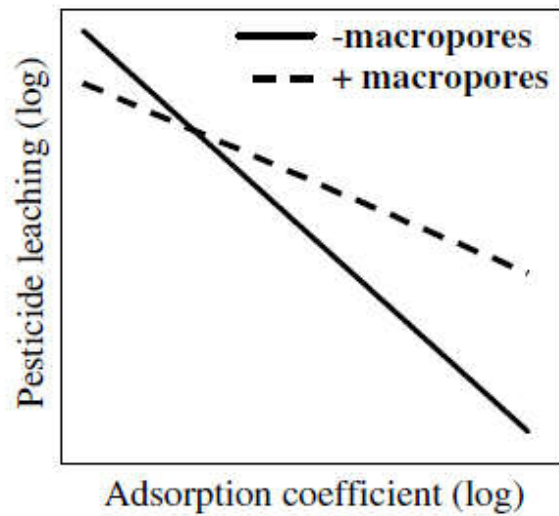


Figure 4 – Diagram illustrating the effect of macropores on the relationship between leaching of dissolved pesticides and the adsorption coefficient (Jacobsen and Kjær, 2007).

2.3.3 Drain flow and transport pathways to subsurface drains

Drainage water consists of a mixture of water of different origins and reflects the various transport pathways that move water to tile drains (Figure 5).

When the water table is located below the drain depth (i.e. outside the drainage season), transport is dominated by vertical flow through the soil profile (Figure 5a). If the soil is relatively dry and precipitation moderate, percolation input will mainly occur as matrix flow. Macropore flow will occur if the matrix hydraulic conductivity is exceeded. Villholth *et al.* (1998) performed a series of chloride tracer drain plot experiments on a silty to sandy loam soil in Denmark. The rapid and relatively deep penetration of the tracer in the soil profile that were observed suggested that macropore transport between the drains was involved. Kjær *et al.* (2004a) observed analogous behaviour: following a single rain event, pesticides were rapidly transported to monitoring screens located in the uppermost part of the shallow groundwater (1.5 – 2.5 m depth). When the water table is located below drain depth, drain flow is normally not

expected because a drain does not exert any capillary pressure, and a positive water potential at drain depth is needed to force water into the drain (Jacobsen and Kjær, 2007).

In the drainage season the water table will rise as precipitation input exceeds the hydraulic conductivity of the deeper soil layers. When the water table reaches drain depth water will flow laterally into the drain (Figure 5b). Rapid high lateral transport was observed in tracer studies in fractured Danish till (Nilsson *et al.*, 2000). The first arrival of the bromide tracer revealed that horizontal transport at shallow depths was about 200 times faster than vertical transport to a depth of 5 m. The rapid lateral transport to the drains and uppermost groundwater screen (1.5 – 2.5 m) was attributed to stratification of the bulk permeability and the presence of thin sand lenses and the horizontally oriented fracture system to a depth of 4 m (Jacobsen and Kjær, 2007).

During period of high precipitation, the water table between drains will rise further (Figure 5c). Water will flow to the drains following the pressure gradient, and drain flow will peak. Water flow will be highest in areas with high hydraulic conductivity (e.g. along the plough pan or along the soil surface). Bypass transport of pesticides in macropores consisting of earthworm burrows, shrinkage cracks, and ploughing cracks has been reported by Haria *et al.* (1994). This transport followed horizontal pathways connected to the fracture system of the mole drains, thus feeding the drains. Low bulk hydraulic conductivity in heavy clay soils is likely to promote lateral transport in structures with higher conductivity. In general, if vertical flow is restricted because of heavy clay or compact layers, or very high precipitation, water will flow laterally in the layer with the highest lateral hydraulic conductivity. When the water reaches the area above the drain, it starts infiltrating because vertical flow is not restricted. Vertical flow downwards can also be eased if the hydraulic conductivity of the backfill is higher than that of the undisturbed soil (Jacobsen and Kjær, 2007).

A number of studies report that macropores can be in direct contact with a drain, generating a direct pathway from the soil surface to the drain. It has therefore suggested that it might lead to higher macroporosity in the area above the drains than in the area between the drains. However, experimental data supporting this hypothesis are very limited (Shipitalo *et al.*, 2004).

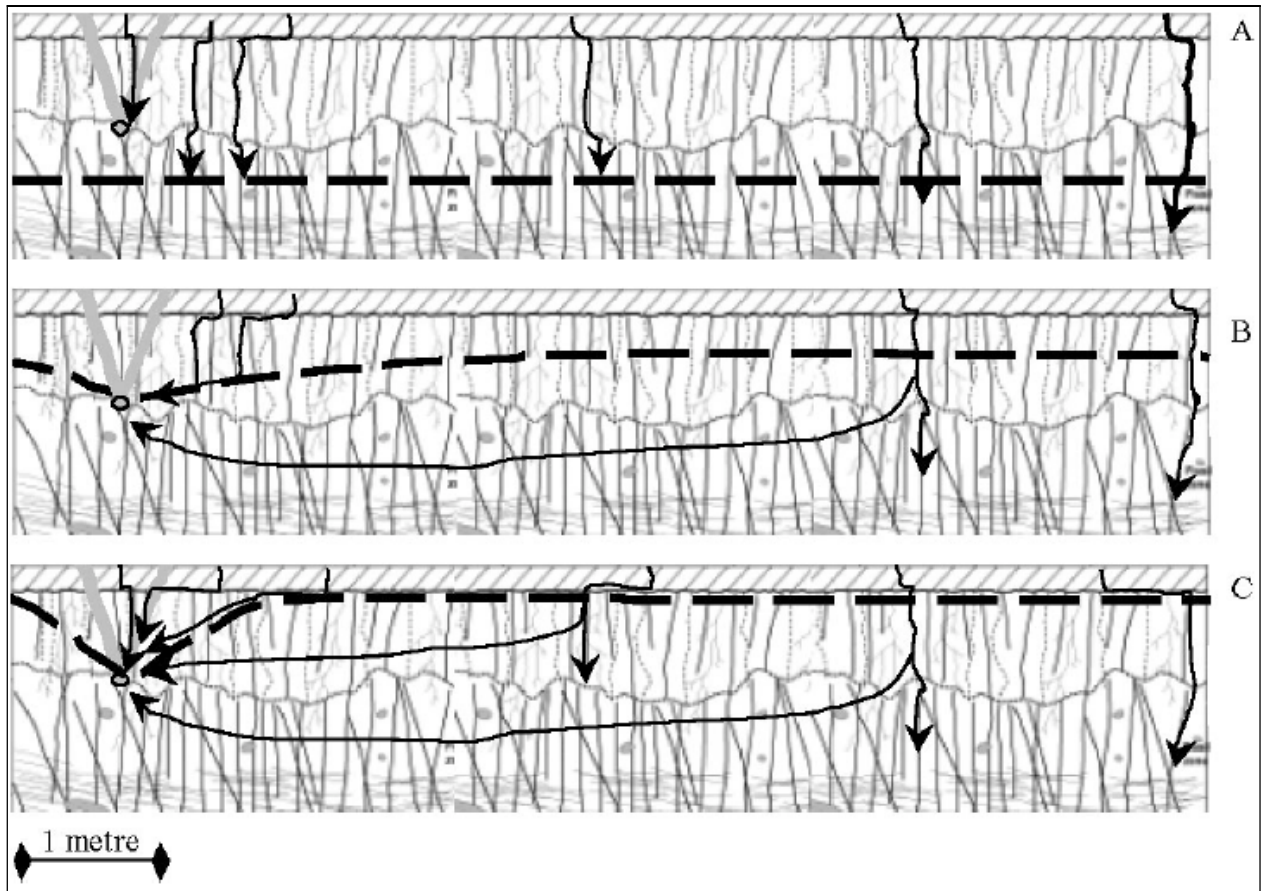


Figure 5 – Soil profile showing the various water pathways from the surface to drains and groundwater (solid lines with arrows) for three water table levels. The location of the drainage trench and water table are indicated by thick grey and dotted lines respectively. An open circle indicates a drain at 1 m depth. The soil profile consists of a plough layer, a layer dominated by biopores, and a deeper calcareous layer mainly dominated by tectonic fractures (Jacobsen and Kjær, 2007).

Different transport pathways may be involved in pesticide transport to drains. Petersen *et al.* (2003) showed that the leaching patterns observed for particles, particle-bound pesticide, and dissolved pesticide were very similar, suggesting that the same transport pathways were used by the dissolved and particle-bound pesticide during storm events. In this study leaching only occurred during storm events, with highest concentration in the first samples, dropping rapidly as the event progressed. It therefore seems to indicate direct transport from the top layer to the drains through macropores. Other studies, though, suggest that the loss of strongly sorbing compounds does not only occur during

storm events: Kjær *et al.* (2004a, 2004b) found high glyphosate concentrations between storm events, suggesting that transport also occurred via other pathways than drain-connected earthworm burrows (Jacobsen and Kjær, 2007).

In poorly drained soils in wet conditions (when the water table is located above drain depth), much of the pesticide leaching occurs in macropores connected to high-permeability layers (see Figure 5b). Pesticide leaching through macropores not connected to high-permeability layers is much lower, allowing more sorption to the macropore walls, and more diffusion of particle-bound pesticides. In such macropores, solutes and particles will probably not leach as deeply as in the “connected” macropores (Jacobsen and Kjær, 2007).

2.4 Pesticide movement in soils

2.4.1 Solute movement in soils

Movement of a solute in soil depends on three mechanisms: advection, dispersion, and reaction (Freeze and Cherry, 1979). The mass flow of water will carry solutes by advection which, in the absence of other processes, results in chemicals being transported at the same rate as the macroscopic velocity of the water. However, the velocity of solutes in practice is different from this rate due to hydrodynamic dispersion. This results from two processes: mechanical dispersion and molecular diffusion. The latter is usually smaller than the former in most environmental systems and results from the random motion of molecules. It occurs regardless of whether or not there is net water movement. Hydrodynamic dispersion in porous media results from the fact that individual solute molecules take different pathways through the matrix. Some of these pathways may be relatively rapid and others relatively slow (Ward and Robinson, 1990). Some molecules may be transported into pores which are “stagnant” or immobile and are exchanged with the mobile pore space via slow processes, such as diffusion. The net effect of these phenomena is a spreading out of a solute pulse as it moves through the system. It is very

difficult to distinguish the effects of molecular diffusion from hydrodynamic dispersion and the two are often bulked together in mathematical descriptions of solute transport in porous media. Changes in concentrations may also take place due to chemical reactions, including adsorption to the solid matrix and a variety of transformation and degradation processes (e.g. Ward and Robinson, 1990). The combined effects of these processes on solute movement are usefully presented using breakthrough curves (BTC). BTCs depict the change in solute concentration observed in the outflow of a system, fed with either a pulse or a step change solute input. The system considered could be as simple as a laboratory soil column, although the principles can also be applied to fields or even catchments. In the case of simple systems such as homogeneous porous media, BTCs can be described quite well using the physical theory of advection and dispersion which is the basis for the convection dispersion equation (CDE). However, this theory has been shown to be inappropriate when preferential flow pathways exist.

In the case of macropore flow (a form of preferential flow), water can move rapidly through larger pores and may not come into chemical equilibrium with the bulk soil matrix (Köhne *et al.*, 2009a). Reaction (including sorption) is restricted to the soil immediately adjacent to the macropores, although there will be some lateral diffusion into the matrix as well. As a consequence, a significant amount of chemical can pass unchanged through the soil.

Soil macropores are formed in different ways: by shrinkage at natural planes of weakness on drying (Brewer, 1964); freeze-thaw cycles, mole draining, and subsoiling (Beven and Germann, 1982); plant roots (Aubertin, 1971); and soil fauna like earthworms (Green and Askew, 1965; Ehlers, 1975). Although they may comprise only a small fraction of the total soil volume (0.001 to 0.05), they can have a profound effect on the rate of infiltration and redistribution of water under the right conditions (White, 1985). Beven and Germann (1982) suggest that rainfall rates between 1 and 10 mm may be sufficient to trigger macropore flow. Macropores can greatly decrease the time taken for dissolved and suspended matter applied on the soil surface to reach subsurface drains or ground water (Thomas and Phillips, 1979; Hagedorn *et al.*, 1981; Bouma *et al.*, 1983) (White, 1985).

Macropore flow tends to be most important when the rate of surface water input is high. Under these circumstances, a high fraction of surface applied solute may bypass the matrix and penetrate beyond the reach of plant roots. This results in an early rise of the BTC while sorption to soil solids (absorption into the organic matrix or adsorption to solid surfaces) phase and solute diffusion from the mobile porespace to immobile zones will cause a delay (manifested as a long tail in the BTC).

2.5 Pesticide characteristics

Pesticide transport is dependent on hydrological processes, but it is also affected by pesticide-specific physico-chemical and degradation properties. The most important characteristics of a pesticide in terms of its environmental fate are: its degradability, and its affinity for soil solids. The degradability of a chemical is often described using a DT_{50} (the median dissipation time or dissipation half life). This is the time needed for 50% of a compound to dissipate (Maly *et al.*, 2005). Strictly speaking “dissipation” includes *in situ* processes such as volatilisation as well as various degradation processes, including hydrolysis and photolysis as well as microbially mediated biodegradation. However, for many chemicals, biodegradation is the dominant loss process and the DT_{50} is often assumed to be equivalent to a biodegradation half life, at least implicitly. Representing loss rate using a half life assumes that the process can be well described using first order kinetics. However, this may be inappropriate for many chemicals in many different environmental matrices. The DT_{50} value is usually obtained experimentally from field and laboratory experiments by fitting a first-order kinetic model to observed degradation patterns (Beulke and Brown, 2001). The affinity of many organic chemicals to soil solids can be described using linear sorption isotherms normalised to the organic carbon content. This means that sorption is assumed to occur only to soil organic carbon and that the slope of the relationship between the chemical concentration associated with this carbon (mol kg C^{-1}) and that in the soil pore water (mol l^{-1}) is constant (i.e. the organic carbon to water partition coefficient: K_{OC} , l kg^{-1}). This means that mineral solids are

assumed to play no part in chemical sorption. The overall distribution of chemical between solids and the pore water is described by the distribution coefficient K_d ($l\text{ kg}^{-1}$), where:

$$K_d = f_{oc} \cdot K_{OC} = \frac{C_s}{C_w} \quad (1)$$

and where f_{oc} is the mass fraction of organic carbon in the soil (kg kg^{-1}), C_s (mol kg^{-1}) is the concentration of chemical sorbed to the soil solids (mineral and organic) and C_w (mol l^{-1}) is the chemical concentration in the pore water at equilibrium.

The validity of the above assumptions for different pesticides varies considerably. They are probably most appropriate for describing the behaviour of neutral compounds. For polar chemicals or chemicals which ionise (which include many acid herbicides) sorption may not be well described by K_{OC} . For neutral organic compounds, on the other hand, they probably work well. In this case, the K_{OC} can be estimated using the octanol: water partition coefficient (K_{ow}), which is the ratio of the concentration of a chemical in octanol to that in water at equilibrium and at a specified temperature. Octanol is an organic solvent that is used as a surrogate for natural organic matter. The lower the K_{ow} the more likely the substance will partition to water and, indeed there is often a reasonable correlation between K_{ow} and aqueous solubility. Leaching potential is generally thought to be related to both K_{OC} and DT_{50} . A low value for K_{OC} indicates that a substance will have a low affinity for soil carbon and, therefore, have a higher concentration in the pore water, implying high potential mobility. A high K_{OC} , on the other hand, suggests that a chemical should have relatively low mobility. Substances with long DT_{50} are expected to degrade slowly in the soil, implying that they could be available for transport a long time after they have been applied. Conversely, short DT_{50} s imply that substances should degrade quickly and, hence, should be unlikely leachers (where leachability is expressed as a fraction of chemical applied) because they are not present at high concentrations when water movement occurs. The GUS index (Groundwater Ubiquity Score:

Gustafson, 1989) was devised to describe the leachability of a chemical using K_{OC} and DT_{50} . The GUS equation is:

$$GUS = \log(DT_{50}) \cdot [4 - \log(K_{oc})] \quad (2)$$

If the GUS is lower than 1.8 the probability for the pesticide to leach is low and if GUS is greater than 2.8 the pesticide has a high leachability. If the GUS index is greater than 1.8 and lower than 2.8 the leaching potential is moderate. Contour plots for the GUS, derived from Equation 2 are shown in Figure 6. It should be stressed, though, that the GUS equation has got some limitations in giving information about leachability to surface waters: it was based on empirical data of chemical presence in groundwater, in California, which are very specific conditions. Solubility, which is only compound-specific and not site-specific might be a better index for leachability.

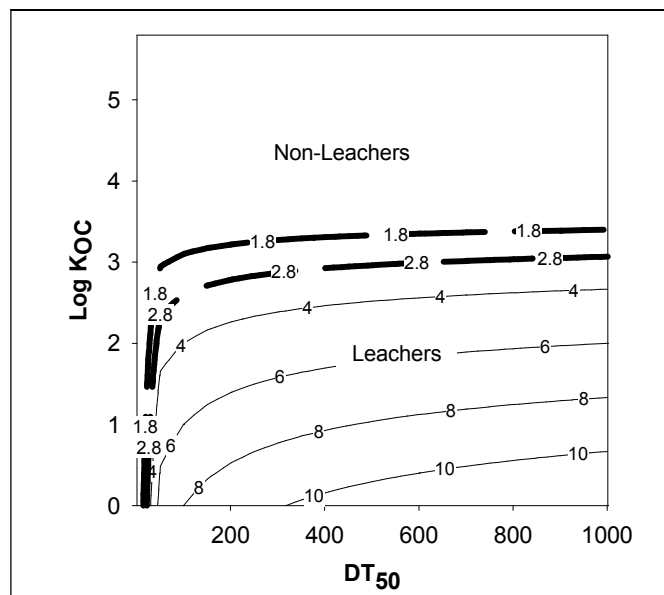


Figure 6 - GUS (Groundwater Ubiquity Score) index, which expresses pesticide leaching potential (Source: Mick Whelan, personal communication, constructed using Equation (2)).

It should be noted that although leaching potential is likely to be some function of chemical specific properties, this does not mean that chemicals with low leaching potential are never transferred from land to water. Other factors such as soil properties (and, of course, the hydrological processes, discussed above) will also influence leaching.

In general soils with high organic matter content (high foc in Equation 1) would be expected to decrease the movement of pesticide in soil because of increased K_d . In addition, soils with low water transfer rates (e.g. because of hydraulic conductivity through the matrix) might also be expected to pose a low risk to pesticide leaching (Boivin *et al.*, 2005). However, such soils (e.g. clays) may also be prone to cracking in summer, in which case such general expectations break down because much of the water (and pesticide) may be able to bypass the matrix. Soil pH and temperature can also potentially affect pesticide transport by influencing hydrolysis rates and dissociation of ionisable compounds, thus changing their sorption behaviour (e.g. Whitford *et al.*, 2001).

2.6 Pesticide fate modelling

Many field- and catchment-scale models have been developed to describe the transfer of pesticides from soil to ground and surface waters, ranging from simple empirical models, like the GUS index (Gustafson, 1989) to comprehensive, physically-based, distributed models that require complex parameterisation (Jarvis, 1994). Routine use of catchment models for assessment and management of pesticides requires a tool that is comprehensive in being able to address all major routes of entry of pesticides into surface water and that has reasonable parameter requirements. Pesticide fate models for application in simulation of small catchments can be divided into three groups (Renaud *et al.*, 2008):

- One-dimensional soil column leaching and/or overland flow: These models lack the capability of simulating surface processes and/or are restricted in

scale (i.e. plot scale). An example is MACRO (Jarvis, 1994) (see Paragraph 2.6.1).

- Field-scale models of hydrological processes, and contaminant fate (nutrients and/or pesticides): Models belonging to this group are limited to field-scale simulations and do not provide representation of flow routing to low order streams and ditches. In addition, they do not provide adequate representation of spatial variability typically present in catchments. EPIC (Erosion Productivity Impact Calculator) is an example of these models (Williams, 1995). It was first developed to simulate long-term effects of soil erosion on soil productivity. Nutrient cycling and pesticide fate routines were added later on. The various developments of EPIC are given by Gassman *et al.* (2005) (Bouraoui *et al.*, 2006).
- Catchment-scale models of hydrological processes and contaminant fate (nutrients and/or pesticides): These models include a capability of representing flow routing and spatial heterogeneity. The SWAT (Soil and Water Assessment Tool) model is one example. This model was developed by the USDA to assess the effect of land management decisions on water, sediment, nutrient and pesticide yields in large river basins (Arnold *et al.*, 1998). It integrates information about weather, soil properties, topography, natural vegetation, and cropping practices within a GIS interface. Sub-basins are divided into hydrologic response units (i.e. unconnected units with the same land use and soil).

Of course, such model classification systems do not capture all models. Notable exceptions include SWATCATCH (Hollis and Brown, 1996), which is a semi-empirical catchment-scale model which takes account of the distribution of soil types and land uses in the catchment and makes predictions of weekly pesticide transfers. Flow predictions are based on responses embedded in the HOST classes and pesticide concentrations are predicted based on land use-specific usage and hydrological response.

A number of attempts have been made to describe the behaviour of so-called dual-phase solute transport in porous media (i.e. including the effects of mobile and immobile regions). Many of these attempts have applied the CDE to describe the transport of solute in the soil matrix and an advection model to describe macropore flow (e.g. van Genuchten and Wierenga, 1976; Jarvis, 1994; Jarvis *et al.*, 1997). Conceptually similar attempts have also been made using “capacity” type models (e.g. Addiscott *et al.*, 1986).

2.6.1 MACRO – mono-dimensional pesticide leaching model

MACRO (Jarvis, 1994) is a one dimensional gravity-driven dual-permeability (preferential flow) model of solute transport in a layered soil profile which takes explicit account of macropore flow (see Figure 7 for an illustration). Water and solute transport are described in the soil matrix using “classical” physical equations: i.e. Richards’ equation for water flow and the CDE for solute. However, water and solute advection in soil macropores is described using a kinematic wave model. Water transfer into the matrix is treated as a first-order approximation to the water diffusion equation and is proportional to the difference between actual and saturated matrix water contents. Reverse transfer of water in excess of matrix saturation is instantaneously routed from the matrix into macropores (Köhne *et al.*, 2009a). The Freundlich adsorption isotherm is assumed for both micro- and macropores, with the total sorption partitioned into two fractions for the two domains (Köhne *et al.*, 2009b). A more detailed description of this model is reported in Chapter 6 (Paragraph 6.2).

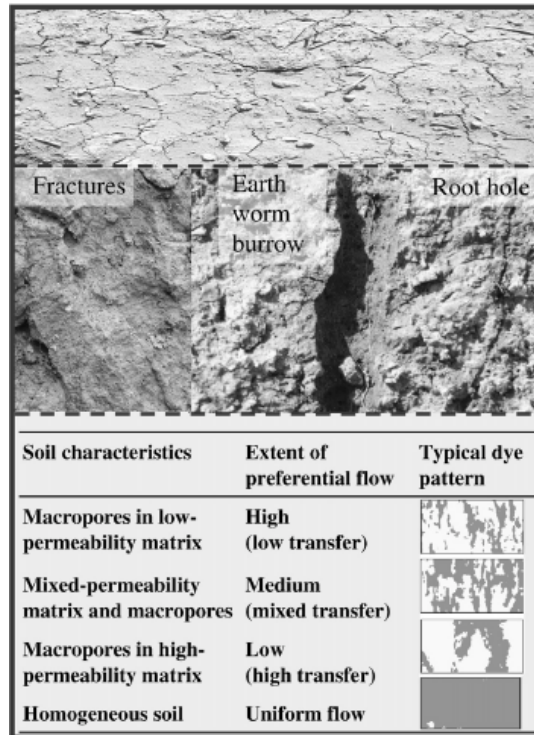


Figure 7 – Fractures and microtopography are triggers for preferential infiltration (top). Diverse structure/matrix interfaces stained by dye tracer visualise different preferential transport paths; these interfaces may affect lateral diffusion, sorption and degradation (middle). Soil matrix and macropore characteristics and resulting transport patterns; actual patterns also depend on the characteristics of rainfall and of overlaying soil horizons (simplified after Weiler and Flühler, 2004) (bottom) (Source: Köhne et al., 2009b).

Conclusions

The river catchment is a fundamental unit of landscape organisation and process integration. The catchment concept is important for understanding diffuse pollution because it links a specified land area to a given point in the channel network.

In agricultural areas the main hydrological routes for pesticides in surface waters include leaching to field drains and overland flow. These sources are difficult to handle since they are influenced by numerous interacting factors.

An enormous amount of work has been done to develop field- and catchment-scale models to describe pesticide transfer from soil to waters, but not many studies have been carried out in the field. The collection of data for real field situations is difficult because

there are many processes which affect the results. Furthermore, the weather and the farming practice are not decided by the experimenter. However, field results can provide clues about the important processes involved.

This thesis presents field investigations carried out in a heavy clay artificially drained field in the Upper Cherwell catchment (see Chapter 5), and subsequent modelling. The field work was set up in real field conditions, which are more difficult to control, but likely provide a more realistic picture of the processes. It includes the monitoring of the outflow from a main field drain, water sampling and sample analysis for key herbicides, and additional monitoring of weather and soil conditions. Chapter 6 and 7 report herbicide transfers prediction at the field and catchment scale, respectively. The one-dimensional model MACRO was evaluated against field measurements, with the aim to provide a theoretical framework to the pesticide transport issue. This work has contributed to the development of a preliminary catchment-scale model of pesticide transfers (Chapter 7).

Chapter 3 – THE UPPER CHERWELL CATCHMENT

3.1 Pesticides in the Upper Cherwell

The River Cherwell (catchment area approximately 906 km²) is a tributary of the River Thames, joining the Thames at Oxford. The upper part of the catchment (Figure 9) is used for drinking water supply to the town of Banbury via Grimsbury Reservoir. It is defined as the area draining to the reservoir abstraction point, much of which lies in Northamptonshire. The reservoir is operated by Thames Water, which regularly samples the raw water used for reservoir supply. The monitoring conducted by Thames Water has revealed that concentrations of a number of commonly used herbicides significantly exceed the DWD MAC, each year. The Thames Water monitoring has prompted significant interest in the pesticide problem in catchment from regulators such as the Environment Agency of England and Wales and from the pesticide industry via the Voluntary Initiative (VI). A key objective of all interested parties is a reduction in herbicide contamination. However, there is considerable uncertainty about the origins and principal transport pathways taken by these chemicals.

3.2 The Voluntary Initiative

Widespread monitoring has confirmed that many raw water sources in the UK contain pesticides at levels above the DWD MAC (Humphrey, 2007). Pesticides at such levels do not necessarily cause harm to ecosystems or pose risks to human health. However, if water is to be used for potable supply it will require expensive treatment to ensure that it meets EU standards. Such treatment requires high initial capital expenditure, high operating costs and large amounts of energy to operate. In addition, it cannot always cope with high peak pesticide concentrations.

In 2000 the Crop Protection Association (CPA), supported by a number of other farming organisations, proposed a programme of measures that could be used to address the environmental impacts of pesticide usage, as an alternative to the introduction by the government of a pesticide tax. This programme is called Voluntary Initiative (VI). A key VI project was the “Pilot Water Catchment Project”. The project chose six catchments with pesticide problems, with the objective of developing tools to reduce the levels of pesticides in water both in the pilot catchments and in others with similar problems.

The six pilot catchments are:

- Blythe (Staffordshire);
- Boston Park (East of Doncaster);
- Upper Cherwell (above Banbury);
- Ingbirchworth (North of Penistone South Yorkshire);
- Leam (Warwickshire);
- Ugie (Aberdeenshire).

At a national level, the VI set specific indicators and targets. These included a national objective of reducing pesticide levels in surface water by 30% but as the pilot catchment project progressed, more specific targets have been set. In the Blythe, Upper Cherwell and Leam catchments the targets were (Humphrey, 2007):

- An average 50% reduction in pesticide concentrations;
- No peak values higher than $0.5 \mu\text{g l}^{-1}$.

A number of measures have been implemented in the Cherwell catchment by the VI, including awareness raising campaigns to reduce spillages on farm yards and to avoid applications during or just before wet weather. However, despite these measures, concentrations of some herbicides still exceed the target values

http://www.foe.co.uk/resource/briefings/vol_initiative_water_poll.pdf [accessed 7th December 2009]).

3.3 The Upper Cherwell catchment

3.3.1 Catchment characteristics

At the start of this project the area of Upper Cherwell catchment was calculated to be 199 km² (Figure 9). However, the boundaries have been modified to exclude areas which drain to the Oxford Canal and do not contribute to river flow at Grimsbury reservoir. The main tributaries to the River Cherwell (Figure 8) are Byfield Brook (6.2 km), Ashby Brook (12.8 km), Culworth Brook (5.4 km), High Furlong Brook (16.8 km) and Chacombe Brook (8.9 km). Some smaller tributaries, typically less than 3 km in length, also enter the main channel within the study area (May *et al.*, 2001).



Figure 8 – River Cherwell at Edgcote (approximately 10 km Northeast of Banbury) (<http://www.geograph.org.uk/> [accessed on 12th October 2010]). © Copyright Stephen McKay and licensed for reuse under the Creative Commons Attribution-ShareAlike 2.0 Licence.

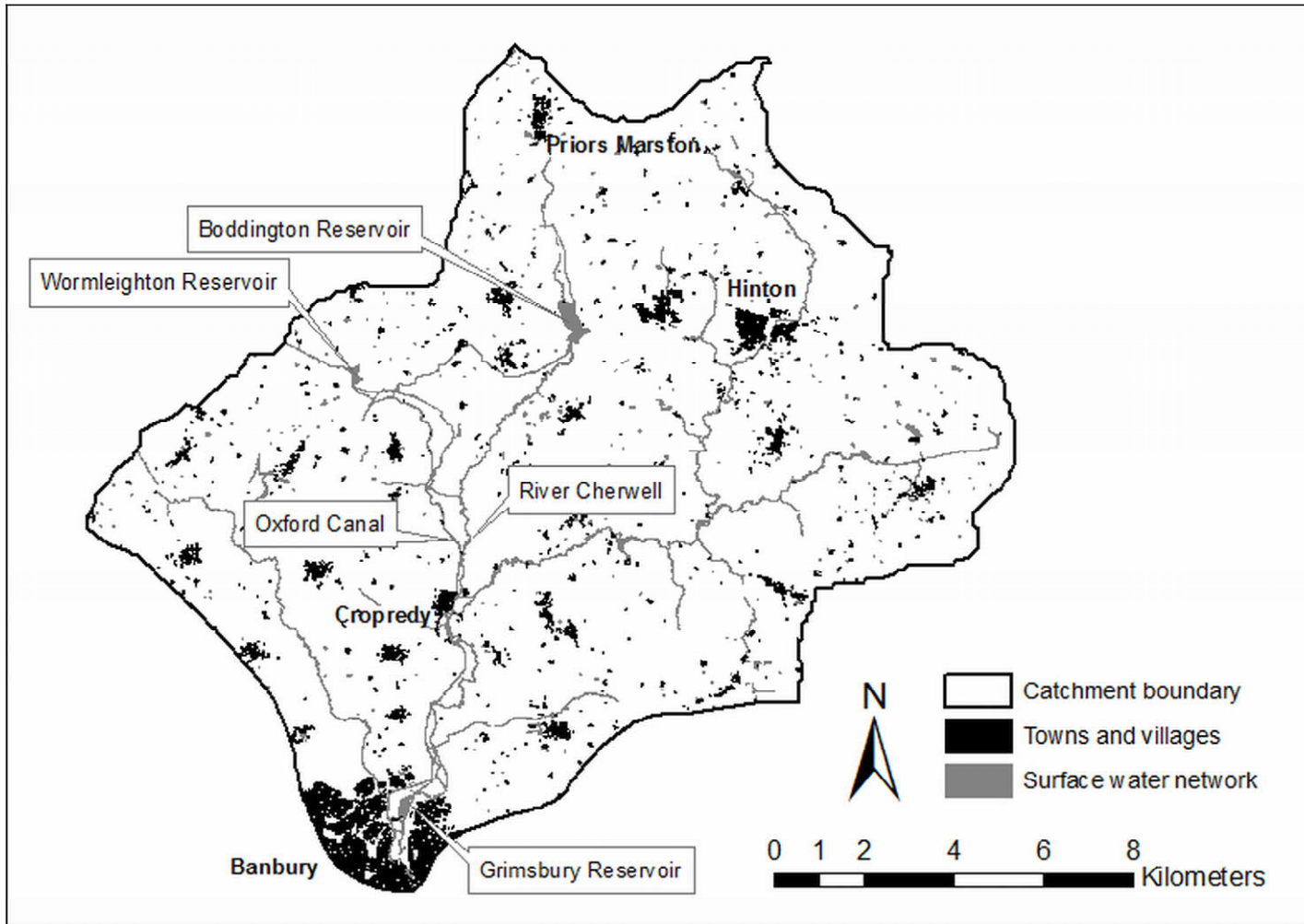


Figure 9 – Catchment of the upper River Cherwell above Banbury. Note that some areas shown here drain to the Oxford Canal and are not strictly part of the catchment draining to Grimsbury reservoir (see Appendix 2).

The predominant land use in the catchment is agriculture (about 95% of the total area is agricultural land, see map in Figure 10), dominated by arable rotations which are typically based around oilseed rape and cereals, with beans used as a break crop. Various cultivation systems are employed, including reduced and no tillage. There is also some permanent grassland, which makes up about 33% of the total area (Table 1).

Table 1 – Agricultural land use for the Local Authority ‘Cherwell’ (DEFRA statistics, 2007).

Crop	As a % of total agricultural area
Wheat	27.1
W. Barley	3.1
Oats	1.6
<i>Total Cereals</i>	<i>31.8</i>
Maize	1.4
Oilseed Rape	10.3
Potatoes	0.1
Temp. Grass	7.7
Permanent Grass	33.2

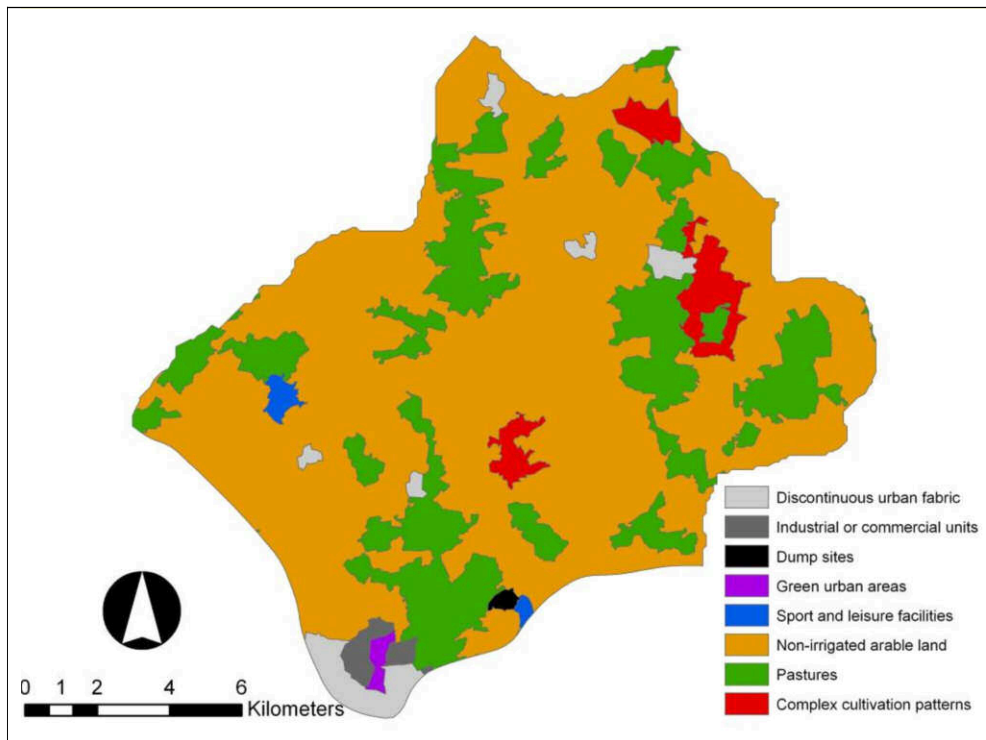
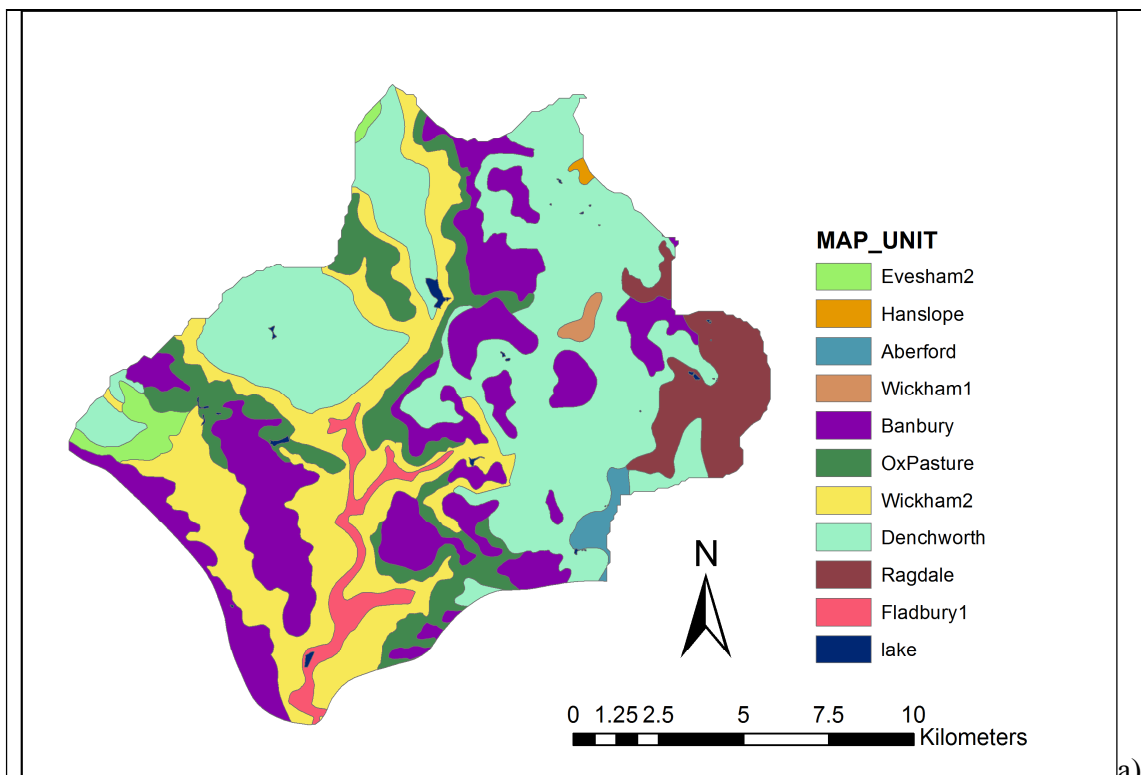


Figure 10 – Vector land use map of the Upper Cherwell catchment (Intellectual property rights IMAGE2000 of JRC, based on Landsat 7 ETM+ © ESA, distributed by Eurimage; ortho-correction EU15 © Metria, ortho-correction other countries GISAT; mosaic production GISAT).

The soils of the catchment are predominantly seasonally waterlogged clays, although there are also lighter and freely drained sandy loamy soils on ironstone (purple in Figure 11a), mainly on hill tops. Soil associations are shown in Figure 11a. A brief description of the main associations within the catchment is shown in Figure 11b. Lighter soils of the Banbury Soil Association occupy approximately 15% of the catchment, possibly 30% of the arable land [T. R. E. Thompson, personal communication]). Most of the heavier soils in agricultural use are artificially drained. Land drainage in the area is likely to date back to the 18th century and there are a wide range of drain types present (i.e. clay, plastic). The majority of the field drainage system was probably installed by the 1970s, when the Government stopped subsidising this kind of works (Land Drainage Grants terminated in the 1970s) (Thompson, 2009).



Soil Association	Brief Description
OxPasture	Fine loamy over clayey and clayey soils with slowly permeable subsoils and slight seasonal waterlogging.
Denchworth	Slowly permeable seasonally waterlogged clayey soils or loamy over clayey soils.
Wickham 2	Slowly permeable seasonally waterlogged fine loamy over clayey, fine silty over clayey and clayey soils. Small areas of slowly permeable calcareous soils on steeper slopes.
Fladbury 1	Stoneless clayey soils variably affected by groundwater, some with sandy subsoils. Occurs on flat land with some risk of flooding.
Banbury	Well drained brashy fine and coarse loamy ferruginous soils over ironstone. Some deep fine loamy over clayey soil with slowly permeable subsoils and slight seasonal waterlogging.

Figure 11 – (a) Soil map of the catchment (Source: Natmap, NSRI) and (b) description of the main soil associations (Source: Jarvis et al., 1984).

The UK HOST (Hydrology Of Soil Types: Boorman *et al.*, 1995) classes of the main soils in the Upper Cherwell are shown in Table 2. The HOST system groups all soils of the UK into 29 classes and characterises them according to dominant hydrological similarities, which complements existing soil classification schemes. The Standard Percentage Runoff (SPR) is an estimate of the average percentage of rainfall in individual events that is translated into short-term stream flow response. The higher the value of SPR, the flashier the catchment hydrology tends to be. The HOST class of the Denchworth and Wickham 2 soil associations, which predominate in the Upper Cherwell catchment, is the same.

Table 2 – HOST classification and SPR coefficients of the Upper Cherwell catchment (Source: Boorman *et al.*, 1995).

Soil Association	HOST	SPR %
OxPasture	20	60.0
Denchworth	25	49.6
Wickham 2	25	49.6
Fladbury 1	9	25.3
Banbury	2	2

The Banbury soil association has the best drainage characteristics of the soil associations listed in Table 2, although in certain areas, this association contains loamy soils over clay, which gives drainage characteristics similar to OxPasture soils (Jarvis *et al.*, 1984). The high SPR value of the other soil associations suggests that a high proportion of rainfall will be translated into runoff during storm events. This may have important implications in pesticide transfers in the catchment.

Many springs are present within the catchment and some at least still have a surface expression as wet seeps or act as sources for primary tributaries of the river network. The springs often occur along the boundary of the Banbury and Denchworth soils.

The topography of the catchment is not particularly steep. The catchment is characterised by rolling farmland some of which, especially in the northern reaches, is located on steeply sloping valleys (Clarke, 2007). The average relief is about 140 m (maximum and minimum values are respectively 92 m and 223 m).

Hydrology of the catchment

Mean annual rainfall for the Upper Cherwell is 664 mm y⁻¹ (National River Flow Archive, www.nwl.ac.uk [accessed 8th December 2009]). Monthly average rainfall varies from a minimum of 39.3 mm in June to a maximum of 76.2 mm in October (data series 1996 to 2008) (Figure 12).

The mean annual discharge at Banbury (Table 3) is 1.08 m³ s⁻¹ (www.nwl.ac.uk; Figure 13), which is equivalent to a mean annual runoff of 170.8 mm y⁻¹. It should be noted that flows are measured downstream Grimsbury Reservoir (see Paragraph 5.1.2).

Table 3 – Banbury gauging station characteristics (Source: www.nwl.ac.uk [accessed 8th December 2009]).

Grid Reference:	42 (SP) 458 411
Operator:	EA
Local number:	1420
Catchment Area:	199.4 km ²
Level of Station:	88.7 mOD
Max. Altitude:	222.0 mOD
Mean flow:	1.08 m ³ s ⁻¹
95% exceedance (Q95):	0.016 m ³ s ⁻¹
10% exceedance (Q10):	2.84 m ³ s ⁻¹
61-90 Av. Ann. Rainfall:	664 mm

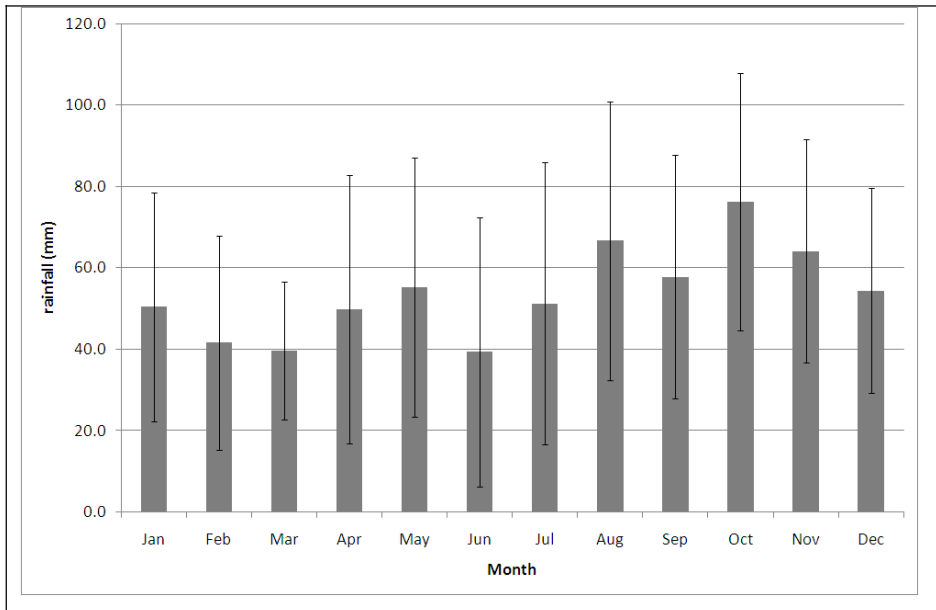


Figure 12 – Monthly average rainfall from 1996 to 2008, Grimsbury gauging station (Error bars show the mean \pm one standard deviation) (Source: EA [Thames West]).

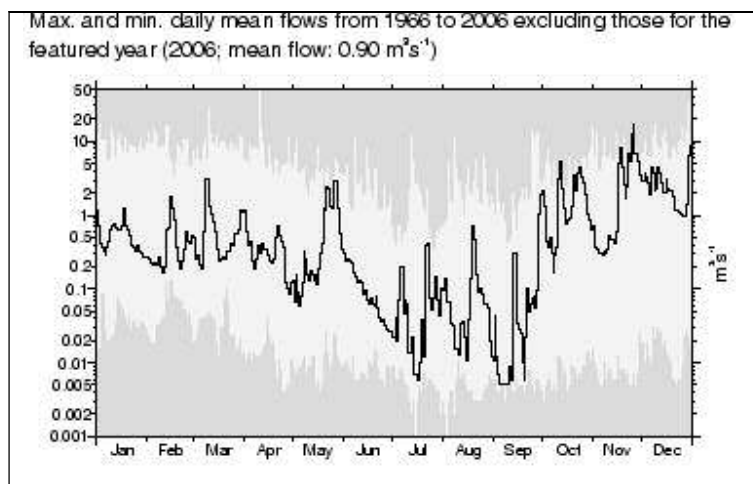


Figure 13 – Discharge from 1966 to 2006 at Banbury (Source: www.nwl.ac.uk [accessed 8th December 2009]).

Figure 14 shows the Integrated River Monitoring Map of the catchment (Thames Water, personal communication).

Grimsbury and Bodicote Intakes

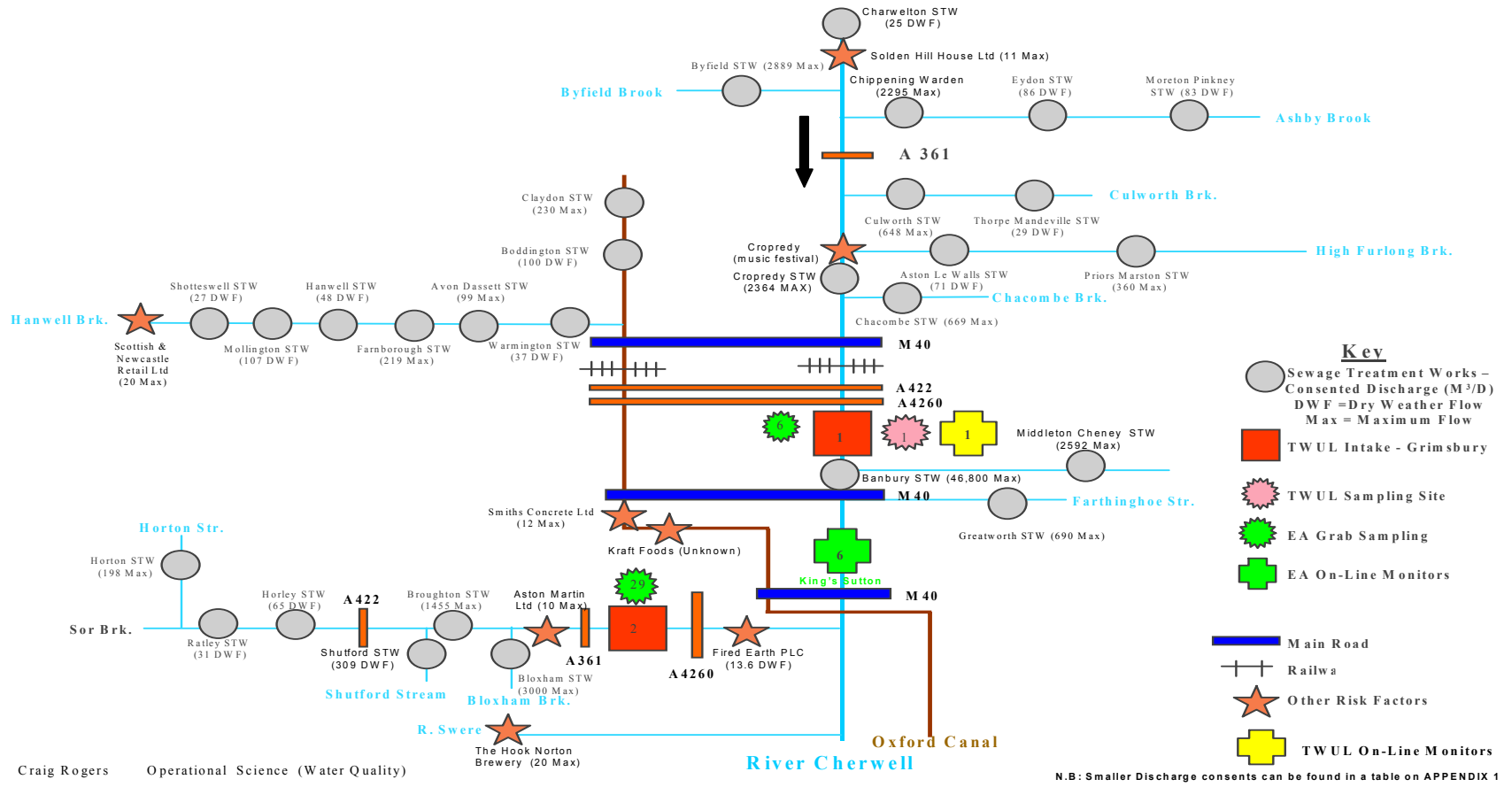


Figure 14 – Integrated River Monitoring Map of the Upper Cherwell catchment (Source: Thames Water, personal communication). Flow direction is shown (black arrow).

The catchment regime is rather responsive but the large upstream abstraction (Grimsbury reservoir) can appreciably distort the low flow hydrograph (www.nwl.ac.uk). The hydrology of the catchment is also affected by:

- Eleven sewage treatment works that discharge upstream of Banbury;
- Offtake from the river to the Oxford Canal at Cropredy (Figure 15);
- Offtake from Boddington Reservoir to the Oxford Canal;
- Offtake from Wormleighton Reservoir to the Oxford Canal.

Note that the Sor Brook enters the Cherwell downstream of the reservoir and should be excluded from the catchment for the purposes of this project. Water is occasionally used to feed Grimsbury reservoir, but not often (Thames Water, direct communication).

Although a catchment boundary was supplied by the EA at the start of the project, it was important to ascertain the extent to which the above artificial influences affected the importance of different areas for potential pesticide transfer to the outlet. A digital channel network was derived by redigitising the Ordnance Survey raster map (see Appendix 1). In addition, investigations were conducted to evaluate the influence of British Waterways and Thames Water operations on the effective hydrology of the catchment. This analysis suggested that four significant areas should be excluded from the catchment draining to the Thames Water abstraction point at Banbury. These include the catchments of Boddington and Wormleighton Reservoirs, the catchment of Hanwell Brook and an area close to Cropredy, which all feed the Oxford Canal and do not influence water and pesticide transfers in the main river channel. Details are documented in Appendix 2. The area of the modified catchment is 129 km².

Grimsbury Reservoir has a total volume of 234,154 m³, and a usable volume of 187,323 m³ (20% of the total volume is never used because of the high ammonia levels at the bottom of the reservoir). The reservoir provides 23.4 days supply (based on an average output of 8 ML d⁻¹) (Thames Water, personal communication).

Records of water transfer from the river Cherwell at Cropredy to the Oxford Canal were supplied by British Waterways for the period January 2004 to May 2009. The average offtake was 8.9 l s^{-1} . This compares with an average river discharge of 800 l s^{-1} . The average offtake in August was 20 l s^{-1} , when river discharge is usually low (typically 240 l s^{-1}), implies that the offtake can represent up to 10% of streamflow. However, since pesticides are mainly transferred between autumn and late spring the Cropredy offtake was assumed not to influence the magnitude and temporal pattern of herbicide concentrations at the catchment outlet.



Figure 15 – Map of the River Cherwell and the Oxford Canal between Banbury and Cropredy. The insets show Cropredy and the Cropredy Lock (GEOProjects, 2004).

3.3.2 Pesticide usage in the catchment

A number of active ingredients have been monitored in the Cherwell at Grimsbury Reservoir for several years. Concentrations of some herbicides exceed the DWD MAC (98/83/EC) at least once a year, but some more frequently. Data were available for this project for atrazine, carbetamide, propyzamide, simazine, mecoprop-p, isoproturon (IPU), 2-methyl-4-chlorophenoxyacetic acid (MCPA) and chlortoluron for the period November 1995-November 2009.

In the UK, recent attention has been directed towards two herbicides used mainly for black-grass control in winter oilseed rape production: carbetamide and propyzamide. These herbicides are now frequently measured in monitored surface water catchments draining arable land with high seasonal peaks. Maximum annual concentrations of propyzamide and carbetamide measured in the Upper Cherwell at Banbury between March 1996 and the end of 2008 for propyzamide and between January 2002 and the end of 2008 for carbetamide are shown in Figure 16. The data suggest that peak concentrations have increased over the monitored period. Peak concentrations of both active ingredients have exceeded $4 \mu\text{g l}^{-1}$ in the last two years. It should be noted though that in recent years the monitoring frequency (and therefore the chance of detecting high concentrations) has increased.

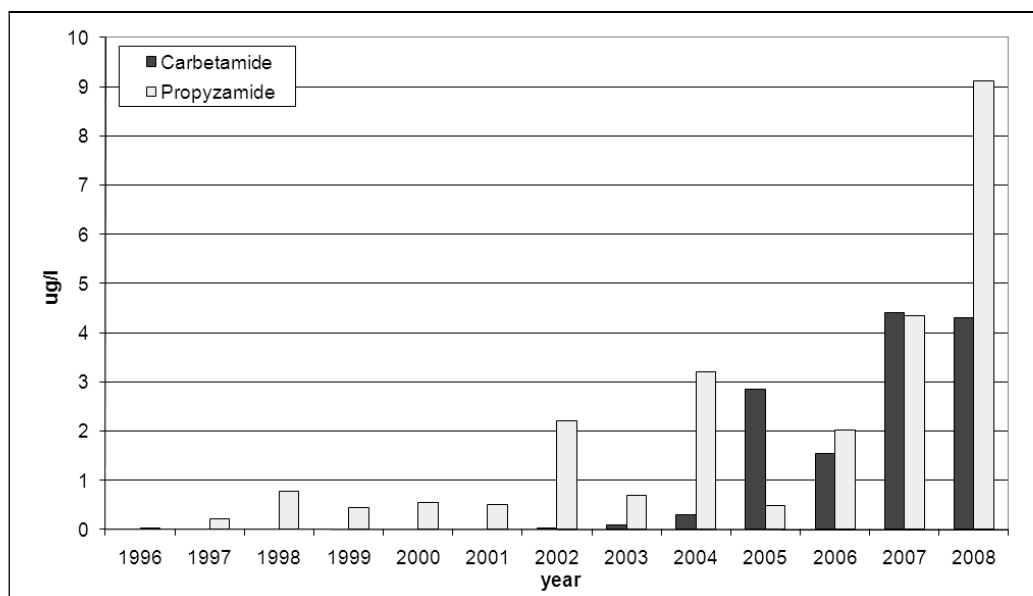


Figure 16 – Maximum concentrations of carbetamide and propyzamide observed in the Upper Cherwell at Banbury between 1996 and 2008.

Carbetamide (predominantly used in the product Crawler[®]) and propyzamide (predominantly used in the product Kerb[®]) have very different leaching potential and physico-chemical properties (Tables 4-5). Label guidance for both herbicides allows only one application per crop.

Table 4 – Key properties of propyzamide and carbetamide pertinent to the potential for leaching loss (www.eu-footprint.org [accessed 7th December 2009]). DT₅₀ is the median dissipation time, K_{OC} is the organic carbon to water partition coefficient and GUS is the Groundwater Ubiquity Score (Gustafson, 1989).

	Propyzamide	Carbetamide
DT₅₀ [days]	56 (moderate)	8 (non persistent)
K_{OC} [l kg⁻¹]	840 (slight)	89 (moderate)
Leachability (GUS index)	1.83 (transition state)	2.87 (high)

Table 5 – Physico-chemical properties of propyzamide and carbetamide (www.eu-footprint.org [accessed 7th December 2009]).

		Propyzamide	Carbetamide
Solubility - In water at 20°C (mg l⁻¹)		9	3300
Solubility - In organic solvents at 20°C (mg l⁻¹) (acetone)		139000	250000
Melting Point (°C)		156	110
Flashpoint (°C)		not highly inflammable	not highly inflammable
Octanol-water partition coefficient at pH 7, 20°C	P:	2.00 X 10 ⁰³	4.68 X 10 ⁰¹
	Log P:	3.3	1.67
Bulk density (g ml⁻¹)/Specific gravity		1.33	1.18
Dissociation constant (pKa) at 25°C		Not applicable	11.3
Vapour pressure at 25°C (mPa)		0.0267	0.0003
Henry's law constant at 25°C (Pa m³ mol⁻¹)		7.60 X 10 ⁻⁰⁴	1.93 X 10 ⁻⁰⁸

Propyzamide is less water-soluble and more lipophilic than carbetamide, suggesting that it is less mobile in soil. However, it has a significantly longer half life than carbetamide which provides better residual herbicidal activity, especially in mild and wet autumns. Kerb[®], the most common propyzamide product, is, therefore, usually applied in autumn. Research has shown that on average over a number of years and different seasons propyzamide is best applied in the last 2 weeks of November (Jon Bellamy, personal communication, March 2010). This also avoids the risk of residual activity carry over to following crops. For this reason it can not be used after the 1st of February (label cut off date). The maximum label application rate for propyzamide in Kerb[®] is 840 g ha⁻¹.

Carbetamide is, in theory, much more rapidly degraded in soil but it is also more mobile, which ensures a quicker and better distribution in the soil but facilitates leaching. Crawler[®] (granular carbetamide) is generally used between mid-October and February but tends to be used later on in the season (February) compared with Kerb[®], when weeds are deeper rooted and soil conditions improved (Jon Bellamy, personal communication, October 2009). Crawler has no label cut off date, due to its low persistence. The maximum label application rate for carbetamide in Crawler[®] is 2100 g ha⁻¹.

Unfortunately, more detailed and accurate information was not available on actual usage rates or application timing of carbetamide and propyzamide in the catchment. This is a major limitation for developing an understanding of the processes contributing their transfer in the catchment.

Chapter 4 – ANALYSIS OF EXISTING DATA

A preliminary analysis of historical data on herbicide concentrations was carried out to provide a framework to herbicide issues in the catchment. Existing data on herbicide concentrations in the River Cherwell were analysed to investigate the extent of any seasonality and to explore possible relationships between concentration and hydrological processes. The aim of this analysis was to gain a better understanding which could help plan field investigations and modelling.

4.1 Data sources

4.1.1 Rainfall data

Rainfall data (daily totals derived from a tipping-bucket gauge) were provided by the Environment Agency of England and Wales (Thames West) for the period January 1996 to March 2010 at Banbury. Weather station details are shown in Table 6.

Table 6 – Grimsbury weather station location and details.

Station ID	257039TP
Name	Grimsbury R31
NGR	SP4576041797
Region	Thames

4.1.2 Discharge data

Mean daily river discharge data for the same period were also provided by the Environment Agency of England and Wales (Thames West) for the outlet of the catchment, downstream of Grimsbury reservoir. Station details are reported in Table 7. It should be stressed that gauged flows are likely an underestimate of the flows in the river, since the reservoir is an abstraction point for drinking water supply (see Paragraph 3.3.1).

Table 7 – Banbury gauging station details.

Station ID	1420TH
Name	BANBURY G.STN
NGR	SP45844108
Region	Thames

4.1.3 Herbicide concentration data

Herbicide concentrations are regularly monitored at the catchment outlet both in the river and in the reservoir. The herbicide concentration data used in this project were monitored in the river at the reservoir abstraction point. Two different data sets were analysed:

- Grab sample data: Grab sample data for the following eight herbicides at the catchment outlet were available: atrazine, IPU, CTU, mecoprop-p, MCPA, carbetamide, propyzamide and simazine. Data for different herbicides were available for different periods. Concentrations were determined in the laboratory on grab samples by Thames Water.
- SAMOS data: Data were also available for limited periods from Thames Water's "on-line" SAMOS (System for the Automated Monitoring of Organic Substances) located on the River Cherwell just downstream of the intake to

Grimsbury Reservoir. Ten herbicides have been monitored (atrazine, simazine, carbetamide, propyzamide, isoproturon, MCPA, MCPP, 2,4-dichlorophenoxyacetic acid, 2,4,5-trichlorophenoxyacetic acid, chlortoluron). The SAMOS (e.g. Lacorte *et al.*, 1998), consists of preconcentrating water samples on solid-phase extraction (SPE) precolumns, which are available in C₁₈ or polymeric materials (Brinkman, 1994). Using this technique, the percolation of 100 ml of water is enough to efficiently trap compounds of diverse polarities, including pesticides (Lacorte and Barceló, 1994). Automation of SPE is possible both with gas chromatograph (GC) (Kwakman *et al.*, 1992) or liquid chromatography (LC) (Slobodnik *et al.*, 1993). This analysis is considered to be less reliable than laboratory analysis, but it allows daily concentrations to be monitored. This is very useful in the context of drinking water abstractions but also provides invaluable insights into temporal changes in pesticide concentrations at the catchment-scale.

Details of carbetamide and propyzamide concentration data sets are reported in Table 8.

Table 8 – Available carbetamide and propyzamide concentration data sets examined in this project.

	Grab sample data (laboratory analysis)	On line SAMOS data
Carbetamide	Jan 2002 – May 2008	Jan 2007 – September 2010
Propyzamide	Nov 1995 – May 2008	Jan 2007 – September 2010

4.2 Methodology

4.2.1 Statistical analysis of historical data (1996 – 2008)

Statistical analysis was carried out on grab-sample herbicide concentration data for the period March 1996 to May 2008, in an attempt to better-understand historical herbicide contamination in the catchment. SAMOS data were not analysed statistically because a much shorter time series was available.

First, some simple descriptive statistics were calculated in order to summarise the extent and timing of the herbicide issues in the Upper Cherwell. Secondly, the degree of correlation between herbicide concentration and rainfall and river discharge was investigated. Correlation coefficients were determined between concentration and concurrent rainfall and discharge and between concentration and temporally lagged rainfall and discharge values to determine whether concentration peaks could have been triggered by storm events occurring on the same day or earlier (lag 1 to 10 days). Pearson product moment correlation matrices were generated using STATISTICA (StatSoft Inc, Tulsa, OK, USA) for each herbicide. All values reported at or less than the analytical limit of detection (LOD) were removed prior to performing the correlation analysis. Since the concentration distribution was log-normal, a logarithmic transformation was used prior to calculating the coefficients.

For those correlations which were statistically significant, linear regression models were generated in order to provide additional information about the relationship.

The relationship between log-transformed concentration (y) and discharge (x) was described by:

$$y = \beta_0 + \beta_1 x + \varepsilon \quad (3)$$

where β_0 is the y -intercept, β_1 is the slope of the linear fit and ε is the random error.

Although models are usually used to predict the independent variable behaviour, in this case they were used only to investigate whether any correlation existed and whether

it was significant. As a matter of fact it is not possible to predict herbicide concentrations, since not only do they depend on discharge or rainfall, but also on other variables (i.e. application timing and rates), which are unknown.

It is important to stress that the concentration data used for this analysis are not daily. This means that it is likely that some concentration peaks have not been detected. Moreover the number of records is not constant for each month.

4.2.2 Qualitative analysis of daily carbetamide and propyzamide concentrations in 2009 measured using SAMOS

Daily concentration data collated during 2009 using Thames Water's SAMOS was analysed qualitatively together with patterns of rainfall, discharge and soil moisture content in the catchment. Temporal patterns of relevant data were plotted and observations made about apparent relationships and possible drivers.

4.3 Results

4.3.1 Statistical analysis of historical data (1996-2008)

The statistical analysis of existing data focused on carbetamide and propyzamide, which have become a key issue in the Upper Cherwell catchment in recent years.

The number of days in which measured concentrations exceeded the DWD MAC shows that the catchment has got a long history of herbicide problem, with a peak in 2006 and 2007 (Figure 17). Considering the values exceeding the MAC over the total measurements (Figure 18), carbetamide is characterised by an increasing trend from 2004 to 2007 (passing from 8% to 17.7% of measurements above the MAC); propyzamide is more variable, but an average of 20.8% of the observed values exceeded $0.1 \mu\text{g l}^{-1}$

between 1996 and 2008. Table 9 shows maximum concentrations measured every year for both carbetamide and propyzamide.

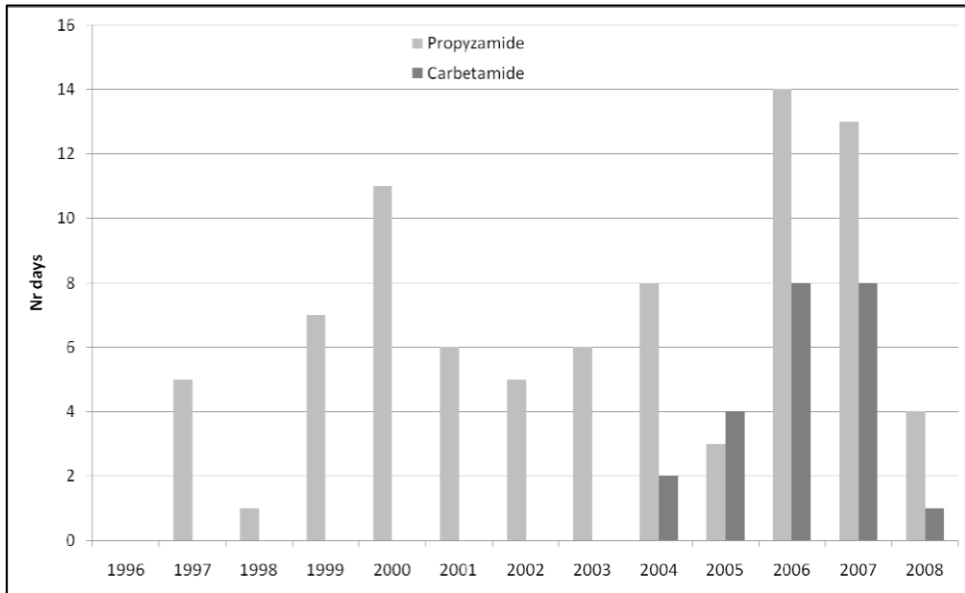


Figure 17 – Number of days with observed herbicide concentration above the MAC.

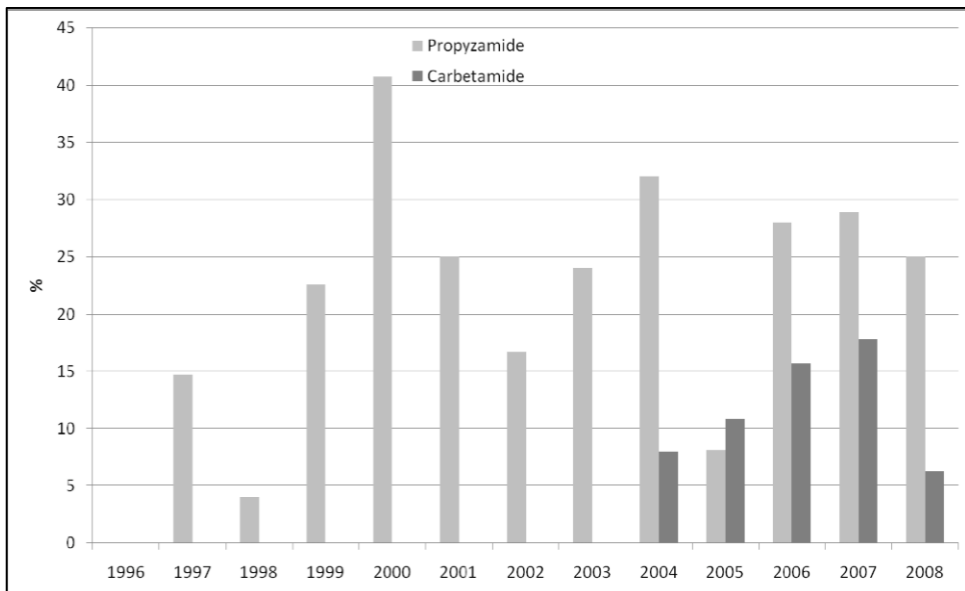


Figure 18 – Fraction of measurements above the MAC over the total number of concentration measurements (%).

Table 9 – Maximum concentrations measured every year (1996-2008), for carbetamide and propyzamide.

Year	Carbetamide – max concentration ($\mu\text{g l}^{-1}$)	Propyzamide – max concentration ($\mu\text{g l}^{-1}$)
1996		0.04
1997		0.21
1998		0.77
1999		0.44
2000		0.55
2001		0.51
2002	0.02	2.20
2003	0.08	0.70
2004	0.31	3.20
2005	2.85	0.48
2006	1.55	2.03
2007	4.40	4.35
2008	0.74	1.33

Average monthly concentrations of carbetamide and propyzamide monitored at the catchment outlet are presented in Figures 19 and 20, respectively. There appear to be clear seasonal patterns to the concentration of each herbicide. Concentrations of both herbicides peak in the winter period, which is consistent with their typical usage for black grass control in winter oil seed rape and beans. The peak mean monthly concentration is similar for each chemical (approximately $0.6 \mu\text{g l}^{-1}$), although the timing of peak monthly concentration differs. Average carbetamide concentrations are highest in February and March (although the concentration is also very variable in these months). For propyzamide, concentrations are highest in November and December. Again, concentrations are most variable in the month with the highest mean concentration. These differences in timing seem to reflect differences in the relative application timing of each chemical, to some extent, although information about usage in the catchment is not precise so it is not possible to be unambiguous. Propyzamide use is restricted to the period prior to the beginning of February (label cut-off) due to the higher potential for residual carry-over to the following crop. Differences in chemical properties may also affect their environmental behaviour. Propyzamide is more hydrophobic (and thus less mobile in the dissolved phase) than carbetamide but it is also more persistent. This

implies that transport to water could be triggered several weeks or even months after application. Carbetamide is fairly water-soluble but should rapidly degrade (based on its DT₅₀). This would imply that any carbetamide losses from soil should occur relatively soon after application.

Lack of information about usage is one of the most fundamental limitations of the data set of the Upper Cherwell because usage is likely to be a key driver for loss. Without usage data it is difficult to establish clear relationships between other variables.

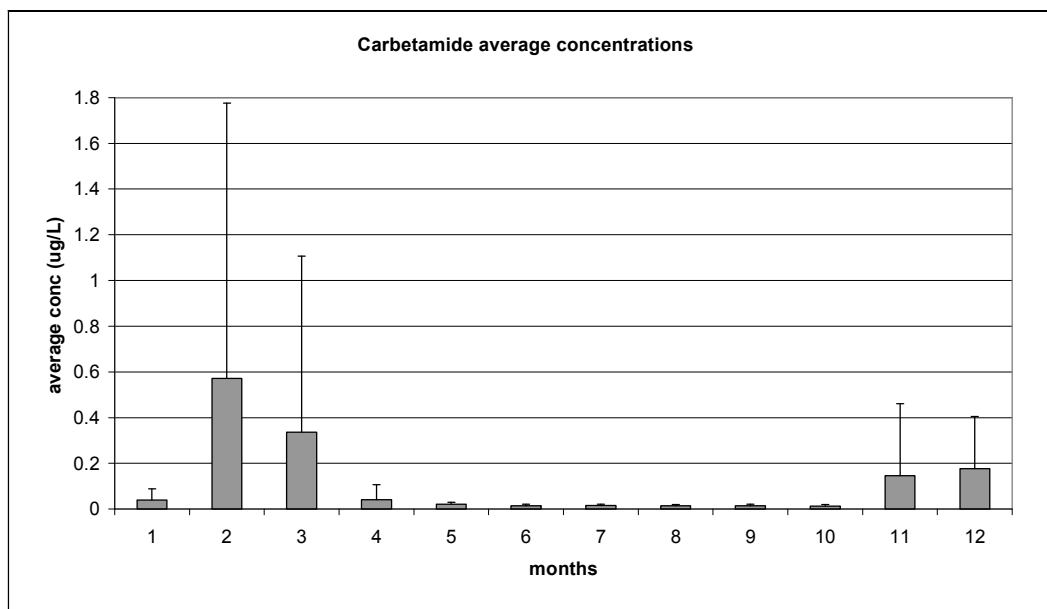


Figure 19 - Average concentration of carbetamide for each month of the year over the period 1996-2008. Error bars show the mean \pm one standard deviation.

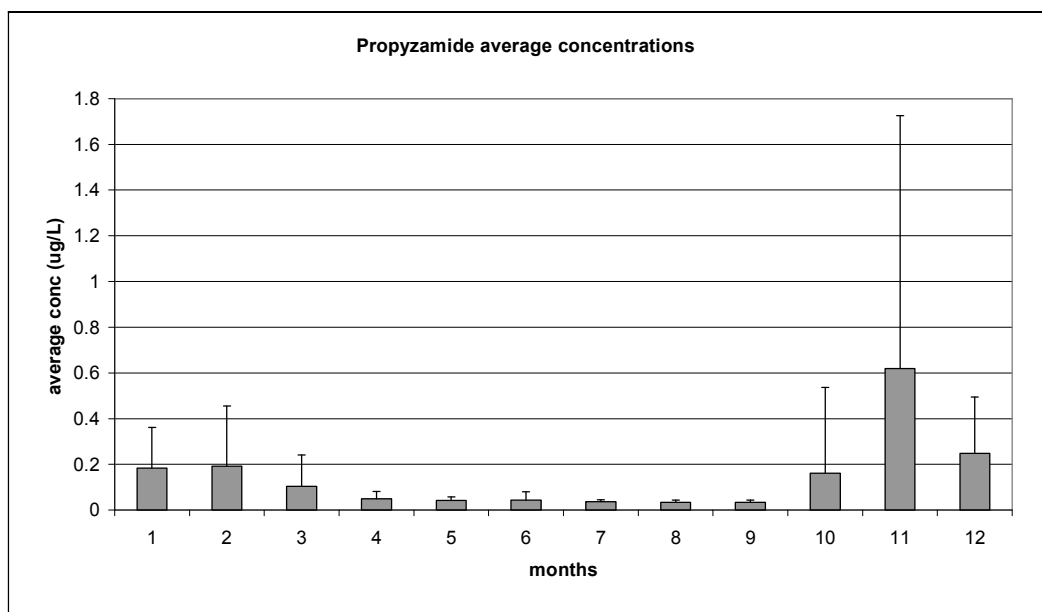


Figure 20 - Average concentration of propyzamide for each month of the year over the period 1996-2008. Error bars show the mean \pm one standard deviation.

The results of the correlation analysis show that herbicide concentrations are more significantly correlated with discharge than with precipitation. The highest correlation coefficients were derived between concentration and discharge lagged by 1 to 2 days for propyzamide (significant correlations were obtained for lags 0 to 5 days). For carbetamide the most significant correlation was obtained between concentration and discharge lagged by three days (significant correlations were obtained for lags 0 to 6 days). The relationships between the correlation coefficient and the temporal lag for river discharge and precipitation are shown in Figures 21 and 22 for carbetamide and propyzamide, respectively.

The best linear regression model is the one for carbetamide with a lag of three days. The slope of the linear regression (*beta*) was high and significant (0.604) and the adjusted R^2 value was 0.35. This means that the model based on discharge explains the 35% of the variation in concentration. A satisfactory statistical model was also obtained for propyzamide. The slope of the relationship was significant (> 0.4) for models constructed using discharge with lags of one and two days. The adjusted R^2 suggest that these models explain 18% and 16%, of the variance in concentration, respectively.

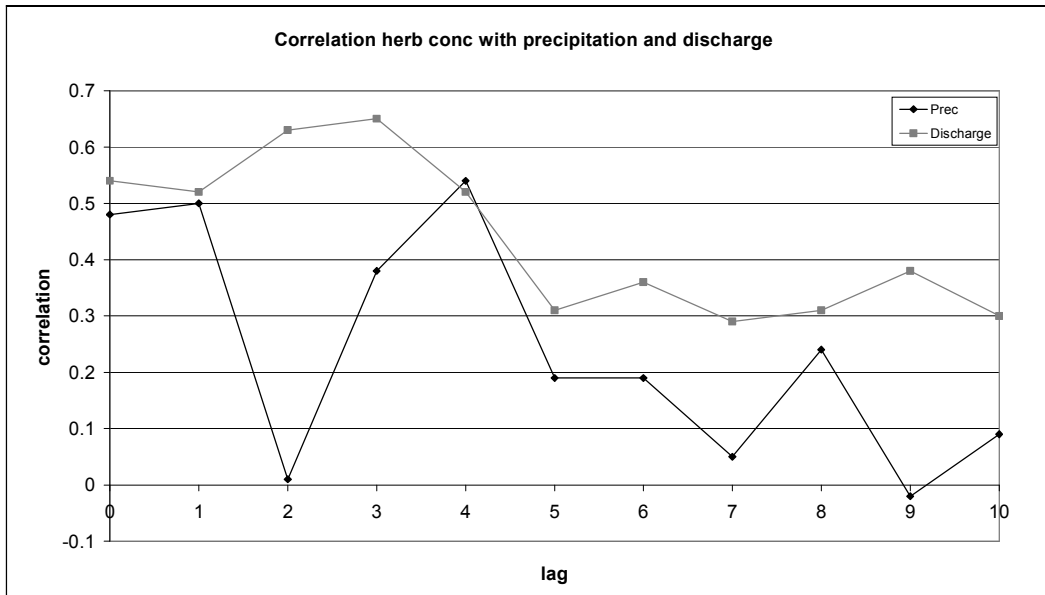


Figure 21 – Correlation coefficients between carbetamide concentration and precipitation and discharge for different lag periods (days).

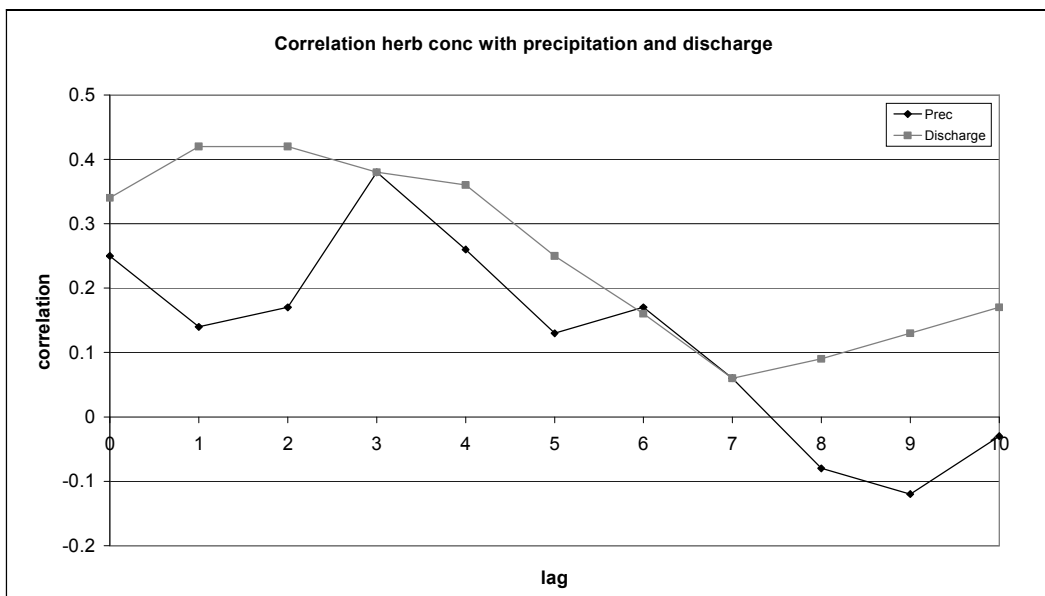


Figure 22 – Correlation coefficients between propyzamide concentration and precipitation and discharge for different lags (days).

Although limited by the low temporal frequency of sampling, these results suggest that there is some delay in the response of herbicide concentrations at the catchment outlet and the storm events (rainfall and stream discharge) which probably trigger herbicide movement between the soil and the river network. The delays of a few days implied by the correlation analysis are longer than the delays that might be expected for transport in overland flow. Overland flow is usually connected to intense events with high rainfall. Consequently one might expect that if the main transport pathway were overland flow, the most significant correlation would be between herbicide concentration and precipitation. Moreover, overland flow responds relatively quickly to rainfall. The combination of short overland flow travel times on the hillslopes of the catchment and short solute travel times in the channel network, particularly during storm events are likely to result in overall travel times of the order of hours which would give highest correlation coefficients between concentration and precipitation and or discharge with lags of 0-1 days. However, it is difficult to be conclusive without good information on the amount and timing of applications and without more frequent sampling. It is possible that some peak concentrations occurring concurrently with or shortly after rainfall or flow peaks were not captured by the sampling programme considered.

There are a number of possible explanations for the differences in the most significant lag between concentration and discharge for propyzamide and carbetamide, including different chemical properties and the prevailing timing of applications. Propyzamide is mainly applied in the autumn, when soils are wetting up, but have often not yet reached their field capacity (FC). At this time of year, macropores which have developed in the summer period (i.e. soil cracks) are often still open and allow more rapid movement of solutes and particle-associated materials from the near-surface soil horizons towards field drains. Carbetamide is usually applied later, in mid-winter, when soils are wetter (at or above FC) and when drains are regularly flowing. Under these conditions, hydraulic conductivity of the soil matrix will be probably higher but macroporosity is reduced so the movement of solutes to the drainage system could be slower.

The differences between carbetamide and propyzamide properties may explain different transport mechanisms, but not specific pathways. Carbetamide has the highest GUS index (suggesting high leachability) due to its low K_{OC} (organic carbon to water partition coefficient) and low DT_{50} (dissipation half life in soil). Propyzamide is less mobile (higher K_{OC} , longer DT_{50}). It can, therefore, be hypothesised that carbetamide is more likely to be transported in solution to field drains whereas propyzamide may be more likely to be transported in sorbed form, via macropores.

4.3.2 Analysis of carbetamide and propyzamide peaks in 2009 using the SAMOS data

Two main contamination “events” from 2009 were analysed in detail using data supplied by Thames Water from the SAMOS station at Grimsbury reservoir. One event occurred in March 2009 (subsequently referred to as the spring event) and the other in November 2009 (subsequently referred to as the autumn event).

As far as the spring event is concerned (Figure 23), there are three obvious peaks in carbetamide concentration and one peak in propyzamide concentration. The propyzamide peak (which occurred on the 5th of March) is smaller but is coincident with the first peak in carbetamide ($5.3 \mu\text{g l}^{-1}$) and occurred about two days after the peak daily rainfall of 13 mm (3rd of March) and about one day after the peak in discharge. This delayed response is approximately consistent with the results of the statistical analysis that was carried out on the historical data series. For carbetamide a second (minor) peak is apparent on the 8th of March which appears to be associated with a very minor increase in river discharge, followed by a much larger peak of $5.9 \mu\text{g l}^{-1}$ on the 13th of March (8 days after the first peak). This peak appears 10 days after peak precipitation and is not associated with a significant increase in river discharge.

A possible interpretation of these observations is as follows. The short DT_{50} of carbetamide would suggest that the peaks observed in the spring event are the consequence of relatively recent application. The propyzamide peak, on the other hand,

may have resulted from much earlier applications (much longer DT_{50}). It tends to be applied in late autumn/early winter and only a limited amount is likely to be available for leaching in spring. This is consistent with knowledge that carbetamide is more often applied in springtime compared to propyzamide (which has a cut off latest use date on 1st of February). The first carbetamide peak, occurred just after a significant (13.4 mm) rainstorm (3rd of March), which, in turn, triggered a 5.56 mm discharge peak the following day. The second peak may have been due to delayed transport in the unsaturated or saturated zone in some parts of the catchment or may simply have been due to spatially limited rainfall which was not captured by the rain gauge used in the analysis. Rainfall recorded between 7th and 10th March (5 mm) appeared to trigger more significant movement of carbetamide to the river network, although the consequent increase in discharge is limited. The limited discharge response may be due to the limited spatial extent of this rainfall. Propyzamide concentrations appear not to respond to this event.

It should be noted that there appeared to be very little evidence for any significant overland flow in the catchment over the spring period. A number of visits were made to different parts of the catchment during this period and very few rills or deposition fans were identified.

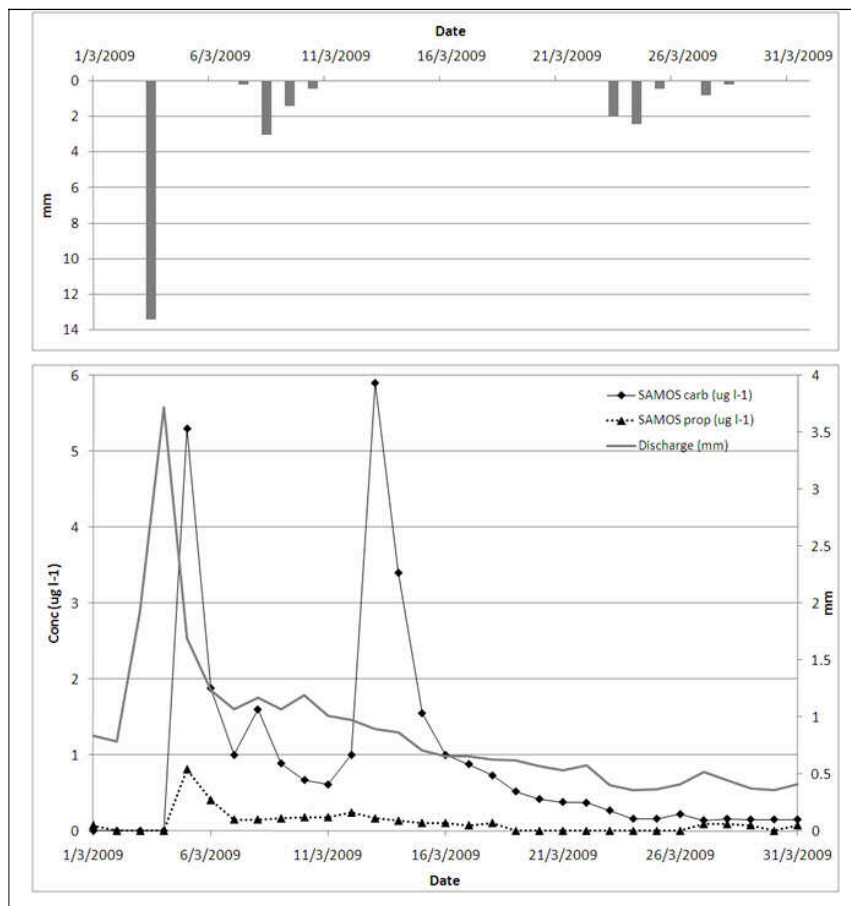


Figure 23 – Daily rainfall totals measured at Grimsbury (columns), river discharge in the Cherwell at Banbury (grey line), and carbetamide (carb) and propyzamide (prop) concentrations measured using SAMOS (black solid and dashed lines) at the catchment outlet in March 2009.

The autumn event (Figure 24) also shows a quick rise in carbetamide and propyzamide concentrations following the rainfall which fell between the 10th and the 16th of November. From local knowledge and observations we know that propyzamide was applied approximately one week before on one of the farms in the north of the catchment and it is likely that carbetamide and propyzamide were applied on other farms around this time too. The peak carbetamide concentration ($7.7 \mu\text{g l}^{-1}$) was observed on the same day as the peak discharge (14th November), which was delayed about one day after peak rainfall (10.6 mm day^{-1}). The peak propyzamide concentration was observed

on the 15th of November, after which concentrations decreased pseudo-exponentially. Such a recession in concentrations is consistent with the tail of a solute breakthrough curve and suggests that propyzamide is transported to the catchment outlet via a range of pathways with different travel times. This is further discussed in detail later in the thesis.

A second peak in carbetamide concentration was observed on the 17th of November, following some rainfall on the 16th. However, this rainfall appears not to have resulted in a significant discharge response and the hydrograph is in recession during this period. This would suggest that this rainfall was not widespread over the catchment, but may have resulted in an additional carbetamide pulse. There is no knowledge of applications in the catchment in this period.

Rainfall and associated discharge response were observed in the catchment in the period following the 20th of November. However, there was no apparent increase in concentrations of either carbetamide or propyzamide in this period, suggesting an exhaustion of sources for both chemicals. Exhaustion of carbetamide sources would be consistent with its low DT_{50} . The longer DT_{50} of propyzamide may be responsible for the minor increase in propyzamide concentration on the 30th November. Of course, this may also be simply a reflection of additional applications in the catchment in the preceding period.

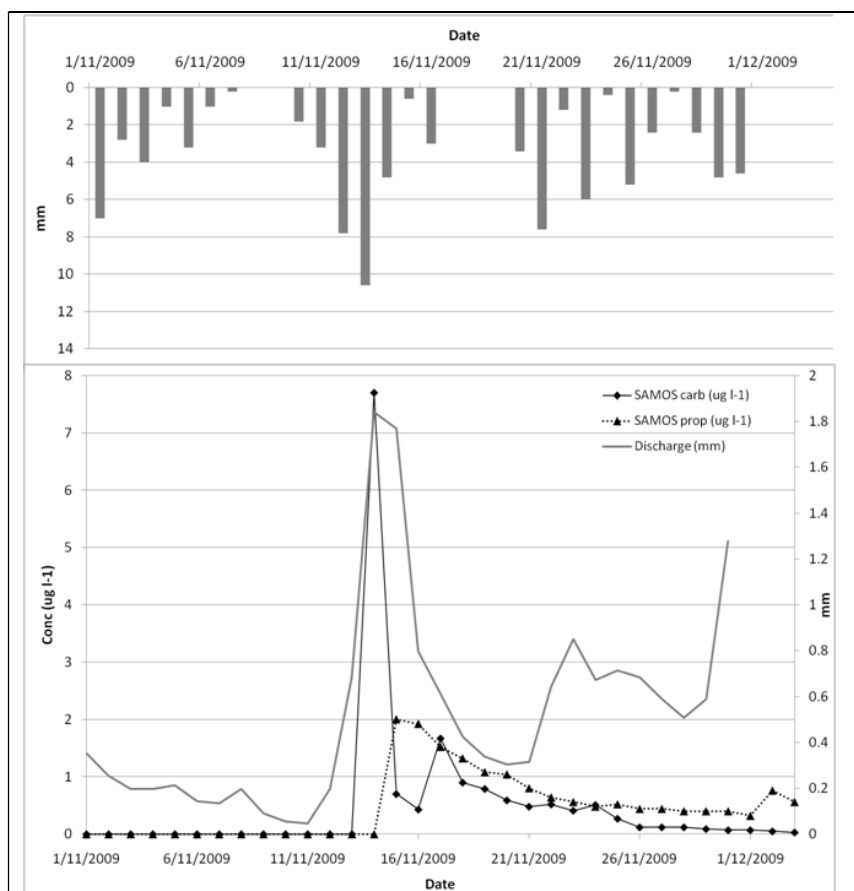


Figure 24 - Daily rainfall totals measured at Grimsbury (columns), river discharge in the Cherwell at Banbury (grey line), and carbetamide (carb) and propyzamide (prop) concentrations measured using SAMOS (black solid and dashed lines) at the catchment outlet in November 2009.

In both the spring and the autumn events, peak concentrations of carbetamide are generally much higher than concentrations of propyzamide. This may reflect the higher mobility of carbetamide compared with propyzamide. It might also reflect the relative usage of each chemical across the catchment but this is unlikely, as at a national scale herbicide usage on OSR is split in 77% and 23% in favour of propyzamide (FERA, 2008). The slope of the concentration “recession curve” for propyzamide also appears to be shallower.

In all cases, it must be remembered that the temporal concentration patterns observed in the river channel at Banbury result from spatially and temporally discrete applications throughout the contributing catchment. Many of these applications do not occur on the same day. Similarly the reader is reminded that rainfall is also spatially variable. Some concentration peaks at the catchment outlet may result from rainfall not captured in the rain gauge used in the analysis.

Conclusions

The analysis of historical data suggests that herbicide concentrations are significantly correlated to discharge and that their response appears to be delayed. Possible explanations for the differences in the most significant lag between concentration and discharge for propyzamide and carbetamide include different chemical properties (i.e. mobility and persistency) and the prevailing timing of applications. Such a delay would suggest that herbicide transport to the river network occurs via relatively slow pathways.

The next three chapters will present the work which was done in order to investigate which pathways play a key role in herbicide transfers in the Upper Cherwell. The methodology includes monitoring activities in a clay soil field, and both field- and catchment-scale modelling.

Chapter 5 – FIELD INVESTIGATIONS

This chapter presents field investigations which were carried out in the Upper Cherwell catchment over the period March 2009 – April 2010. Field work included environmental variable monitoring and water sampling:

- The most intensive monitoring was conducted in an arable field on the Denchworth soil in the North of the catchment (described in Paragraph 5.1). Soil moisture content and temperature were monitored continuously at different depths, in a single profile. Air temperature and hourly rainfall totals were also recorded at this site. Water sampling was conducted at the outlet of a single field drain (in OSR) in the following periods:
 - In the autumn period during the period of soil moisture recovery, before and after the application of propyzamide;
 - In late winter, before and after the application of carbetamide.
- Water quality was also monitored in various points in the catchment, including the outlets of a number of agricultural field drains in two periods (spring 2009 and autumn 2009). These samples were analysed for carbetamide in the spring and for propyzamide in the autumn (Paragraphs 5.2.3 and 5.3.3).

The key objectives of the monitoring work were: (i) to evaluate the importance of field drains as conduits for herbicide transfers to surface waters, (ii) to investigate transport mechanisms and processes, and (iii) to obtain sufficient data for the modelling (see Chapters 6 and 7).

5.1 Site description

The monitoring activity was carried out in an arable field (Figures 25 and 26), in the Northeast of the catchment draining to the River Cherwell.

The field is 8.6 ha in area and is located at the base of a hill, with maximum and minimum altitude of 197 m and 177 m. It is dominated by heavy clay soil which is seasonally waterlogged (Denchworth) with a small part occupied in one corner by the Banbury soil series (Thompson, 2009). The Denchworth soil portion develops on rocks called Upper Lias, which are predominantly greyish-brown, locally silty clays with several thin limestones. At the top of the hill – where the Banbury soils are – rocks are Northampton Sands, which consist of calcareous ferruginous sandstones. They are typically above the Upper Lias and they cap many of the isolated hills in the catchment (Edmonds *et al.*, 1965) (Figure 27).

This field was chosen for a number of reasons:

- It is characterised by heavy clay artificially drained soils (Denchworth soil association), which are hypothesised to be the main soils responsible for herbicide losses (see Chapter 2);
- The field is artificially drained with a well defined outlet (the drainage system was probably installed in the 1970s at a depth of approximately 0.7 m with an interdrain spacing of about 18 m);
- It appears to be hydrologically isolated: considering the topography of the field there are unlikely significant interactions with other fields;
- It has already been used for other experiments and the land owner and farm staff were very cooperative.

The field was in winter wheat during the 2008 – 2009 growing season but it was put under oilseed rape in autumn 2009. Oilseed rape is currently the most interesting crop from the point of view of carbetamide and propyzamide contamination.

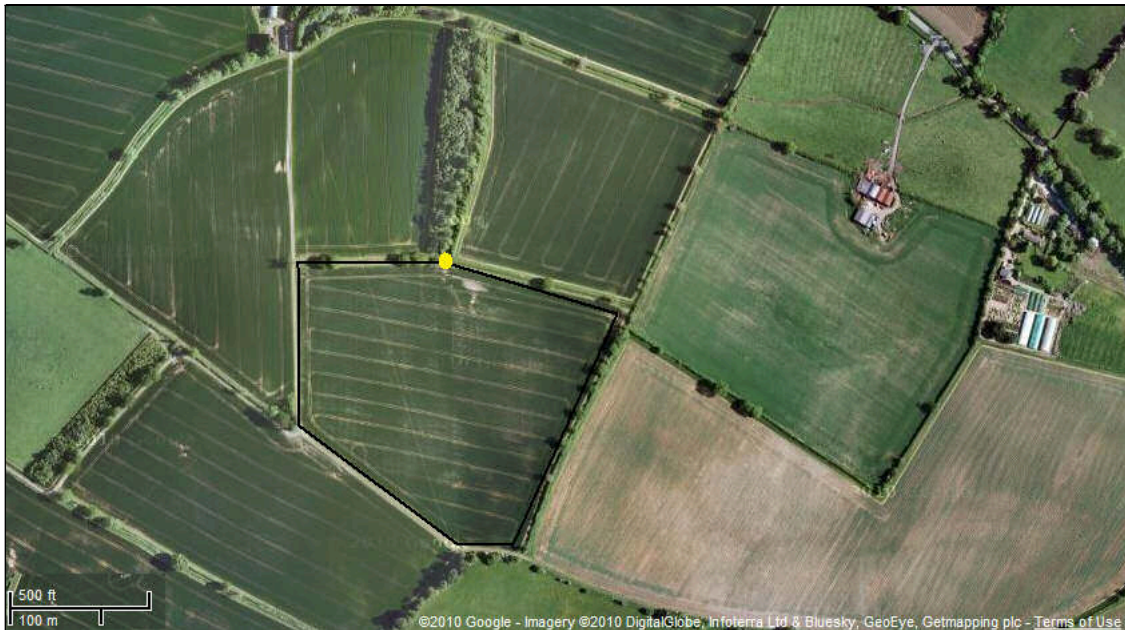


Figure 25 – Experimental Field (black line; the yellow marker shows the outlet of the main field drain).



Figure 26 – Photograph of the Experimental Field which was monitored. The apparatus visible was installed by ADAS to measure in-field overland flow and was not connected with the project described in this thesis.

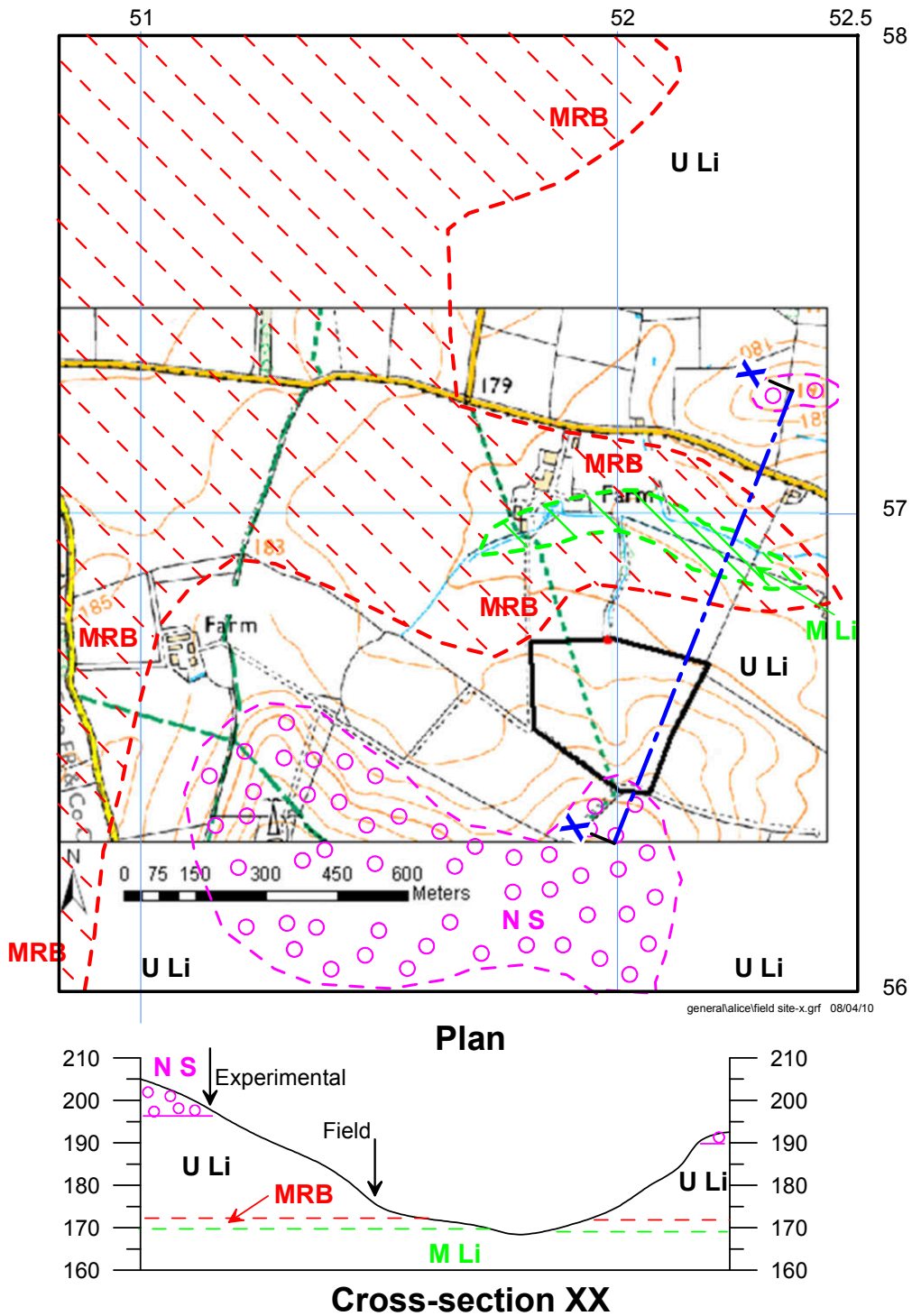


Figure 27 – Experimental Field (black thick line): 1:25,000 map (Ordnance Survey) with geology map (British Geological Survey; 1:50,000) superimposed. ULi = Upper Lias; NS = Northampton Sands; M Li = Middle Lias; MRB = Marlstone Rock Bed. A cross-section is also shown (Ken Rushton, personal communication, 2010).

5.2 Methodology

The monitoring activity at the experimental site was focused on assessing pesticide transport via the artificial drainage.

In addition, grab samples were taken at different sites (field drains and stream water) within the upper reaches of the catchment, in order to attempt to identify and understand spatial and temporal patterns of herbicide transport.

5.2.1 Drain flow characterisation at the Experimental Field

Weather and soil conditions

The Experimental Field was monitored for soil and weather conditions, in order to provide information on environmental drivers for herbicide transport from land to water. A Delta-T multi-channel Datalogger, powered by an external 12 volt battery, was installed in the field (Figure 28a). Hourly rainfall total and air temperature were monitored using a tipping-bucket rain gauge and thermocouple sensor respectively. Hourly soil moisture content was measured at four depths (5, 10, 20, and 25 cm) using SM200 soil moisture probes. Soil temperature was measured at three depths (5, 10, and 15 cm) using thermocouple sensors. The soil moisture probes installed in the soil are shown in Figure 28b.

Data were periodically retrieved from the data-logger using a laptop.

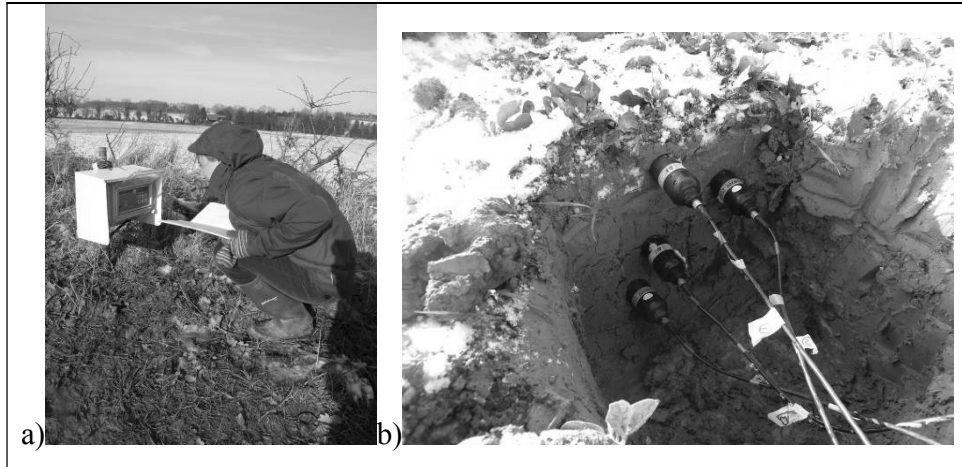


Figure 28 – (a) The Delta-T datalogger installed at the Experimental Field, and (b) SM200 soil moisture sensors installed in the field.

Drain flow

The flow coming out of the main field drain was monitored continuously using a WSC (Washington State College) flume coupled with stilling well containing a pressure transducer (level logger). A barometric logger was installed in parallel in order to make corrections for changes in atmospheric pressure. Drain flow was monitored from 5th October 2009 to the 27th December 2009 and from 11th February 2010 to 5th May 2010.

The WSC flume is a variant of the Venturi or critical-depth flume and is used for the measurement of discharge in open channels. It is particularly useful for making spot measurements of small flows in unlined streams or channels (Chamberlain, 1952: Figure 29). The flume used in this study was prefabricated in GRP (glass-reinforced plastic) and has a pre-supplied calibration equation relating depth on the upstream flume wall to discharge up to 7.5 l s⁻¹ (Table 10). The equation which relates the measured head (h) to discharge (Q) is as follows and is shown graphically in Figure 30:

$$Q = 0.0000155 \cdot h^{2.5} \quad (4)$$

where Q is expressed in l s⁻¹ and h in mm.

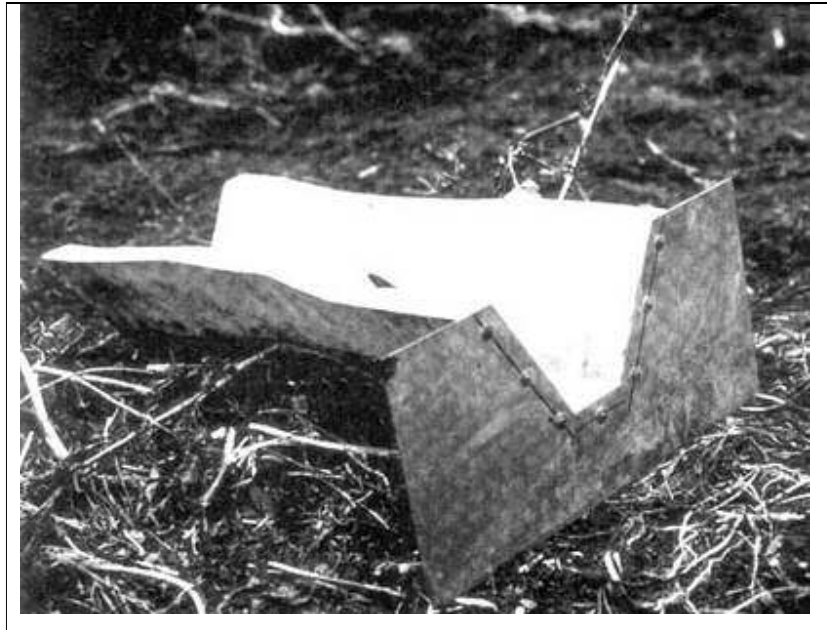


Figure 29 – A WSC flume (photo from M.G. Kay).

Table 10 – Characteristics of the WSC flume used for the monitoring conducted at the Experimental Field.

Height (mm)	230
Width (mm)	350
Depth (mm)	780
Minimum discharge ($l\ s^{-1}$)	1.0
Maximum discharge ($l\ s^{-1}$)	7.5

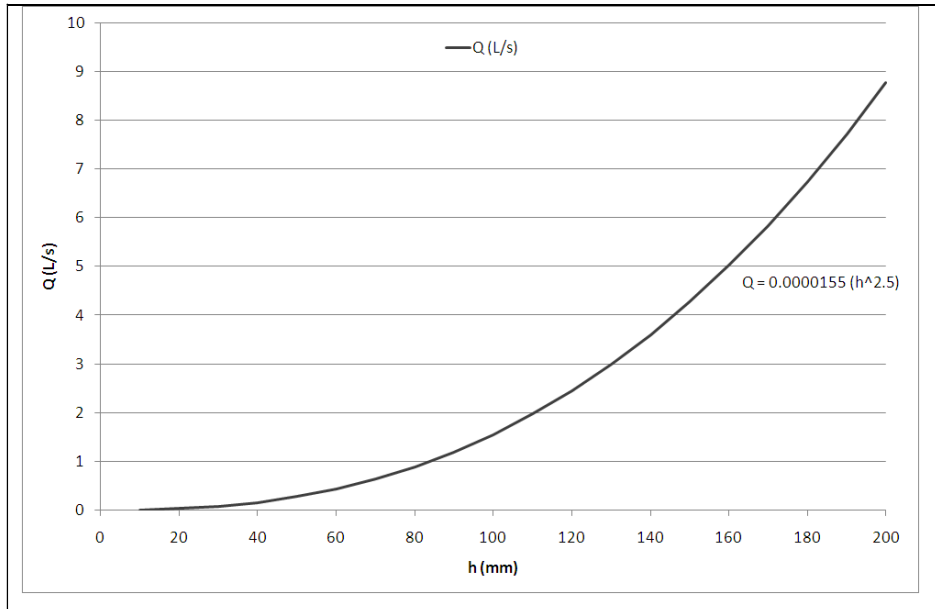


Figure 30 – Calibration curve for the WSC flume installed at the drain monitored at the Experimental Field.

The WSC flume is designed for channels with no sudden head change (drop off). In the case of the Experimental Field, flow emanated from a pipe drain above the flume. A bespoke stainless steel box was therefore fitted to the upstream end of the flume, which collected water from the drain pipe (Figure 31) before water flowed through the flume.

The water level (head) in the box was measured in a connected stilling well. This head was used to calculate an equivalent water level in the flume by manually constructing a calibration curve.

Depth measurements were recorded continuously with a Solinst Levellogger Model 3001 M10 and a Solinst Barologger Model 3001 (Table 11). The Levellogger measures absolute pressure (total head of water in the stilling well plus the barometric pressure). This was compensated to net water level using data from a Barologger, which simultaneously measures barometric pressure. The sample rate was 5 minutes. The

equation relating the actual water head in the stilling well to the measurements recorded with the loggers is as follows:

$$h_{sw}^* = 1.0292 \cdot h_{sw} - 3.3273 \quad (5)$$

where h_{sw}^* (cm) is the water head in the stilling well, and h_{sw} (cm) is the measurement. The R^2 was 0.9874. Equation (5) is also displayed graphically in Figure 32.



Figure 31 – The WSC flume installed at the outlet of the main field drain in the Experimental Field.

Table 11 – Characteristics of the Barologger and Levelogger used for recording the head of water in the stilling well installed at the main drain monitored at the Experimental Field.

Model	Resolution	Accuracy (typical)	Water fluctuation range
Barologger	0.002% FS	± 0.003 ft.0.1 cm	Air Only
F30, M10	0.0006% FS	± 0.016 ft.0.5 cm	29.5 ft., 9 m

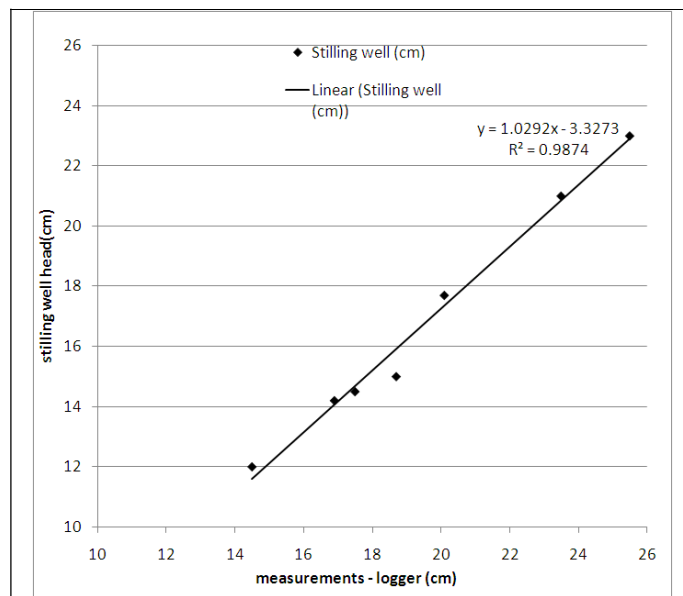


Figure 32 – Linear equation for calculating the actual water head in the stilling well.

Another calibration equation was required to relate the water head in the stilling well to the head in the flume (Figure 33):

$$h = 0.9458 \cdot h_{sw}^* - 9.8672 \quad (6)$$

where h_{sw}^* (cm) is the calibrated level in the stilling well and h (cm) is the water head in the flume. The R^2 was 0.9764.

Discharge was then calculated applying Equation (4). The accuracy of the calculated discharge was checked manually each week via the volumetric method (measuring the time taken to fill a given volume in a bucket placed at the drain outlet).

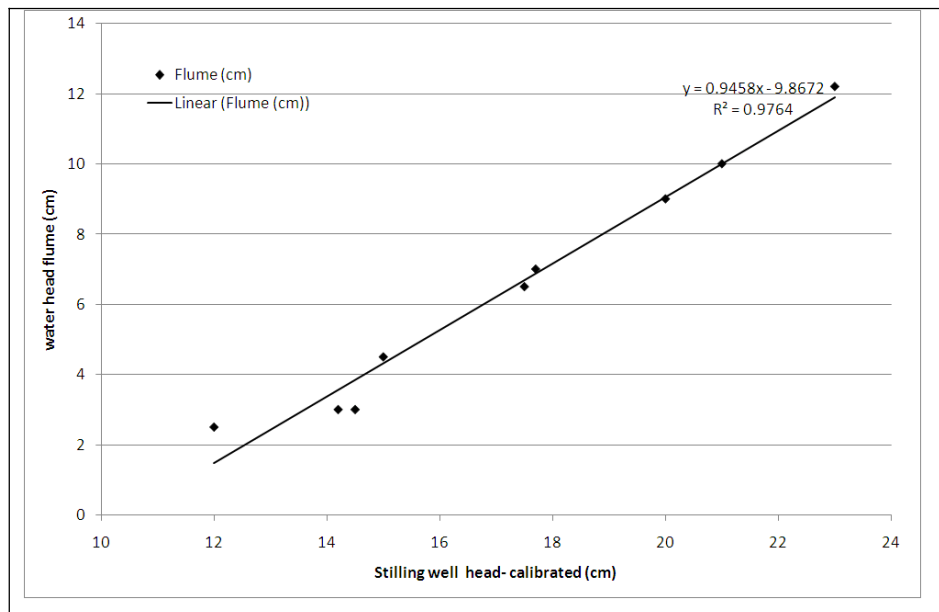


Figure 33 – Linear equation for calculating the water head measured in the WSC flume.

5.2.2 Herbicide concentrations in the Experimental Field

Samples were collected via a combination of manual grab sampling and via an Automatic Water Sampler (Lange Xian 1000) installed at the flume (Figure 34).

The container module of the sampler has 24 one-litre plastic bottles. The sampler was set to take one sample every 8 hours (3 samples per day). Therefore the bottles had to be emptied at least once every eight days. Samples were transferred into solvent-washed one-litre glass bottles supplied by the EA analytical laboratory and the plastic sampler bottles were rinsed with deionised water in order to reduce the risk of contamination by residues from previous samples. All samples were kept in the dark at 4

°C before being sent to the EA laboratory for analysis. Carbetamide was analysed by liquid chromatography - mass spectrometry (LC-MS) and propyzamide was analysed by gas chromatography - mass spectrometry employing Selective Ion Monitoring (GC-MS SIM).

Information about herbicide applications at the farm were supplied by the farm staff. Oilseed rape fields were treated with Kerb Flo[®] (800 g ha⁻¹ propyzamide), on the 7th of November 2009. Herbicide concentrations were monitored in the drain flow from the 5th of November to the 9th December 2009.

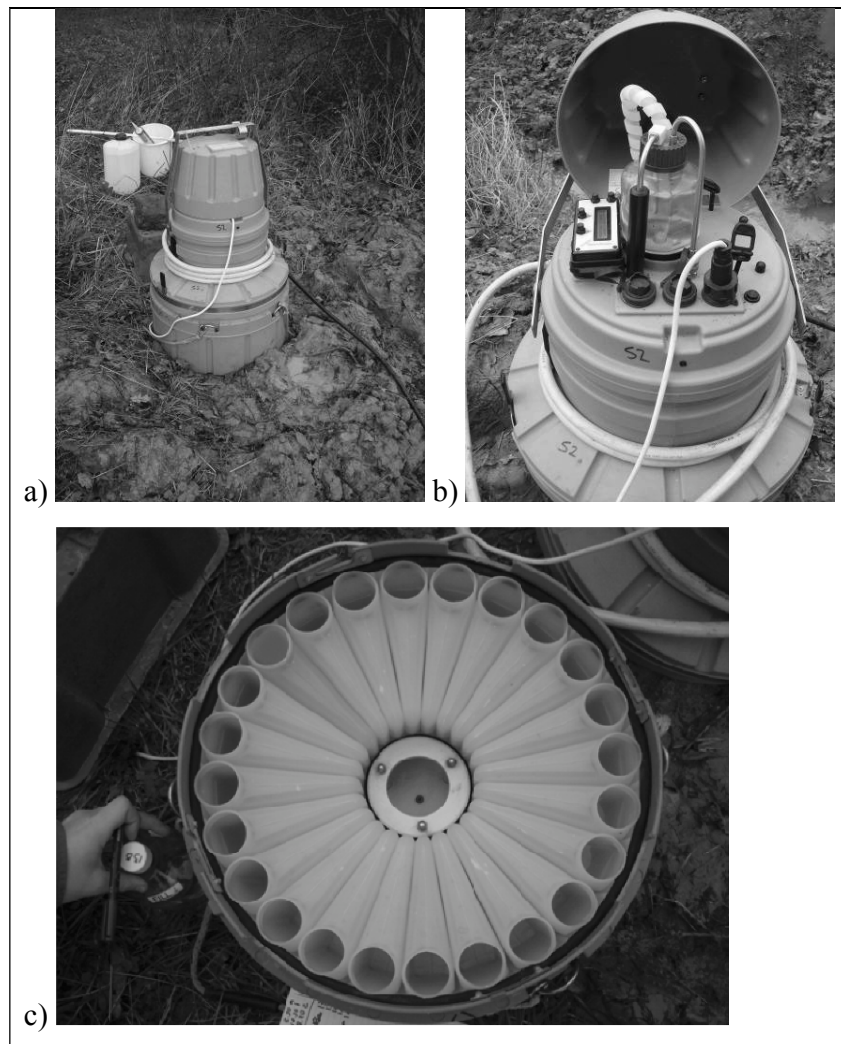


Figure 34 – (a) Lange Xian 1000 Automatic Water Sampler set up at the WSC flume. (b) Sampling module, and (c) the container module.

The field was therefore sprayed with *Crawler*[®] (label rate, 2100 g ha⁻¹ carbetamide), on the 15th of February 2010. Note that this treatment was for research purposes only, since the Experimental Field had already been treated with propyzamide for black-grass control in the autumn (November 2009). The application of carbetamide, therefore, had little agronomic value. Herbicide concentrations were monitored in the drain flow from the day of application to the 4th March 2010.

5.2.3 Manual grab samples

A number of stream and drain outlet sites in the catchment were monitored in spring 2009 and autumn 2009. Water sampling was aimed at gaining an insight into the contribution of different sub-catchments and fields to herbicide contamination in the upper reaches of the catchment.

Water samples were collected in three different areas of the catchment on the first order river Cherwell and on Ashby Brook (see Figure 35) at eight different sampling points (field drains and in-stream). Sampling points are listed in Table 12.

Carbetamide and propyzamide are measured in different analytical suites. Spring samples were collected between March and May 2009 and were tested only for carbetamide. No information was available about herbicide application rates or timing in this period. However, carbetamide is generally applied in winter and early spring.

Autumn grab samples were collected, on approximately a weekly basis, in November and December 2009. Although no precise information about applications at the catchment scale was available, propyzamide treatment on oilseed rape at the Experimental Field occurred on 7th of November. The timing and magnitude of increases in both propyzamide and carbetamide concentrations measured using Thames Water's SAMOS at the catchment outlet (Chapter 4) suggest that a significant fraction of the oilseed rape in the catchment was probably sprayed in the same period. Analysis of autumn samples focused on propyzamide, mainly for reasons of cost.

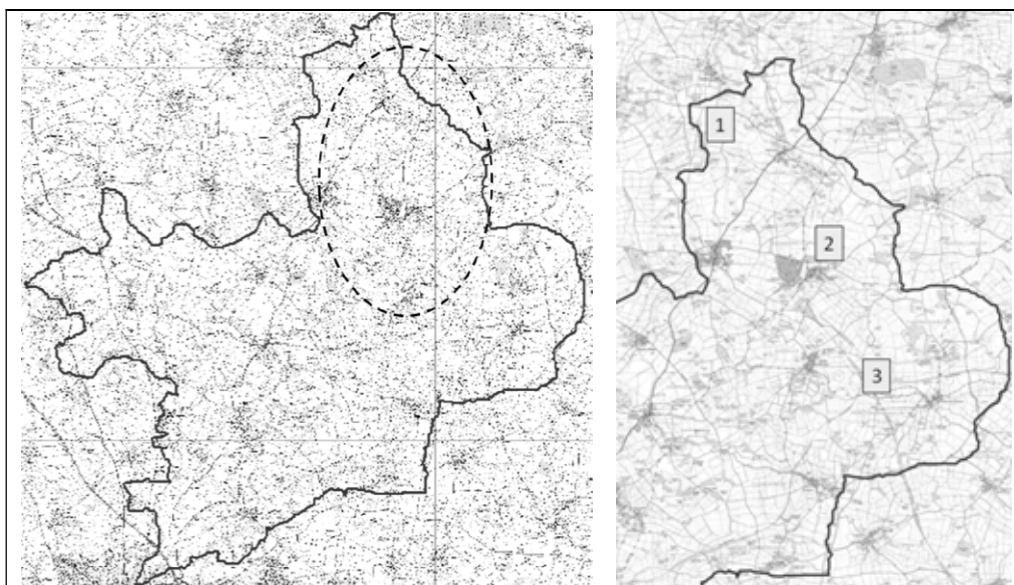


Figure 35 - Sampling areas (numbers 1 to 3 refer to sampling point locations: 1. Experimental Site; 2. upstream Woodford Halse; 3. Ashby Brook between Eydon and Moreton Pinkney).

Table 12 – Sampling points monitored during spring and autumn 2009.

Sampling site location (see Figure 45)	Sampling point	Sampling period	Description
1	drain 1	Spring and Autumn	Main drain of the Experimental Field
	drain 2	Spring and Autumn	Main drain of another field close to the Experimental Field, which was in winter wheat in Spring 2009 and in OSR in the Autumn
	stream	Spring and Autumn	Stream downstream of Drains 1 and 2
2	stream	Spring and Autumn	River Cherwell upstream of Woodford Halse
	drain 1	Spring	Field drain issuing to the Cherwell (the field was in OSR during Spring 2009 and in winter wheat in Autumn)
	drain 2	Spring	Field drain issuing to the Cherwell (the field was in OSR during Spring 2009 and in winter wheat in Autumn)
3	drain	Spring and Autumn	Field drain issuing to the Ashby Brook (the field was in OSR during Spring 2009 and in winter wheat in Autumn)
	stream	Spring and Autumn	Ashby Brook

5.3 Results

5.3.1 Drain flow

Discharge from the Experimental Field drain was monitored from the 5th of October to the 27th of December 2009, and from the 11th of February to the 31st of March 2010. Unfortunately no records are available for the period end December 2009 to 10th February 2010, because of technical problems with the data loggers. Note that the flow in the flume was exclusively drain flow (no overland flow was intercepted) over the whole period, except for one storm at the end of February 2010 in which overland flow was observed to inundate the steel box at its upstream end.

Figure 36 shows rainfall, soil moisture content (average for 5 to 25 cm depth), and drain discharge. Total drain flow over the monitored period is 148.03 mm, representing 58.7% of the total rainfall measured on this site (252.2 mm). It should be noted that drain flow was calculated dividing the cumulative flow by the total area of the field. However no precise information was available about the actual extent of the drains, which may not cover the whole of the field (some parts of the field may not feed into the drainage pipe). If so, the percentage of the total rainfall would be higher. Monthly values are shown in Table 13.

Table 13 – Monthly rainfall and drain flow at the Experimental Field.

Month	Total rainfall (mm)	Total drain flow (mm)	As % of total rainfall
October ¹	41.6	2.58	6.2
November	90.4	28.07	31.05
December ²	47	41.38	88.04
January	44.8	-	-
February ³	54.6	43.47	79.61
March	18.6	32.53	174.9

¹ from 5th October.

² from 1st to 27th December.

³ from 11th February

Drain flow increased significantly at the beginning of November, following the heavy storm event on the 1st of November (13 mm), which pushed soil moisture content close to saturation. For the Denchworth soils, volumetric soil moisture content at a tension of 10 kPa (usually referred to as field capacity $FC = \theta_{10}$) is $0.435 \text{ cm}^3 \text{ cm}^{-3}$ at 20 cm depth and $0.48 \text{ cm}^3 \text{ cm}^{-3}$ at 50 cm depth (www.landis.org.uk [accessed 15th December 2009]). These values appear to be corroborated by observations at the Experimental Field. Drain flow was observed to increase when the topsoil FC values were exceeded. In contrast, the intense rainfall events that occurred at the beginning of October (9.8 mm and 8.2 mm on the 6th and 7th of October) did not trigger any significant increase in drain flow, as soil moisture was below FC. The highest peaks were recorded at the end of February (four peaks at or above 9 l s^{-1} between the 24th and 27th February), in correspondence with heavy rainfall events (2.4 mm, 9.8 mm, 7.2 mm, and 4.6 mm): it must be noted, though, that the pre-supplied calibration equation for the WSC flume installed in the Experimental Field theoretically works up to a maximum discharge of 7.5 l s^{-1} . In practice the flume appeared to work well up to 9 l s^{-1} . So measurements were considered to be genuine up to this threshold.

Drain flow seems to include two different components. Peaks are a quick response to rain events and water transport to the drainage system may predominantly occur via macropores. A second flow component is represented by base flow, which slowly increases over the monitoring period, and starts decreasing towards the end of March. This seems to be completely separate from the clay soil hydrology. It must be noted that at the southern end of the field, on the high ground, there are some ironstone (light) soils (Banbury over Northampton Sands). There is a dry valley running off this high ground down the centre of the field towards North-Northwest (Dick Thompson, personal communication, May 2010). This valley is visible on old maps as a stream and it is likely that the field drainage system was designed to drain the spring from which this stream derived (wet patches near the top of the field were observed both in winter and spring). If this is the case, it could explain this increased base flow component. Moreover, water which passes through Banbury soils may enter the drainage system with a certain delay, which might partially explain the high drain flow measured in March (174.9% of total rainfall; see Table 13).

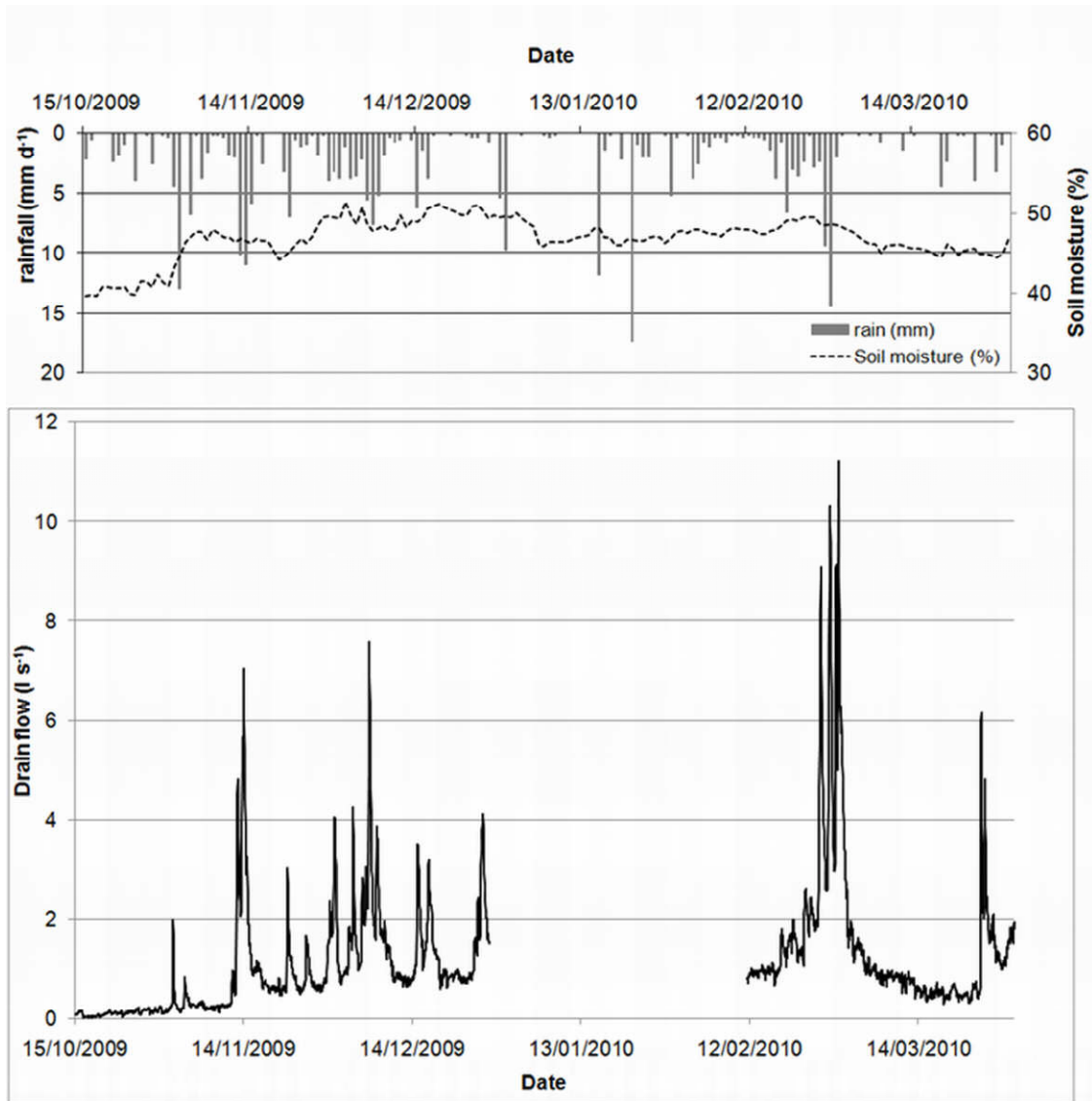


Figure 36 – Drain flow ($l s^{-1}$) measured in the WSC flume installed at the main field drain. Also shown are daily rainfall totals (primary axis [$mm d^{-1}$]), and daily soil moisture content (secondary axis [% total volume]) (average at 5 cm to 25 cm depth). The period 15th October 2009 to 31st March 2010 is shown.

5.3.2 Herbicide concentrations and drain flow

Propyzamide

Propyzamide was applied at the Experimental Field on the 7th of November 2009. Prior to this date, no significant concentrations were detected in any of the drains monitored at the site (concentrations all below the limit of detection [LOD] on the 5th of November).

Drains were next sampled on the 12th of November. At this time, a significant concentration increase was observed (to 29.3 $\mu\text{g l}^{-1}$). This followed a fairly wet period (14.8 mm of rain fell in the 6 days following propyzamide application) which caused a steady rise in drain flow (Figure 37) with a minor drain flow peak on the 11th of November. This was followed by a major storm event between the 12th and 16th of November. Propyzamide concentrations peaked during this event (the highest concentration was detected in the sample taken at 2:30 a.m. on 14th November at 55.7 $\mu\text{g l}^{-1}$). This was at approximately the same time as the drain flow peak. Concentration then decreased gradually, during the hydrograph recession to the 16th of November another peak was observed (24 $\mu\text{g l}^{-1}$ in the sample taken at 10:30 a.m.), in response to increased drain flow, triggered by rainfall on the 14th and 15th of November (14.2 mm in total). Concentrations decrease again in a very clear recession, following the recession of the hydrograph, until discharge events on the 21st and 25th of November appear to force concentrations to rise again. In each event, the concentration response to rainfall is very rapid and the concentration peak is observed at about the same time as the discharge peak. There then follows a steady quasi-exponential decrease in concentration. The shape of the concentration recession after the event of the 25th of November follows the hydrograph again, decreasing until the 1st December when no propyzamide is detected in the sample taken at 10:30 a.m. Concentration rises again concurrently with the drain flow peak observed on 3rd December. Another recession follows this event. From the 4th to the 9th December drain flow response is very quick. 22.8 mm of rain fell in these 6 days, triggering four drain flow peaks.

The total herbicide loss over the monitored period is 1.1% of the total amount applied (72.7 g). Total loss was calculated on the basis of linear interpolation of measured concentrations and 5-minute drain flow measurements. In the UK, total losses have been reported to vary between < 0.1 and approximately 5% depending on the chemical properties (i.e. sorption) (Brown *et al.*, 2004). In particular, Harris and Catt (1999) reported that loadings of the moderately sorbed isoproturon (K_{OC} of $122 \text{ cm}^3 \text{ g}^{-1}$) were 0.2% of applied. Total losses < 0.1% have been reported for strongly sorbed compounds such as trifluralin (K_{OC} of $8765 \text{ cm}^3 \text{ g}^{-1}$) and deltamethrin (K_{OC} of $1.02 \cdot 10^7 \text{ cm}^3 \text{ g}^{-1}$) (Brown *et al.*, 1995; Turnbull *et al.*, 1997). Transport of the weakly sorbed herbicide triasulfuron (K_{OC} of $16 \text{ cm}^3 \text{ g}^{-1}$) from a heavy clay soil in southern England resulted in total losses of about 5% of applied (Jones *et al.*, 1995). Propyzamide is slightly mobile (K_{OC} of $840 \text{ cm}^3 \text{ g}^{-1}$) and total losses would be expected to be between < 0.1 and 0.2%. However the results suggest higher losses.

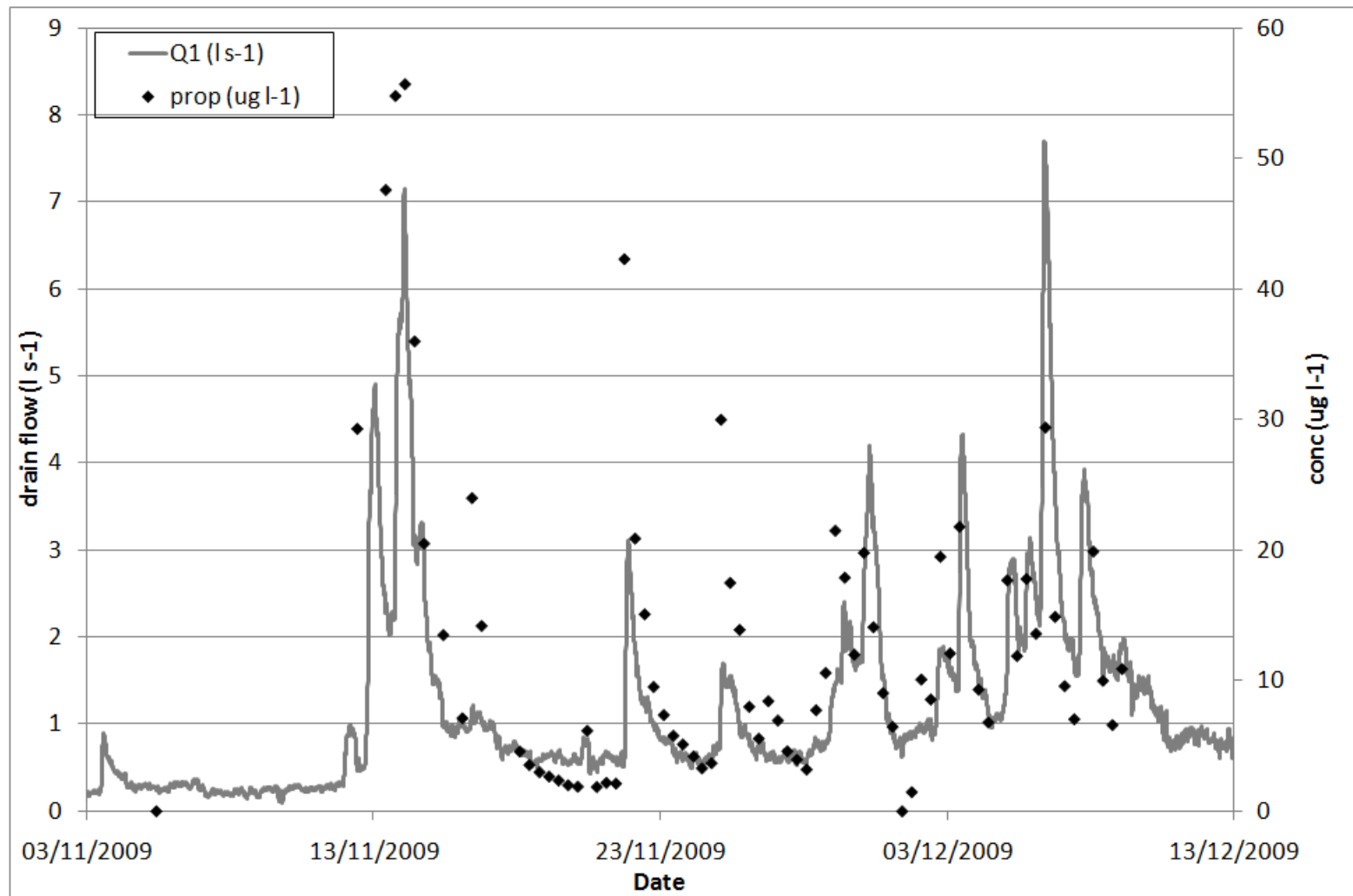


Figure 37 – Drain flow ($l s^{-1}$) and propyzamide concentrations (black points [$\mu g l^{-1}$]) at the main field drain.

For a better understanding of the processes involved in propyzamide transport in the soil, concentration/discharge relationships were investigated (Figures 38-41). In fact it has been long noted that solute concentrations vary systematically with respect to rising and falling limb discharge on the hydrograph (Toler, 1965; Rose, 2003). Such variation often results in a non-unique solute concentration for a given discharge or hysteresis (Rose, 2003). Figure 38 shows how propyzamide concentration varies with respect to discharge during the storm event occurring just after propyzamide application. Concentration varies following a clockwise rotation: in the rising limb of the hydrograph concentration increases with discharge and it then decreases in the falling limb. 31.6 mm of rainfall fell between 7th and 14th November, of which 22 mm between 12th and 14th November. Therefore herbicide contamination might be connected to storm water pushing the chemical through the soil, with concentration receding with the hydrograph in the falling limb (where, at a given discharge, lower concentrations are observed).

During the storm event on 16th November an anticlockwise rotation is observed: in the falling limb a higher concentration is observed for a given discharge (at least when discharge is below 1 l/s) (Figure 39). This means that there might be other contribution than storm water (soil water, or groundwater, as the water table might be at drainage depth at this time of the year). In fact this rain event is rather small (2.6 mm) and it does not trigger any drain flow peaks; drain discharge only slightly increases. Moreover 10 days after application the chemical might have reached deeper soil layers and might move more easily to the drains, even without storm water pushing through the soil.

During the 21st – 23rd November event the rising limb is characterized by a rapid concentration increase, but then a more intense rain event (5.6 mm between 3:00 and 10:00 a.m.) triggers a quick discharge increase (Figure 40). Here concentration decreases, although the hydrograph is still rising. This suggests that storm water dilutes the chemical, which comes from a different source (soil water or groundwater). So the concentration increase observed at the beginning of this event might be due to soil or ground water, which is later mixed with storm water. In the falling limb concentration slowly decreases, with the water table going down or with the hydrograph recession.

During the two following events (24th November and 6th December) similar patterns are observed. Figure 41 represents the storm cycle of the 6th December. Concentration

increases in the rising limb and it decreases in the falling limb. This would suggest exhaustion of supply due to the fact that a few weeks after application a relevant amount of the chemical has already been lost or degraded. Therefore high discharges are necessary to push the chemical still available through the soil and concentration peaks are observed concurrently to discharge peaks.

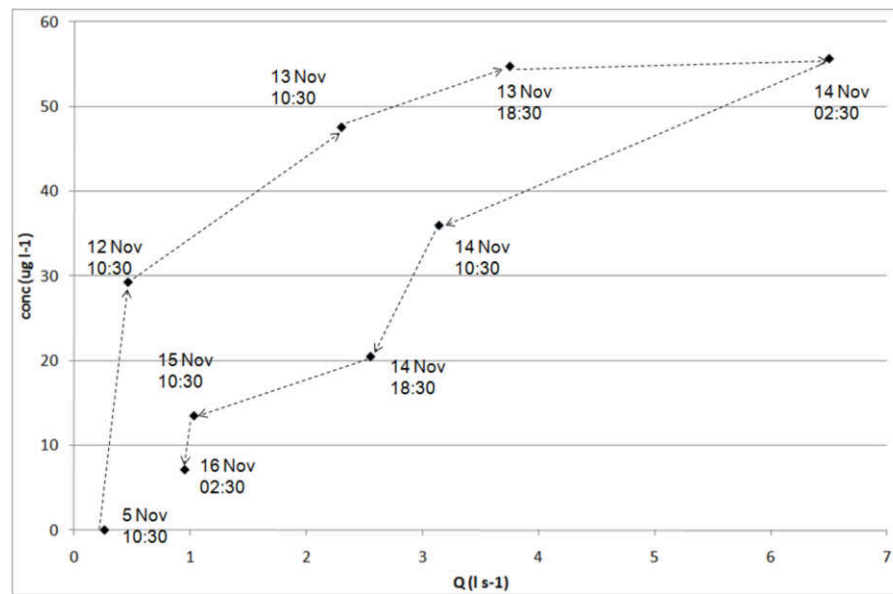


Figure 38 – Solute rating curve: propyzamide concentration with respect to discharge for the period 5th to 16th November 2009 is shown.

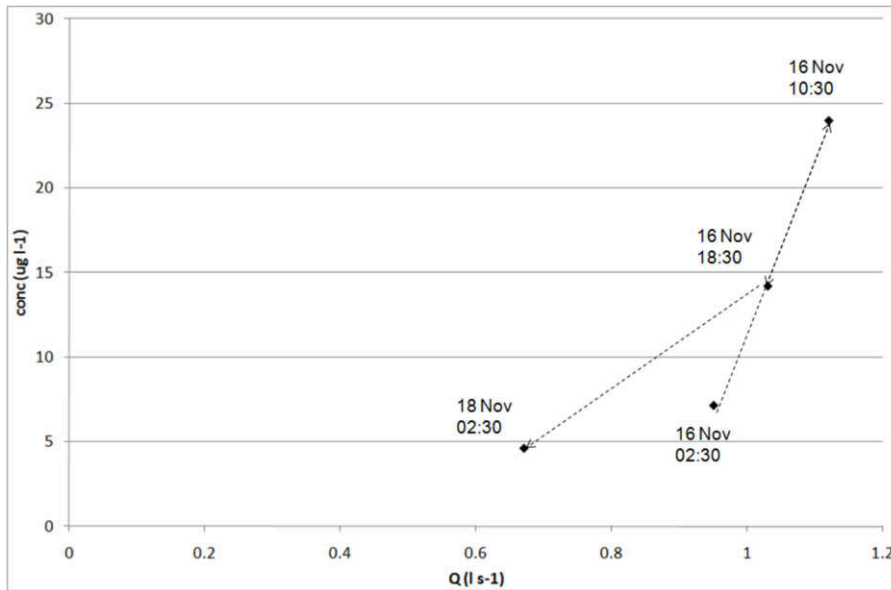


Figure 39 - Solute rating curve: propyzamide concentration with respect to discharge for the period 16th to 18th November 2009 is shown.

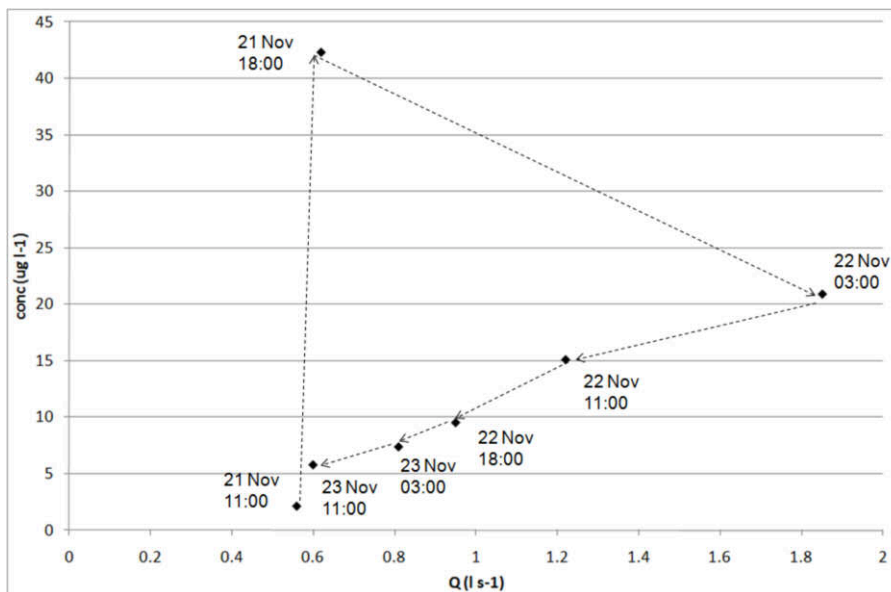


Figure 40 - Solute rating curve: propyzamide concentration with respect to discharge for the period 21st to 23rd November 2009 is shown.

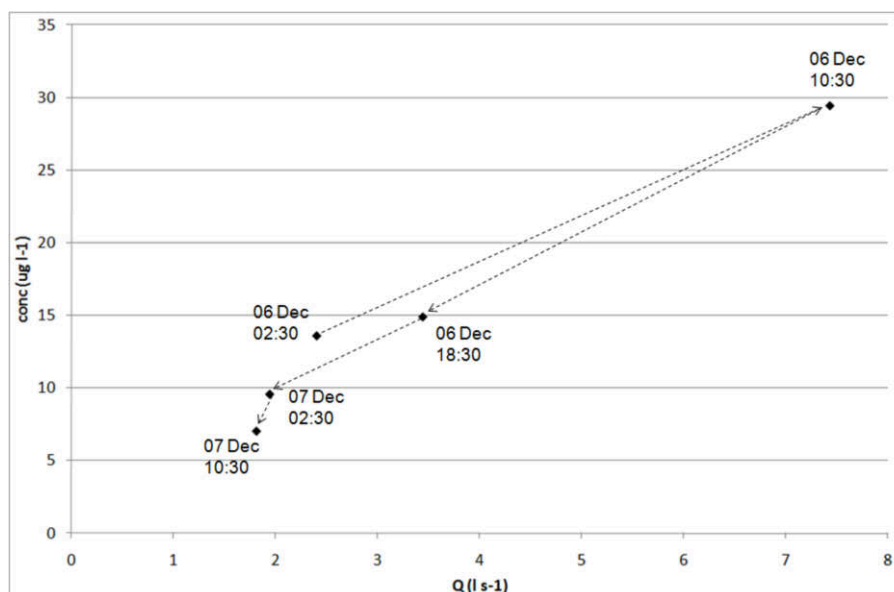


Figure 41 - Solute rating curve: propyzamide concentration with respect to discharge for the period 6th to 7th December 2009 is shown.

Carbetamide

Carbetamide was applied at label rate at the Experimental Field on the 15th of February 2010. In the two samples prior to application, no significant concentrations were detected at the site (concentrations below the limit of detection [LOD]). Some carbetamide was detected in the sample taken at 8:00 p.m. ($0.19 \mu\text{g l}^{-1}$), likely after application (the exact application timing was not provided, but it likely occurred before 8:00 p.m.) (Figure 42).

A significant concentration increase was observed on 17th February at 12:00 a.m. (up to $621 \mu\text{g l}^{-1}$) concurrently with a rain event (1 mm of rain between 11:00 a.m. and 12:00 a.m.) with a minor drain flow peak, which does not seem to be relevant (drain flow increases in the afternoon, with 2.8 mm of rain between 12:00 a.m. and 6:00 p.m.). This carbetamide concentration peak seems to occur before any important rain event and drain flow rise. The water sampled came straight out of the drain pipe, without any chance to mix with any other sources. High concentration peaks (above $500 \mu\text{g l}^{-1}$) were observed on 19th and 21st February (in the samples taken at 8:00 p.m.), following 6.6 mm and 3.6 mm rainfall respectively, and consequent drain flow increase. Another carbetamide peak

(694 $\mu\text{g l}^{-1}$) was measured on 25th of February at 2:00 a.m., triggered by a drain flow peak occurred on 24th February in the evening, after 2.4 mm of rain measured on the same day. Carbetamide concentrations peaked again during an intense rain event between the 25th and 26th of February (11 mm between 8:00 p.m. and 12:00 a.m.). The highest concentration was detected in the sample taken at 10:00 a.m. on 26th February at 623 $\mu\text{g l}^{-1}$. This was at approximately the same time as the drain flow peak. Another carbetamide peak was observed on 27th February (658 $\mu\text{g l}^{-1}$ at 8:00 p.m.), triggered by a high drain flow peak at the same time, following very intense rainfall on the same day (8.2 mm in the morning and 6.2 mm in the afternoon – this explains the double drain flow peak observed). In each event, the concentration response to rainfall is very rapid and the concentration peak is observed at about the same time as the discharge peak. Concentration then decreased gradually, during the hydrograph recession to the 4th of March when the monitoring stopped. Concentrations decreased in a very clear recession, following the falling limb of the hydrograph.

The reader is reminded that carbetamide was applied at the Experimental Field although the field had already been treated to control black-grass in the autumn (propyzamide was applied in November 2009). This is not a usual practice, but in this way it was possible to observe carbetamide behaviour in the same site monitored for propyzamide. Agronomist, farmer, and farm staff agreed on this.

The total carbetamide loss over the monitored period was calculated to be approximately 8.6% of the applied. Carbetamide, being more mobile than propyzamide, was more easily lost to field drains. This loss is very high, though: for moderately and weakly sorbed compounds total losses have been reported between 0.1 and 0.5%, and 5% respectively (Brown *et al.*, 2004; Harris and Catt, 1999; Jones *et al.*, 1995). This could be explained considering the soil conditions on the day of application, which were very wet, and that February was very rainy (65.4 mm of rainfall). Moreover total losses also depends on soil type, drain spacing and type, and rainfall patterns shortly after application (Flury, 1995).

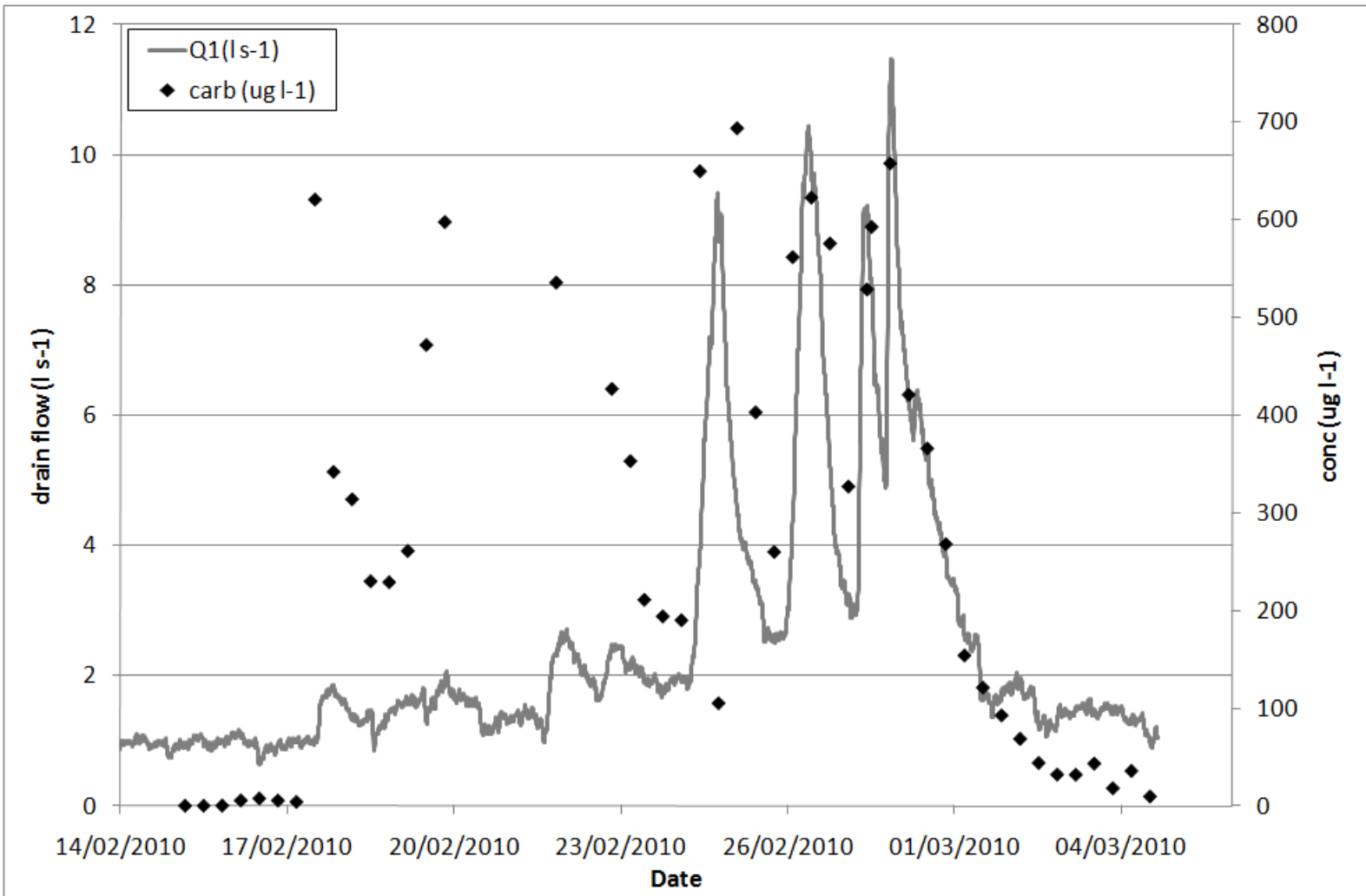


Figure 42 - Drain flow ($l s^{-1}$) and carbetamide concentrations (black points [$\mu g l^{-1}$]) at the main field drain.

Concentration/discharge relationships were investigated also for carbetamide (Figures 43-46). Figure 43 shows how carbetamide concentration varies with respect to discharge just after application. The hysteresis pattern observed here is an anticlockwise rotation: concentration starts to increase just after application (in the sample taken on 15th February at 8:00 p.m.), concurrently with discharge, even with no rain. Carbetamide is likely to move very easily through the soil, even without storm water pushing the chemical through the soil. It should be noted that the soil at the time of application was very wet. Two rain events (0.6 mm recorded between 8:00 p.m. and 10:00 p.m. and 1.4 mm between 2:00 a.m. and 5:00 a.m. the next day) triggered concentration and discharge peaks, which are observed on 16th of February in the early morning. At this point carbetamide may be mobilised, and therefore it keeps flowing to the drains: concentration increase may be due to decreasing discharge. Concentration starts to decrease when discharge rises again and dilutes the chemical. Here it seems that herbicide transport is not strictly connected to storm water. Carbetamide moves to the drains thanks to high soil moisture (which is probably at saturation) and water constantly feeding the drains.

During the 17th February event (3.8 mm between 11:00 a.m. and 6:00 p.m.) the rising limb is characterized by a rapid concentration increase ($621 \mu\text{g l}^{-1}$), and a following quick discharge peak (Figure 44): here concentration decreases, although the hydrograph is still rising. This suggests that storm water dilutes the chemical, which comes from a different source (soil water, or groundwater if the water table is at or above drain depth). So the concentration increase that is observed at the beginning of this event might be due to soil or ground water, which is later mixed with storm water. In the falling limb concentration slowly decreases. The small discharge increase which is observed on 18th February is due to some rain (0.8 mm between 12:00 a.m. and 6:00 p.m.), which –again– causes chemical dilution.

During the rain event on 24th February no clear hysteresis is observed (Figure 45). Also here we observe a concentration peak first, and subsequently a concentration decrease, while discharge keeps rising. This seems to be a frequent pattern for carbetamide observations, suggesting that the chemical is mobilised by storm water, which triggers very high peaks. Then discharge keeps increasing and storm water dilutes the chemical, which is in the soil. When the hydrograph recedes, concentration increases

for some time ($698 \mu\text{g l}^{-1}$ on 25th February at 2:00 a.m.) and then starts falling with the hydrograph.

Also during the event shown in Figure 46, no clear hysteresis is observed. In the rising limb of the hydrograph concentration increases up to $658 \mu\text{g l}^{-1}$. This peak is triggered by 8 mm of rainfall. In the falling limb of the hydrograph concentration gradually decreases. Measured concentrations at a given discharge generally seem to be smaller in the recession of the hydrograph than in the rising limb, but this is not very clear. This behaviour may suggest that the chemical is exhausting and that at this point it needs to be pushed through the soil by storm water to reach the drains.

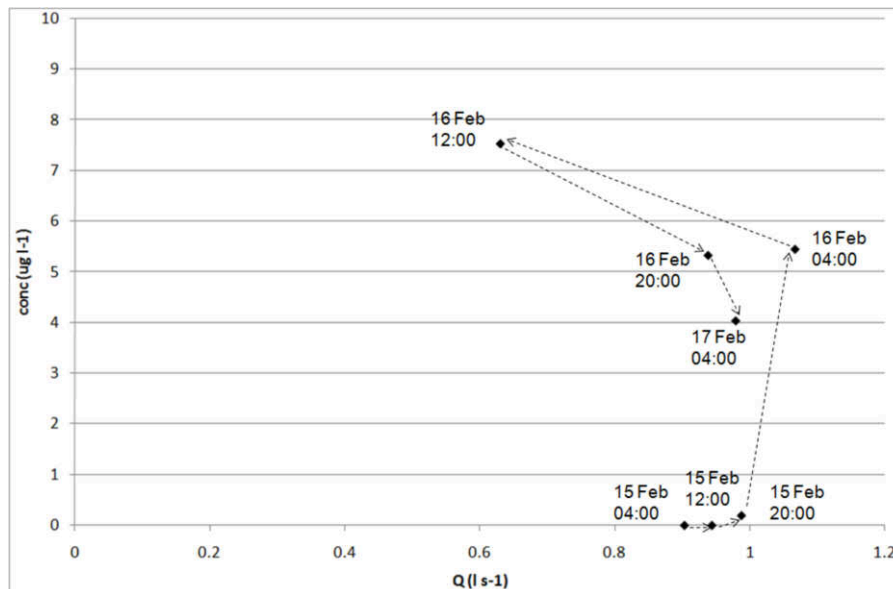


Figure 43 – Solute rating curve: carbetamide concentration with respect to discharge for the period 15th to 17th February 2010 is shown.

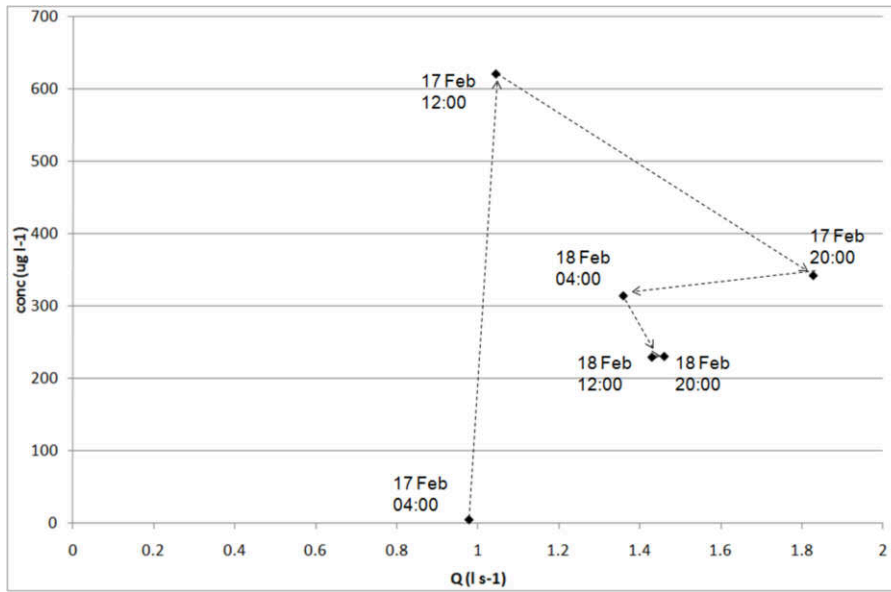


Figure 44 – Solute rating curve: carbetamide concentration with respect to discharge for the period 17th to 18th February 2010 is shown.

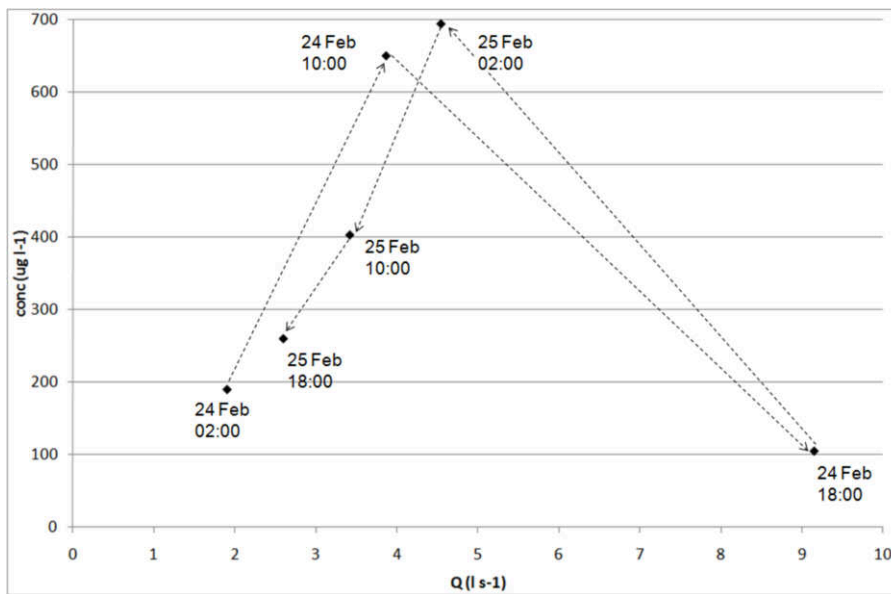


Figure 45 - Solute rating curve: carbetamide concentration with respect to discharge for the period 24th to 25th February 2010 is shown.

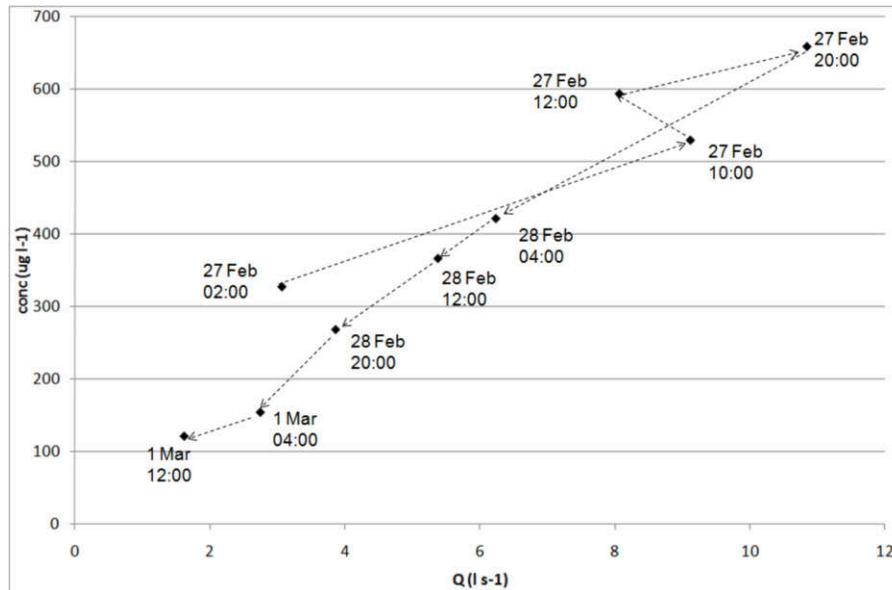


Figure 46 - Solute rating curve: carbetamide concentration with respect to discharge for the period 27th February to 1st March 2010 is shown.

Comparison between carbetamide and propyzamide

Observed carbetamide concentrations were about an order of magnitude higher than those observed for propyzamide. This may be due, in part, to a higher application rate (2.6 times higher for carbetamide), but also to carbetamide's higher aqueous solubility and lower K_{OC} . However, propyzamide concentrations seemed to stay high for a longer period than carbetamide. This cannot be certain, though, as monitoring stopped and no further storm events and drain flow peaks were monitored beyond mid-December and the beginning of March for propyzamide and carbetamide respectively. Total carbetamide loss was also much higher than propyzamide loss (8.6% versus 1.1%), likely because of higher mobility and solubility.

A gradual recession curve was observed in both propyzamide and carbetamide concentrations, although they were applied in different times of the year. Also, peaks seemed to occur approximately at the same time as drain flow. This suggests that herbicide transport to drains is a quick process.

Carbetamide appeared to respond more dramatically to moderate rainfall events. No difference in terms of peak concentration was observed between low and high drain flow

peaks. A general drain flow increase seemed to be sufficient to trigger concentration peaks (not always: also steady low drain flow generated a concentration peak on 17th of February). This might be connected to carbetamide properties: being more soluble than propyzamide, it dissolves into water more easily, even when drain flow is relatively small. Dissolving in a smaller quantity of water, concentrations are also higher.

Calculations of the fraction of chemical in the dissolved phase suggest that $\gg 90\%$ of both chemicals is likely to be in the dissolved phase. An approximate f_{OC} of 0.1 grams C/g sediment was used to calculate the distribution coefficient K_d (see Equation 1, Paragraph 2.5). The fraction of chemical in the dissolved phase in water was calculated using measured concentration of suspended solids (C_{SS}). Suspended solids were measured in two samples taken from the drain monitored in the Experimental Field, in November 2009 and February 2010. The laboratory analysis gave values of 11.3 and 5.4 mg/100 ml for November and February respectively. Despite the different chemical properties both herbicides seem to be transported mainly in solution.

Propyzamide movement to the drains seem to be triggered by intense rain events first, which push the chemical through the soil, reaching the drainage system. When the chemical is mobilised concentration peaks do not appear to be triggered by heavy rain events. Storm water at this point might dilute the chemical, which is in the soil or ground water. As far as carbetamide is concerned, transport to the drains seem to occur, even without storm water pushing it from the upper soil layers downwards. In fact relevant concentrations were observed even before intense rain events (high soil moisture might be sufficient to trigger solute flow to drains). In correspondence with intense rainfall events very high peaks are triggered. Concentrations appear to decrease very quickly: this suggests that storm water triggers concentration peaks first, but then contributes to chemical dilution.

5.3.3 Manual grab samples

Sampling during spring 2009 yielded rather limited insights into relevant processes operating in the catchment – principally because of lack of information on herbicide application rates and timing during winter 2008 and spring 2009.

Concentrations of carbetamide above the LOD were detected only in the stream at Woodford Halse (site 2) (Table 14). The decreasing trend observed in these samples suggest that carbetamide was applied in some areas of the catchment some time beforehand and by mid-March concentrations were in recession.

In the drains which were monitored no carbetamide was detected. This may be because carbetamide was not applied to the fields served by these drains; another reason may be that it was applied, but that concentrations had decreased below the LOD by the time the samples were taken.

Table 14 – Concentrations of carbetamide ($\mu\text{g l}^{-1}$) observed in grab samples collected from the River Cherwell at Woodford Halse (site 2).

Date	Concentration ($\mu\text{g l}^{-1}$)
19/03/2009	1.31
27/03/2009	0.663
01/04/2009	0.163
01/05/2009	0.082

Sampling during the autumn, in contrast, was more interesting. This was due to better knowledge of the timing and magnitude of herbicide applications in the catchment but also because of a better knowledge of the catchment and of the processes driving herbicide transfers to water. The monitoring focused on:

- Stream water at three different points in the channel network (the river Cherwell at the experimental site, the Cherwell at Woodford Halse and the Ashby Brook, which is a major tributary of the Cherwell);
- One drain draining a field that was under OSR during autumn 2008 - winter 2009;

- One drain draining a field that was in OSR during the 2009 – 2010 season.

Manual grab samples were taken on five different days in autumn 2009: the 5th, 12th, 13th, 18th, and 25th of November (Table 15). The first set of samples was intended to act as a baseline concentration data set, before propyzamide application. Indeed all concentrations were below the LOD in samples taken in the river Cherwell (sites 1 and 2). In the Ashby Brook sub-catchment (site 3), however, propyzamide was detected. The concentration in the stream was 0.432 $\mu\text{g l}^{-1}$ on the 5th of November, presumably due to applications in this catchment before this date. Note that at some farms in the catchment propyzamide treatment was planned for the 5th of November but postponed because of high winds. Concentrations were also above LOD in a field drain issuing to the Ashby Brook (at 0.11 $\mu\text{g l}^{-1}$), despite the fact that the field which this drain serves was under winter cereals at the time of sampling and had not received propyzamide since the previous growing season, when it was in OSR. This suggests that the propyzamide present in the drain (and possibly some of the substance found in the stream) was applied prior to the label cut off date of the beginning of February. This is plausible, given the relatively long DT_{50} for this substance.

Propyzamide concentrations determined in manual grab samples collected from “drain 2” on the same farm as the Experimental Field show a very similar pattern to those measured at the Experimental Field itself. Concentrations were also of a similar magnitude (Table 15).

Propyzamide concentrations in stream water samples collected after the 5th of November (Table 15) show different trends. At the experimental site, the stream (which is essentially the source of the River Cherwell) was monitored downstream of an on-line pond, where water draining the land upstream accumulates before flowing downstream. There was no flow from the pond on the 5th and 12th of November. On 13th, 18th, and 25th November very high concentrations were detected, which reflect the peaks observed in the drains contributing to the pond. Concentrations in the outflow were generally lower than the concurrent concentrations in the drains (with the exception of the samples collected on the 18th of November), but seem to decrease more slowly. This is consistent

with the probable role of the pond as a buffer, mixing, diluting, delaying (and possibly degrading) substances passing through it.

Concentrations in the Cherwell at Woodford Halse gradually increase in the second and third weeks of November, probably in response to applications in the contributing catchment.

Table 15 – Concentrations of propyzamide ($\mu\text{g l}^{-1}$) observed in the grab samples.

Date	Drain 2 – adjacent to the Experimental Field	River Cherwell-downstream of pond	River Cherwell-Woodford Halse	Ashby Brook	Drain - Ashby Brook
05/11/2009	< 0.02500	no flow	< 0.005	0.432	0.114
12/11/2009	34.4	no flow	0.0247	0.0858	0.1
13/11/2009	46.7	15.2	0.0534	0.918	0.119
18/11/2009	1.39	10.7	0.819	0.157	0.108
25/11/2009	11	5.34	0.294	0.232	0.0725

Conclusions

The monitoring conducted at the Experimental Field has provided insights into the processes controlling herbicide transfers from land to water in the Upper Cherwell catchment. The results suggest that artificial drainage systems serving the heavy clay soils in the catchment transport significant quantities of herbicide to the channel network. This corroborates the key starting hypothesis that drains are the principal pathway for herbicide transfers. In the period immediately after herbicide applications, concentrations in drain water at the Experimental Field increased significantly. Concentrations tended to follow the hydrograph, peaking rapidly and decreasing gradually during hydrograph recession. Concentration peaks tended to occur concurrently with peak discharge, suggesting that transport to drains occurs via rapid pathways (i.e. macropore flow).

Data collected at the experimental site and reported in this chapter will be used for the modelling presented in Chapter 6 and Chapter 7.

Chapter 6 – FIELD-SCALE MODELLING

This chapter reports the application of the MACRO pesticide leaching model to represent field observations (reported in Chapter 5). This could provide a theoretical framework and help understand and interpret processes and mechanisms observed at the Experimental Field. The aim of the MACRO application is to test the hypothesis that macropore flow to drains is a major source of herbicide contamination.

Data collected at the Experimental Field (see Chapter 5) are used in this chapter to prepare and calibrate the model.

6.1 Data sources

6.1.1 Meteorological data

The meteorological data required for the modelling were: hourly rainfall, and daily maximum and minimum air temperature.

Rainfall and air temperature were monitored at the Experimental Field and they were available for the period March 2009 to April 2010. These data were used to calculate potential evapotranspiration (PET), which is required for MACRO to work. PET was calculated using the empirical Hargreaves equation, which is based upon minimum and maximum air temperature and a theoretical solar radiation flux density for the latitude and time of year under consideration (e.g. Hargreaves and Samani, 1985):

$$ET_p = 0.0023 \cdot R_a \cdot (T + 17.8) \cdot \sqrt{T_{max} - T_{min}} \quad (7)$$

where R_a is the incoming extraterrestrial solar radiation flux density (W m^{-2}), T is the air temperature ($^{\circ}\text{C}$) and T_{max} and T_{min} are the maximum and minimum air temperature ($^{\circ}\text{C}$).

6.1.2 Soil data

Data on soil type and properties were obtained from the 1:250,000 Natmap vector data set (National Soil Map: Figure 47). This is a product of the NSRI (National Soil Resources Institute) and represents 297 soil associations within the United Kingdom (www.landis.org.uk [accessed 15th December 2009]). The correspondence between map units and soil associations is shown in Table 16.

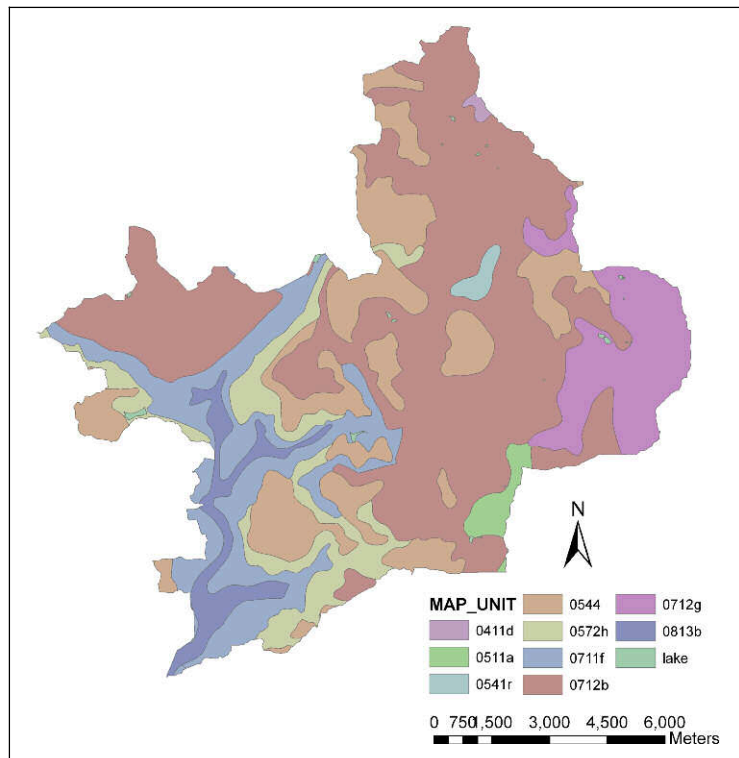


Figure 47 – National Soil Map, scale 1:250,000 (NATMAP vector © Cranfield University and for the Controller of HMSO, 2009).

Table 16 – Description of the soil associations represented in Figure 47 (NATMAP data set).

Map unit	Soil association	Description
0411d	Hanslope	Slowly permeable, calcareous clayey soils
0511a	Aberford	Shallow, locally brashy well drained calcareous fine loamy soils over limestone
0541r	Wickham 1	Deep well drained coarse loamy and sandy soils locally over gravel
0544	Banbury	Well drained brashy fine and coarse loamy ferruginous soils over ironstone
0572h	OxPasture	Fine loamy over clayey and clayey soils with slowly permeable subsoils and slight seasonal waterlogging
0711f	Wickham 2	Slowly permeable seasonally waterlogged fine loamy over clayey, fine silty over clayey and clayey soils
0712b	Denchworth	Slowly permeable seasonally waterlogged clayey soils with similar fine loamy over clayey soils
0712g	Ragdale	Slowly permeable seasonally waterlogged clayey and fine loamy over clayey soils
0813b	Fladbury 1	Stoneless clayey soils, in places calcareous variably affected by groundwater

6.2 Methodology

The main approach which has been taken here was the application of the MACRO model (see Paragraph 2.6.1) to represent drain flow and pesticide leaching at the Experimental Field.

The MACRO pesticide leaching model (version 5.1: http://bgf.mv.slu.se/ShowPage.cfm?OrgenhetSida_ID=5658 [accessed 24th May 2010]) was used to assess pesticide transfers in the soil. MACRO (Jarvis, 1994) has been endorsed by the FOCUS (FORum for the Co-ordination of pesticide fate models and their USE) working group (FOCUS, 2000), and it is submitted as part of pesticide registration dossiers in the European Union to assess the leaching potential for compounds to surface waters via drainage and to groundwater. MACRO has been evaluated in a significant number of studies (e.g. Jarvis *et al.*, 1994; Vanclooster *et al.*, 2000), and was recommended for use within pesticide registration in a comparative study investigating the potential for five preferential flow models to simulate field (Beulke *et al.*, 2001) and lysimeter (Beulke *et al.*, 1998) data (Holman *et al.*, 2004).

The reasons why MACRO was chosen for this study are explained below:

- It accounts explicitly for the transport of materials (solutes and colloids) in macropores (such as shrinkage cracks) which are typically present in heavy clay soils (Figure 48). A dual-permeability model was considered to be necessary to simulate this field situation.
- Among the different types of dual-porosity and dual-permeability approaches used, several are very complicated and require many parameters to describe the water flow. MACRO, which uses the kinematic wave approach (see Paragraph 2.6.1), requires only 10 parameters to describe the porous medium. This makes its application easier, as it is generally hard to obtain this kind of parameters.
- Although two- and three-dimensional modelling approaches should be more appropriate for field situations, they require considerable time (Gärdenäs *et al.*, 2006).



Figure 48 - Photograph of the surface of a Denchworth soil taken on the 27th of July 2009, illustrating the formation of significant cracks at the surface. The mobile telephone is placed for scale and measures approximately 7 cm long by 4 cm wide.

6.2.1 The MACRO model

The MACRO 5.1 model is described here briefly; a full description is given in Larsbo and Jarvis (2003).

MACRO considers non-steady state fluxes of water, heat, and solute for a variably-saturated layered soil profile. Total porosity is partitioned into two flow regions (micropores and macropores), each characterised by a degree of saturation, conductivity, water flow rate, solute concentration, and solute flux density (Larsbo and Jarvis, 2003).

A full water balance is simulated, including treatments of precipitation, evapotranspiration and root water uptake, deep seepage and horizontal fluxes to tile drains (Larsbo and Jarvis, 2003).

Vertical water and solute fluxes are first calculated in the micropores. Updated values of water storages are used to determine the excess amount of water routed to the macropores. Water fluxes originating in the macropores are then calculated and the solute concentrations in both domains which solve the solute balance are derived (Larsbo and Jarvis, 2003).

The Richards equation is used to calculate the vertical movement of water in the micropores:

$$C \frac{\partial \psi}{\partial t} = \frac{\partial}{\partial z} \left(K \left(\frac{\partial \psi}{\partial z} + 1 \right) \right) - \sum S_i \quad (8)$$

where $C = \partial\theta/\partial\psi$ is the differential water capacity (cm^{-1}), θ is the volumetric water content ($\text{cm}^3 \text{ cm}^{-3}$), ψ is the soil water pressure head (cm), t is time (days), z is depth (cm), K is the unsaturated water conductivity (cm day^{-1}), and S_i are source/sink terms for water exchange with macropores, drainage, and root water uptake (day^{-1}).

Soil water retention in the micropores is described by a modified form of the van Genuchten equation (van Genuchten, 1980), whilst hydraulic conductivity is calculated with the Mualem model (Mualem, 1976). A simplified approach is used to describe water flow in macropores, assuming a non-capillary gravity-driven process:

$$\frac{\partial \theta_{ma}}{\partial t} = \frac{\partial K_{ma}}{\partial z} - \sum S_i \quad (9)$$

where θ_{ma} and K_{ma} are the macropore water content ($\text{cm}^3 \text{ cm}^{-3}$) and hydraulic conductivity (cm day^{-1}). K_{ma} is assumed to be a power law function of θ_{ma} :

$$K_{ma} = (K_s - K_b) \cdot S_{ma}^{n^*} \quad (10)$$

$$S_{ma} = \frac{\theta_{ma}}{\theta_s - \theta_b} \quad (11)$$

where K_s is the saturated hydraulic conductivity (cm day^{-1}), K_b is the saturated hydraulic conductivity of micropores (cm day^{-1}), S_{ma} is the macropore degree of saturation ($\text{cm}^3 \text{ cm}^{-3}$), n^* is a kinematic exponent related to the macropore size distribution; θ_s is the saturated volume fraction of liquid phase ($\text{cm}^3 \text{ cm}^{-3}$), and θ_b is the volume fraction of liquid phase at the micropore/macropore boundary ($\text{cm}^3 \text{ cm}^{-3}$).

Water exchange rates between micropores and macropores are calculated as a function of an effective diffusion pathlength (related to aggregate size), d (cm), using an approximate physically-based first-order function, which neglects the influence of gravity and assumes a rectangular slab geometry for the aggregates (Booltink *et al.*, 1993; van Genuchten and Dalton, 1986; Šimůnek *et al.*, 2003):

$$S_w = \left(\frac{G_f \cdot D_w \cdot \gamma_w}{d^2} \right) \cdot (\theta_b - \theta_{mi}) \quad (12)$$

where G_f is a dimensionless geometry factor, D_w is an effective water diffusivity ($\text{cm}^2 \text{ day}^{-1}$), and γ_w is a dimensionless scaling factor to match the approximate and exact solutions to the diffusion problem (van Genuchten, 1985; Gerke and van Genuchten, 1993; Jarvis, 1994).

The top boundary condition for water flow determines the partitioning of net precipitation and/or irrigation between micropores and macropores (Beven and Germann, 1981; Bronswijk, 1988).

The drainage rate for saturated micropore and macropore domains in each layer of the soil profile (q_d [cm day⁻¹]) is calculated using seepage potential theory for layers above drain depth (Leeds-Harrison *et al.*, 1986), and the Hooghoudt equation (Hooghoudt, 1940) for layers below (Larsbo and Jarvis, 2003). Total drain flow is given by the sum of drain flow from both domains.

Percolation to groundwater (i.e. vertical flow out of the bottom layer of the profile), q_{out} (cm day⁻¹), is calculated using the following equation, function of the water table height (H):

$$q_{out} = q_{const} \left(\frac{K}{K_s} \right) \cdot H \quad (13)$$

where q_{const} (day⁻¹) is an empirical parameter controlling percolation to groundwater, K is the saturated hydraulic conductivity (cm day⁻¹) of either macropore or micropore domain in the deepest horizon of the soil profile, and K_s (cm day⁻¹) is the overall saturated hydraulic conductivity in the deepest horizon of the profile.

Solute transport in the micropores is calculated using the convection-dispersion equation:

$$\frac{\partial(\theta_{mi} C_{L,mi} + (1-f)X\rho)}{\partial t} = \frac{\partial}{\partial z} \left(D\theta_{mi} \frac{\partial C_{L,mi}}{\partial z} - qC_{L,mi} \right) - \sum U_i \quad (14)$$

where $C_{L,mi}$ is the concentration of solute in the liquid phase in the micropores (g cm⁻³), f is the fraction of sorption sites attributed to the macropores, X is the content of solute sorbed onto the solid phase (g g⁻¹), ρ is the dry soil bulk density (g cm⁻³), D is the dispersion coefficient (cm² day⁻¹), q is the volume flux of water in soil (cm day⁻¹), and $\sum U_i$ represents the source/sink terms regarding mass exchange between flow domains, solute uptake by crop, solute transformation and losses to drains. Coefficient D is given by:

$$D = D_v \nu + D_0 f^* \quad (15)$$

where D_0 is the diffusion coefficient in free water ($\text{cm}^2 \text{ day}^{-1}$), f^* is the impedance factor for diffusion in the liquid phase (Millington and Quirk, 1961), D_v is the dispersivity (cm), and v is the pore water velocity (cm day^{-1}). In the macropores solute dispersion is neglected because solute transport is assumed to be dominated by convection. The partitioning of reactive solutes between liquid and solid phases is described using the Freundlich isotherm:

$$s = k_f (C_L)^m \quad (16)$$

where k_f is the sorption coefficient ($\text{cm}^3 \text{ g}^{-1}$), C_L is the solute concentration in the liquid phase (g cm^{-3}), and m is the Freundlich exponent.

The rate of solute exchange between micropores and macropores, U_e ($\text{g cm}^{-3} \text{ day}^{-1}$), is given by a combination of a diffusion component and a mass flow component:

$$U_e = \left(\frac{G_f \cdot D_e \cdot \theta_{mi}}{d^2} \right) \cdot (C_{L,ma} - C_{L,mi}) + S_w C_L \quad (17)$$

where D_e is an effective diffusion coefficient ($\text{cm}^2 \text{ day}^{-1}$), $C_{L,mi}$ and $C_{L,ma}$ are mass concentrations of solute in the liquid phase (g cm^{-3}) in micropores and macropores respectively, and C_L is $C_{L,mi}$ or $C_{L,ma}$ depending on the direction of the water flow. D_e is approximated by:

$$D_e = D_0 f^* S_{ma} \quad (18)$$

The loss of solute to drains and to lateral groundwater seepage (U_t [$\text{g cm}^{-3} \text{ day}^{-1}$]) is calculated assuming complete mixing within a flow domain in the horizontal dimensions:

$$U_t = \frac{q_d}{\Delta z} \cdot C_L \quad (19)$$

The solute uptake by roots, U_c ($\text{g cm}^{-3} \text{ day}^{-1}$), is modelled as a passive process as a function of root water uptake and the solute concentration:

$$U_c = f_c \cdot S_r \cdot C_L \quad (20)$$

where f_c is an empirical concentration factor (Boesten and van der Linden, 1991), and S_r is the root water uptake (day^{-1}).

Solute transformation in each soil phase and flow domain is described with first-order kinetics. The actual transformation rate in the field (μ [day^{-1}]) is predicted from a laboratory-measured reference value (μ_{ref}), using reduction factors to account for the influence of environmental conditions (Boesten and van der Linden, 1991):

$$\mu = \mu_{ref} \cdot F_w \cdot F_t \quad (21)$$

where functions F_w and F_t are used to account for the effects of soil moisture and temperature respectively. F_w is given by:

$$F_w = \left(\frac{\theta}{\theta_b} \right)^B \quad (22)$$

where B is an empirical exponent.

The soil temperature function is calculated by a numerical approximation of the Arrhenius equation (Boesten and van der Linden, 1991) modified for low soil temperatures:

$$\begin{aligned} F_t &= e^{\alpha(T-T_{ref})}; & T > 5^\circ\text{C} \\ F_t &= \left(\frac{T}{5} \right) \cdot e^{\alpha(5-T_{ref})}; & 0 \leq T \leq 5^\circ\text{C} \\ F_t &= 0; & T < 0^\circ\text{C} \end{aligned} \quad (23)$$

where T is the soil temperature ($^{\circ}\text{C}$), T_{ref} is the temperature ($^{\circ}\text{C}$) at which μ_{ref} is measured, and α ($^{\circ}\text{C}^{-1}$) is a parameter depending on T , T_{ref} , the gas constant, and the molar activation energy (Boesten and van der Linden, 1991).

The water routed into the macropores is characterised by a concentration C_{ma} (g cm^{-3}), which is calculated assuming complete mixing with solute stored in the soil liquid phase of a shallow mixing depth z_d (cm) at the soil surface (Steenhuis and Walter, 1980):

$$C_{ma} = \frac{Q_s + (PC_p)}{P + (z_d(\theta_{mi,sur}) + (1-f)\rho_{sur}K_f)} \quad (24)$$

where Q_s is the amount of solute stored in z_d (g cm^{-2}), C_p is the solute concentration in the precipitation (g cm^{-3}), $\theta_{mi,sur}$ is the volumetric fraction of liquid phase in the mixing depth z_d ($\text{cm}^3 \text{ cm}^{-3}$), and ρ_{sur} is the dry soil bulk density in the mixing depth (g cm^{-3}).

6.2.2 MACRO calibration

Field data collected at the Experimental Field (see Chapter 5) were used to calibrate MACRO. Model calibration was considered to be necessary in order to ascertain whether MACRO could capture the most important physical processes observed at the field.

The model was calibrated manually.

The approach which was taken here is concentrating on flow to drains first, and then later on herbicide leaching. Therefore the model was first calibrated using the field measurements of drain flow. Subsequently, the calibrated parameters for drain flow were used in a number of simulations run for carbetamide and propyzamide leaching. Results were compared with herbicide leaching measured at the Experimental Field.

As to water balance the calibration process was performed varying three different parameter types (Table 17):

- Soil moisture initial condition;
- Drainage system characteristics;

- Soil physical parameters.

Table 17 –Parameters which were used for the model calibration.

Parameter type	Parameter (unit of measurement)
Initial condition	Initial water content (%)
Drainage system	Depth (m)
	Spacing (m)
Soil physical parameters	Boundary soil water tension (cm)
	Boundary hydraulic conductivity (mm h ⁻¹)
	Boundary water content (%)
	Effective diffusion pathlength (mm)

The initial water content (%) was calibrated first, defining the soil initial condition, and then drain depth and spacing. After that, the soil physical parameters were calibrated simultaneously, which control the boundary between micropores and macropores:

- boundary water content: water content at the boundary between macropores and micropores (i.e. when micropores are saturated and macropores drained);
- boundary soil water tension: the water tension corresponding to the boundary water content;
- effective diffusion pathlength: it controls the exchange of water (and solute) between the two flow domains;
- boundary hydraulic conductivity: the hydraulic conductivity when micropores are saturated and macropores empty (i.e. at the boundary water content).

The calibration process focused on these parameters because Denchworth soils have a high clay content and are known to crack significantly in summer. Although these cracks close up as the soil re-wets in autumn, it is possible that they function as conduits for preferential flow also for some considerable time during the re-wetting period.

Once the model hydrological parameters were calibrated, the same process was performed for solute parameters. In particular the model prediction was evaluated

against herbicide flux, which was calculated using herbicide concentration and drain flow measured at the Experimental Field. The reason why the model was evaluated against herbicide flux instead of concentration is that for the purpose of this work mass losses were considered to be more appropriate than concentrations, which depend on discharge.

The only parameter which was calibrated is K_{OC} , as it was considered the most influential parameter affecting solute leaching, among those required by MACRO.

Simulations were carried out for the period from 1st October 2009 to 31st March 2010. The model was evaluated against drain flow and herbicide flux measured at the Experimental Field during the period 4th October 2009 to 27th December 2009 and 11th February 2010 to 31st March 2010 (subsequently referred to as autumn 2009 and winter 2010).

6.2.3 Simulation characteristics

Simulations were run for the monitoring period October 2009 to March 2010. Each simulation in MACRO was defined for a specific scenario (crop, soil, and climate), weather data, and pesticide (properties and application pattern).

The soil scenario defined represented the Denchworth soil association, which covers the most part of the field. Winter oilseed rape was the considered crop. The climate was defined using the meteorological data collected on site. All the inputs required are shown in Tables 18-20.

As far as chemical parameterisation is concerned (parameters shown in Table 21), the application dates and rates were provided by farm staff for both propyzamide and carbetamide.

The full list of parameter values used in these simulations is reported in Appendix 4.

Table 18 – Soil properties (NATMAP, www.landis.org.uk [accessed 15th December 2009]) used in simulations performed with MACRO (Denchworth soil series).

Horizon	Thickness (cm)	OC (%)	Clay (%)	Silt (%)	Sand (%)	Bulk density (g cm ⁻³)	pH
A	20	2.9	43	40	17	1.17	6.3
Bg1	30	1.2	64	30	6	1.26	6.9
Bg2	20	0.8	64	31	5	1.31	7
BC	30	0.4	58	36	6	1.40	7.4

Table 19 – Crop information (oilseed rape) used in simulations performed with MACRO.

Day of emergence (Julian day) ¹	250
Day of maximum leaf area/root depth (Julian day) ¹⁻³	120
Day of harvest (Julian day) ¹	210
Maximum root depth (m) ²	1.1 (limited by drainage depth to 0.6)
Maximum leaf area (-) ³	3.2
Leaf area at harvest (-)	0.4

¹ Scarisbrick and Ferguson (1995)

² Scarisbrick and Daniels (1986)

³ Behrens and Diepenbrock (2006)

Table 20 - Weather data and site characteristics used in simulations performed with MACRO.

Annual average temperature (°C)	10.52
Average annual amplitude in temperature (°C)	7.71
Latitude (degree)	52
Rainfall correction factor (-) ¹	1
Snowfall correction factor (-) ¹	1
Snowmelt factor (mm/°C/day) ¹	4.5
Ditch/drainage depth for secondary system (m)	1
Residence time for regional groundwater flow rate (days) ¹	0

¹ MACRO default values.

Table 21 – Key properties and application details of the herbicides considered in this thesis.

	Carbetamide	Propyzamide
K_{OC} (cm³ g⁻¹)¹	89	840*

Number of applications per crop	1	1
Day of application	46	311
Application rate (g ha⁻¹)	2100	800
Irrigation amount (mm)	0.03	0.06

¹ www.eu-footprint.org (accessed 13th July 2010)

*modified in the calibration process (see Paragraph 6.4.1)

6.3 Evaluation of MACRO performance

The performance of MACRO was assessed by using the Nash-Sutcliffe efficiency index (Nash-Sutcliffe, 1970), and visually by graphical displays.

The efficiency proposed by Nash and Sutcliffe (1970) is defined as one minus the sum of the absolute squared differences between the predicted and observed values normalized by the variance of the observed values during the period under investigation:

$$NSE = 1 - \frac{\sum_{i=1}^n (y_i - x_i)^2}{\sum_{i=1}^n (x_i - \bar{x})^2} \quad (25)$$

where x_i and y_i are the observed and predicted values at corresponding times, and \bar{x} is the mean of the observed values.

The range of NSE lies between 1.0 (perfect fit) and -1 . An efficiency of lower than zero indicates that the mean value of the observed time series would have been a better predictor than the model.

This criterion is a widely used and potentially reliable statistic for assessing the goodness of fit of hydrological models (McCuen *et al.*, 2006) and it is easy to understand, since it is based on the proportion of the observed variance “explained” by the model. One advantage of the Nash–Sutcliffe index is that it can be applied to a variety of model types. The ASCE Watershed Management Committee (ASCE, 1993) recommends the Nash–Sutcliffe index for evaluation of continuous moisture accounting models. Erpul *et al.* (2003) used the index to assess nonlinear regression models of sediment transport. Merz and Blöschl (2004) used it in the calibration and verification of catchment model parameters. Kalin *et al.* (2003) used the index as a goodness-of-fit indicator for a storm event model. It is also widely used with continuous moisture accounting models (Birikundavyi *et al.*, 2002; Johnson *et al.*, 2003; Downer and Ogden, 2004). The use of the index for a wide variety of model types indicates its flexibility as a goodness-of-fit statistic (McCuen *et al.*, 2006).

However, according to Pappenberger *et al.* (2004) even large time or mass shifts result in still acceptable levels for the Nash-Sutcliffe value. MacLean (2005) reported that the most important shortcoming of the Nash-Sutcliffe statistic is that, because of its definition, it puts more emphasis on extreme events than on average flows.

The model was evaluated also by visual inspection, which can reveal some of the inadequacies of the model which are not so perceptible through the exclusive use of numerical criteria (World Meteorological Organization, 1986). Visual graphical evaluation was based on the simple plotting of two curves (modelled and observed variables).

6.4 Results

6.4.1 Calibrated parameter values

The initial water content is 40% in the first 20 cm. This value was obtained in the calibration procedure. Measured soil water content at 25 cm depth was used for the 20-25 cm layer and extended to the deeper layers (25 cm to 100 cm), for which no measurements were available.

Calibrated drainage system depth and spacing are 0.6 m and 10 m respectively. According to general information about artificial drainage system of the farm where the Experimental Field is, drain depth and spacing should be about 0.7 m and 18 m. However, these values gave very low drain flow, which was inconsistent with field observations. Therefore these values were decreased during the calibration process. It should be noted that the MACRO method of representing drains is only very approximate, as it is a one-dimensional (i.e. vertical) model (Paragraph 6.2.1).

Soil physical parameter values (boundary soil water tension, boundary water content, effective diffusion pathlength, and boundary hydraulic conductivity) are reported in Table 22. Boundary hydraulic conductivity was calibrated for the first layer only (0-20 cm); values calculated using the Pedotransfer Functions (PTFs) implemented in MACRO

were used for the deeper layers. The large boundary water content and effective diffusion pathlength values imply that macropores should play a major role.

Table 22 – Soil physical parameter values.

Horizon	Thickness (cm)	Boundary soil water tension (cm)	Boundary water content (%)	Effective diffusion pathlength (mm)	Boundary hydraulic conductivity (mm h⁻¹)
A	20	10	53	100	0.029
Bg1	30	10	50	100	0.10
Bg2	20	20	49	50	0.098
BC	30	20	46	50	0.12

As to herbicide leaching, a number of simulations were run varying K_{OC} values (Table 23). The first values used were those found in the literature (<http://www.eu-footprint.org/> [accessed on 13th July 2010]). The K_{OC} values which gave the best herbicide flux prediction are 89 dm³ kg⁻¹ (literature value) and 250 dm³ kg⁻¹, for carbetamide and propyzamide respectively. Herbicide losses appeared to be very sensitive to K_{OC} variations, especially in the case of propyzamide. As far as propyzamide is concerned the simulation with a K_{OC} of 840 dm³ kg⁻¹ (i.e. literature value) gave poor prediction of herbicide leaching, which was heavily underestimated (the highest peak was one order of magnitude smaller than measured peak and many minor peaks were missed). A possible explanation might be that field conditions at the Experimental Field during the monitoring activity were different from those reported in the literature. Therefore a smaller value is required to represent field observations. Soil/water/pesticide systems in real conditions exhibit more complex behaviour than in laboratory conditions, because of experimental artefacts and theoretical simplifications.

Table 23 - K_{OC} values used in the model calibration and Nash-Sutcliffe efficiency index.

Herbicide	K_{OC} (dm ³ kg ⁻¹)	Nash-Sutcliffe index
Propyzamide	840*	-0.12
	420	0.34
	250	0.64
	230	0.57
	200	0.30
Carbetamide	89*	0.58
	45	0.45
	40	0.42
	35	0.39
	30	0.36
	10	0.24

*<http://www.eu-footprint.org/> [accessed on 13th July 2010]

6.4.2 Hydrology

The model was evaluated against observed drain flow. Figures 49-50 show modelled and measured drain flow for autumn 2009 and winter 2010 respectively. Nash-Sutcliffe efficiency index is 0.22 for the period October 2009 to March 2010.

Peaks simulated in the period mid-November to mid-December occur at the right time and they are roughly the correct magnitude (Figure 49). However the model does not predict the high peak recorded on 26th of December. A possible reason may reside in the driving data (measured rainfall does not show any intense rainfall event at that time). Also in winter 2010 drain flow is heavily underestimated. Two problems are observed: first, no drain flow is simulated until the 20th February, whereas the monitored drain was flowing at that time; moreover, the model does not represent the high drain flow peak observed on 24th February 2010 (Figure 50). It should be stressed that measured drain flow peaks at the end of February are not reliable. In fact, the flume used to monitor

drain flow in the Experimental Field worked well up to about 0.37 mm h^{-1} ; values above this threshold might be unreal.

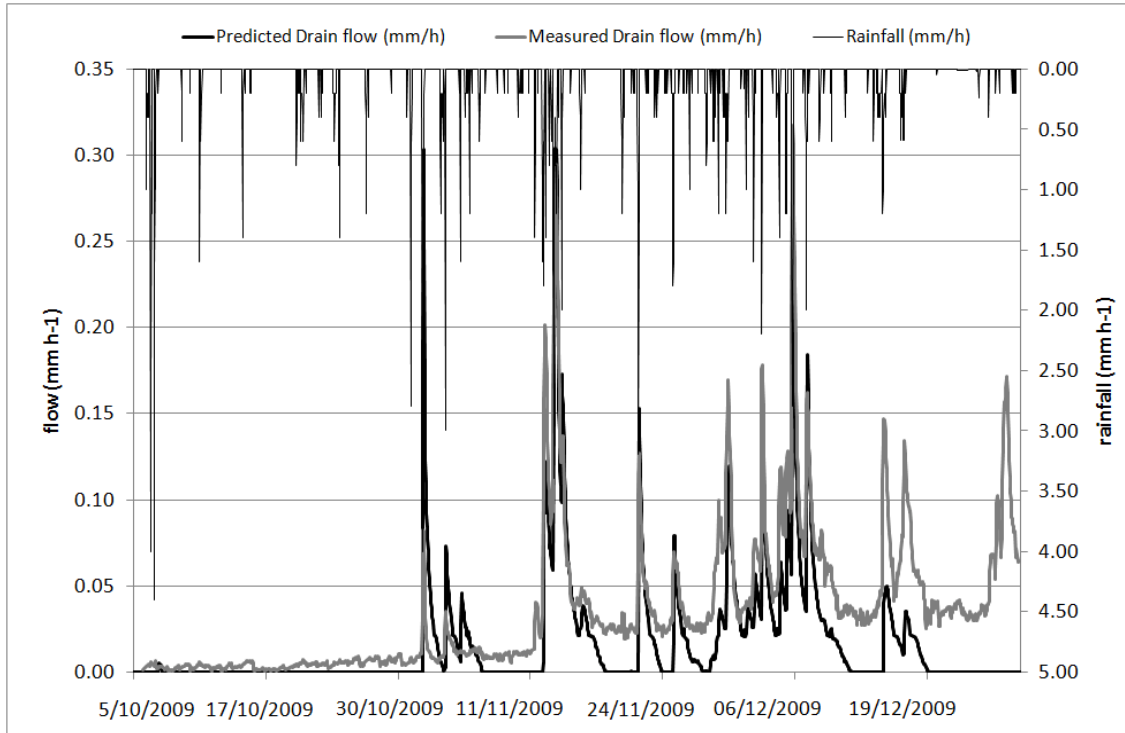


Figure 49 – Predicted (black line) and measured (grey line) hourly drain flow (mm h^{-1}), and measured rainfall (black line, secondary axis); 6th October to 27th December 2009.

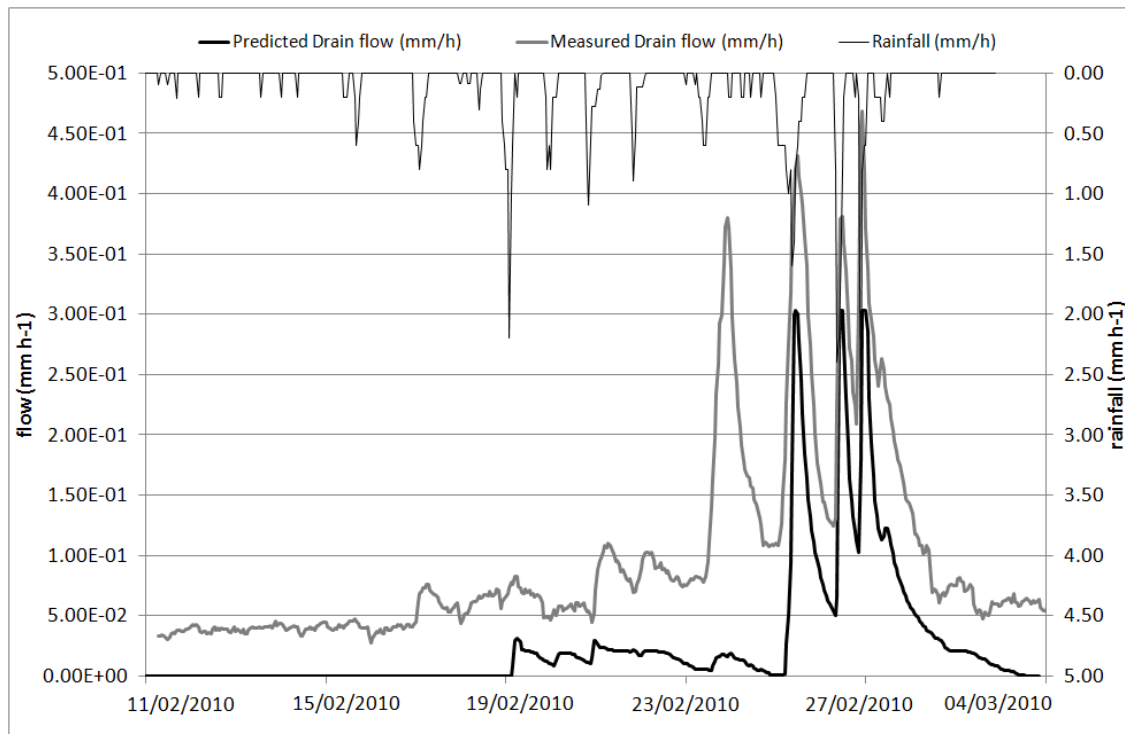


Figure 50 – Predicted (black line) and measured (grey line) hourly drain flow (mm/h), and measured rainfall (black line, secondary axis); 11th February to 4th March 2010.

Figures 51-52 show predicted and measured soil moisture for the first 25 cm of the soil profile. Soil moisture is generally overestimated in the first 20 cm, whereas at 25 cm depth predicted values are close to measurements (estimated values are 96% to 102% of measured values). It should be noted that soil moisture probes were installed at the field edge, where conditions might have been different from the average conditions of the field. In general the Experimental Field seemed to be characterised by spatially variable water content because of its topography and possibly the presence of perched water table.

The model seems to work better during winter (December to February) and worse in the wetting up and drying out periods (November and March). In general the model does not seem to represent the variability which was observed in the field: modelled soil moisture tends to be more homogeneous than observations along the profile.

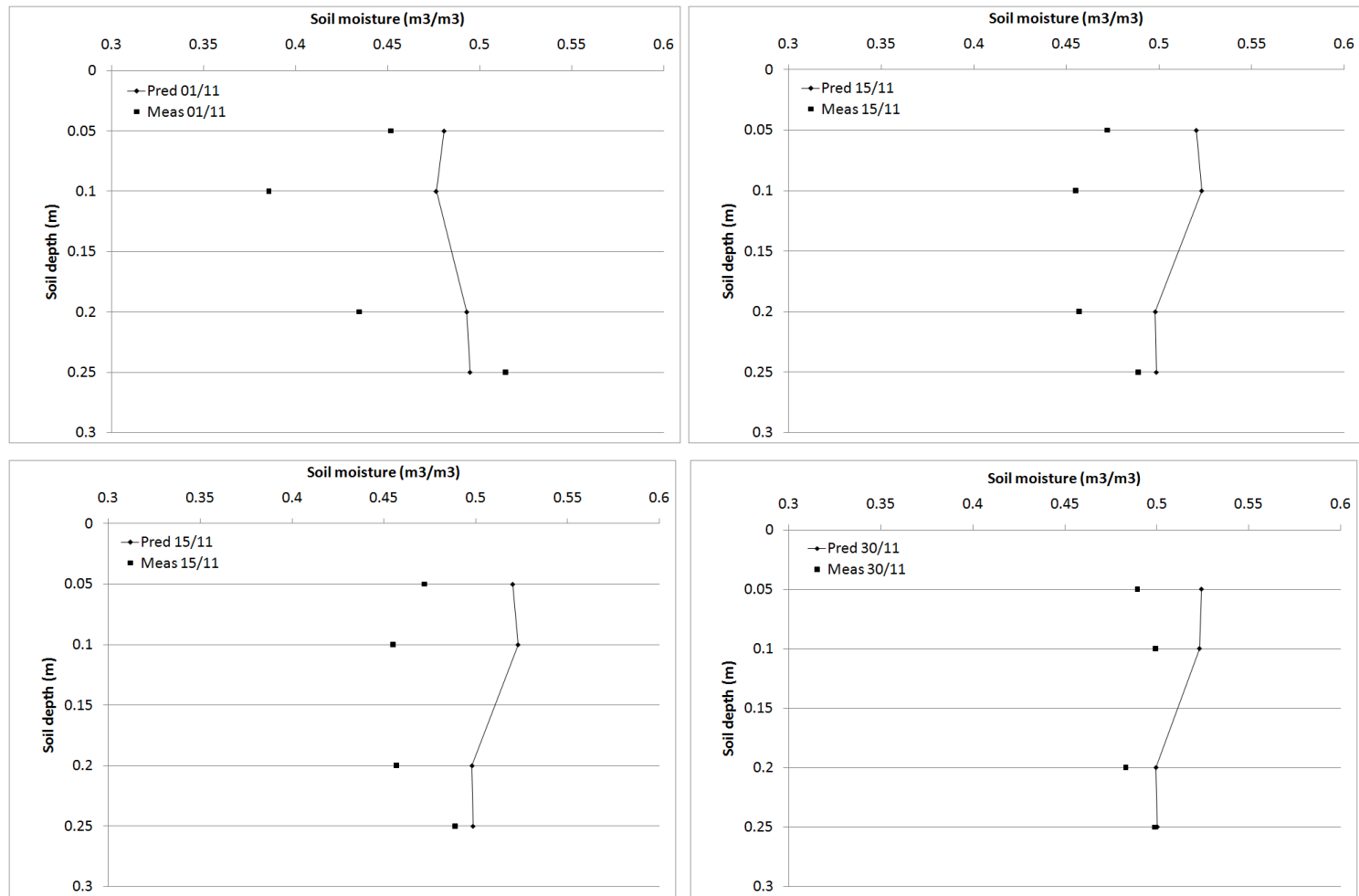


Figure 51 – Predicted (black line) and measured (black symbols) soil moisture ($m^3 m^{-3}$) along the soil profile (0-25 cm) for autumn 2009.

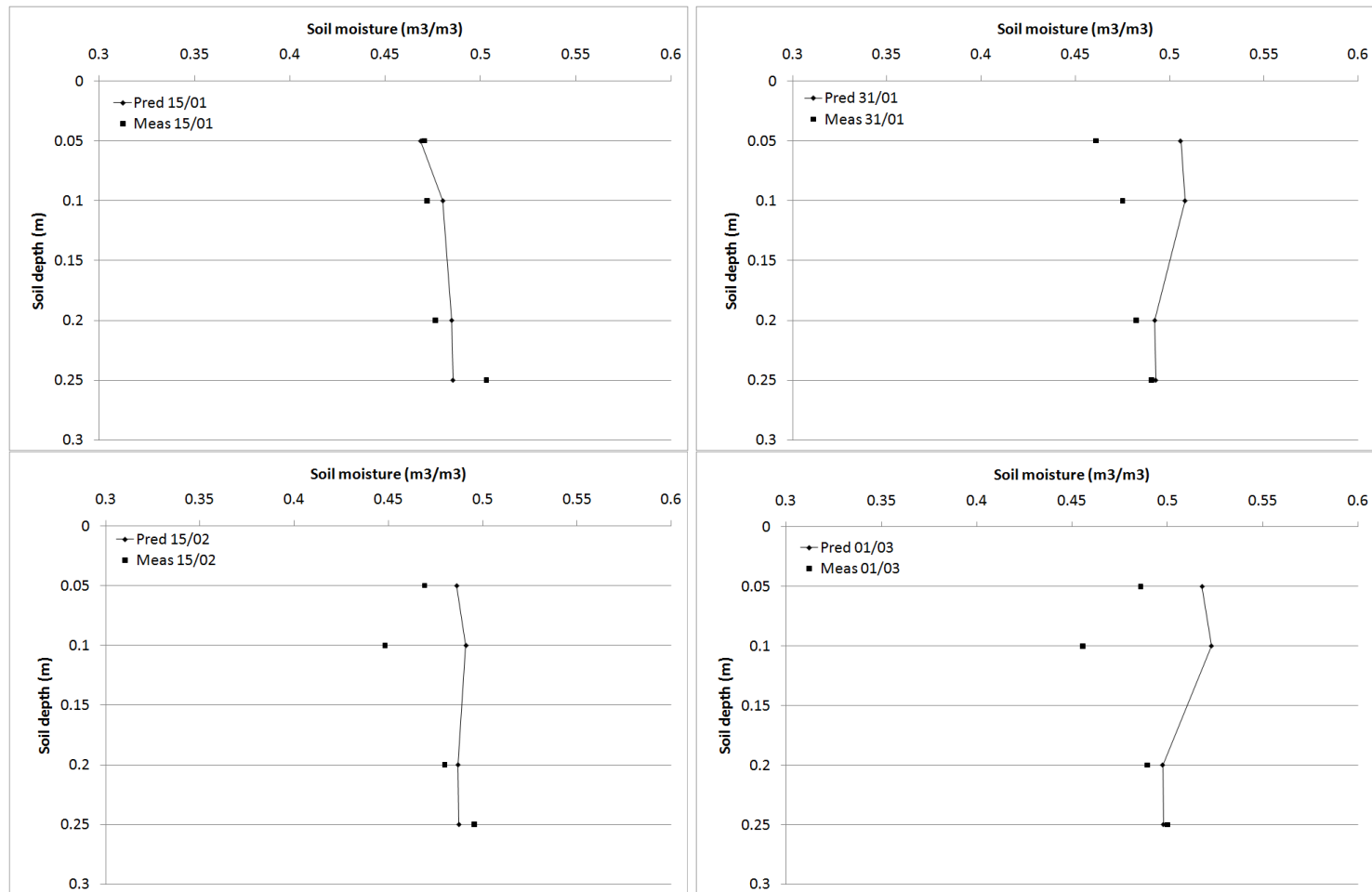


Figure 52 - Predicted (black line) and measured (black symbols) soil moisture ($m^3 m^{-3}$) along the soil profile (0-25 cm) for winter 2010 (daily average values).

Discussion

In general, looking at measured drain flow, an increasing base flow is observed along the monitoring period (from the beginning of October to the beginning of March) (see Paragraph 5.3.1, Figure 36). This phenomenon is not simulated by the model and it may explain the underestimation of drain flow: predicted drain flow over the whole monitoring period is 49 mm (40% of measured drain flow). A possible explanation may be connected to the light soils at the Southern end of the Experimental Field (see Paragraph 5.3.1): base flow from the Banbury soils over Northampton Sands might enter the monitored drain. The cross-section in Figure 53 shows geological strata of the Experimental Field area. Seepages were identified in the field (Figure 54), approximately at the boundary between Upper Lias and Northampton Sands on 30th March 2010, when the rest of the field was already dry. The existence of seepages may be due to a spring, with water flowing from the Northampton Sands intercepted by the drainage system. The quantity of water is likely to be very low during the summer. Measurable flows should start when the soil moisture deficit approaches zero (i.e. November) and flows should increase as more recharge occurs during the winter. There will be peaks in spring flows during periods of very heavy rainfall. The recession may continue for several months after recharge ceases. However, seepages might be also due to limited capacity of the drainage system.

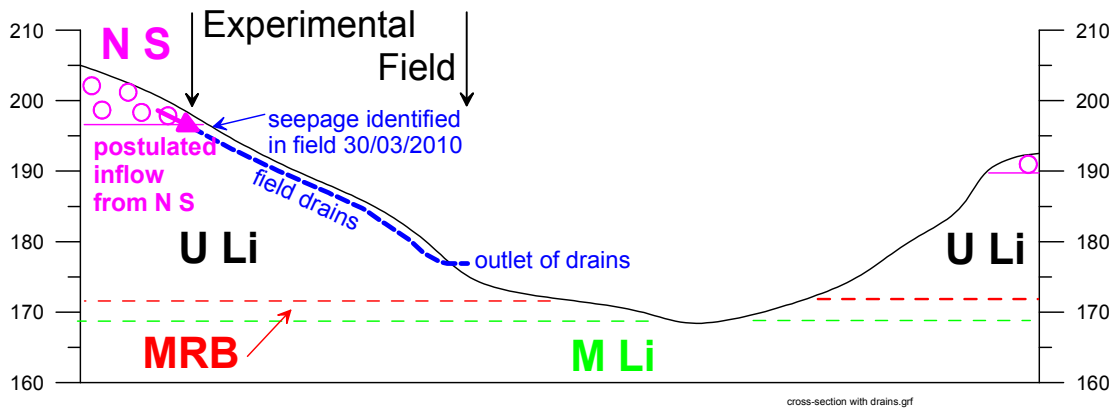


Figure 53 – Cross-section of the Experimental Field: geological strata are shown (British Geological Survey; 1:50,000). ULi = Upper Lias; NS = Northampton Sands; MLi = Middle Lias; MRB = Marlstone Rock Bed. (Ken Rushton, personal communication, 2010) (see Figure 26).



Figure 54 – Seepage observed at the top of Experimental Field on 30th March 2010 (photograph taken by Ken Rushton).

Measured drain flow was therefore used to define a possible base flow originating in the Northampton Sands. Base flow was identified graphically. A number of techniques exist for base flow separation, which vary in complexity (for a review Brodie and Hostetler, 2005; http://www.connectedwater.gov.au/documents/IAH05_Baseflow.pdf [accessed on 23rd September 2010]). These techniques were not considered appropriate for this piece of work, as very little is known about drainage system layout, and it would not be possible to be precise about the way in which any water from the Northampton Sands may enter the drainage system.

Base flow was subsequently added to predicted drain flow and a total flow of 103 mm was obtained, which is about 85% of measured drain flow. In this case Nash-Sutcliffe index is 0.69.

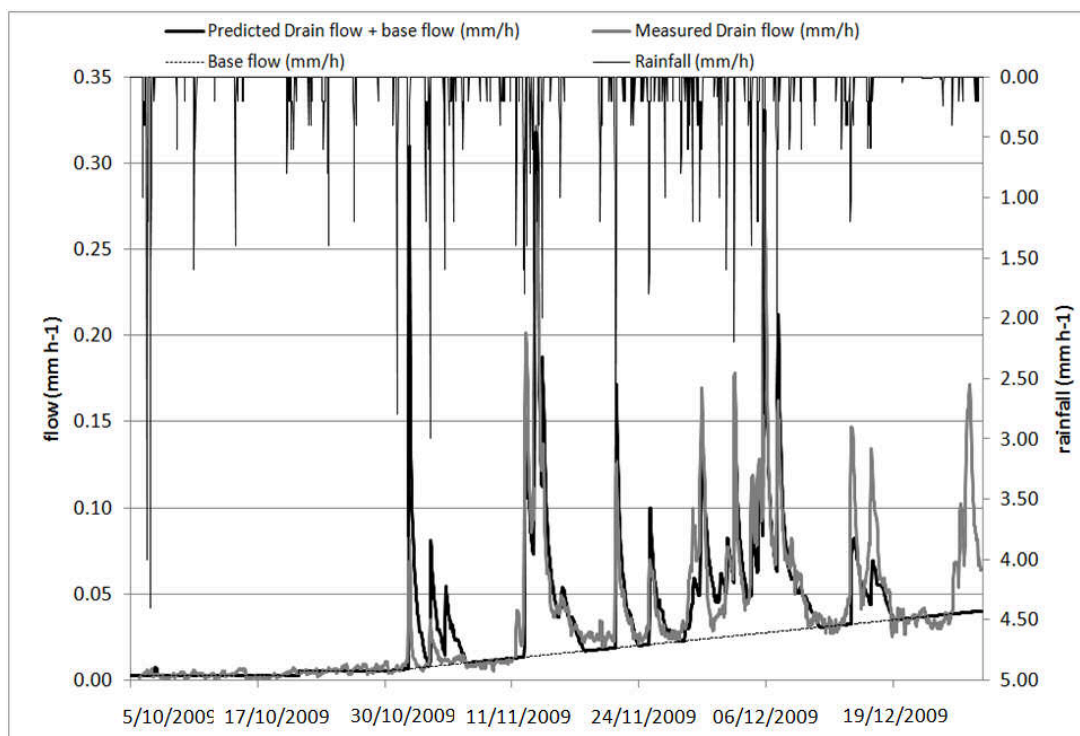


Figure 55 - Measured (grey solid line) hourly drain flow (mm h^{-1}), base flow (black dotted line [mm h^{-1}]), and predicted drain flow plus base flow (black solid line [mm h^{-1}]). Measured rainfall is also shown (black line, secondary axis); 6th October to 27th December 2009.

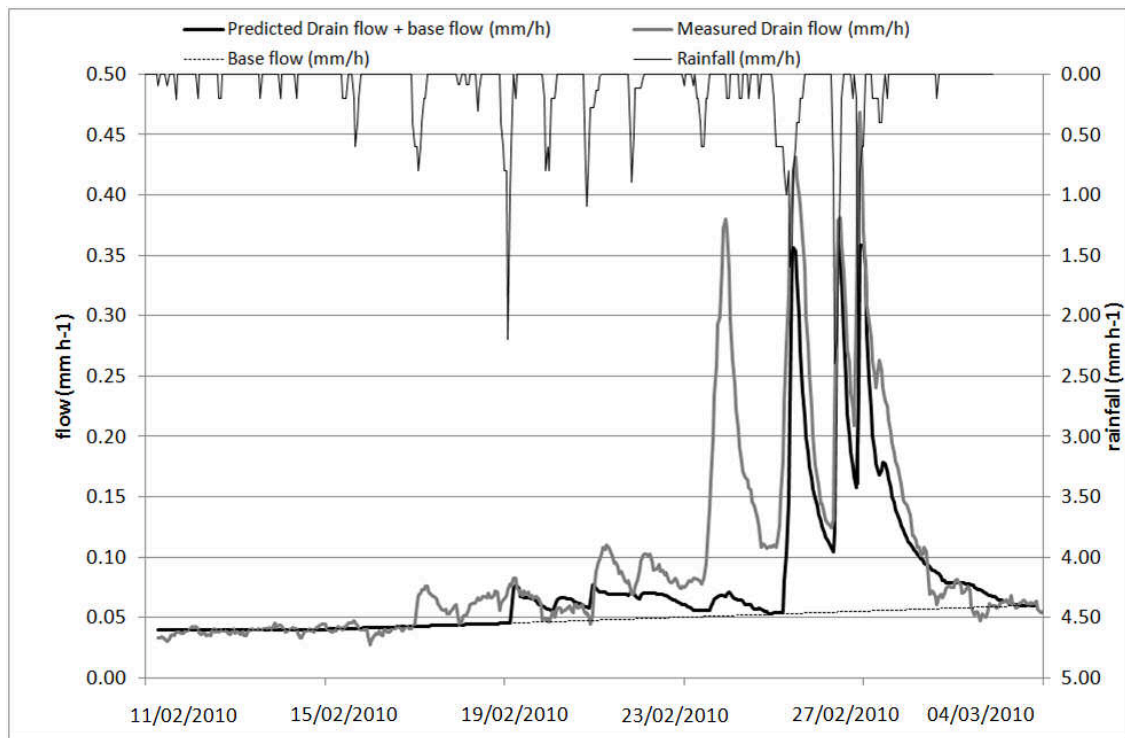


Figure 56 - Measured (grey solid line) hourly drain flow (mm h^{-1}), base flow (black dotted line [mm h^{-1}]), and predicted drain flow plus base flow (black solid line [mm h^{-1}]). Measured rainfall is also shown (black line, secondary axis); 11th February to 4th March 2010.

Conclusions

MACRO represented peaks satisfactorily; only two peaks (observed on 26th December 2009 and 24th February 2010) were not simulated (see Figures 49-50), but this seemed to be connected to driving data, since no heavy rain was recorded, which could trigger drain flow peaks.

Total drain flow was heavily underestimated, as base flow monitored at the field could not be represented by the model. This flow seems to be a second flow component completely separate from the Denchworth soil hydrology (Dick Thompson, personal communication), which may explain why it is not simulated by MACRO. A possible explanation is that seepages from the Northampton Sands present at the top of the Experimental Field enter the drainage system. In fact, when a possible base flow was

added to modelled drain flow a much better agreement between prediction and observation was obtained (Nash-Sutcliffe index of 0.69) (Figures 55-56).

6.4.2 Herbicide leaching

Once the model was evaluated for water flow, the calibrated parameters were used in the model to represent herbicide leaching.

Propyzamide

Propyzamide flux was evaluated against measurements over the period 3rd November to 9th December 2009. The overall performance of the model was considered to be satisfactory: Nash-Sutcliffe index is 0.64. Peaks seem to be represented accurately (Figure 57). The peak observed on 14th November is slightly overestimated ($19.6 \mu\text{g h}^{-1} \text{m}^{-2}$), but the timing is right and the gradual recession following each peak is predicted well.

Note that no herbicide leaching is represented before 14th November. Model prediction could not be improved in this respect, since solute transport to drains occurs only when drains flow, and the model did not predict any drain flow between 7th November (propryzamide application date) and 12th November 2009. This may partly explain the overall underestimation of total herbicide loss: according to the model only 424 μg herbicide are lost over the period November 2009 to March 2010, which is 50.2% of the total loss measured at the Experimental Field.

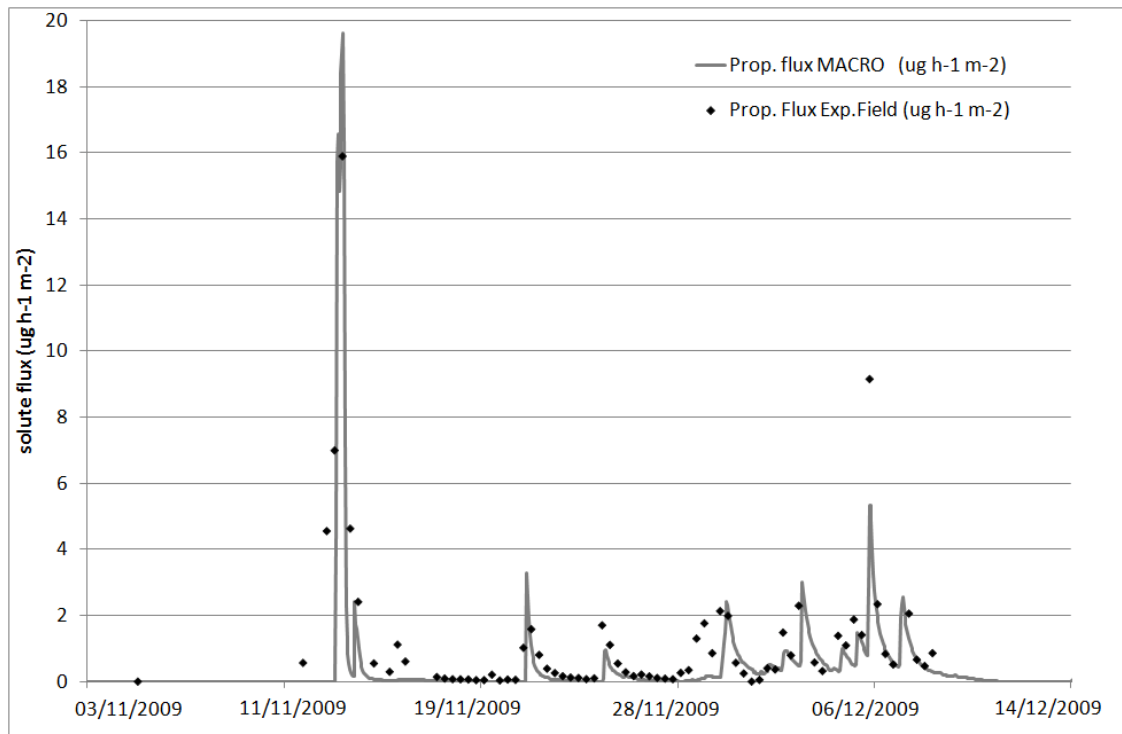


Figure 57 – Predicted (grey line) and measured (black symbols) propyzamide flux ($\mu\text{g h}^{-1} \text{m}^{-2}$); 3rd November 2009 to 14th December 2009. K_{oc} used in the model parameterisation is $250 \text{ dm}^3 \text{ kg}^{-1}$.

Propyzamide transport to drains seems very rapid: about 90% of the chemical lost in the period November – March is leached in the first month after application (Figure 58). Solute flow to drain via micropores starts later after the application (Figure 58); however it appears to play a minor role: only 0.02% ($0.1 \mu\text{g}$) of total loss occurs via micropores. The result suggests that macropore flow is the major pathway for propyzamide transport to drains in the Experimental Field.

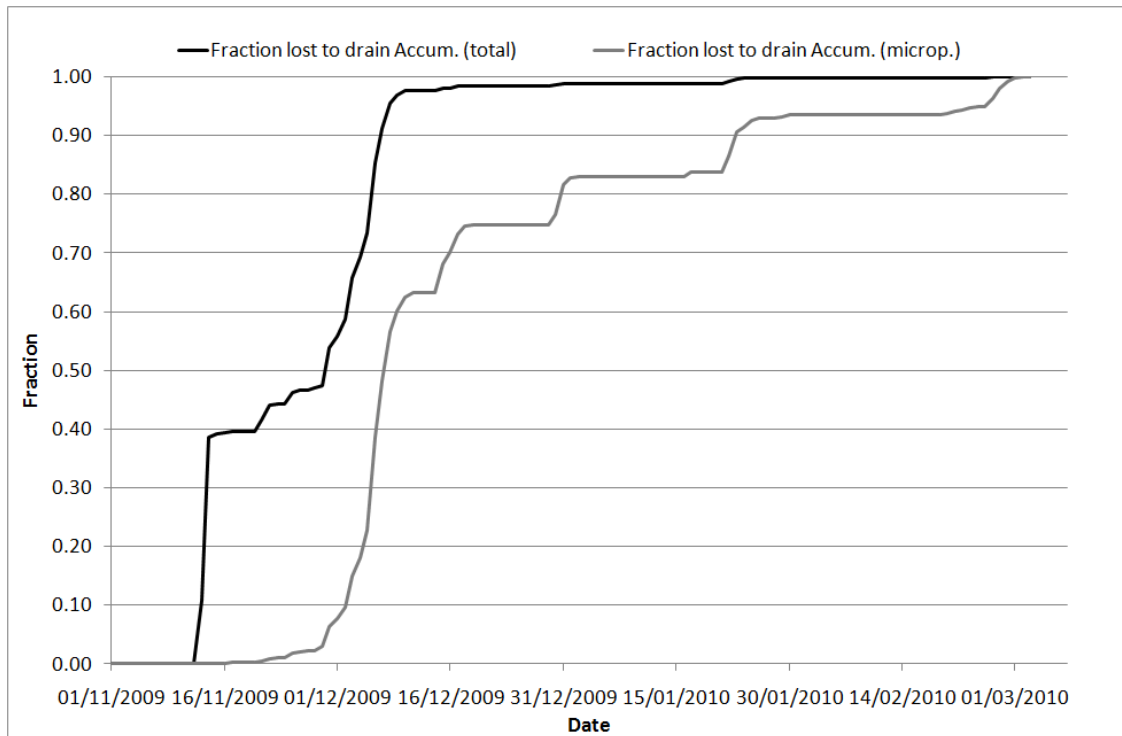


Figure 58 – Accumulated propyzamide loss to drain: total flow (macropore and micropore flows; black solid line), and micropore flow (grey line).

Carbetamide

Modelled carbetamide flux was evaluated against measurements over the period 11th February to 1st March 2010. A Nash-Sutcliffe index of 0.58 was obtained.

Herbicide flux is heavily underestimated from 15th February (day of application) to the end of February (Figure 59). In particular, no herbicide flux is modelled for the period 15th to 19th February, and very low values (order of magnitude of $10^{-2} \mu\text{g h}^{-1} \text{m}^{-2}$) are simulated from 19th to 26th February. This is due to the late start of modelled drain flow (see Paragraph 6.4.2 and Figure 50). Once drain flow starts, though, carbetamide leaching to drains is represented well. The peak observed on 26th February ($260 \mu\text{g h}^{-1} \text{m}^{-2}$ at 10:30 a.m.) is only slightly underestimated ($246 \mu\text{g h}^{-1} \text{m}^{-2}$), and the timing is right (modelled peak occurs at 9:30 a.m., only one hour before the observed peak). On 27th February two peaks were observed (at 10:30 a.m. and 8:30 p.m.; 202 and $299 \mu\text{g h}^{-1} \text{m}^{-2}$ respectively). The morning peak is represented an hour before (at 9:30 a.m.) and it is

overestimated (266 against 202 $\mu\text{g h}^{-1} \text{m}^{-2}$). So the one-hour lag is observed also here, but it is impossible to be conclusive, as it may be that the highest flux during this event occurred at some point between the two water samples collected at 2:30 a.m. and 10:30 a.m. The evening peak is underestimated of nearly one third, and it occurs one hour later than the monitored peak. The model represents the recession at the of February rather accurately, with herbicide leaching decreasing gradually until the beginning of March, when the monitoring stopped (4th March).

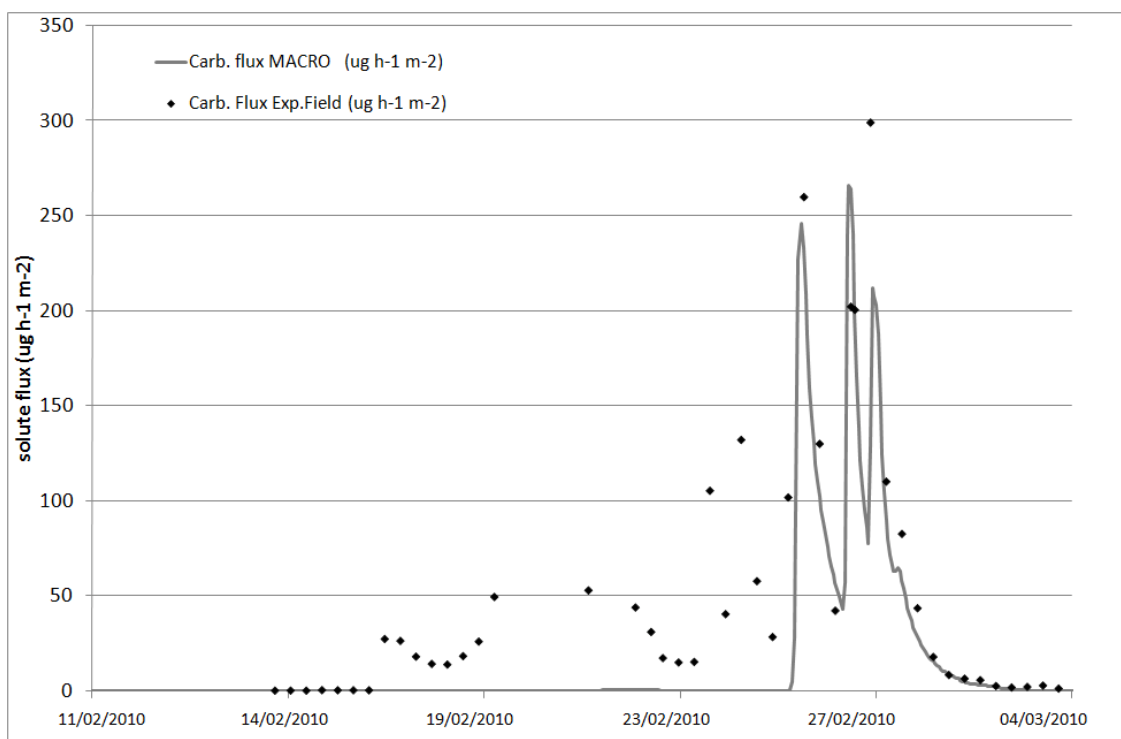


Figure 59 - Predicted (grey line) and measured (black symbols) hourly carbetamide flux ($\mu\text{g h}^{-1} \text{m}^{-2}$); 11th February 2010 to 4th March 2010. K_{oc} used in the model parameterisation is $89 \text{ dm}^3 \text{ kg}^{-1}$.

Predicted herbicide loss is 7710 μg over the period February-March 2010, which is 43% of the total loss measured at the Experimental Field. This may be due to the late start of drain flow modelled by MACRO.

Solute transport to drains appears to be rapid: more than 95% of the total loss occurs by the end of February (Figure 60). Solute flow via micropores and macropores start concurrently. This may result from different soil conditions (i.e. higher soil moisture) compared to November (see Figure 58). Like for propyzamide, microporosity seems to be irrelevant in herbicide transport to drains: only 0.02% (1.42 μg) is lost in micropore flow, which is approximately the same rate as for propyzamide. Also in this case macropore flow seems to be the major pathway for herbicide transport to the artificial drainage system.

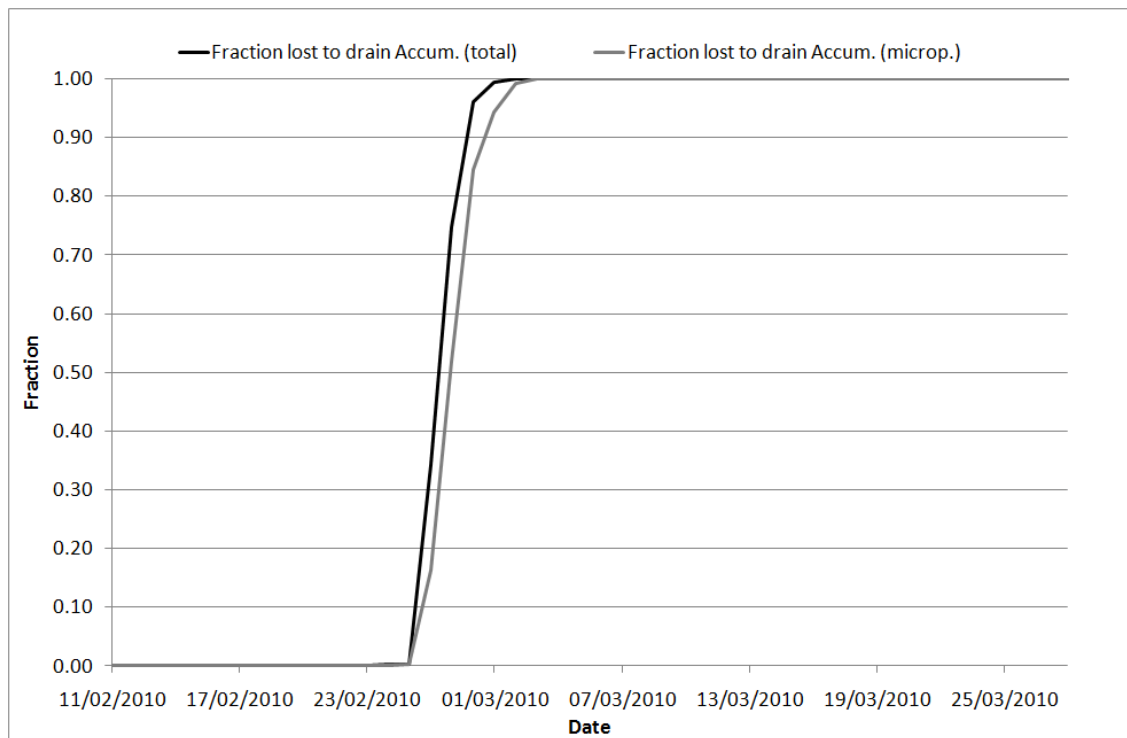


Figure 60 - Accumulated carbetamide loss to drain: total flow (macropore and micropore flows; black solid line), and micropore flow (grey line).

Conclusions

The results suggest that the model predicts herbicide leaching reasonably well. Modelled herbicide flux is not simulated when the drains are not flowing and this is the main reason why overall herbicide leaching is underestimated. When drains are flowing prediction is considered to be satisfactory for the purposes of this thesis.

Both propyzamide and carbetamide seem to peak very soon after the first relevant rain event following application. However carbetamide peaks are 10-fold bigger than propyzamide peaks. This may be due to higher application rate and higher mobility (lower K_{OC}).

According to the model nearly 100% of solute leaching to drains occurs via macropore flow (for both propyzamide and carbetamide). This result supports the hypothesis that the main process responsible of herbicide contamination in heavy clay artificially drained soils is macropore flow to drains.

6.5 Conclusions: is MACRO a valid approach?

The work presented in this chapter demonstrates that MACRO can be a valid approach to represent the substantial processes observed at the field scale. Calibration appeared to be a key step to obtain satisfactory results. This is supported by Dubus *et al.* (2002), who state that only in rare instances a decent description of field data was obtained using 'blind' or 'cold' simulations. Therefore data collection becomes a prerequisite for satisfactory modelling.

According to Dubus and Surdyk (2006) in cases where data for measurements for water, bromide, and pesticide fluxes are available, models tend to be unable to provide a good description to the three variables on the basis of a single parameter set. A satisfactory simulation of soil moisture profiles in the soil may not be linked to a good description of drainage fluxes (Vanclooster *et al.*, 2000). Similarly, a good description of pesticide concentrations in soil and leachate can be obtained despite transport of water through soil profile is not adequately simulated. In this study, MACRO seemed to

represent both drain flow and herbicide losses satisfactorily, using the same parameter set.

The uncertainties of field experiments and data (i.e. uncontrolled field conditions, field-scale variability, reliability of measured data) must be recognised. The drain flow peaks that were not reproduced by the model did not coincide with substantial measured rainfall. Apart from driving data, another problem encountered in the MACRO simulations was connected to the second flow component (base flow), which was observed at the main field drain monitored at the Experimental Field, and which could not be represented by the model. This base flow may come from the lighter soils present in a small portion of the field, on Northampton Sands. Much more information would be necessary to model this component; however base flow was separated graphically from total monitored flow and a much better agreement between observed and modelled was obtained (Nash-Sutcliffe efficiency index equal to 0.69).

As far as herbicide leaching is concerned prediction is considered to be satisfactory. The main limitation is that herbicide flux is not simulated when the drains are not flowing, and this is the main reason why overall herbicide leaching is underestimated and some peaks are not represented.

As MACRO appeared to be a valid approach for representing the most important processes observed at the field scale, it was decided to use it also in the following steps of this study (see Chapter 7). In particular it was used to represent herbicide leaching and flows in different scenarios (i.e. weather data, crops, and soil types), relevant to the Upper Cherwell catchment.

Chapter 7 – CATCHMENT-SCALE MODELLING

Herbicide contamination problems in the Upper Cherwell are strictly connected to the drinking water reservoir in Banbury, where high concentrations (above the DWD MAC) have been detected for years. When this happens, water needs to be treated to ensure that it meets EU standards. Such treatment is very expensive and cannot always cope with high peak pesticide concentrations. Therefore the understanding and the representation of the processes involved in chemical transport from fields to the catchment outlet are a key issue.

It was thought to develop a catchment-scale model, which aims to represent herbicide contamination at the catchment outlet, where water quality is monitored. This model originates from the work presented in the previous chapters (Chapters 5 and 6), which helped understand the processes involved in herbicide transfers at the field scale. The catchment-scale model includes transport along the river network.

One of the difficulties in pesticide fate modelling is that the model developer is often tempted to add description of new processes in their model. Although this can in theory contribute to a better simulation of the observed pesticide behaviour in the field, the addition of extra parameters in the model leads to difficulties in the model parameterisation. Also, the model becomes less suited to extrapolation and large-scale applications (Dubus and Surdyk, 2006). It is therefore important to find the right balance between model complexity and parameterisation problems. The modelling presented in this thesis aims to analyse the opportunities to develop and use simple tools for pesticide fate, both at field and catchment scale.

A simple assumption was made here: the hydrological behaviour of one single field can be observed anywhere in the catchment. Hence, it was assumed that the same hillslope hydrograph and pollutograph could be extended to the whole catchment. The challenge is to see whether this approach is acceptable and this will be analysed in this chapter.

This work is a preliminary analysis, but the attempts to reproduce flows and herbicide losses at the catchment-scale which are presented in this chapter can be a valuable contribution for the development of a more complex model. However, a lot more information would be needed.

The monodimensional pesticide fate model MACRO (described in Paragraph 6.2.1) was considered to be a valid approach to represent field-scale herbicide transport (see Chapter 6). Therefore it was incorporated in this model and used to generate flow and herbicide flux.

7.1 Data sources

7.1.1 Meteorological data

In addition to daily rainfall data (described in Paragraph 4.1.1), daily minimum and maximum air temperature data were obtained from the Radcliffe Meteorological Observatory in Oxford (Table 24) for a 13-year period (1996 to 2008). The simulation period was October 2008 to March 2010, so the temperature time series was extended for the missing period January 2009 to March 2010. A description of the methodology used to produce the data needed is reported in Appendix 5.

Table 24 – Location of Radcliffe Meteorological Observatory, Oxford (<http://www.geog.ox.ac.uk/research/climate/rms/>).

Altitude (m)	63.4
Latitude	51°46' N
Longitude	1°46' W

7.1.2 Soil map

Data on soil properties were derived from the 1:250,000 Natmap vector data set (National Soil Map, NSRI), already described in Paragraph 6.1.2.

7.1.3 Land use and herbicide usage data

The land use information utilised for the modelling at the catchment scale comes from land use statistics from DEFRA (www.defra.gov.uk agricultural census data for 2007 [accessed 7th April 2009]) (Table 25). These data refer to the Local Authority ‘Cherwell’, of which the Upper Cherwell is only a part.

Table 25 – Agricultural land use (DEFRA agricultural census 2007).

Land use	%
Permanent grassland	33.19
Wheat	27.11
Oilseed rape (OSR)	10.29
Temporary grassland	7.72
Set aside	5.97
Winter barley	3.11
Field beans	2.69
Woodland	2.14
Bare fallow	1.88
Rough grazing	1.77
Oats	1.59
Maize	1.43
Peas	0.40
Other arable crops	0.38
Other crop stock	0.10
Potatoes	0.09
Sugar beet	0.04
All other vegetables and salad	0.04
Top fruit	0.02
Small fruit	0.02

In terms of herbicide usage and its timing, most of the information was provided by agronomists working in the catchment and farm staff. In the Upper Cherwell OSR is usually treated to control black-grass. If herbicides were to be banned, OSR production would no longer be effective because of yield losses. The use of propyzamide and carbetamide in the catchment is split in 90% and 10% in favour of propyzamide (Jon Bellamy, TAG agronomist, personal communication, February 2010). According to national-scale statistics 77% of OSR is treated with propyzamide, 23% with carbetamide (FERA, 2008).

Propyzamide is best applied in the last two weeks of November and this is the timing most growers aim for. Carbetamide has a similar optimum timing but it can be used later in the season (January and February) with satisfactory effectiveness. Therefore it tends to be used by growers who have, for whatever reason, missed the optimum timing for propyzamide and so post Christmas. Carbetamide has a latest use up to end of February so it is often used in February as ground conditions improve (Jon Bellamy, personal communication, March 2010).

Propyzamide and carbetamide are also approved on winter beans. In this case, though, the use is split almost in reverse 90%/10% in favour of carbetamide and this is often applied in February. Carbetamide also has some off label approvals on minor crops allowing it to be used, in very specific situations, outside the recommended timings (but within the statutory 8 weeks harvest interval) (Jon Bellamy, personal communication, March 2010).

7.2 Methodology

The catchment-scale model takes into account transport at the field scale first (simulated using MACRO), and then along the river network as pure delay at the catchment outlet. Hillslope hydrographs and hillslope herbicide flux are generated via the MACRO model application (see Paragraph 7.2.1). Water and herbicide transfers from the field to the outlet is based on travel times, which are calculated using stream velocity and area

function. In particular, the area function is used to integrate hillslope responses through the river network to simulate flows and herbicide fluxes at the catchment outlet.

7.2.1 Conceptual model

As far as herbicide transport is concerned, the catchment-scale model takes into account the artificially drained land only, as flow to tile drains appeared to be the main contamination mechanism (see Chapters 5 and 6). The conceptual model is based on the components described below (Figure 61):

- a) Vertical movement from the soil surface down the soil profile (including transport in macropores) to field drains;
- b) Lateral movement in the saturated zone (e.g. along the gradient at the phreatic surface) to the drains;
- c) Movement along the field drain network to reach the surface water network;
- d) Movement along the surface water network to the catchment outlet. Note that only artificially drained land contributes to herbicide transport (white colour in Figure 61d).

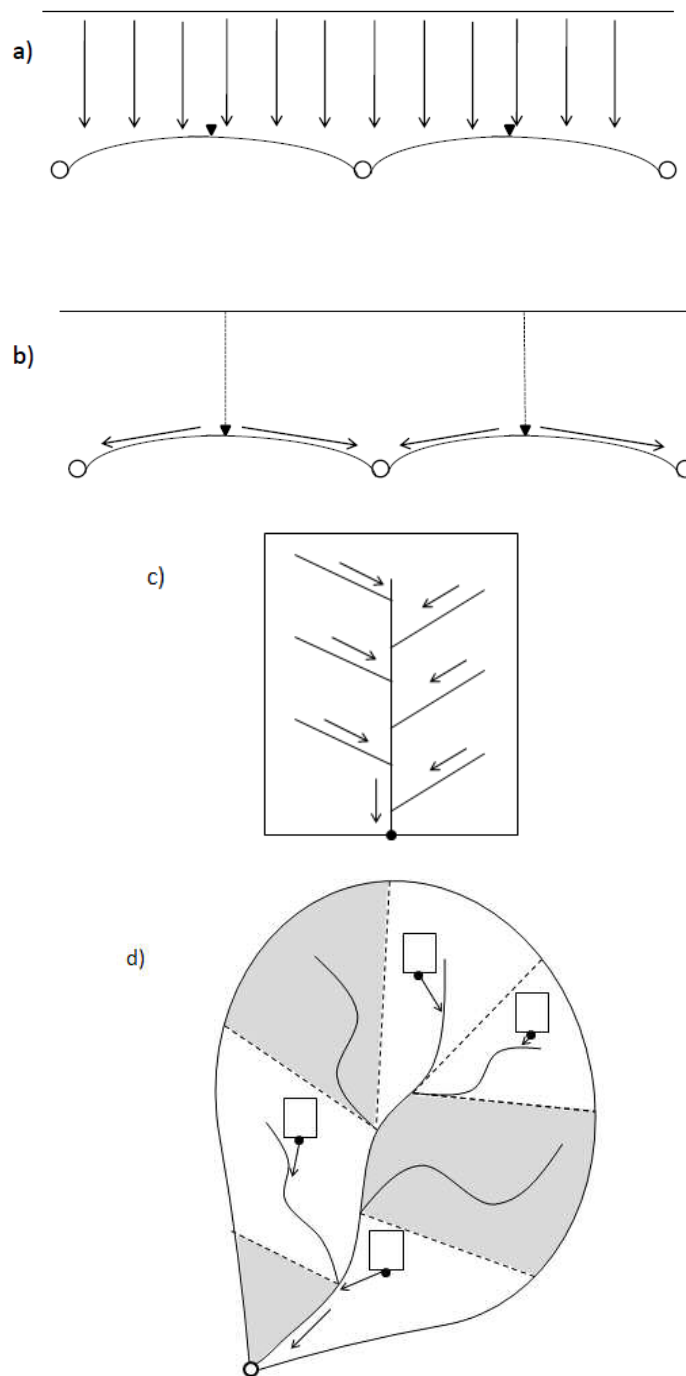


Figure 61 – Conceptual model of pesticide transport from the soil surface to the catchment outlet: a) vertical movement from the soil surface down the soil profile; b) Lateral movement in the saturated zone to field drains; c) movement along the field drains to reach the surface water network; d) movement along the surface water network to the catchment outlet (grey areas do not contribute to pesticide leaching as they are not artificially drained).

As to water flow, the model is characterised by additional components, since more processes are involved. In fact, flow is not generated via the drainage system only. Therefore both artificially drained and undrained areas are included. In undrained land water flow is mainly generated by percolation and overland flow. In artificially drained soils the main mechanism is drain flow, like for herbicide leaching. Movement from the field edge along the surface water network to the catchment outlet is the same for artificially drained and undrained soils and is represented in Figure 62 (see Figure 61d for a comparison).

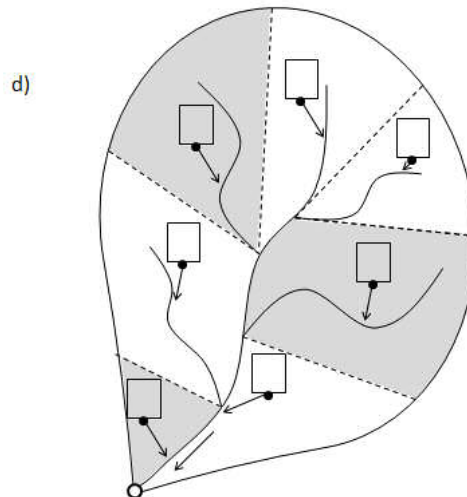


Figure 62 – Water flow: movement along the surface water network to the catchment outlet: the whole catchment contributes to total flow.

7.2.2 Model description

Hillslope hydrographs and hillslope herbicide fluxes to drains are generated via using outputs from the one-dimensional MACRO model application. The following Outputs are from the MACRO model, used to calculate total flows at the field edge, include : drain flow, overland flow, percolation, and flow to the secondary drainage system (i.e. streams, canals, or perimeter field ditches - Larsbo and Jarvis, 2003). In undrained areas, drain flow and flow to the secondary drainage system are not considered (see Paragraph 7.2.1). Herbicide leaching occurs only in artificially drained soils.

Herbicide load (L_i) and concentrations (c_i) at the catchment outlet are calculated as follows:

$$L_i = F_i \cdot A_h \quad (26)$$

$$c_i = \frac{L_i}{Q_i} \quad (27)$$

L_i (g h^{-1}) is calculated from the herbicide flux F_i ($\text{g h}^{-1} \text{m}^{-2}$), (based on MACRO outputs) using the total area treated with herbicide, A_h , (m^2); c_i is calculated using the herbicide load and discharge at the catchment outlet Q_i ($\text{m}^3 \text{h}^{-1}$), also based on MACRO outputs. An hourly simulation time step is used (with i indicating the number of the time step).

Considering the herbicide flux modelling first, the herbicide flux F_i at the catchment outlet is calculated using the following equations:

$$f'_i = \sum_{j=1}^n (f_{j,i} \cdot p_j) \quad (28)$$

$$F_i = \sum_{k=t_0}^{t_{\max}} (f'_{i-k} \cdot p_k) \quad (29)$$

The value $f_{j,i}$ in Equation 28 is the herbicide flux ($\text{g h}^{-1} \text{m}^{-2}$) for the i^{th} hour simulated by MACRO due to a herbicide application on the j^{th} day. p_j is the fraction of the total area that is expected to be treated on that day (p_j can be also seen as the probability of a random field to be treated on the j^{th} day). The probability distribution functions of p_j are reported in Paragraph 7.3.2. The sum of the n values of p_j is 1.0. j starts from 1 (the first possible application day in the simulation period), to n (the last possible application day). So, Equation 28 is used to calculate f'_i , the average herbicide flux at the field edge, from all the artificial drains of the catchment in the i^{th} day.

In the following step transport from the field edge to the catchment outlet is considered. Transport is simulated using Equation 29, where a time delay of k hours is applied to a fraction, p_k , of the flux $f'_{j,i}$. The factor p_k is proportional to the area treated. Times t_0 and t_{max} are minimum and maximum delays respectively (i.e. minimum and maximum travel times). As explained before for p_j , p_k can also be considered as the probability for a random field (treated with herbicide) to have a k -hour travel time. The probability distribution function for p_k is reported in Figures 68-69 and, once again, the sum of all p_k values is 1.0.

Considering Equation 27, Q_i is water flow at the i^{th} hour of the simulation, and it is calculated from the water flow of a single field q_{zi} ($\text{mm h}^{-1} \text{m}^{-2}$). q_{zi} is calculated according to Equation 30 where the subscript z indicates one of the m combinations soil type – crop: different combinations soil type – crop are taken into account, as soil type and crop affect soil hydrological response (see Paragraph 7.3.1):

$$q_{z,i} = df_{z,i} + olf_{z,i} + perc_{z,i} + sdf_{z,i} \quad (30)$$

$$Q_{z,i} = \sum_{k=t_0}^{t_{\text{max}}} (q_{z,i-k} \cdot p_{z,k}) \quad (31)$$

$$Q_i = \sum_{z=1}^m (Q_{z,i} \cdot A_z) \quad (32)$$

where $df_{z,i}$ is drain flow, $olf_{z,i}$ is overland flow, $perc_{z,i}$ is percolation, and $sdf_{z,i}$ is flow to secondary drainage system, All these terms are outputs from a MACRO simulation.

In equation 31 $Q_{z,i}$ ($\text{mm h}^{-1} \text{m}^{-2}$) represents the water reaching the catchment outlet in the i^{th} hour of the simulation generated by each z sub-catchment,. Similarly to Equation 29, $p_{z,k}$ in Equation 31 is the probability of the delay k to occur in each z sub-catchment (i.e. portion of the catchment represented by each combination soil type - crop). k varies between t_0 and t_{max} with hourly time step. Equation 32 sums the flows from each sub-catchment weighted on the corresponding areas A_z (m^2).

Stream velocity

Information about stream velocity is necessary to assess time delay. However no stream velocity measurements were available for the catchment. Velocity varies in relation to discharge. However herbicide transport mainly occurs in correspondence with intense rain events and in these conditions velocity is unlikely to vary dramatically. Therefore this assumption should be a sensible. Velocity was assessed using area function and peak delay, as explained below:

- 1) Area function: it is defined as the distribution of the catchment area with respect to flow distance from the outlet, which is expressed as contributing area per unit distance (Yang *et al.*, 2002). It was derived from the DTM (see Appendix 1, Paragraph A1.1) using an ESRI ArcGIS tool for hydrological spatial analysis. Figure 63 shows the catchment area function.

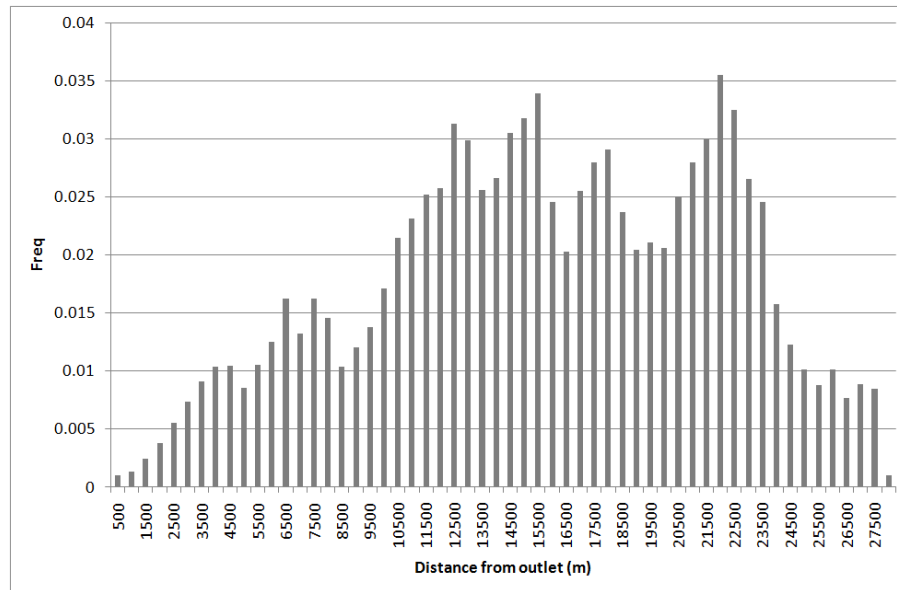


Figure 63 – Catchment area function: distance from the outlet (x axis) is along the river network; the area function is expressed as a frequency distribution.

- 2) Peak delay: for November - December 2009 and February – March 2010 both drain flow measurements at the Experimental Field and discharge measured at Banbury were available. Figure 64 shows drain flow monitored at the Experimental Field and discharge at Banbury (only December 2009 is shown). It is possible to observe that generally peaks monitored at the field (point A) are also observed at the outlet (point B), with a certain lag due to the distance between A and B. 26 peak events of different magnitude were identified on the hillslope hydrograph (point A), with corresponding peak in the hydrograph at the outlet (point B). The observed lags range from 4.67 to 22.17 hours (Table 26).

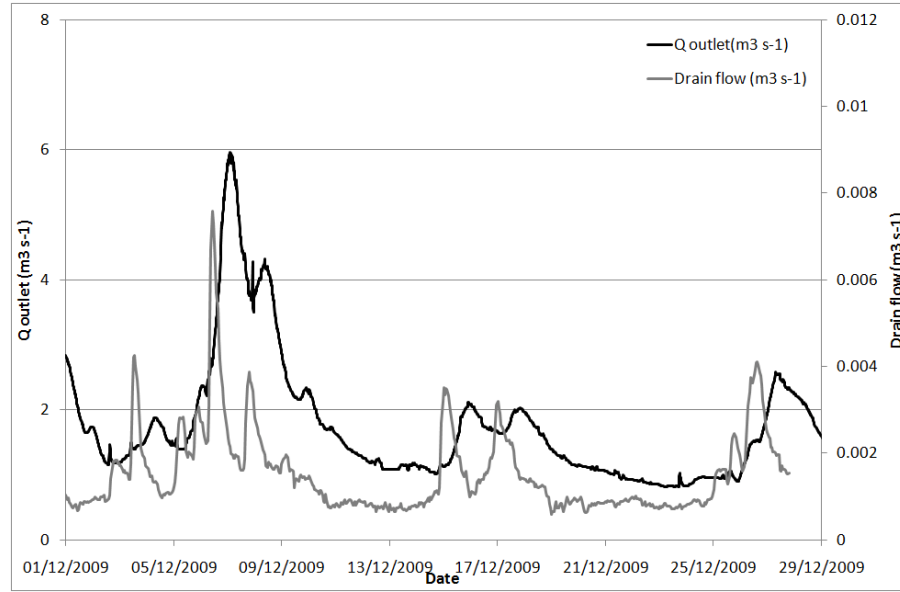


Figure 64 – Discharge measured at the catchment outlet (primary axis [$m^3 s^{-1}$], and drain flow (secondary axis [$m^3 s^{-1}$]) monitored at the Experimental Field.

An average lag of about 13.8 hours was calculated, considering only the events where the ratio of the peak discharges at the field and at the outlet were similar (Figure 66). This means that they were likely triggered by rain events with similar characteristics (i.e. uniform in the whole catchment). The aim was to minimise the chance of using flow peaks in this calculation, which were triggered by local rain events.

The criterion used to identify peaks with similar magnitude is the normalised distance (d) between the two peaks:

$$d = \left| \frac{x_i}{x_{\max}} - \frac{y_i}{y_{\max}} \right| < \alpha \quad (33)$$

where x_i is drain flow (i identifies each one of the peaks considered) ($m^3 s^{-1}$); y_i is discharge measured at the outlet ($m^3 s^{-1}$); x_{\max} and y_{\max} are maximum drain flow measured at the Experimental Field and maximum discharge at the outlet respectively. The parameter α was set equal to 0.15.

Table 26 – Drain flow peaks recorded at the Experimental Field (Q_{field} [$\text{m}^3 \text{s}^{-1}$]), flow peaks at the catchment outlet (Q_{outlet} [$\text{m}^3 \text{s}^{-1}$]), and observed lag (hours).

Day	Time	Q_{field} ($\text{m}^3 \text{s}^{-1}$)	Day outlet	Time outlet	Q_{outlet} ($\text{m}^3 \text{s}^{-1}$)	Lag (h)
12/11/2009	03.40.00	0.0011543	12/11/2009	19.45.00	0.758	16.0833
13/11/2009	3.15.00	0.0047146	13/11/2009	18.30.00	2.16	15.25
14/11/2009	1.05.00	0.0070507	14/11/2009	12.30.00	3.25	11.41667
14/11/2009	1.25.00	0.0075281	14/11/2009	17.00.00	3.58	15.833
16/11/2009	9.30.00	0.0011861	16/11/2009	17.00.00	1.81	7.5
20/11/2009	11.20.00	0.0008905	20/11/2009	16.00.00	1.11	4.67
21/11/2009	20.05.00	0.0032596	22/11/2009	7.30.00	0.818	11.41667
25/11/2009	4.10.00	0.00181	25/11/2009	19.15.00	1.15	15.0833
30/11/2009	6.50.00	0.004426	30/11/2009	23.30.00	2.83	16.667
02/12/2009	17.45.00	0.0019367	03/12/2009	10.00.00	1.5	16.25
03/12/2009	12.00.00	0.0044971	04/12/2009	6.30.00	1.87	18.5
6/12/2009	10.20.00	0.00792	7/12/2009	5.30.00	5.81	19.1667
7/12/2009	19.30.00	0.00401	8/12/2009	9.15.00	4.32	13.75
15/12/2009	0.05.00	0.00388	15/12/2009	22.15.00	2.12	22.167
17/12/2009	0.00.00	0.00344	17/12/2009	15.15.00	2	15.25
26/12/2009	14.00.00	0.00436	27/12/2009	7.30.00	2.58	17.5
17/02/2010	15.58.25	0.00181	18/02/2010	7.15.00	1.77	15.25
21/02/2010	22.12.25	0.0026677	22/02/2010	14.45.00	5.96	16.5
22/02/2010	20.02.25	0.002447	23/02/2010	7.30.00	3.02	11.5
24/02/2010	17.42.25	0.0094218	25/02/2010	1.00.00	4.88	7.28
26/02/2010	8.32.25	0.010677	26/02/2010	15.00.00	2.92	6.5
27/02/2010	11.27.25	0.0083313	27/02/2010	23.00.00	10.2	11.5
27/02/2010	20.27.25	0.0117907	28/02/2010	11.15.00	10.6	14.78
25/03/2010	3.52.25	0.0058123	25/03/2010	12.15.00	3.9	8.367
25/03/2010	17.47.25	0.0023484	25/03/2010	23.45.00	6.27	6
27/03/2010	3.17.25	0.0019801	27/03/2010	9.15.00	3.36	6

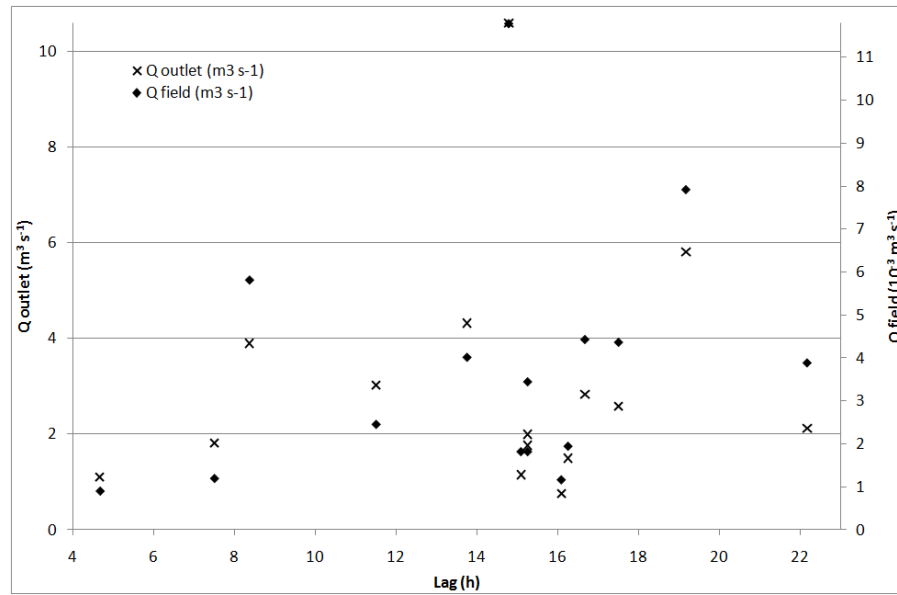


Figure 65 – Discharge at the catchment outlet ($m^3 s^{-1}$)(primary axis), and drain flow measured at the Experimental Field ($10^{-3} m^3 s^{-1}$) with respect to the observed lag (hours). Only peaks with similar magnitude are shown ($\alpha < 0.15$).

Note that x_i (in Equation 33) is drain flow (i.e. discharge monitored at the drain pipe outlet) whereas y_i is total discharge. However in artificially drained soils drain flow is usually the main contribution to total flows. It was therefore assumed that the two data series could be compared.

The calculated lag is used to estimate velocity. It should be noted that velocity calculated here is likely closer to wave celerity (i.e. the speed at which a peak moves between two points) than to stream velocity, but no sufficient information was available to estimate the possible difference between stream velocity and wave celerity. However, this difference is expected to be small, and it was therefore decided to assume they were alike, and no distinction was made between the two.

Figure 66 shows the data points used for the estimation of the average delay.

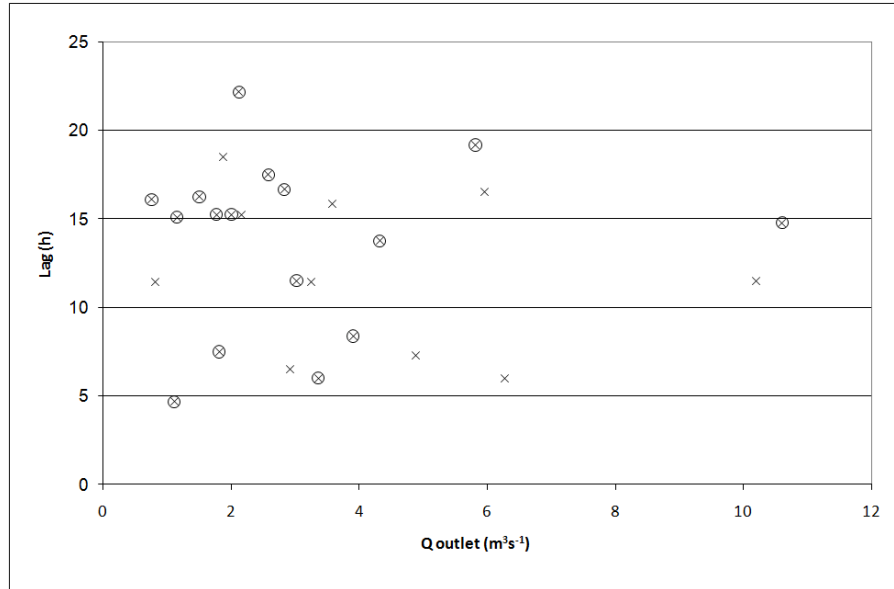


Figure 66 – Discharge at the catchment outlet ($m^3 s^{-1}$) on the x axis, and time delay (hours). All the peaks are shown: the ones with similar magnitude ($\alpha < 0.15$) are marked with a circle.

This lag refers to the Experimental Field, which is in the Northern edge of the catchment and it is the average time required to water to go from the field to the catchment outlet. Assuming uniform rainfall in the whole catchment, 13.8 hours after a rainfall event, water draining from this field would arrive at the outlet. This discharge would be in the tail of the hydrograph, since most part of the catchment is closer to the outlet than the Experimental Field.

The hypothesis on which this work is based is that this field is representative of all the clay soils in the catchment and so any clay field would have the same behaviour and the same hydrograph. Therefore, in order to calculate velocity, it was decided to hypothesise that the hydrograph monitored at the Experimental Field was observed at the weighted average distance from Banbury (15.7 km along the river network). In this way discharge draining out of this field would arrive at the catchment outlet during the peak of the hydrograph. The average weighted distance (expected value E) was derived from the area function (Figure 63), and it was calculated as follows:

$$E = \sum_{i=1}^n \left(\frac{A_i}{A} \cdot X_i \right) \quad (34)$$

$$A_i = F_i \cdot x \quad (35)$$

$$A = \sum_{i=1}^n A_i \quad (36)$$

where X is the distance from the outlet, which can be divided into n equal distances (x); X_i is therefore the distance from the outlet at each step x . A_i is the area calculated multiplying x by the portion of the catchment which is at the distance X_i from the outlet; and A is the total area. Figure 67 gives a graphical interpretation of this procedure.

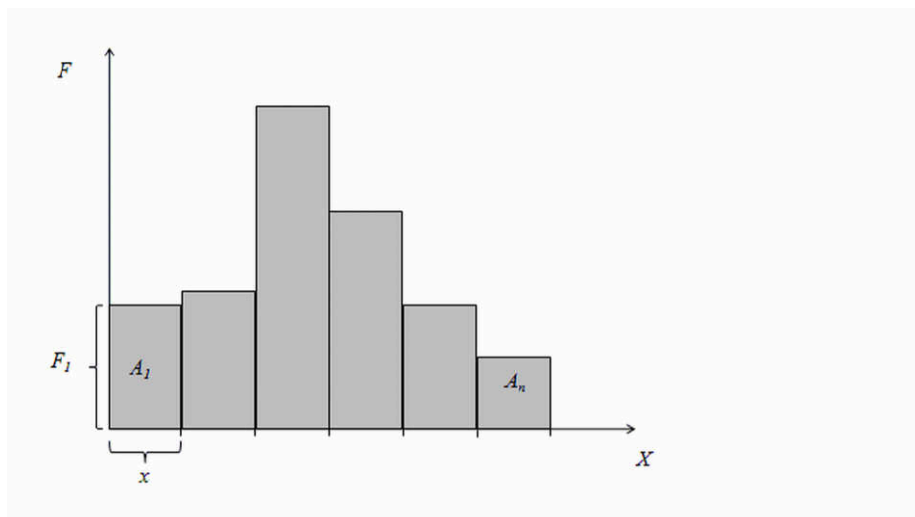


Figure 67 – Area function: X is the distance from the outlet and it is divided in n equal distances (x). At each distance from the outlet X_i corresponds an area F_i .

Hence it can be assumed that - on average - water moves along a distance of 15.7 km in 13.8 hours time. The following equation was therefore used to calculate stream velocity (v) (i.e. the speed at which a certain distance is travelled):

$$v = \frac{E}{l} \quad (37)$$

where l is the average lag and E is defined in Equation 34. Stream velocity v was calculated to be equal to 0.32 m s^{-1} .

Travel times

The area function was also used, together with stream velocity, to integrate hillslope hydrographs and herbicide fluxes. The catchment was divided into two sub-catchments characterised by different hydrology and therefore different hydrographs. One of them includes Banbury soil areas only; the second one all the other soils, which are clay. Area functions were calculated for each sub-catchment (Figures 68-69). Note that the catchment was divided into two subcatchments only and not four as the number of combinations soil type – crop, as land use is hypothesised to be uniformly distributed.

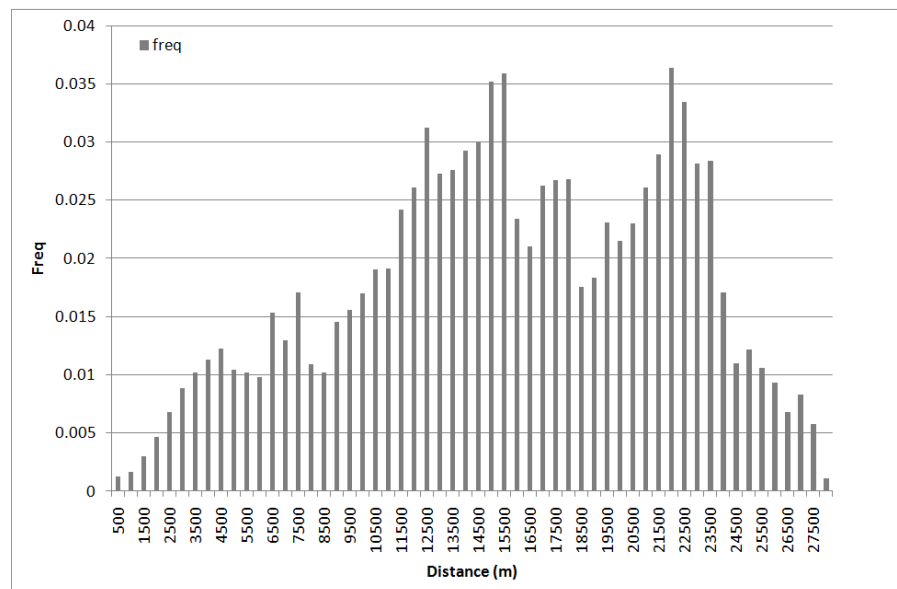


Figure 68 – Area function for all the clay soil areas in the Upper Cherwell catchment.

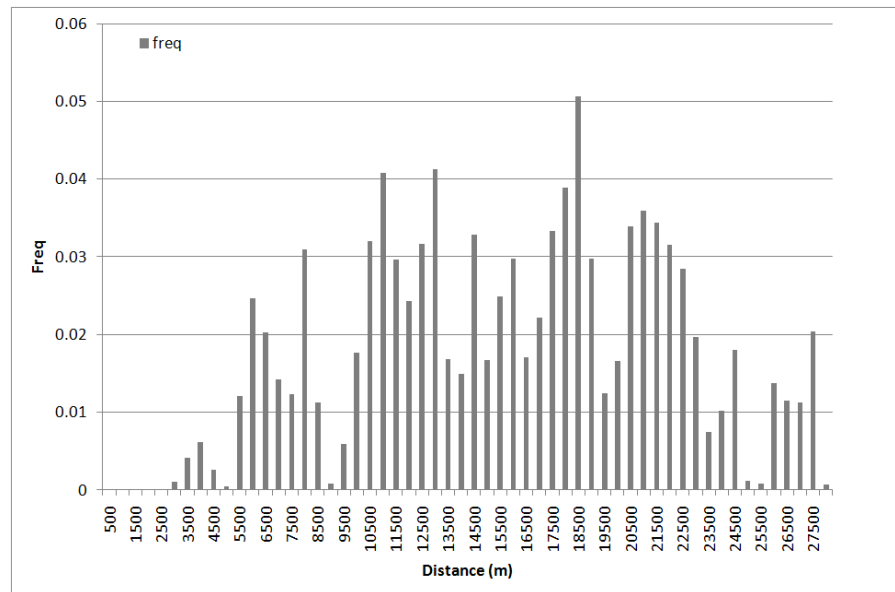


Figure 69 – Area function for Banbury soil areas in the Upper Cherwell catchment.

Travel times (T_D) (i.e. the delay k in Equations 29 and 31) were calculated using the following equation (Kent, 1972):

$$T_D = \frac{D}{v} \tag{38}$$

where D are the hydraulic distances from the outlet (i.e. along the river network), which are given by the area function, and v is stream velocity.

Then it was possible to generate an analogous frequency distribution for travel times. An hourly time step was used. The maximum travel time is 25 hours.

7.3 Simulation characteristics

The simulation period is October 2008 to March 2010, which was split into two seasons: October 2008 to September 2009, and October 2009 to March 2010 (subsequently referred to as first season and second season respectively). The second season is shorter because meteorological and hydrological data were collected only until end of March 2010. Simulations were run with an hourly time step.

7.3.1 Hillslope responses

Water flow simulations

A number of simulations were run for different soil types and crops, since all soils and land uses contribute to flow generation. In particular, two soil types and two crops were identified.

The soil associations simulated are: Denchworth, which covers about 37% of the catchment and was considered to be representative of all clay (underdrained) soils, and Banbury, which covers about 21% of the total catchment area and is characterised by a completely different hydrology as it is light sandy loamy without waterlogging problems (undrained soils). Water which passes through these soils usually enters an aquifer and it can take weeks or months for the water to exit from springs on the edge of these aquifers.

Two representative crops were chosen, an annual arable crop and a permanent one. The most interesting crops were considered to be: permanent grassland, which covers 33.19% of the agricultural area, and OSR, which represents 10.29% of the total agricultural area. Permanent grassland was assumed to represent all grassland areas (permanent grassland, temporal grassland, and other grazing areas) (42.68%); OSR was considered as representative of all other agricultural land uses. Winter cereals (31.81%) could also have been simulated as they are widespread in the catchment but it was decided to limit the number of crops for simplicity's sake. Permanent grassland and OSR were hypothesised to be uniformly distributed in the catchment since no up-to-date information about spatial distribution was available.

Parameters for Denchworth soils and OSR are reported in Chapter 6 (Tables 18-19); parameters for Banbury soils and permanent grassland (i.e. a mixture of ryegrass and white clover) are shown in Tables 27-28.

A simulation was run for each combination of soil type and crop (i.e. 4 simulations; m in Equation 31).

Table 27 – Soil properties (NATMAP, www.landis.org.uk [accessed 15th December 2009]) used in simulations performed with MACRO (Banbury soil series).

Horizon	Thickness (cm)	OC (%)	Clay (%)	Silt (%)	Sand (%)	Bulk density (g cm ⁻³)	pH
A	25	1.9	25	30	45	1.32	6.8
Bw1	25	0.8	24	31	45	1.33	7.5
BC	20	0.3	20	23	57	1.48	7.7

Table 28 – Crop information (permanent grassland) used in simulations performed with MACRO.

Root depth (m) ¹	0.7 (limited by the profile depth)
Leaf area (-) ²	2
Height (m) ¹	0.3

¹ Allen et al. (1998)

² Woledge et al. (1989)

Herbicide leaching simulations

A set of MACRO simulations was defined for herbicide leaching according to the following assumptions:

- Herbicide flux is generated only from heavy clay soils, which are represented by the Denchworth soil association (see Table 17 for parameters). This assumption is supported by some preliminary simulations of herbicide leaching in Banbury soils, which gave low predicted concentrations (order of magnitude of 10^{-13} $\mu\text{g l}^{-1}$). This is because water is assumed to freely percolate through the soil matrix, which provides significant opportunities for

adsorption to soil solids and reduces dissolved concentrations in the mobile pore volume. It should be noted that MACRO was not calibrated for Banbury soils due to lack of data;

- All Denchworth soils are artificially drained (no artificial drainage maps were available, but generally heavy clay soils are underdrained in order to cope with waterlogging problems);
- A number of application dates were defined for each one of the chemicals investigated (propryzamide and carbetamide), and simulations were run for each application date: the application timing was restricted to November - December for propryzamide and January - February for carbetamide; herbicide application could not take place in wet days (rainfall above 5 mm d⁻¹), as it is generally recommended not to spray on rainy days. A probability distribution of application dates was defined for each chemical (see Paragraph 7.2.2), giving the probability of an application to occur on each possible date;
- Propryzamide and carbetamide were assumed to be applied only on OSR, which was therefore the only parameterised crop for these simulations (they can be used also on field beans and other minor crops but these cover a very small area in the catchment and were considered to be negligible).

All the simulation properties and parameters are the same of the ones reported in Chapter 6 for the Experimental Field, apart from the meteorological input data. For the catchment-scale model data measured at the catchment outlet were used instead of those measured at the Experimental Field (Paragraphs 4.1.1 and 7.1.1).

For each chemical a number of simulations were run equal to the number of possible application dates (j). Hence, for each simulation a herbicide flux series (f_j) was obtained.

7.3.2 Transport to the catchment outlet

Water flow simulations

Simulations were run using both the redefined catchment area (129 km²; see Appendix 2), and the original catchment area (199 km²). It must be noted that the area function

generated for the 129-km² catchment was used for both simulations, assuming that the soil type distribution in the 70 km² difference was approximately the same of the rest of the catchment.

Herbicide leaching simulations

Herbicide leaching simulations were performed for the period October to March for both seasons, since propyzamide and carbetamide are mainly transferred between autumn and spring. Two sets of simulations were run, considering either a 1- or 2-month window for herbicide application. These will be subsequently referred to as *sim1* and *sim2*, respectively. Each application date was given a probability to occur; the probability distribution was constant within each week and varying from week to week; wet days (rainfall above 5 mm d⁻¹) were *a priori* removed from the possible application dates. Note that it was assumed that application could take place on Saturdays, Sundays, and holidays with the same probability of working days. For the 1-month application window (*sim1*) the following patterns were used:

- A 1-2-3-3 pattern for November: propyzamide tends to be applied in the last two weeks of November (Jon Bellamy, personal communication, March 2010) but the 1st and 2nd weeks were also included, as early applications can occur (see Experimental Field in 2009);
- A 1-2-2-1 pattern for February: carbetamide tends to be applied in February (Jon Bellamy, personal communication, March 2010); no more precise information was available. A normal distribution with higher probability on the 2nd and 3rd weeks was chosen.

For *sim2* the application window was extended, as herbicide application timing is characterised by high variability. The 2-month application window is November – December and January – February for propyzamide and carbetamide, respectively. Probability distributions (for the first season only) are shown in Figures 70-71.

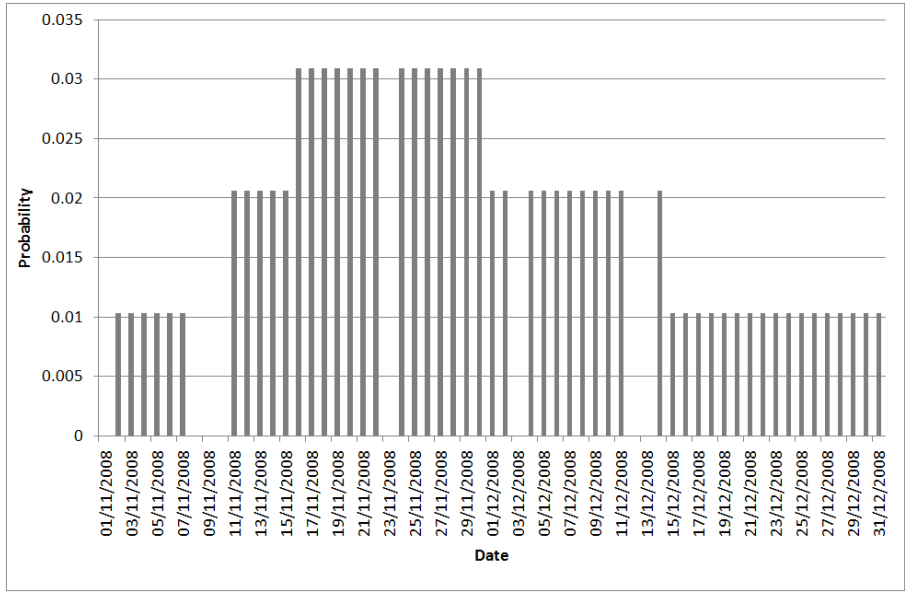


Figure 70 – Probability density function for propyzamide application in November - December 2008.

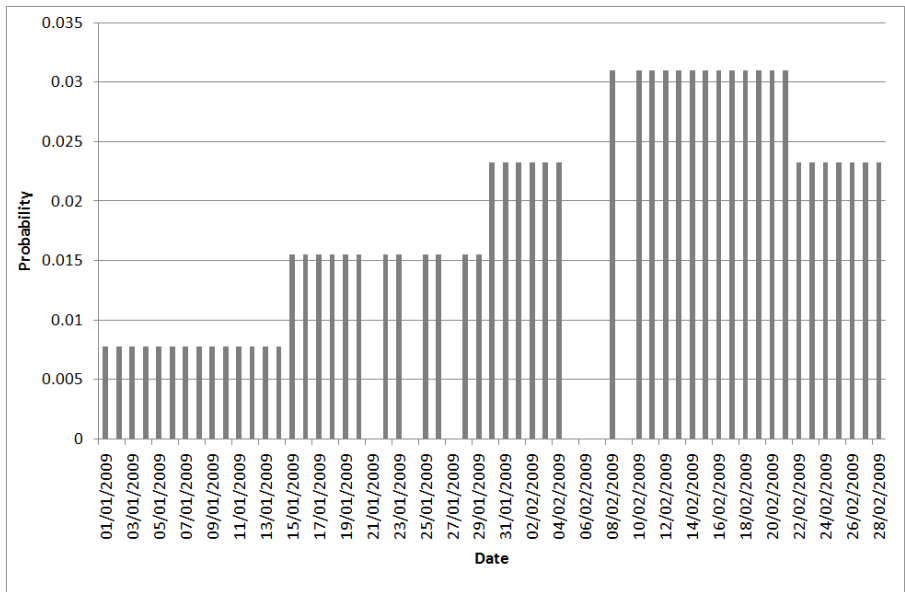


Figure 71 – Probability density function for carbetamide application in January - February 2009.

7.4 Results

Catchment-scale model results are presented here. Flows will be considered first and then herbicide leaching. First season and second season will be presented in chronological order.

7.4.1 Water flow

Before presenting the results it is important to point out that they were post-processed by adding a 0.005-mm base flow over the whole simulation period, since the model could not represent it. This issue will be discussed later on in this section. Model prediction was evaluated by visual inspection and by using the Nash-Sutcliffe efficiency index (see Paragraph 6.3).

It should be noted that measured flows used to evaluate the model performance are gauged downstream of Grimsbury Reservoir; they might therefore be smaller than flows in the river (see Paragraph 4.1.2). Unfortunately it was not possible to assess flows upstream the reservoir, since no sufficient data were available.

First season (2008 – 2009)

A first set of simulations was run assuming a catchment area of 129 km², which is the hydrologically active catchment (see Appendix 2). In the first season it is possible to observe that discharge is generally underestimated (Figure 72). A Nash-Sutcliffe efficiency index of 0.38 was obtained. Over the whole season predicted discharge is generally below measured data and predicted discharge is only 62% of measured discharge at Banbury.

The high peaks observed at the beginning of the season (on 4th November, 10th November, and 12th December 2008) are twice as high as the modelled peaks. Results from end of January to mid-February 2009 suggest that the rainfall events which triggered discharge peaks were not uniform in the catchment. Measured discharge peaks were likely triggered by local storm events, which did not occur simultaneously to the

event recorded at the catchment outlet. In this case it seems that spatial variability of weather conditions may have a relevant impact on the model performance. Prediction seems to improve in summer (Nash-Sutcliffe index of 0.41 for April to September 2009), when modelled discharge is 74% of measured discharge.

In terms of model efficiency the values obtained are considered to be acceptable; this may be due to the right timing of the modelled peaks to occur. In terms of total flows though model prediction is definitely unsatisfactory.

A number of checks on the soil water balance were carried out to exclude any problem in the input generation step. It was therefore hypothesised that the hydrologically active catchment was bigger than expected. In fact the assumption made in the redefinition of the catchment boundary was that the Oxford Canal and the river Cherwell could be considered separately. During wet periods, though, there will be flows into the canal from streams, and drainage from farm land. Moreover the reservoirs that feed the canal will fill and possibly spill into the canal. Therefore during autumn and winter, flows in the canal probably increase and there might also be losses from the canal to the river by means of overflow weirs into the river system. According to information and measured data provided by British Waterways, Boddington Reservoir, which is the main reservoir that feeds the Oxford Canal, is full for most of the winter time (November 2008 to February 2009, and December 2009 to March 2010). The reservoir collects drainage from farm land upstream. When the reservoir is full it likely overflows, feeding the Oxford Canal. When the water level in the canal increases water may pass to the river via overflow weirs and therefore increase the contributing area. The area contributing to the actual discharge at Banbury may vary between approximately 129 km² and 199 km², although even a bigger area might contribute to flows at Banbury, as the canal might transfer water which comes also from outside the Upper Cherwell catchment.

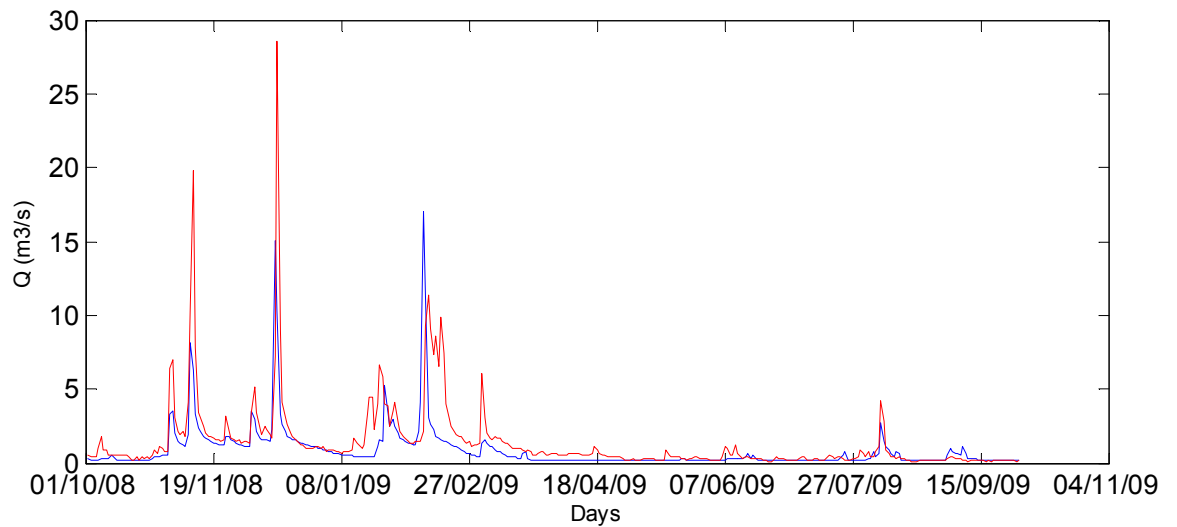


Figure 72 – Mean daily discharge ($m^3 s^{-1}$) at Banbury: measured (red line), and modelled (blue line). Catchment area used in this simulation is $129 km^2$.

So the same period was also simulated considering the original catchment area ($199 km^2$) (Figure 73). Nash-Sutcliffe index worsens in this simulation (Table 29), but total flow prediction improves. In particular, a total runoff of about 210 mm was predicted, which is 96% of measured flow (Table 30). During the dry season (April to September 2009) though, runoff is overestimated (Table 30).

Runoff was calculated to be 34% of total rainfall, which is consistent with measured data (measured runoff is 35% of total rainfall). Much lower values were obtained using a catchment area of $129 km^2$ (Table 31).

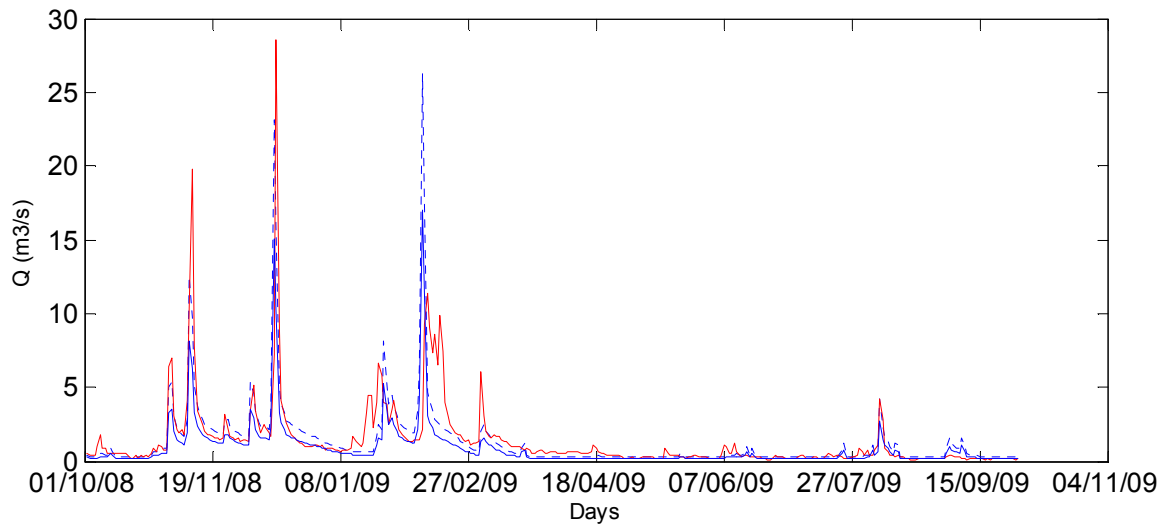


Figure 73 - Mean daily discharge ($m^3 s^{-1}$) at Banbury: measured (red line), and modelled (blue solid line refers to $129 km^2$ catchment area; blue dotted line refers to $199 km^2$ catchment area).

Table 29 – Nash-Sutcliffe efficiency index for 2008 – 09 season (A is the catchment area used in the simulation).

	A=129 km ²	A=199 km ²
2008 - 09 season	0.38	0.29
Oct 08 - Mar 09	0.25	0.14
Apr 09 - Sep 09	0.41	0.34

Table 30 – Predicted and measured runoff considering a catchment area of $199 km^2$ for the first season (2008 – 09) (in brackets values referred to $129-km^2$ area).

	Predicted runoff (mm)	Measured runoff (mm)	Predicted/Measured runoff
2008 - 09 season	209 (136)	218	0.96 (0.62)
Oct 08 - Mar 09	176 (114)	189	0.93 (0.60)
Apr 09 - Sep 09	26 (17)	23	1.13 (0.73)

Table 31 – Measured and predicted total runoff in relation to total rainfall (2008 – 09).

	Measured rain (mm)	Predicted runoff/rain (A=129 km ²)	Predicted runoff/rain (A=199 km ²)	Measured runoff/rain
2008 - 09 season	623	0.22	0.34	0.35
Oct 08 - Mar 09	468	0.24	0.38	0.40
Apr 09 - Sep 09	228	0.08	0.12	0.10

These results suggest that during winter the catchment area is approximately 200 km², possibly slightly bigger because of the contribution from land outside the catchment. During summer the contributing area may be smaller, likely between 130 and 200 km², which is reasonable since the interactions river – canal should be limited.

Second season (2009 – 2010)

The same simulations were run for the second season. Results are shown in Figures 74-75.

In the simulation using a catchment area of 129 km² model efficiency over the simulation period (October 2009 to March 2010) is 0.42. Total flow is 133 mm, which is 95% of measured flow. Prediction can be therefore considered satisfactory.

By visual inspection, though, it is possible to observe that discharge is generally overestimated in the period November 2009 to mid-January 2010, and underestimated from mid-January to the end of March (Figure 72). Therefore the acceptable efficiency index and total flow prediction may be connected to a compensation of errors.

Discharge is represented reasonably well in October 2009. The overestimation observed in the period November to mid-January might be explained by the interactions river-canal once again. Summer 2009 was dry: only 81 mm rainfall were recorded in August and September, compared to 181 mm over the same period in 2008. For the period April to September mean rainfall is 300 mm (average calculated over the 13-year period 1996 – 2008), whilst in 2009 only 228 mm were measured. As a consequence, water level in the Oxford Canal might have been low, and possibly the reservoirs that

usually feed it could not supply sufficient discharge. It should be noted that British Waterways has got a statutory duty as a navigation authority and therefore discharge in the canal has to be maintained at a certain level. There is an offtake point at Cropredy (in the South of the catchment) where discharge from the river can be diverted into the Canal (see Paragraph 3.3.1). This could partly explain the discrepancy between modelled and measured discharge, although any offtake could not have such an impact on total discharge at the outlet. Records of water transfer from the river Cherwell at Cropredy to the Oxford Canal were supplied by British Waterways for the period January 2004 to May 2009 (see Paragraph 3.3.1). The offtake can represent up to 10% of stream flow only (in August). Unfortunately data beyond May 2009 were not available.

From mid-January 2010 discharge is underestimated (only the peak recorded on 23rd January is well simulated).

These results imply that the area draining in the river varies over the simulation period: from mid-January onwards it may be bigger than 129 km².

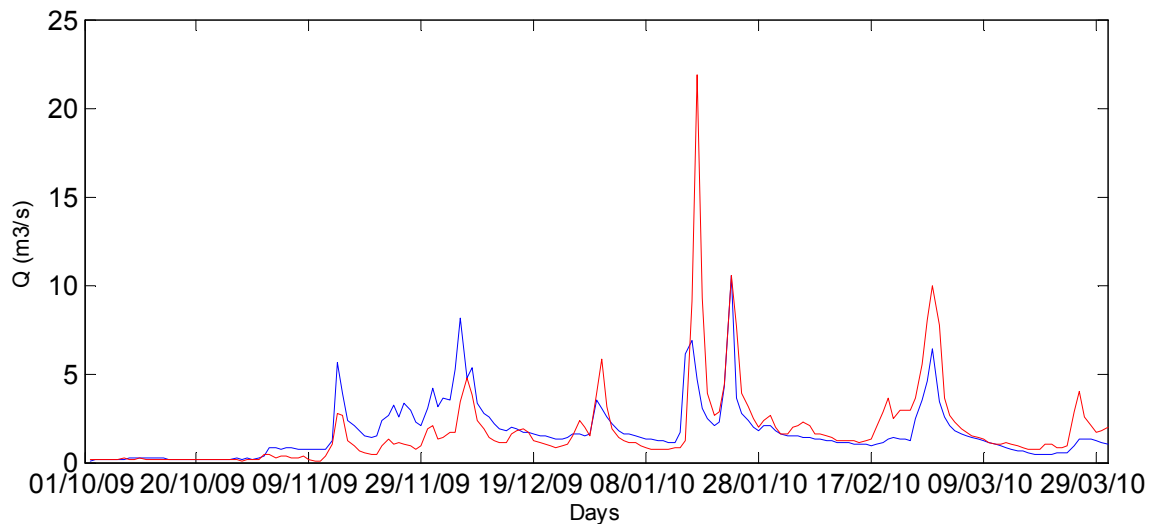


Figure 74 - Mean daily discharge ($m^3 s^{-1}$) at Banbury: measured (red line) and modelled (blue line). Catchment area used in this simulation is 129 km².

Hence a simulation was run also using a catchment area of 199 km² (Figure 75).

Over the whole simulation period Nash-Sutcliffe index worsens (0.18), like total flow prediction (493 mm which is 146% of measured runoff), which is heavily overestimated. Predicted runoff is 61% of total rainfall (338 mm rainfall), which is considerably above measured runoff (42% of total rainfall) (Tables 32-33).

However, in the period January to March 2010 prediction improves: Nash-Sutcliffe index is 0.49 and predicted runoff is 106% of measured runoff (for the same period the simulation with 129 km² area gave a total runoff equal to 70% of measured runoff) (Tables 32-33). The discharge increase starting on 29th December is represented reasonably well although the recession is too slow; hence modelled values stay above measured data. The peak recorded on 17th January is represented by the model but it is underestimated and it occurs one day earlier (10.6 m³ s⁻¹ versus 22 m³ s⁻¹). The following peak (on 23rd January) is overestimated (16.2 m³ s⁻¹ versus 10.5 m³ s⁻¹), but the timing is right. Also in this case a possible explanation could be related to driving data (rainfall) and the hypothesis of uniform weather conditions in the catchment. The peak observed on 28th February is well simulated, both in terms of magnitude and shape of the hydrograph. From mid-February to the end of March a couple of minor peaks are not represented by the model, probably because they were triggered by local rain events, which did not occur at the catchment outlet or occurred with minor magnitude or intensity. The reader is reminded that the weather station used for these simulations is in Banbury.

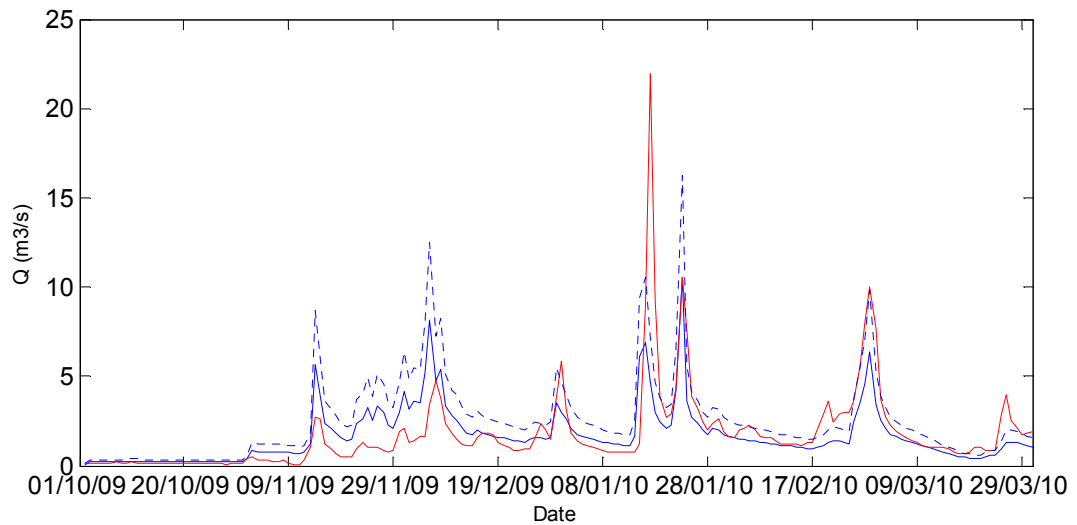


Figure 75 - Mean daily discharge ($\text{m}^3 \text{s}^{-1}$) at Banbury: measured (red line), and modelled (blue solid line refers to 129 km^2 catchment area; blue dotted line refers to 199 km^2 catchment area). Day 1 is 1st October 2009.

Table 32 – Nash-Sutcliffe efficiency index for 2009 – 10 season (A is the catchment area used in the simulation).

	A=129 km ²	A=199 km ²
Oct 09 - Mar 10	0.42	0.18
Jan 10 – Mar 10	0.39	0.49

Table 33 – Predicted and measured runoff considering a catchment area of 199 km^2 for the second season (2009 – 10) (in brackets values referred to 129-km^2 area).

	Predicted runoff (mm)	Measured runoff (mm)	Predicted/Measured runoff
Oct 09 - Mar 10	471.2 (305.4)	322.9	1.46 (0.95)
Jan 10 – Mar 10	251.3 (162.9)	235.5	1.06 (0.70)

Conclusions

Flow prediction at the catchment scale suggests that the definition of the hydrologically active catchment is a key issue. However it was not possible to completely eliminate the uncertainty of the contributing area nor to define general patterns of its variation. In the

first season the area seems to be always very close to 199 km². In the second season it seems to be smaller than 129 km² in the period October to December and just below 199 km² in January to March. Much more information about reservoir policies and canal management, and more resources would be necessary to model the interactions between river, reservoirs, and canal. A better knowledge of the interactions between river and Oxford Canal would be helpful in defining the catchment area. Collecting data on water levels in the Canal and or monitoring overflow weirs would be useful.

As far as low flow hydrograph is concerned, the model could not represent base flow observed in the dry period (April to September) and in the re-wetting period (October). This is due to MACRO representation of flows. A possible explanation might be that percolation from Banbury soils is much more delayed than in the model representation. In fact water percolating from these soils might reach the surface water network even months later, especially when flow originates above an impermeable geological stratum far from any spring where water can intercept the surface water network. This is not represented by MACRO, since it is a monodimensional model.

Peaks are generally well simulated, but the recession following the peaks is not represented very accurately. Also this might be due to Banbury soils and the delayed response they might have at the catchment scale.

Some uncertainties also reside in the fact that flows are measured at Banbury: the gauging station is upstream of Grimsbury reservoir; therefore measurements are likely affected by drinking water abstractions.

7.4.2 Herbicide leaching

Herbicide leaching simulations were performed with a catchment area of 199 km² for both seasons, although the area may vary and be smaller especially in autumn 2009 (see Paragraph 7.4.1), in order to have a worst case scenario.

Herbicide leaching was evaluated against measured data in terms of mass loads at the catchment outlet. Measured loads at the catchment outlet were calculated from measured flows (Banbury gauging station), and measured concentrations (SAMOS data). In the

charts reported in Figures 76-79 they are represented by discontinuous lines: gaps are due to the lack of SAMOS concentration measurements.

Model prediction was evaluated by visual inspection and in terms of mean and standard deviation. The aim here was to assess whether or not the model could represent the kind of variability observed instead of goodness-of-fit, since herbicide application timing was unknown. Each simulation results are analysed in the following paragraphs.

Propyzamide

Propyzamide loads modelled for the first season are shown in Figure 76. Total loss predicted by the model depends on the application timing chosen for the simulation, and varies between 6.2 kg (*sim2*) and 7.2 kg (*sim1*), that is 30% and 34% of measured losses respectively (Table 34). Total losses by the end of the simulation period were calculated to be 0.5% and 0.6% of the total applied. Measured losses are 1.9% of the total amount applied. Given the lack of information about the actual area treated with propyzamide, it is assumed that the actual amount applied is the estimate used in the simulations. Mean and standard deviation values suggest that *sim1* gives better results than *sim2*; however in both cases representation of measured data is not very accurate.

Measured data show a first peak on 2nd November (209 g h^{-1} triggered by 22 mm rainfall on 1st November), which is missed by the model; this means that propyzamide was applied before the optimum application timing (i.e. November). As a consequence the peak observed on 14th December is overestimated by the model (both in *sim1* and *sim2*): at this point a relevant amount of chemical has already been lost, whereas in the simulation most part of it is still in the soil. Both measured and modelled peaks occurred on 14th December, after two rain events (19.2 mm and 12.6 mm on 12th and 13th December). The peaks monitored in January and February are not represented by the model because of the absence of modelled drain flow (therefore no leaching to the drains can take place). The reader is reminded that herbicide flux is generated only by clay underdrained soils (represented by Denchworth soil association). A possible explanation might be that those peaks were generated by different transport mechanisms (i.e. overland

flow, spray drift), or sources other than artificially drained soils (i.e. light soils, or heavy soils without artificial drainage or with blocked drains). However field observations suggest that in January and February most part of the drains in the catchment are flowing.

Table 34 – Propyzamide losses for the period October 2008 to March 2009.

	<i>sim1</i>	<i>sim2</i>	Measured
Total loss (g)	7208	6253	21270
Lost/applied (%)	0.6	0.5	1.9
Mean (g h⁻¹)	1.65	1.43	4.87
Standard Deviation (g h⁻¹)	12.4	10.4	18.50

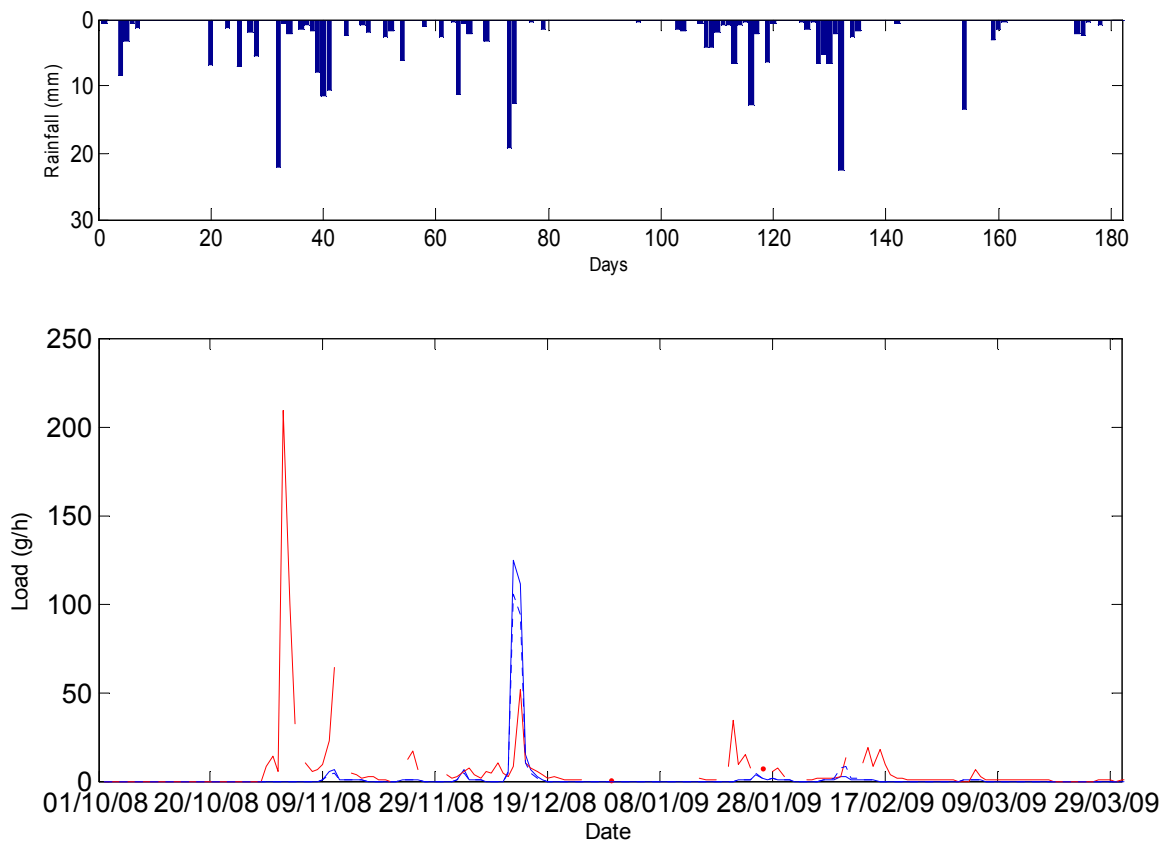


Figure 76 – Daily mean propyzamide loads (g h⁻¹) at Banbury: measured (red line), and modelled (blue solid line refers to sim1; blue dotted line refers to sim2). Period 1st October 2008 to 31st March 2009. Also shown are daily rainfall totals (columns [mm d⁻¹]).

Results for the second season are shown in Figure 77. Total loss predicted by the model is about 7.1 and 7 kg, that is 145% and 142% of measured losses for *sim1* and *sim2* respectively (Table 35). Total losses by the end of the simulation period were calculated to be 0.62% and 0.61% of the total applied. Measured losses are 0.43% of the estimated total amount applied. Mean and standard deviation values suggest that *sim2* gives better results than *sim1*. However in both cases the represented average load is approximately 1.4 times the observed mean.

Total losses for *sim1* and *sim2* are close, but using a wider application window (*sim2*) peaks are spread over a longer period and they are more homogeneous compared to *sim1*, where about 83% of the chemical is lost between mid-November and mid-December.

The first modelled peak occurs on 12th November, 3 days before the measured peak; a possible reason may be that the real application window started a few days later than the one used in the model. Another peak (8.9 g h⁻¹) is observed on 7th December, following a very wet period (59.2 mm of rain in the previous two weeks). Modelled peak (for both *sim1* and *sim2*) occurs on 6th December, likely triggered by the 9-mm rainfall event recorded on 5th December. Another peak is represented on 8th December, following another rain event monitored on 7th December (5 mm). This discrepancy may be due to a non-uniform rainfall distribution in the catchment. The peak represented on 16th January, which is triggered by 11.4 mm rainfall on 15th January. However the first measured peak after this rain event is on 23rd January and follows 11.2 mm rainfall recorded the previous day. Also in this case a possible explanation is connected to weather data spatial variability: the 15th-January rain event may have been a local event at the catchment outlet.

Likely applications in the catchment took place also beyond December, since relevant peaks were still monitored between 15th February and the end of March, when modelled herbicide supply is exhausting.

Table 35 – Propyzamide losses for the period October 2009 to March 2010.

	<i>sim1</i>	<i>sim2</i>	Measured
Total loss (g)	7088	6951	4904
Lost/applied (%)	0.6	0.6	0.4
Mean (g h⁻¹)	1.62	1.59	1.12
Standard Deviation (g h⁻¹)	6.7	5.4	2.8

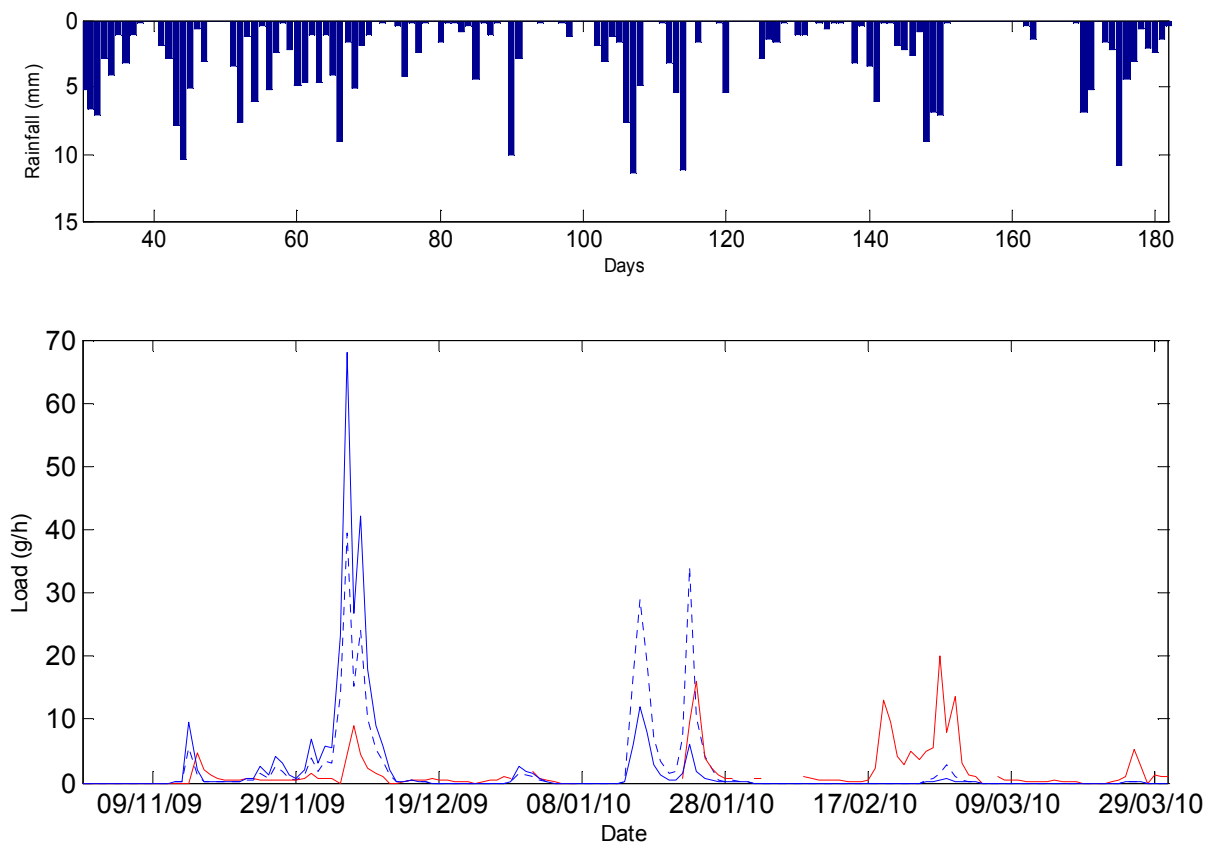


Figure 77 – Daily mean propyzamide loads (g h⁻¹) at Banbury: measured (red line), and modelled (blue solid line refers to sim1; blue dotted line refers to sim2). Period 1st November 2009 to 31st March 2010. Also shown are daily rainfall totals (columns [mm d⁻¹]).

In terms of concentrations, in both seasons, the model tends to overestimate them, but observed data remain high (above the DWD MAC) for a longer time (Table 36). This may suggest that reality is more variable than the model prediction: the application window may be wider, or the probability of application dates might be more homogeneous. Also, herbicide flux to drains might be different because of the presence of other soil types, which might contribute to total losses with a slower response (i.e. longer tail of the curve). The reader is reminded that the model considers only one soil type as source of herbicide flux.

Table 36 – Comparison between measured and predicted propyzamide concentrations ($\mu\text{g l}^{-1}$): mean values and range of variation, and number of days exceeding the DWD MAC ($0.1 \mu\text{g l}^{-1}$).

First season

	<i>sim1</i>	<i>sim2</i>	Measured (SAMOS)	<i>sim1/measured</i>	<i>sim2/measured</i>
Mean conc ($\mu\text{g l}^{-1}$)	0.95	0.79	0.43	2.21	1.84
Range ($\mu\text{g l}^{-1}$)	70.43	59.33	9.12	7.72	6.51
Nr days > MAC	23	23	78	0.29	0.29

Second season

	<i>sim1</i>	<i>sim2</i>	Measured (SAMOS)	<i>sim1/measured</i>	<i>sim2/measured</i>
Mean conc ($\mu\text{g l}^{-1}$)	0.98	0.8	0.12	8.17	6.67
Range ($\mu\text{g l}^{-1}$)	42.63	24.8	1.25	34.10	19.84
Nr days > MAC	43	46	58	0.74	0.79

Carbetamide

Carbetamide loads modelled for the first season are shown in Figure 78 (only January to March is shown). Total loss predicted by the model varies between 1.6 kg (*sim1*) and 3.5 kg (*sim2*) (Table 37), that is 37% and 79% of measured losses respectively. Total losses were calculated to be 0.5% and 1.1% of the total applied, whilst measured losses are 1.3% of the total amount applied. Given the lack of information about the actual area treated, also here it is assumed that the actual amount applied is the estimate used in the

simulations. Mean and standard deviation values *sim2* gives satisfactory results (Table 37).

Measured data show that carbetamide was likely applied later than in the simulations. Neither *sim1* nor *sim2* represents carbetamide peaks well. Modelled peaks occur approximately one month before observed peaks, which means that in the catchment farmers probably sprayed at the end of February, with an application window much shorter than those used in the simulations. As a consequence most of the chemical is predicted to be lost after the rain events recorded on 24th January (14.1 g h⁻¹ on 25th January in *sim2*) and 9th February (30.7 g h⁻¹ and 48.9 g h⁻¹ on 10th February in *sim1* and *sim2* respectively). Measured data do not record any losses at this point (all values are below LOD), so it is likely that application has not occurred yet. In fact carbetamide is detected only after the rain event of 3rd March, which triggered a relevant peak (58.6 g h⁻¹) the following day. The lag between rain event and herbicide peak is one day for both measured and modelled data.

Table 37 – Carbetamide losses for the period October 2008 to March 2009.

	<i>sim1</i>	<i>sim2</i>	Measured
Total loss (g)	1663	3537	4490
Lost/applied (%)	0.5	1.1	1.3
Mean (g h⁻¹)	0.38	0.81	1.03
Standard Deviation (g h⁻¹)	3.0	5.1	5.2

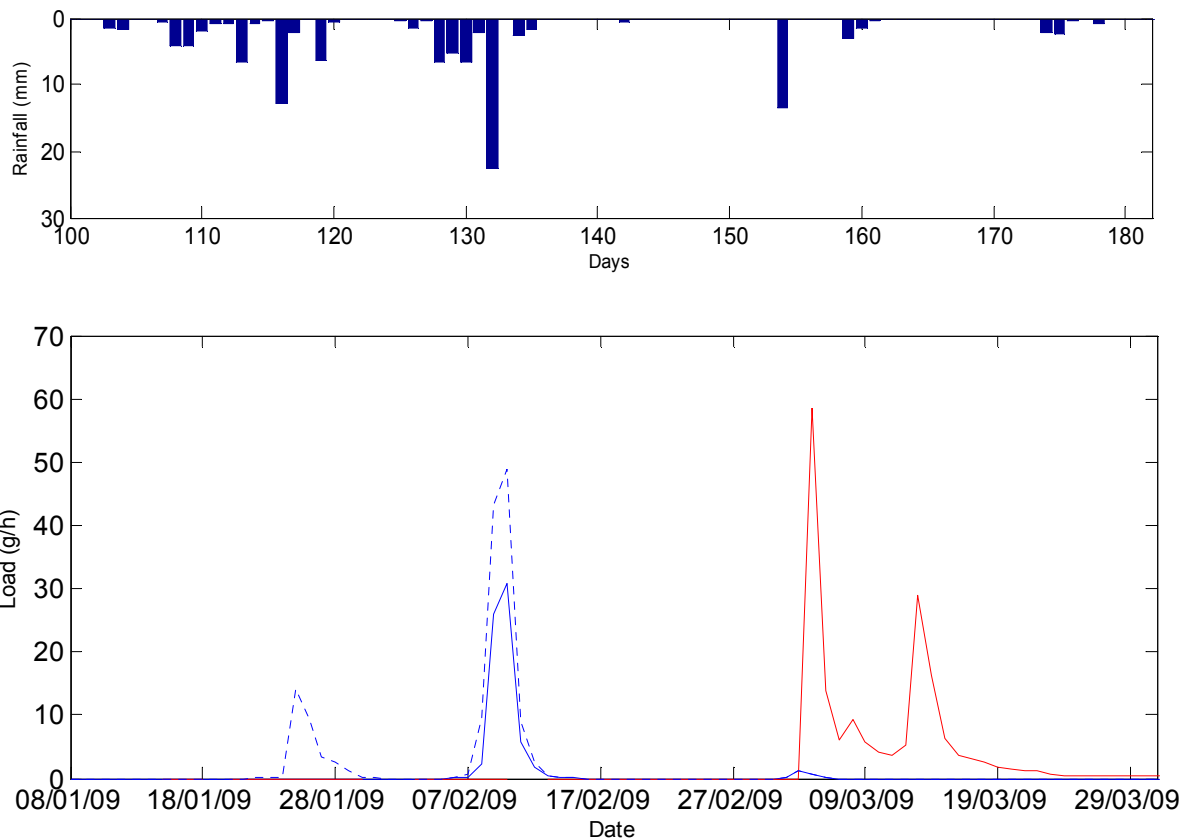


Figure 78 – Daily mean carbetamide loads (g h^{-1}) at Banbury: measured (red line), and modelled (blue solid line refers to *sim1*; blue dotted line refers to *sim2*). Period 8th January 2009 to 31st March 2009. Also shown are daily rainfall totals (columns [mm d^{-1}]).

Modelled loads for the second season are shown in Figure 79. Total loss predicted by the model is about 5.7 and 6.1 kg, that is 62% and 66% of measured losses for *sim1* and *sim2* respectively (Table 38). Total losses predicted by the model are 1.7% and 1.8% of the total applied. Measured losses are 2.8% of the estimated total amount applied. Standard deviation values suggest that *sim1* is very close to measurements; however average loads are far from observations (Table 38).

Like for propyzamide total losses for *sim1* and *sim2* are close (Table 38).

In *sim1* only one major peak is predicted (28th February), as carbetamide is applied late in the season (February). In *sim2* the first peak modelled is on 16th January. No measurements were taken from 8th to 21st January, so the comparison between modelled

and measured values is not possible. Monitoring starts again on 22nd January. The peak observed on 23rd January follows 11.2 mm rainfall on the day before. It is represented by the model (in *sim2*) on the same day, but heavily underestimated. A possible explanation is that in the simulation applications occur in January and February - with higher probability in February than in January. Therefore at this point a relevant part of the catchment has not been treated yet, and a smaller amount of chemical is in the soil. On the contrary according to measured data carbetamide might have been applied earlier in the season (high peaks were detected even before mid-November).

Table 38 – Carbetamide losses for the period October 2009 to March 2010.

	<i>sim1</i>	<i>sim2</i>	Measured
Total loss (g)	5707	6076	9228
Lost/applied	0.017	0.018	0.028
Mean (g h⁻¹)	1.31	1.39	2.11
Standard Deviation (g h⁻¹)	10.2	7.7	10.1

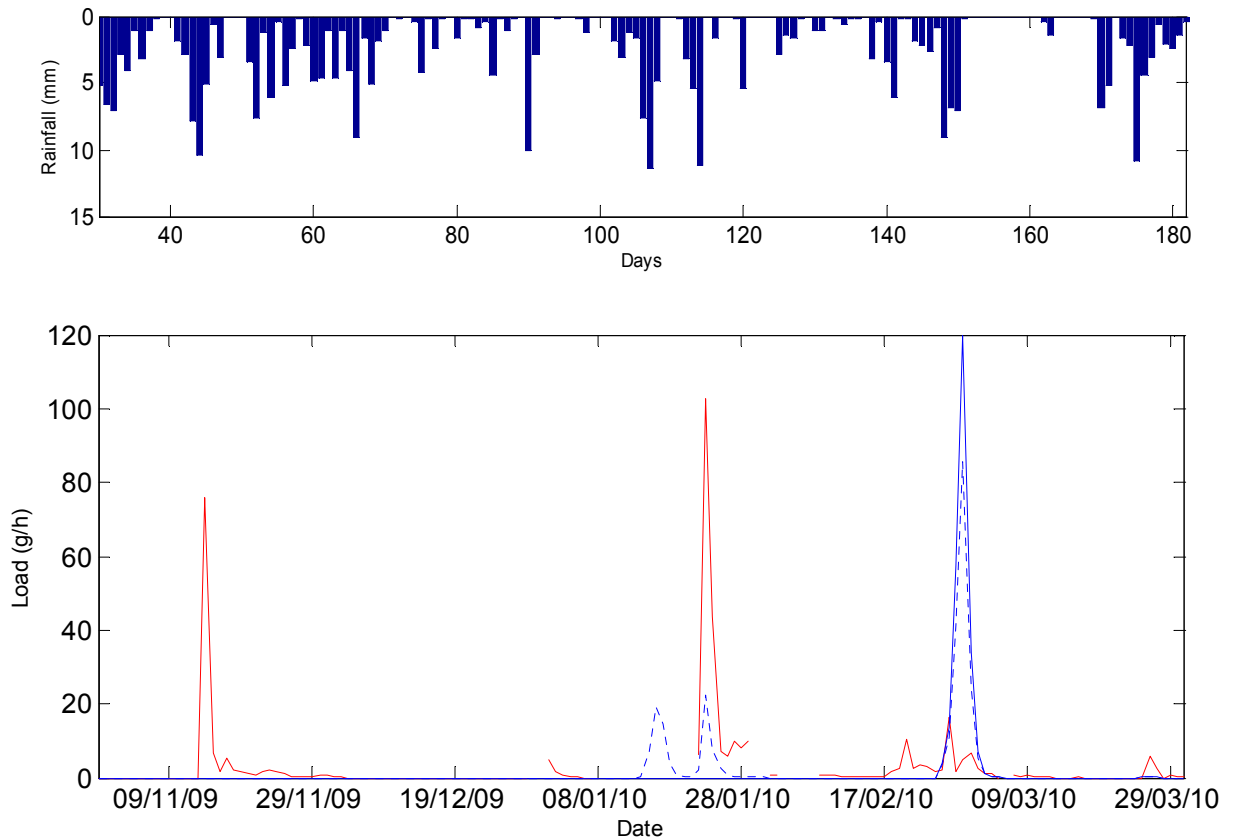


Figure 79 – Daily mean carbetamide loads (g h^{-1}) at Banbury: measured (red line), and modelled (blue solid line refers to sim1; blue dotted line refers to sim2). Period 1st November 2009 to 31st March 2010. Also shown are daily rainfall totals (columns [mm d^{-1}]).

In terms of concentrations, like for propyzamide, peaks tend to be overestimated by the model, although they are closer to observed data (1 to 4 times bigger). Moreover observations remain high (above the DWD MAC) for a longer time (Table 39). Also these results suggest that reality is more variable than the model prediction.

Table 39 – Comparison between measured and predicted carbetamide concentrations ($\mu\text{g l}^{-1}$): mean values and range of variation, and number of days exceeding the DWD MAC ($0.1 \mu\text{g l}^{-1}$).

First season

	<i>sim1</i>	<i>sim2</i>	Measured (SAMOS)	<i>sim1/measured</i>	<i>sim2/measured</i>
Mean conc ($\mu\text{g l}^{-1}$)	0.12	0.26	0.2	0.60	1.30
Range ($\mu\text{g l}^{-1}$)	9.66	15.41	5.9	1.64	2.61
Nr days > MAC	8	14	27	0.30	0.52

Second season

	<i>sim1</i>	<i>sim2</i>	Measured (SAMOS)	<i>sim1/measured</i>	<i>sim2/measured</i>
Mean conc ($\mu\text{g l}^{-1}$)	0.36	0.43	0.21	1.73	2.05
Range ($\mu\text{g l}^{-1}$)	33.21	23.69	7.7	4.31	3.08
Nr days > MAC	7	17	45	0.16	0.38

Conclusions

The main limitation of herbicide leaching prediction seems to be connected to the uncertainty of application timing. General application trend and rough information (e.g. optimum application timing) are not sufficient when the aim is to represent observations. So more precise information about when herbicides are applied is necessary to improve prediction.

It should also be noted that the model does not take into account the variability of soils in terms of herbicide contamination, which might lead to a spreading out of herbicide losses at the catchment outlet. Moreover, the MACRO application at the field scale showed that herbicide mass lost is very sensitive to K_{OC} value (see Paragraph 6.4.1). In the whole catchment simulation it was assumed that all fields have the same K_{OC} . However even slightly different values of K_{OC} (which are almost certain to occur in different fields) would lead to different masses lost and possibly different peaks.

To a certain extent also the spatial variability of weather conditions may be responsible of the discrepancy between modelled and measured loads, although its impact seems to be related to specific events only. The overall prediction does not seem to be relevantly affected by the assumption of uniform weather conditions in the catchment. It

must be stressed that the Upper Cherwell is a relatively small catchment, with a rather homogeneous topography.

The model seems to generally underestimate total herbicide losses at the catchment outlet. This might be at least partly due to herbicide flux inputs, generated with MACRO, as also at the field scale predicted total losses were smaller than measured losses (see Chapter 6). Another possible reason may be the uncertainty of the area treated; a number of assumptions were made on:

- Catchment hydrologically active area;
- Crops treated with carbetamide and propyzamide (only OSR, although these chemicals are allowed also on field beans and other minor crops);
- Proportion between area treated with carbetamide, and with propyzamide;
- Area of the catchment which is responsible of herbicide contamination of surface waters.

Moreover actual application rates are known roughly, so total amounts applied can be assessed only by approximation.

Discrepancy between measured and modelled herbicide losses might be also due to contamination processes other than drain flow: this model considers drain flow the only source of herbicide losses. Results suggest that it is the main source but other sources might, in part, contribute to total losses (i.e. overland flow, runoff from hard surfaces).

Peak timing is generally well represented, with herbicide peaks usually occurring 1 day after rainfall event. These results suggest that herbicides are transported very quickly to the catchment outlet. The first 2-4 intense rain events after application are very critical in terms of herbicide losses. Peaks are followed by a slow recession, which is represented by the model, although it is usually quicker than the observed. This might be due to other contamination sources, which contribute with low constant herbicide flux to the outlet (light soils, or inputs from the Oxford Canal).

Chapter 8 – CONCLUSIONS

Context

Many raw waters in the UK contain pesticides at levels above the DWD MAC. Pesticides at such levels do not necessarily cause harm to ecosystems or pose risks to human health. However, if water is to be used for potable supply it has to meet EU standards.

The Upper Cherwell catchment is defined by a drinking water reservoir abstraction point at Banbury, where concentrations of a number of crop protection product active ingredients have been monitored for several years. Several chemicals have been identified as problematic for drinking water supply in the catchment since monitoring began, including isoproturon, which is now banned. Recent attention has been directed towards two key herbicides used for black grass control in OSR and field beans: carbetamide and propyzamide. OSR is widely grown in the catchment and many arable fields are currently under a three year rotation consisting of two cereal crops followed by OSR. About 50% of the catchment is considered suitable for OSR production at some stage (unpublished data supplied by the EA), although not all of this area will be in OSR in any single year.

Towards a conceptual model of pesticide transfers

The preliminary analysis of historical data on the temporal pattern of herbicide concentrations, rainfall, and river discharge suggests that concentrations at the catchment outlet are significantly correlated with discharge and that their response appears to be delayed relative to flow. The fact that concentrations are well correlated with flow indicates that spray drift is not a major contributor to the herbicide problem at the catchment outlet because surface water exposure from spray drift would be expected on the day of application (which should normally be dry). Other rapid pathways such as overland flow and runoff from hard surfaces (such as farm yards) are also probably not

major pathways because these would be expected to generate short lived peak concentrations on the same day as the storm event. Not only does peak concentration tend to occur some time after the discharge peak but the concentration for both active ingredients tends to remain elevated for a significant period following peak flow – gradually receding during the post event period – even when there is no additional rainfall. The delay between peak discharge and peak concentration (which is generally between one and three days) tends to be longer for carbetamide than for propyzamide. This lends support to the hypothesis that carbetamide is more likely to be transported in solution via the bulk soil matrix to field drains whereas propyzamide is more likely to be transported via preferential flow pathways (such as soil macropores or the gravel backfill overlying field drains), bypassing much of the bulk soil matrix.

In contrast, drain flow monitoring described in this thesis suggests that transport to the drainage network is rapid: coincident peaks of drain flow and chemical concentration were observed for both active ingredients. Herbicide peak and drain flow peak occur on the same day are supported by the application of the MACRO model. The results also suggest macropore flow to drains to be the main transport mechanism for both propyzamide and carbetamide. Different timing of application does not seem to have any relevant effect of the role played by macroporosity in herbicide transport.

There appears, therefore, to be a disagreement between the rapid observed and predicted pattern of herbicide transport at the field scale and the somewhat delayed response of herbicide concentrations observed at the catchment outlet, particularly in the case of carbetamide. This could be due to different responses in different fields (herbicide transport to drain outlets may be more delayed in some fields than in others) and or due to delays in solute transport down the river network. The different lag observed for carbetamide and propyzamide might therefore be due to stream velocity, which might vary over the year (and might be slower in February and March than in November, when propyzamide is likely applied). However, it is difficult to be conclusive, given the limitations of the data set used in the analysis. It should be noted that most of the historical data on pesticide concentrations at Banbury are from grab samples collected rather infrequently (interval between sample collections is occasionally as low as one day but is typically 7 days). This means that true peaks in pesticide

concentrations will often be missed by the sampling programme. Thus, the real concentration peaks could occur earlier than the statistical analysis implies. They could, of course, also occur later. Although the low sampling frequency casts some uncertainty on the exact relationship between concentration and river discharge, the fact that concentrations *remain* high for some time after peak flow would still suggest that relatively transport via field drains is very important for pesticide transfers to the channel network. The work presented in Chapters 4-6 has led to the development of a model of catchment scale pesticide transfers in the Upper Cherwell catchment.

Model of catchment-scale pesticide transfers

The catchment-scale pesticide transfers model developed in this thesis must be considered as a first exploratory attempt to represent catchment-scale pesticide transport.

According to this model vertical movement of pesticide to the drains will take place mainly via preferential flow pathways (e.g. in macropores); flow in the soil matrix is likely to play a minor role according to field observations and modelling. Preferential pathways generally by-pass the soil matrix, reducing pesticide sorption and degradation. Macropores include earthworm burrows, mole draining and subsoiling, plant root channels, and soil cracks. They also include, implicitly, any coarse textured (e.g. gravel) back fill which were often used to fill in the trenches in which tile drains were lain. The importance of macropores in chemical transport is also suggested by rapid appearance of herbicide in field drains during storm events observed in the field monitoring. Precisely which of the possible preferential pathways is most important is currently unknown and further work is needed to better understand this process. There is likely to be a distribution of travel times along a range of pathways. Provided chemicals do not degrade rapidly (as is the case of propyzamide), herbicide transport may result in translocation to field drains many months after application. The detection of propyzamide in the drain monitored in the Ashby Brook sub-catchment during the autumn sampling, despite the fact that the field served by this drain was in winter wheat (therefore not treated with propyzamide), tends to confirm this hypothesis.

Once pesticides reach the water table, they move (under advection) laterally to the drain pipes along hydraulic gradients. The velocity of saturated flow will be affected by the hydraulic gradient (which will be determined by the topography of the water table at the surface but by pressure gradients at deeper levels) and the saturated hydraulic conductivity. The transport of solutes and colloids will, again, take place down various pathways with a distribution of velocities. This will also tend to spread out pulse inputs from the unsaturated zone. The monitoring and field-scale modelling presented in this thesis suggest that transport to field drains is a very rapid process, likely a matter of hours.

After reaching the drainage system, pesticides and water will flow through the network of drain pipes until they get to the surface water network. This step should be relatively rapid (about one day). Transport in the channel network to the catchment outlet will also contribute to some spreading out of pulse inputs due to hydrodynamic dispersion (e.g. Gandolfi *et al.*, 2001). Travel times in the stream network will depend on the location of pesticide inputs within the catchment, and the advective velocity. At the catchment scale, herbicides will be applied to different farms at different times and different fields will have different soil properties and different artificial drain constructions and spatial configurations. Finally rainfall inputs will not be spatially uniform. All this means that inputs to the channel network will vary spatially and temporally. The net result at the catchment outlet is likely to be a spreading out of pesticide concentrations compared with the patterns observed at individual drains, such as the one monitored in this project. Figure 80 shows a comparison between propyzamide concentrations monitored at the main drain of the Experimental Field and contemporaneous concentrations observed at the catchment outlet (SAMOS) from the 5th to the 25th of November 2009. Concentrations at the outlet are 100-fold smaller than the ones observed at the field edge, the peak occurs one day later, and the pattern is smoother.

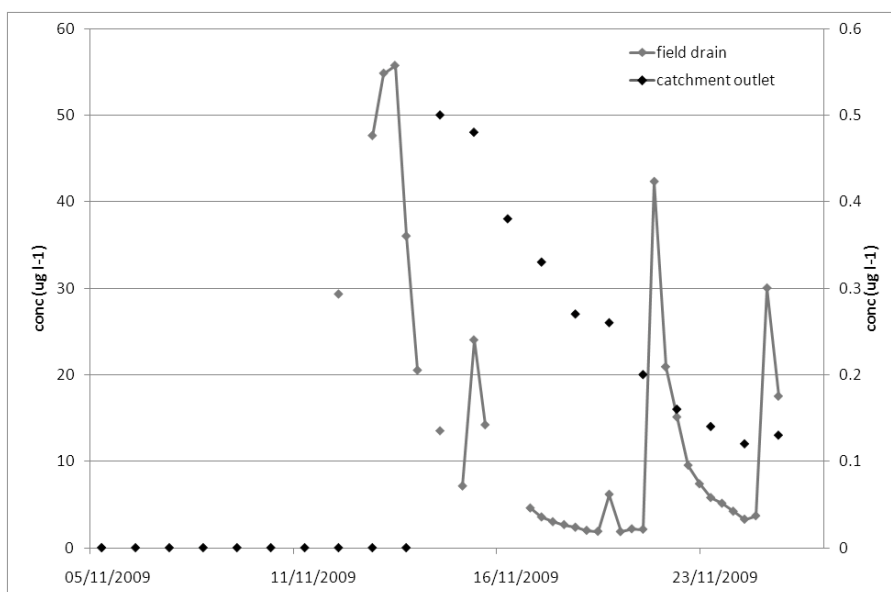


Figure 80 – Propyzamide concentrations monitored at the main drain of the Experimental Field (primary axis, grey symbols), and at the catchment outlet (SAMOS) (secondary axis, black symbols) in November 2009.

Analogous observations could be made for carbetamide. Concentrations monitored at the Experimental Field and concentrations observed at the catchment outlet (SAMOS) are shown in Figure 81 (for the period 22nd February to 3rd March 2010).

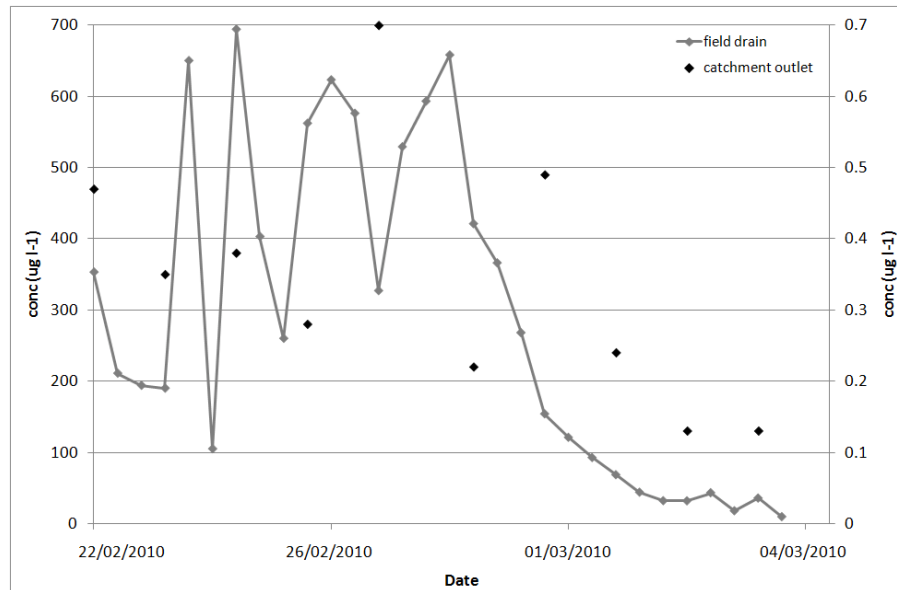


Figure 81 – Carbetamide concentrations monitored at the main drain of the Experimental Field (primary axis, grey symbols), and at the catchment outlet (SAMOS) (secondary axis, black symbols) in the period 22nd February to 3rd March 2010.

Results

Catchment-scale results suggest that herbicide peaks occur concurrently with discharge peaks. This is in contrast with historical data analysis results (see Chapter 4), and it is due to the fact that the same velocity was used for water and solutes. However solutes are likely to move more slowly than water, as water moves at wave celerity, whilst solutes move at stream velocity. In this study data and information available were not sufficient to estimate stream velocity and wave celerity in an unambiguous way.

The results seem to corroborate the hypothesis that drain flow is a major pathway for herbicide transport in the catchment. Estimated concentrations at the catchment outlet are higher than measured data and generally they are one order of magnitude smaller than concentrations measured at the Experimental Field. This behaviour is not consistent with observations (see Figures 80-81), where concentration spreading out is more dramatic; this may be due to factors which have not been included in the model, like:

- Spatial variability of weather data: non-uniform rainfall can have an impact on herbicide dilution. If some portions of the catchment were particularly

rainy but minor sources of herbicide losses (e.g. because of the presence of light soils), at the catchment scale they would dilute total chemical loads;

- Variability of soils: different soil types may have different behaviour; the rough distinction between light and heavy soils might not be sufficient to represent observations accurately;
- Drainage system characteristics and extent: different drainage characteristics likely affect herbicide losses; moreover in this work it was hypothesised that clay soils are artificially drained without having rigorous information.

but also to the uncertainty of application dates and rates. Another factor that may have an impact of herbicide loss prediction is chemical mobility (K_{OC}), which was assumed to be constant in all the fields; however slightly different values are likely to occur.

Limitations of the study and recommendation for further work

This study has a number of limitations, and further work could be done to corroborate and extend the findings presented here. By far the main limitation of the study is the relatively poor knowledge of herbicide application timing, rates, and areas treated. It would be helpful to obtain more detailed and precise information about usage from farmers, farm staff, and or agronomists. Another key issue is represented by the catchment hydrology: more data would be needed for a better-understanding, and a better knowledge of the catchment. A number of assumptions, therefore, had to be made in order to develop a model of the system, which limits the degree of certainty we can attach to the results.

The catchment-scale model developed in this work is a preliminary simple model, which could be improved. A better knowledge of inputs such as herbicide usage, land use distribution, artificial drainage extent, stream velocity, would help set up a more sophisticated model. Spatial variability of rainfall could be taken into account explicitly in such model developments.

With respect to additional field investigations, it would be useful to continue monitoring field drains in order to gain a better-understanding of herbicide transport in the catchment. This monitoring should be extended to other chemicals and to other

drains and soil associations to ascertain if the observations reported here are relevant more widely. This could also provide additional insights, which could be helpful in defining management strategies to reduce herbicide losses to surface waters, such as optimising application timing or limiting the spatial extent of applications. In addition, it would be interesting to explore the impact of different cultural practices on herbicide transport via artificial drainage: i.e. the role of different tillage practices, the effects of no tillage and the role of subsoiling in encouraging or mitigating pesticide transport from land to water. Such experimental work should be conducted on a systematic (and well replicated) basis in the laboratory and or in the field in order to establish scientific credibility. Field investigation should also be extended to other possible contamination processes (e.g. overland flow) in order to ascertain their importance and their effect on pesticide contamination at the field- and catchment-scale.

Implications for managing herbicide pollution in the Upper Cherwell

The findings of this study will be useful for informing future management strategies for herbicide pollution in the Upper Cherwell catchment. It has previously been suggested (in discussions within the VI and the EA) that herbicide losses to water might be managed by improving handling practices on hard surfaces (reducing spills during filling and wash down operations), installing biobeds (biological filters) to reduce concentrations in runoff from hard standings and by installing buffer zones between field edges and water courses to reduce chemical transfers in overland flow. However, the results presented in this thesis suggest that these measures will be relatively ineffective because most of the chemical transport is taking place via field drains. Where field drains are extensive, buffer zones are likely to provide relatively poor mitigation because they are effectively bypassed by the drains. Furthermore, whilst losses from hard standings can have local and short term impacts on concentrations, they are unlikely to be important at the catchment outlet because they take place from very limited areas. Concentrations are, therefore, likely to be reduced significantly by dilution and hydrodynamic dispersion.

Although the findings of this study have a number of limitations, they suggest that managing diffuse-source herbicide contamination at Banbury should focus on adjusting the magnitude of herbicide inputs or possibly the timing. However working on application timing might not be effective: as a matter of fact when rain events are frequent it is hard to avoid pesticide leaching, as the first few rain events after application always appear to be critical. Given the fact that a reduction of application rates would probably diminish chemical effectiveness, working on the area treated might be the most efficient strategy. Short of banning the use of certain herbicides, there are some options which could be examined. One could be to restrict the area of the catchment in OSR (i.e. the area treated with the chemical considered) by extending the length of crop rotations. Another might be to create emissions trading schemes, similar to those which have been devised globally for atmospheric carbon. Drain blocking could also be possible, although this is likely to have an impact on crop production because it will increase the area of land which is seasonally waterlogged. Further work is required to explore these options, in the light of additional studies on herbicide transport in this or similar catchments.

Conclusions and wider applications

The work presented in this thesis focused on carbetamide and propyzamide in the Upper Cherwell catchment; however it provides general insights about pesticide transport in clay catchments, and it may have wider applications.

Heavy clay soils that are artificially drained appear to be very critical in terms of pesticide transport to surface waters. Macropores are preferential pathways for chemical vertical transport. This process seems to be very rapid and appears to be responsible of high pesticide losses both at field and catchment scale. Once pesticides reach the artificial drainage network, they are quickly transported to surface waters. In artificially drained catchments, where chemical usage is widespread, diffuse-source pollution via field drains is likely to occur.

In this context pesticide fate modelling at the catchment scale could become an important tool for providing information, analysing alternative scenarios, and supporting pesticide management. The catchment-scale model developed in this thesis is

characterised by many idealisations and assumptions, which need to be recognised and which led to many uncertainties. However, if more information and more resources were available, a more complex model could be developed, in order to obtain a better representation of observed data. It should be noted, though, that the catchment-scale model presented in this thesis is a first attempt to explore possible options of developing relatively simple models for pesticide fate at the catchment scale.

REFERENCES

- Addiscott, T.M., Heys, P.J., and Whitmore, A.P. (1986). Application of simple leaching models in heterogeneous soils, *Geoderma* 38, 185-194.
- Allen, R. G., Pereira, L. S., Raes, D., and Smith, M. (1998). Crop Evapotranspiration. FAO Irrigation and Drainage Paper 56.
- Anderson, M.G., and Burt T.P. (1978). The role of topography in controlling through flow generation, *Earth Surface Processes* 3:331-344
- Arnold, J. G., Srinivasan, R., Muttiah, R. S., and Williams, J. R. (1998). Large area hydrologic modelling and assessment. Part I: model development, *Journal of the American Water Resources Association* 34:73-89.
- ASCE Task Committee on Definition of Criteria for Evaluation of Watershed Models of the Watershed Management, Irrigation, and Drainage Division (ASCE) (1993). Criteria for evaluation of watershed models, *Journal of Irrigation and Drainage Engineering*, 119,3:429–442.
- Aubertin, G. M. (1971). The nature and extent of macropores in forest soils and their influence on subsurface water movement, *USDA Forest Service Research Paper* NE-192.
- Behrens, T., and Diepenbrock, W. (2006). Using Digital Image Analysis to Describe Canopies of Winter Oilseed Rape (*Brassica napus* L.) during Vegetative Developmental Stages, *Journal of Agronomy and Crop Science*, 192:295—302.
- Bengston, R. L., Carter, C. E., McDaniel, V., and Halverson, B. E. (1984). Corn silage response to subsurface drainage in alluvial soil, *Trans. ASAE* 27, 1391.
- Beulke, S., Brown, C. D., and Dubus, I. G. (1998). Evaluation of preferential flow models to predict the movement of pesticides to water sources under UK conditions. SSLRC research project JF3728 for MAFF PL0516, 101 pp.
- Beulke, S., and Brown, C. D. (2001). Evaluation of methods to derive pesticide degradation parameters for regulatory modelling, *Biology and Fertility of Soils* 33; 558-564.
- Beulke, S., Brown, C. D., Dubus, I. G., and Harris, G. (2001). Evaluation of uncalibrated preferential flow models against data for isoproturon movement to drains through heavy clay soil, *Pesticide Management Science*, 57:537-547.
- Beven, K., and Germann, P. (1981). Water flow in soil macropores. II. A combined flow model, *Journal of Soil Science*, 32:15-29.

- Beven, K., and Germann, P. (1982). Macropores and water flow in soils. *Water Resources Research*, 18:1311-1325.
- Beven, K., and Kirkby M.J. (1979). A physically-based, variable contributing area model of basin hydrology, *Hydrological Sciences Bulletin* 42:43-69.
- Birikundavyi, S., Labib, R., Trung, H. T., and Rousselle, J. (2002). Performance of neural networks in daily streamflow forecasting, *Journal of Hydrologic Engineering*, 7,5:392-398.
- Boesten, J. J. T. I., and van der Linden, A. M. A. (1991). Modeling the influence of sorption and transformation on pesticide leaching and persistence, *Journal of Environmental Quality*, 20:425-435.
- Boivin, A., Cherrier, R. and Schiavon, M. (2005). A comparison of five pesticides adsorption and desorption processes in thirteen contrasting field soils, *Chemosphere* 61; 668-676.
- Booltink, H. W. G., Hatano, R., and Bouma, J. (1993). Measurement and simulation of bypass flow in a structured clay soil: a physico-morphological approach, *Journal of Hydrology*, 148:149-168.
- Boorman, D. B., Hollis, J. M., and Lily, A. (1995). Hydrology of Soil Types: A hydrologically-based classification of the Soils in the United Kingdom, Report no: 126 ed, Institute of Hydrology, Wallingford.
- Bouma, J., Belmans, C., Dekker, L. W., and Jeurissen, W. J. M. (1983). Assessing the suitability of soils with macropores for subsurface liquid waste disposal. *Journal of Environmental Quality*, 12:305-310.
- Bouraoui, F., Grizzetti, B., and Mulligan, D. (2006). Fate of agrochemicals in terrestrial ecosystems; an integrated modelling framework: application to the Loire (FR), EUR22518EN, Institute of Environment and Sustainability, JRC, European Commission.
- Brewer, R. (1964). Fabric and mineral analysis of soils. John Wiley and Sons, New York.
- Brinkman, U. A. Th. (1994). On-line sample treatment for or via column liquid chromatography, *Journal of Chromatography A*, 665(2):217-231.
- Bronswijk, J. J. B. (1988). Modeling of water balance, cracking and subsidence of clay soils, *Journal of Hydrology*, 97:199-212.
- Brown, C. D., Hodgkinson, R. A., Rose, D. A., Syers, J. K., and Wilcockson, S. J. (1995). Movement of pesticides to surface waters from a heavy clay soil, *Pesticide Science*, 43(2):131-140.

- Brown, C. D., Fryer, C. J., and Walker, A. (2001). Influence of topsoil tilth and soil moisture status on losses of pesticide to drains from a heavy clay soil, *Pest Management Science*, 57: 1127-1134.
- Brown, C. D., Dubus, I. G., Fogg, P., Spirlet, M., and Gustin, C. (2004). Exposure to sulfosulfuron in agricultural drainage ditches: field monitoring and scenario-based modelling, *Pest Management Science* 60; 765-776.
- Carlile, W. R. (2006). *Pesticide Selectivity Health and the Environment*, Cambridge University Press, Cambridge.
- Chamberlain, A. R. (1952). Measuring water in small channels with WSC flume. Stations Circular 200, State College of Washington.
- Clarke, M. P. (2007). Assessing the Water Quality Benefits of Riparian Buffer Zones in the Cherwell Catchment, Oxfordshire. Department of Natural Resources, Cranfield University.
- Downer, C. W., and Ogden, F. L. (2004). GSSHA: Model to simulate diverse stream flow producing processes, *Journal of Hydrologic Engineering*, 9,3:161–174.
- Dubus, I. G., Beulke, S., and Brown, C. D. (2002). Calibration of pesticide leaching models: critical review and guidance for reporting, *Pest Management Science*, 58:745-758.
- Dubus, I. G., and Surdyk, N. (2006). State-of-the-art review on pesticide fate models and environmental indicators. Report DL#4 of the FP6 EU-funded FOOTPRINT project [www.eu-footprint.org], 39p.
- Edmonds, E. A., Poole, E. G., and Wilson, V. (1965). Geology of the Country around Banbury and Edge Hill (*Explanation of Sheet 201, New Series*), Memoir of the Geological Survey of Great Britain, Her Majesty's Stationary Office, London.
- Edwards, A. C., Kay, D., McDonald, A. T., Francis, C., Watkins, J., Wilkinson, J.R., and Wyr, M.D. (2008). Farmyards, an overlooked source for highly contaminated runoff, *Journal of Environmental Management* 87; 551-559.
- Ehlers, W. (1975). Observations on earthworm channels and infiltration on tilled and untilled loess soils, *Soil Science*, 119:242-249.
- Erpul, G., Norton, L. D., and Gabriels, D. (2003). Sediment transport from interrill areas under wind-driven rain.” *Journal of Hydrology.*, 276:184–197.

European Commission (2009). Common implementation strategy for the Water Framework Directive (2000/60/EC), Technical Report 2009-026, Guidance Document No. 18 – Guidance on groundwater status and trend assessment.

Fait, G., Nicelli, M., Fragoulis, G., Trevisan, M., and Capri, E. (2007). Reduction of point contamination sources of pesticide from a vineyard farm, *Environmental Science and Technology* 41; 3302-3308.

FERA (2008). Pesticide usage survey, Report 224, Arable crops in Great Britain 2008 (including aerial applications 2007-2008); National Statistics.

Flury, M. (1995). Environmental evidence of transport of pesticides through field soils – A review, *Journal of Environmental Quality*, 25:25-45.

FOCUS (2000). FOCUS groundwater scenarios in the EU review of active substances. Report of the FOCUS Groundwater Scenarios Workgroup, EC Document Reference SANCO/321/2000 rev. 2202pp.

Freeze, R. A. , and Cherry, J. A. (1979). Groundwater, Prentice-Hall, Englewood Cliffs, N. J., 604 pp.

Gandolfi, C., Facchi, A., and Whelan, M.J. (2001). On the relative role of hydrodynamic dispersion for river water quality, *Water Resources Research* 37(9), 2365-2375.

Gärdenäs, A., Šimůnek, J., Jarvis, N. J., and van Genuchten, M. Th. (2006). Two-dimensional modelling of preferential water flow and pesticide transport from a tile-drained field, *Journal of Hydrology*, 329:647-660.

Gassman, P. W., Williams, J. R., Benson, V. W., Izaurralde, R. C., Hauck, L. M., Jones, C. A., Atwood, J. D., Kiriny, J. R., and Flowers, J. D. (2005). Working Paper 05-WP 397. Center for Agricultural and Rural Development, Iowa State University, 43 pp.

Gavrilescu, M. (2005). Review: Fate of Pesticides in the Environment and its Bioremediation, *Engineering Life Science* 5-6; 497-526.

GEOProjects (2004). Thames Ring Atlas. GEOprojects, Reading, RG1 4QS, UK, ISBN 97808 6351 1660.

Gerke, H. H., and van Genuchten, M. Th. (1993). Evaluation of a first-order water transfer term for variably-saturated dual-porosity flow models, *Water Resources Research*, 29:1225-1238.

Gerecke, A. C., Schärer, M., Singer, H. P., Müller, S. R., Schwarzenbach, R. P., Sägerser, M., Ochsenbein, U., and Popow, G. (2002). Sources of pesticides in surface waters in Switzerland: pesticide load through waste water treatment plants-current situation and reduction potential, *Chemosphere* 48 – 3; 307-315(9).

- Green, R. D., and Askew, G. P. (1965). Observations on the biological development of macropores in soils of Romney Marsh, *Journal of Soil Science*, 16:342-349.
- Gustafson, D. I. (1989). Groundwater Ubiquity Score: A simple method for assessing pesticide leachability *Environmental Toxicology and Chemistry* 8; 339-357.
- Hagedorn, C., McCoy, E. L., and Rahe, T. M. (1981). The potential for ground water contamination from septic effluents, *Journal of Environmental Quality*, 10:1-8.
- Hargreaves, G. H. and Samani, Z. A. (1985). Reference Crop Evapotranspiration from Temperature, *Applied Engineering in Agriculture*, 1(2); 96-99.
- Haria, A. H., Johnson, A. C., Bell, J. P., and Batchelor, C.H. (1994). Water movement and isoproturon behaviour in a drained heavy clay soil: 1. Preferential flow processes, *Journal of Hydrology*, 163:203-216.
- Harris, G. L., and Catt, J. A. (1999). Overview of the studies on the cracking clay soil at Brimstone Farm, UK, *Soil Use and Management*, 15:233-239.
- Hayhoe, H.N. (2000). Improvements of stochastic weather data generators for diverse climates, *Climate Research*, 14:75-87.
- Holman, I. P., Dubus, I. G., Hollis, J. M., and Brown, C. D. (2004). Using a linked soil model emulator and unsaturated zone leaching model to account for preferential flow when assessing the spatially distributed risk of pesticide leaching to groundwater in England and Wales, *The Science of the Total Environment*, 318; 73-88.
- Hollis, J. M., and Brown, C. D. (1996). A Catchment-Scale Model for Pesticides in Surface Waters, *Proceedings of the X Symposium of Pesticide Chemistry*, Sep 30-Oct 2, Piacenza, Italy, La Goliardica, pp. 371.
- Hooghoudt, S. B. (1940). Bijdrage tot de kennis van enige natuurkundige gootheden van der grond, *Verslagen van Landbouwkundige Onderzoekingen*, 46:515-707 (in Dutch).
- Humphrey, N. C. B. (2007). The Voluntary Initiative Pilot Catchment Project; Report Ref. No. 07/WR/26/2, UK Water Industry Research. Final Report; Period covered 2002/2006.
- Jacobsen, O. H., and Kjær, J. (2007). Review: Is tile drainage water representative of root zone leaching of pesticides, *Pest Management Science*, 63:417-428.
- Jarvis, M. G., Allen, R. H., Fordham, S. J., Hazelden, J., Moffat, A. J., and Sturdy, R. G. (1984). Soils and their use in south east England. *Bulletin - Soil Survey of England & Wales*, 15.

- Jarvis, N. J. (1994). The MACRO model (Version 3.1). Technical Description and Sample Simulations. Reports and Dissert, 19. Dept. Soil Sci., Swedish University Agric. Sci., Uppsala, Sweden.
- Jarvis, N. J., Stahli, M., Bergström, L., and Jonsson, H. (1994). Simulation of dichlorprop and benazeton leaching in soils of contrasting texture using the MACRO model, *Journal of Environmental Science and Health*, A29;6:1255-1277.
- Jarvis, N. J., Hollis, J. M., Nicholls, P. H., Mayr, T., and Evans, S. P. (1997). MACRO_DB: a decision-support tool for assessing pesticide fate and mobility in soils, *Environmental Modelling & Software*, 12; 2-3; 251-265.
- Johnson, A. C., Haria, A. H., Bhardwaj, C. L., Williams, R. J., and Walker, A. (1996). Preferential flow pathways and their capacity to transport isoproturon in a structured clay soil, *Pesticide Science*, 48:225-237.
- Johnson, M. S., Coon, W., Mehta, V., Steenhuis, T., Brooke, E., and Boll, J. (2003). Applications of two hydrologic models with different runoff mechanisms to a hillslope dominated watershed in the northeastern U.S.: A comparison of HSPF and SMR, *Journal of Hydrology*, 284:57–76.
- Jones, R. L., Harris, G. L., Catt, J. A., Bromilow, R. H., Mason, D. J., and Arnold, D. J. (1995). Management practices for reducing movement of pesticides to surface water in cracking clay soils, *Proc. Brighton Crop Protection Conference BCPC*, Farnham, Surrey, UK, pp. 489-498.
- Kalin, L., Govindaraju, R. S., and Hantush, M. M. (2003). Effect of geomorphological resolution on modeling of runoff hydrograph and sedimentograph over small watersheds, *Journal of Hydrology*, 276:89–111.
- Kent, K. M. (1972). SCS National Engineering Handbook; Section 4: Hydrology; Chapter 15. NEH Notice 4 – 102.
- Kjær, J., Olsen, P., Barlebo, H. C., Juhler, R. K., Plauborg, F., Grant, R., *et al.* (2004a). The Danish Pesticide Leaching Assessment Programme. Monitoring Results May 1999 – June 2003, *4th Report June 2004*, Geological Survey of Denmark and Greenland, ISBN 87-7871-128-2, 146 pp.
- Kjær, J., Olsen, P., Ullum, M., and Grant, R. (2004b). Leaching of AMPA and glyphosate in Danish agricultural soils, *Journal of Environmental Quality*, 34:608-620.
- Kladivko, E. J., Van Scoyoc, G. E., Monke, E. J., Oates, K. M., and Pask, W. (1991). Pesticide and nutrient movement into subsurface tile drains on a silt loam soil in Indiana, *Journal of Environmental Quality*, 20:264-270.

Kladivko, E. J., Brown, L. C., and Baker, J. L. (2001). Pesticide transport to subsurface tile drains in humid regions of North America, *Critical Reviews in Environmental Science and Technology* 31:1-62.

Köhne, J. M., Köhne, S., and Šimůnek, J. (2009a). A review of model applications for structure soils: a) Water flow and tracer transport, *Journal of Contaminant Hydrology* 104; 4-35.

Köhne, J. M., Köhne, S., and Šimůnek, J. (2009b). A review of model applications for structure soils: b) Pesticide transport, *Journal of Contaminant Hydrology* 104; 36-60.

Kreuger, J. (1998). Pesticides in stream water within an agricultural catchment in southern Sweden, 1990–1996. *Science of the Total Environment* 216; 227–251.

Kwakman, P. M. J., Vreuls, J. J., Brinkman, U. A. Th., and Ghijzen, R. T. (1992). Determination of organophosphorus pesticides in aqueous samples by on-line membrane disk extraction and capillary gas chromatography, *Chromatographia*, 34:41-47.

Lacorte, S., and Barceló, D. (1994). Validation of an automated precolumn exchange system (PROSPEKT) coupled to liquid chromatography with diode array detection. Application to the determination of pesticides in natural waters, *Analytica Chimica Acta*, 296:223-234.

Lacorte, S., Vreuls, J. J., Salau, J. S., Ventura, F., and Barceló, D. (1998). Monitoring of pesticides in river water using fully automated on-line solid-phase extraction and liquid chromatography with diode array detection with a novel filtration device, *Journal of Chromatography A*, 795:71-82.

Larsbo, M., and Jarvis, N. J. (2003). MACRO 5.0. A model of water flow and solute transport in macroporous soil. Technical description. Report, *Emergo*, 6, Swedish University of Agricultural Sciences, Uppsala, Sweden, 123 pp.

Leeds-Harrison, P. B., Shipway, C. J. P., Jarvis, N. J., and Youngs, E. G. (1986). The influence of soil macroporosity on water retention, transmission and drainage in clay soil, *Soil Use and Management*, 2:47-50.

Leonard, R. A. (1990). Movement of pesticides into surface waters, in Cheng, H. H. (ed.) *Pesticides in the Soil Environment: Processes, Impacts, and Modeling*, Soil Science Society of America, Inc., Wisconsin, pp. 305-349.

Leu, C., Singer, H., Stamm, C., Müller, S. R., and Schwarzenbach, R. P. (2004). Simultaneous assessment of sources, processes, and factors influencing herbicide losses to surface waters in a small agricultural catchment, *Environmental Science and Technology*, 38:3827-3834.

- Levin J.M., Herman J.S., Hornberger G.M. and Saiers J.E. (2006). Colloid mobilisation from a variably saturated, intact soil core, *Vadose Zone Journal*, 5:564-569.
- MacLean, A. (2005). Statistical evaluation of WATFLOOD, Department of Civil and Environmental Engineering, University of Waterloo, Ontario, Canada.
- Maly, J., Klem, K., Lukavska, A. and Masoj, J. (2005). Degradation and Movement in Soil of the Herbicide Isoproturon Analyzed by a Photosystem II–Based Biosensor, *Journal of Environmental Quality*, 34:1780-1788.
- Mason, P.J., Foster, I. D. L., Carter, A. D., Walker, A., Higginbotham, S., Jones, R. L., and Hardy, I. A. J. (1999). Relative importance of point source contamination of surface waters: River Cherwell catchment monitoring study. In: Del Re, A. A. M., Brown, C., Capri, E., Errera, G., Evans, S. P., and Trevisan, M. Human and environmental exposure to xenobiotics; Eds. La Goliardica Pavese, Pavia, Italy, pp. 405-412.
- Marshall, T. J., and Holmes, J. W. (1980). *Soil Physics*. Cambridge University Press, 345 pp.
- May, L., House, A. W., Bowes, M., and McEvoy, J. (2001). Seasonal export of phosphorus from lowland catchment: upper River Cherwell in Oxfordshire, England. *The Science of the Total Environment*, 269:117-130.
- McCuen, R. H., Knight, Z., Cutter, A. G. (2006). Evaluation of the Nash-Sutcliffe efficiency index, *Journal of Hydrologic Engineering*, 11,6:597-602.
- Merz, R., and Blöschl, G. (2004). Regionalization of catchment model parameters, *Journal of Hydrology*, 287:95–123.
- Millington, R. J., and Quirk, J. P. (1961). Permeability of porous solids, *Transactions of the Faraday Society*, 57:1200-1207.
- Mualem, Y. (1976). A new model for predicting the hydraulic conductivity of unsaturated porous media, *Water Resources Research*, 12:513-522.
- Müller, K., Bach, M., Hartmann, H., Spiteller, M., and Frede, H. G. (2002). Point and Non-Point Source Pesticide Contamination in the Zwesten Ohm Catchment (Germany), *Journal of Environmental Quality*, 31:309-318.
- Nash, J. E., and Sutcliffe, J.V. (1970). River flow forecasting through conceptual models part I — A discussion of principles, *Journal of Hydrology*, 10(3):282–290.
- Neumann, M., Schuls, R., Schäfer, K., Müller, W., Mannheller, W., and Liess, M. (2002). The significance of entry routes as point and non-point sources of pesticides in small streams, *Water Research*, 36:835-842.

Nilsson, B., Brusch, W., Morthorst, J., Vosgerau, H., Abildtrup, H. C., Pedersen, D., *et al.* (2000). Undersøgelse af landovervågningsboringerne DGU No. 165.295-165.297 i LOOP område 4, Lillebæk, Fyns Amt. GEUS Report, No. 47, 48 pp. (in Danish).

Pappenberger, F., Beven, K. J., De Roo, A., Thielen, J., and Gouweleeuw, B. (2004). Uncertainty analysis of the rainfall-runoff model LisFlood within the Generalized Likelihood Uncertainty Estimation (GLUE), *International Journal of River Basin Management*, 2, 2: 123-133.

Petersen, C. T., Holm, J., Koch, C. B., Jensen, H. E., and Hansen, S. (2003). Movement of pendimethalin, ioxynil and soil particles to field drainage tiles, *Pest Management Science* 59:85-96.

Ramwell, C. T., Johnson, P. D., Boxall, A. B. A., and Rimmer, D. A. (2004). Pesticide residues on the external surfaces of field-crop sprayers: environmental impact, *Pest Management Science*, 60(8):795-802.

Renaud, F. G., Bellamy, P. H., and Brown, C. D. (2008). Simulating pesticides in ditches to assess ecological risk (SPIDER): I. Model description, *Science of the Total Environment*, 394:112-123.

Rose, S. (2003). Comparative solute-discharge hysteresis analysis for an urbanized and a 'control basin' in the Georgia (USA) Piedmont, *Journal of Hydrology*, 284:45-56.

Scarisbrick, D. H., and Daniels, R. W. (1986). Oilseed rape. 1986. Collins Professional and Technical Books London, UK.

Scarisbrick, D.H., and Ferguson, A. J. (1995). New Horizons for Oilseed Rape. Semundo Ltd., Cambridge.

Shipitalo, M., Nuutinen, V., and Butt, K. R. (2004). Interaction of earthworm burrows and cracks in a clayey, subsurface-drained, soil, *Applied Soil Ecology*, 26:209-217.

Schwab, G. O., Fausey, N. R., Desmond, E. D., and Holman, J. R. (1985). Tile and Surface Drainage of Clay Soils. IV. Hydrologic Performance with Field Crops (1973-80); V. Corn, Oats, and Soybean Yields (1973-80); VI. Water Quality; VII. Cross Molding over Tile Drains. *Res. Bull.* 1166, OARDC, Wooster, OH. 29 pp.

Šimůnek, J., Jarvis, N. J., van Genuchten, M. Th., and Gärdenäs, A. (2003). Review and comparison of models for describing nonequilibrium and preferential flow and transport in the vadose zone, *Journal of Hydrology*, 272:14-35.

Slobodnik, J., Groenewegen, M. G. M., Brouwer, E. R., Lingeman, H., and Brinkman, U. A. Th. (1993). Fully automated multi-residue method for trace level monitoring of polar pesticides by liquid chromatography, *Journal of Chromatography*, 642:359-370.

Steenhuis, T. S., and Walter, M. F. (1980). Closed form solution for pesticide loss in runoff water, *Transaction of the ASAE*, 23:615-620, 628.

Stone, W. W., and Wilson, J. T. (2006). Preferential flow estimates to an agricultural tile drain with implications for glyphosate transport, *Journal of Environmental Quality*, 35:1825-1835.

Thomas, G. W., and Phillips, R. E. (1979). Consequences of water movement in macropores, *Journal of Environmental Quality*, 8:149-152.

Thompson, T. R. E. (2009). Monitoring of winter soil and surface conditions and water movement in the Upper Cherwell. Unpublished report submitted to the Environment Agency of England and Wales.

Toler, L. G. (1965). Relation between chemical quality and water discharge in Spring Creek, Southwestern Georgia, *US Geological Survey Professional Paper 525-C*, 209-213.

Turnbull, A. B., Harrison, R. M., Williams, R. J., Matthiessen, P., Brooke, D. N., Sheahan, D. A., and Mills, M. (1997). Assessment of the fate of selected adsorptive pesticides at ADAS Rosemaund, *Journal of the Chartered Institution of Water and Environmental Management*, 11:24-30.

United Nations (2002). United Nations Environmental Program (UNEP), Montreal Protocol on Substances that Deplete the Ozone Layer. Report of the Methyl Bromide Technical Options committee, p. 43.

Vanclooster, M., Boesten, J. J. T. I., Trevisan, M., Brown, C. D., Capri, E., Eklo, O. M., Gottesbüren, B., Gouy, V., and van der Linden, A. M. A. (2000). A European test of pesticide leaching models: methodology and major recommendations, *Agricultural Water Management*, 44:1-19.

van Genuchten, M. Th., and Wierenga, P.J. (1976). Mass transfer studies in sorbing porous media. I. Analytical solutions, *Soil Science Society of America Journal*, 40:473-480.

van Genuchten, M. Th. (1980). A closed-form equation for predicting the hydraulic conductivity of unsaturated soils, *Soil Science Society of America Journal*, 44:892-898.

van Genuchten, M. Th. (1985). A general approach for modeling solute transport in structured soils. In *Proceedings 17th International Congress IAH, Hydrogeology of rocks of low permeability*. Memoirs IAH, 17:513-526.

van Genuchten, M. Th., and Dalton, F. N. (1986). Models for simulating salt movement in aggregated field soils, *Geoderma*, 38:165-183.

- Villholth, K. G., Jensen, K. H., and Fredericia, J. (1998). Flow and transport processes in a macroporous subsurface-drained glacial till soil I: field investigations, *Journal of Hydrology* 207:98-120.
- Ward, R. C., and Robinson, M. (1990). Principles of Hydrology, Third edition, McGraw-Hill Book Company Europe, 365 pp.
- Weiler, M., and Flühler, H. (2004). Inferring flow types from dye patterns in macroporous soils, *Geoderma*, 120:137-153.
- Whelan M.J., White S.M. and Howden N.J.K. (2009). River Catchment Contributions to the Coastal Zone, pp 33-58 in Green D. (ed) *Coastal Zone Management*, Thomas Telford, London.
- White, R. E. (1985). The influence of macropores on the transport of dissolved and suspended matter through soil. In *Advances in Soil Science*, Volume 3. Springer-Verlag New York Inc.
- White, R. E., Dyson, J. S., Haigh, R. A., Jury, W. A., and Sposito, G. (1986). A transfer function model of solute transport through soil. 2. Illustrative applications, *Water Resources Research*, 22:248-254.
- Whitford, F. (2002), *The Complete Book of Pesticide Management: Science, Regulation, Stewardship, and Communication*, J. Wiley & Sons, New York.
- Whitford, F., Wolt, J., Nelson, H., Barret, M., Brichford, S., and Turco, R. (2001), *Purdue Pesticide Programs- Purdue University Cooperative Extension Services*, available at: <http://www.btny.purdue.edu/Pubs/PPP/PPP35.html> (accessed 3 Jul 2008).
- Williams, J. R. (1995). The EPIC model. In: Singh, V. P., editor. Computer models of watershed hydrology. Highland Ranch: *Water Resources Publications*, pp. 909-1000.
- Woledge, J., Davidson, I. A., and Tewson, V. (1989). Photosynthesis during winter in ryegrass / white clover mixtures in the field, *New Phytologist*, 113:275-281.
- World Meteorological Organization (1986). Intercomparison of models of snowmelt runoff. WMO No. 646, Geneva.
- Xia, Y., Fabian, P., Stohl, A., and Winterhalter, M. (1999). Forest climatology: estimation of missing values for Bavaria, Germany, *Agricultural and Forest Meteorology*, 96:131-144.
- Yang, D., Herath, S., and Musiake, K. (2002). A hillslope-based hydrological model using catchment area and width functions, *Hydrological Sciences*, 47:49-65.

Appendix 1 – Development of a digital river network map

A1.1 Data sources

Digital Terrain Model (DTM)

Digital elevation models (DEM) are a digital representation of the topography of the Earth surface. This topography is described on a raster cell basis. Each cell in the DEM is assigned a value that corresponds to its elevation. Digital elevation models can be defined into two sub-categories, digital surface models (DSM), and digital terrain models (DTM). Digital surface models include all features on the Earth surface both natural and artificial, for example trees and buildings. Digital terrain models are 'bare Earth' models and model the height of Earth surface without any additional features.

I obtained a 10-metre-resolution DTM from the Ordnance Survey website (DigiMap) (Figure A1.1).

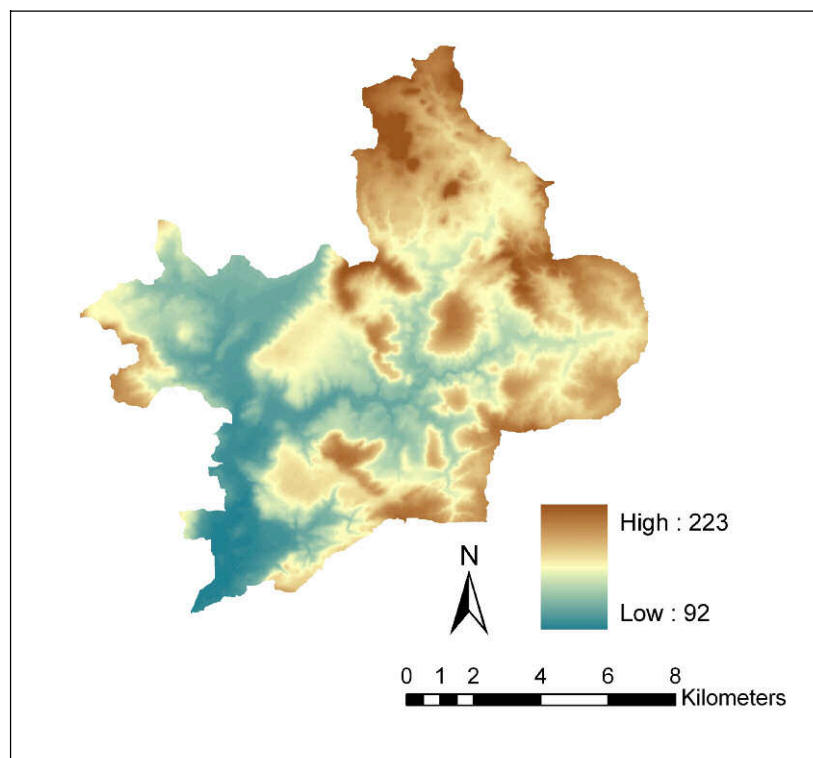


Figure A1.1 - Digital Terrain Model (10-metre resolution) showing a part of the study area. The elevation is expressed in metres.

Topographic map

Topographic maps were downloaded from the EDINA data centre website (<http://edina.ac.uk/digimap/> [accessed 7th December 2009]). In particular I obtained two different maps:

- Vector and raster versions of the 1:25,000-scale topographic map;
- Raster 1:10,000 map.

A1.2 Methodology

A preliminary task for the hydrological modelling was the definition of the catchment boundary and a digital channel network. A comparison of the river network derived from the topographic map (MasterMap, vector format) with the one represented in the topographic raster maps raised some questions regarding the quality of the MasterMap network.

The river network was, therefore, generated using terrain analysis tools. Two flow direction and flow accumulation tools were used: (1) TauDEM: Terrain Analysis Using Digital Elevation Models (Tarboton, 2009; <http://hydrology.usu.edu/taudem/taudem4.0> accessed 15th December 2009) and (2) Algorithms implemented in ArcGIS. Both procedures were unable to represent the location of artificial channels (e.g. ditches) in catchment which make an important contribution to the surface water network. The river network was, therefore, digitised manually from the 1:10,000 and the 1:25,000 Ordnance Survey raster maps, depending on the required detail level. The final map is shown in Figure A1.2.

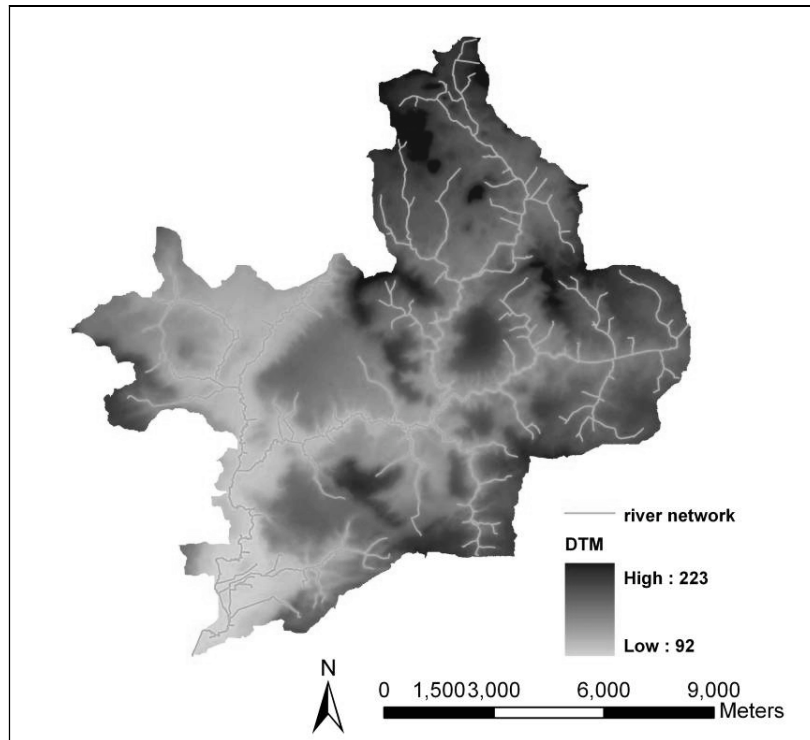


Figure A1.2 - Map of the channel network in the Upper Cherwell catchment, digitised from the OS raster maps, overlain on the digital terrain model (DTM).

Appendix 2 – Redefinition of the catchment boundary

The development of a digital channel network improved understanding of the catchment hydrology, allowing the identification of several non-contributing areas (i.e. areas which drain downstream of the closing section). The hydrologically active catchment is shown in Figure A2.1, superimposed on the original boundary. The numbers 1 to 6 refer to the main areas which were excluded:

1. Boddington Reservoir: This reservoir is operated by British Waterways as a feeder for the Oxford Canal. The reservoir contributes to the channel network of the Upper Cherwell only when the reservoir over spills (i.e. when it is full), although there is also an informal compensation flow, taking water from the canal draw off pipe. Unfortunately, there are no reliable records for overspill discharge (personal communication British Waterways, May 2009). However, given the potential for attenuation of pesticide peaks in the reservoir and the fact that most water feeds the canal, the reservoir catchment was excluded from the revised Upper Cherwell boundary (Figure A2.2). The reliability of this assumption needs to be confirmed via hydrological monitoring of the stream downstream of Boddington Reservoir, combined with sampling and analysis for key pesticides.
2. The area between Boddington Reservoir and Wormleighton Reservoir: This land is drained directly into the Oxford Canal Feeder which, in turn, drains out of the catchment. It is important to stress that the Oxford Canal flows across the catchment, but not into the river (Figure A2.3).
3. Wormleighton Reservoir: The flow from this reservoir drains to the Oxford Canal and the upstream catchment area was therefore excluded (Figure A2.4).
4. Hanwell Brook: Hanwell Brook flows directly into the Oxford Canal and then out of the catchment (Figure A2.5).
5. Cropredy: There is an area west of Cropredy which drains through a number of ditches into the Oxford Canal (Figure A2.6).

6. Grimsbury Reservoir – Banbury: The catchment outlet is assumed to be the abstraction point for Grimsbury Reservoir (Figure A2.7).

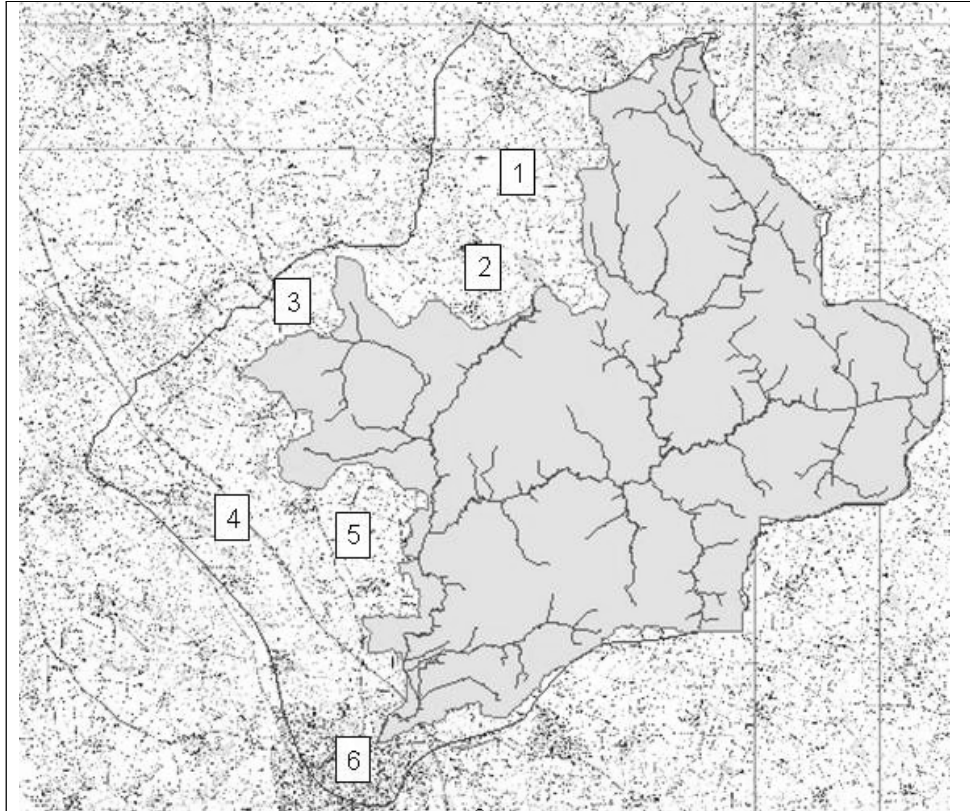


Figure A2.1 – The original and redefined (shaded) boundary of the Upper Cherwell catchment. The numbers refer to notes in the text.

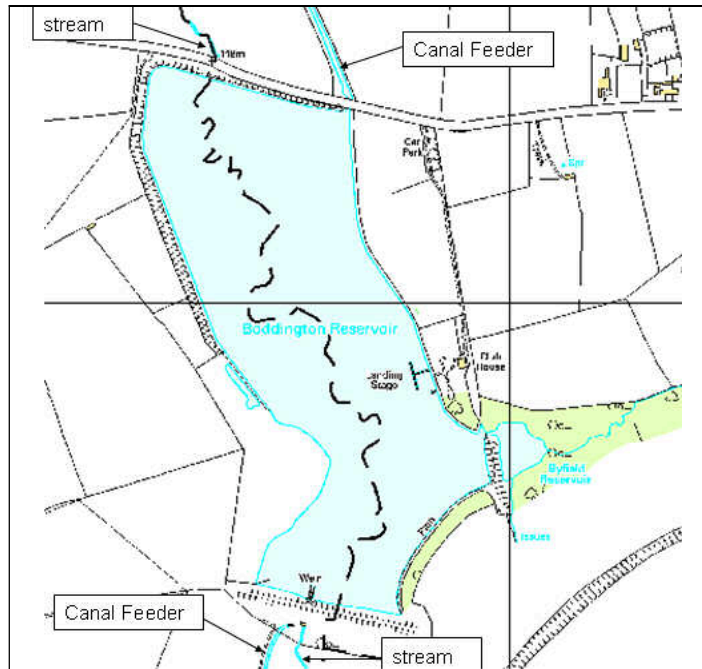


Figure A2.2 - Boddington Reservoir (point 1).

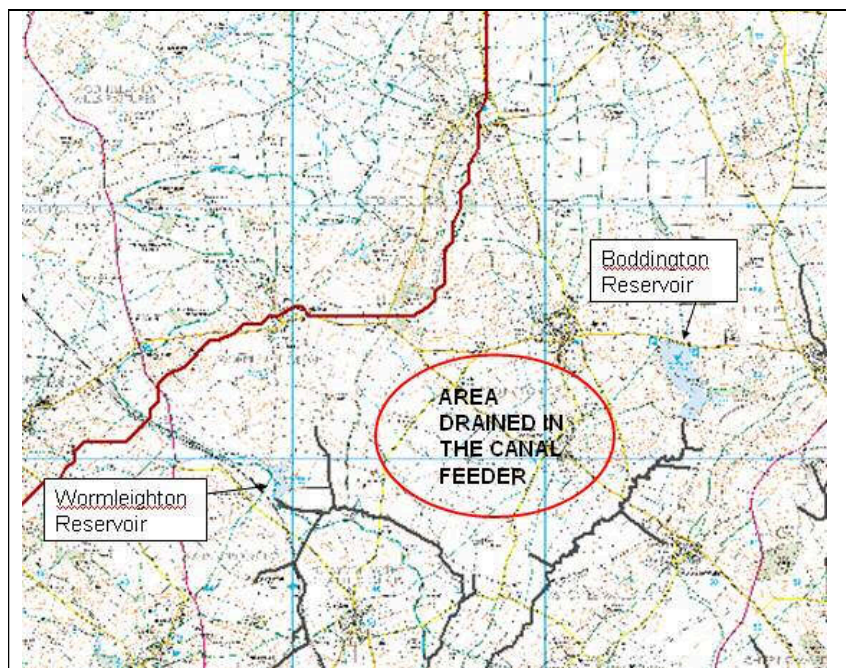


Figure A2.3 - Area between Boddington Reservoir and Wormleighton Reservoir (point 2).

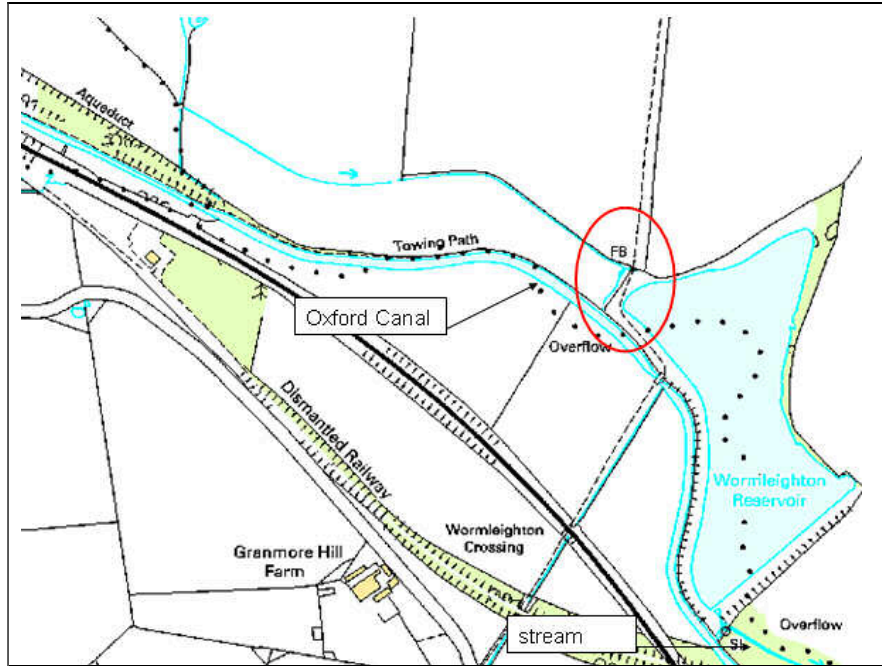


Figure A2.4 – Wormleighton Reservoir (point 3).

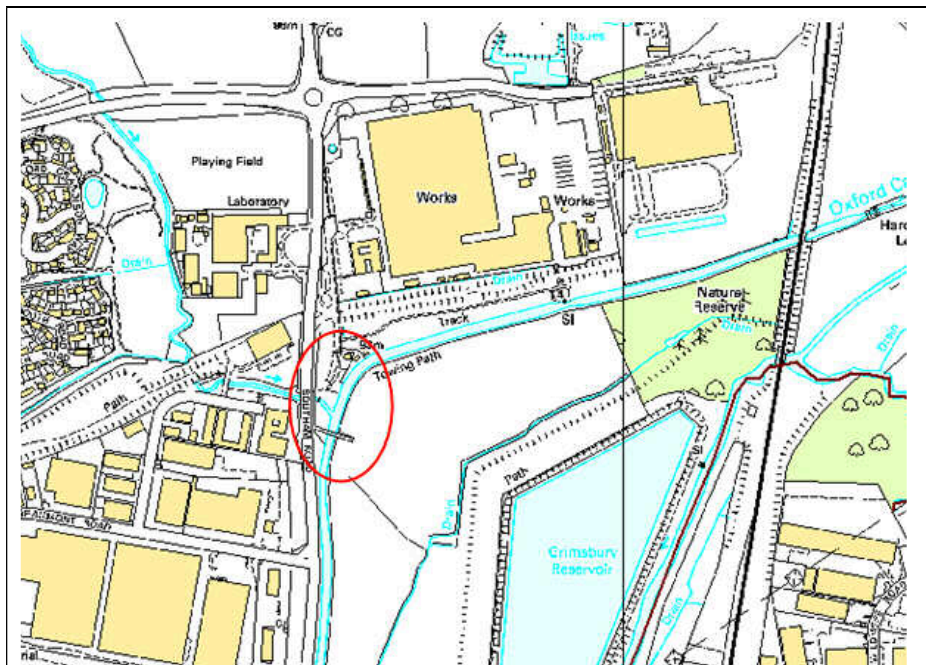


Figure A2.5 - Hanwell Brook (point 4).

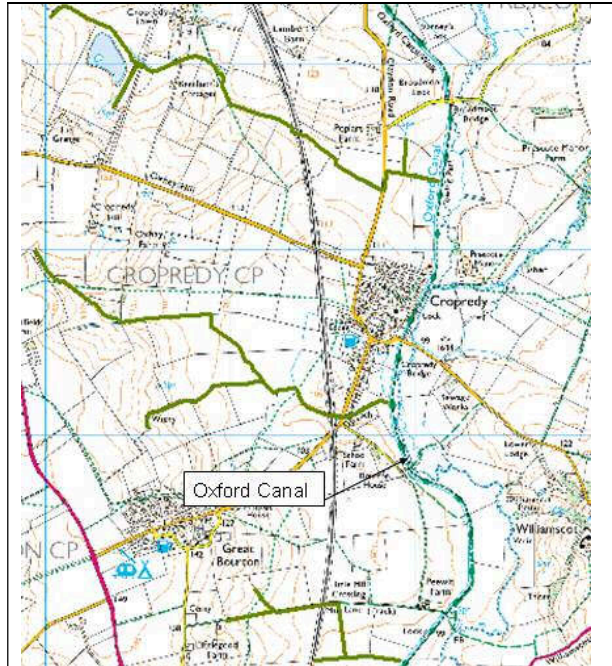


Figure A2.6 – Cropredy (point 5).

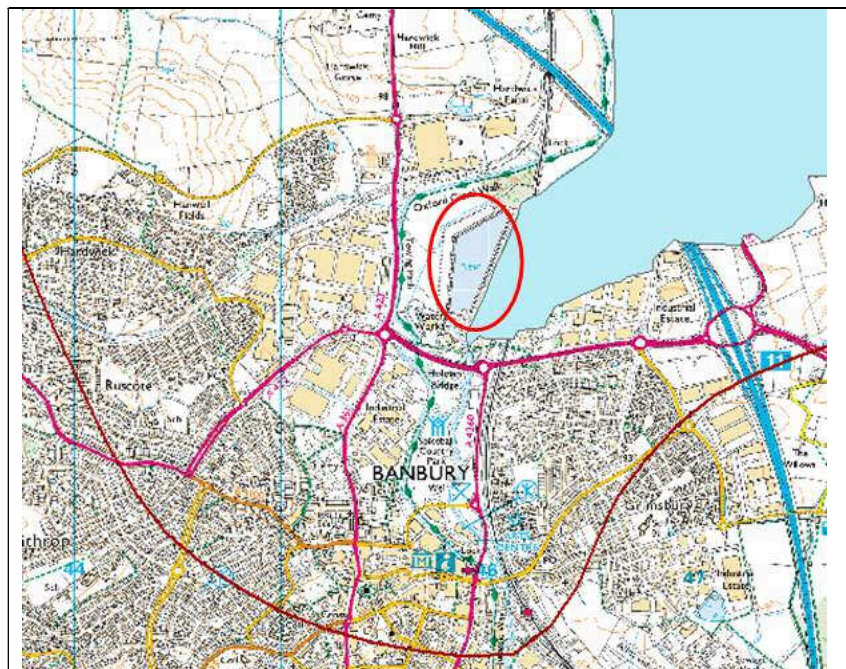


Figure A2.7 – Grimsbury Reservoir – Banbury (point 6).

Appendix 3 – Land use

A3.1 Data sources: land use map and statistics

The land use map I used for this project is the CORINE land cover 2000, scale 1:100,000 (see Figure 3, Chapter 2). The land use is classified using 44 classes of a 3-level CORINE nomenclature. Only 8 classes are included in the study area (Table A3.1).

As this land use classification is rather general the spatial information was integrated with land use statistics from DEFRA (www.defra.gov.uk agricultural census data for 2000 to 2007 [accessed 7th April 2009]). These data refer to the Local Authority ‘Cherwell’, of which the Upper Cherwell is only a part.

A3.2 Methodology

The CORINE land use map was used to derive the total agricultural land in the Upper Cherwell for year 2000. The areas of each land use for the Local Authority ‘Cherwell’ (DEFRA, agricultural census data for 2000 to 2007) were converted into fractions, which were then used for the downscaling.

The calculations were made for year 2000 first, then –knowing the variation of the total agricultural land within the Local Authority ‘Cherwell’- they were carried out also for years 2001 to 2007 (Table A3.2).

Table A3.1 - CORINE and use classes in the Upper Cherwell catchment (CORINE 2000).

Level 1	Level 2	Level 3	Code
Artificial surfaces	Urban fabric	Discontinuous urban fabric	112
Artificial surfaces	Industrial, commercial and transport units	Industrial or commercial units	121
Artificial surfaces	Mine, dump and construction sites	Dump sites	132
Artificial surfaces	Artificial, non-agricultural vegetated areas	Green urban areas	141
Artificial surfaces	Artificial, non-agricultural vegetated areas	Sport and leisure facilities	142
Agricultural areas	Arable land	Non-irrigated arable land	211
Agricultural areas	Pastures	Pastures	231
Agricultural areas	Heterogeneous agricultural areas	Complex cultivation patterns	242

Table A3.2 - Agricultural land use (derived from the DEFRA statistics) of the Upper Cherwell catchment (areas are expressed in hectares).

Agricultural area 2000 – 2007 (hectares)								
	2000	2001	2002	2003	2004	2005	2006	2007
Temporary grassland	805.4	799.6	836.9	759.5	867.8	869.3	811.3	976.2
Permanent grassland	3424.3	3602.0	3498.6	3782.7	3692.7	3830.0	4093.8	4197.9
Rough grazing	171.7	207.1	262.0	214.7	199.4	228.2	156.0	224.3
Woodland	294.3	284.7	264.7	292.3	251.5	270.6	255.2	271.0
Setaside	1044.7	1644.3	1090.2	1236.6	1026.8	1035.1	967.8	755.3
All other land	316.4	302.3	286.8	262.5	215.5	236.1	218.9	0.0
Wheat	3780.9	3016.5	3635.8	3292.1	3463.8	3499.6	3543.2	3428.1
Winter barley	858.7	676.7	752.4	617.0	525.6	453.3	438.2	393.1
Spring barley	0.0	395.5	0.0	0.0	280.8	287.2	293.7	0.0
Oats	208.5	0.0	0.0	0.0	142.5	0.0	0.0	201.7
Other cereals	0.0	0.0	0.0	0.0	7.3	0.0	0.0	0.0
Potatoes	41.0	34.4	31.1	28.5	11.2	18.5	9.4	11.6
Sugar beet	0.0	0.0	0.0	0.0	0.0	0.9	0.0	5.6
Horticulture	9.4	0.0	0.0	0.0	9.4	10.0	0.0	0.0
Field beans	270.3	330.7	403.2	433.8	582.8	490.3	492.4	340.8
Peas hd	136.9	197.0	141.2	161.9	90.2	101.5	66.9	50.2
Oilseed rape	956.8	1197.7	1031.4	1189.4	1027.0	1166.6	1168.2	1301.5
Linseed	177.5	0.0	0.0	49.9	69.0	86.9	0.0	0.0
Turnips etc	8.3	0.0	0.0	0.0	2.8	0.0	0.0	0.0
Other crop stock	17.4	26.9	4.4	12.2	9.3	0.0	0.0	12.5
Maize	146.6	152.0	130.2	130.3	156.0	159.7	170.4	181.1
Other arable crops	23.0	15.8	12.4	10.8	11.0	0.0	51.4	47.8
Bare fallow	38.9	55.1	31.9	29.4	23.0	213.3	223.4	237.5
Peas and beans	0.0	0.0	0.0	0.0	0.3	1.4	0.0	0.0
All other vegetables and salad	0.0	0.0	0.0	5.1	3.9	0.0	0.0	5.2
Area glass plastic	0.0	0.1	0.2	0.0	0.3	0.0	0.0	0.4
Top fruit	0.0	0.0	0.0	0.0	0.9	0.0	1.3	2.4
Small fruit	0.0	0.0	0.0	0.0	2.2	2.6	0.0	2.1
Total area	<i>12731.0</i>	<i>12938.5</i>	<i>12413.4</i>	<i>12508.8</i>	<i>12673.2</i>	<i>12961.3</i>	<i>12961.4</i>	<i>12646.3</i>

Appendix 4 – MACRO application: parameter values

This appendix reports all the parameter values used to represent field observations with MACRO (see Chapter 6). It must be noted that this list of parameters refers to two simulations: the run IDs (R_ID in the tables reported below) 2 and 4 identify the solute simulated (carbetamide and propyzamide, respectively).

General

R_ID	Nlayer	Nhorizon	profilnamn	System	location	Classify	landusage	GeneralID
2	60	4	Denchworth			Denchworth	OSR	46
4	60	4	Denchworth			Denchworth	OSR	48

Crop (the same for R_ID 2 and 4)

R_ID	2
year	1
cropname	OSR
ncrop	1
ROOTINIT	0.01
rootinit_C	1
ROOTMAX	0.6
rootmax_C	1
ROOTDEP	0.7
rootdep_C	1
CFORM	2
cform_C	0
RPIN	60
rpin_C	0
FAWC	0.65
fawc_c	0
CRITAIR	5
critair_C	0
BETA	0.2
beta_C	0
CANCAP	2
cancap_C	0
ZALP	1

zalp_c	0
IDSTART	250
idstart_c	2
IDMAX	120
idmax_C	2
IHARV	210
iharv_C	2
ZHMIN	0.01
zhmin_C	1
LAIC	5
laic_C	1
LAIMIN	0.01
laimin_C	1
LAIMAX	3.2
laimax_C	1
ZDATEMIN	45
zdatemin_C	2
DFORM	0.7
dform_C	0
LAIHAR	0.4
laihar_C	1
HMAX	0
hmax_C	1
RSMIN	80
rsmin_C	0
ATTEN	0.6
atten_C	0
HCROP	0.5
herop_C	1
RSURF	60
rsurf_C	1
idstart2	
idstart2_c	0
zdatemin2	
zdatemin2_c	0
idmax2	
idmax2_c	0
iharv2	
iharv2_c	0
WATEN	2.66497
CROPID	57

RI50	55
RI50_c	0
VPD50	100
VPD50_c	0

Initial boundary conditions (1)

R_ID	2	4
AREA	1	1
area_C	0	0
BGRAD	0.0001	0.0001
bgrad_C	1	1
BOTEN	0	0
boten_C	0	0
CONCIN	0	0
concin_C	0	0
GWFLUX	0.0001	0.0001
gwflux_C	0	0
PARTINIT	0.1	0.1
partinit_C	1	1
CONS_STA	100	100
cons_sta_c	0	0
I_ASCALE	20	20
i_ascale_c	0	0
IBID	46	48

Initial boundary conditions (2) (the same for R_ID 2 and 4)

R_ID	Layer no	THETAINI	thetaini_C	SOLINIT	solinit_C	TEMPINI	tempini_C	IB_ID2
2	1	40	2	0	0	10	0	62
2	2	40	2	0	0	10	0	63
2	3	40	2	0	0	10	0	64
2	4	40	2	0	0	10	0	65
2	5	40	2	0	0	10	0	66
2	6	40	2	0	0	10	0	67
2	7	40	2	0	0	10	0	68
2	8	40	2	0	0	10	0	69
2	9	40	2	0	0	10	0	70
2	10	40	2	0	0	10	0	71
2	11	40	2	0	0	10	0	72

2	12	40	2	0	0	10	0	73
2	13	40	2	0	0	10	0	74
2	14	40	2	0	0	10	0	75
2	15	40	2	0	0	10	0	76
2	16	47	2	0	2	10	0	77
2	17	47	2	0	2	10	0	78
2	18	47	2	0	2	10	0	79
2	19	47	2	0	2	10	0	80
2	20	47	2	0	2	10	0	81
2	21	47	2	0	2	10	0	82
2	22	47	2	0	2	10	0	83
2	23	47	2	0	2	10	0	84
2	24	47	2	0	2	10	0	85
2	25	47	2	0	2	10	0	86
2	26	47	2	0	2	10	0	87
2	27	47	2	0	2	10	0	88
2	28	47	2	0	2	10	0	89
2	29	47	2	0	2	10	0	90
2	30	47	2	0	2	10	0	91
2	31	47	2	0	2	10	0	92
2	32	47	2	0	2	10	0	93
2	33	47	2	0	2	10	0	94
2	34	47	2	0	2	10	0	95
2	35	47	2	0	2	10	0	96
2	36	47	2	0	2	10	0	97
2	37	47	2	0	2	10	0	98
2	38	47	2	0	2	10	0	99
2	39	47	2	0	2	10	0	100
2	40	47	2	0	2	10	0	101
2	41	47	2	0	2	10	0	102
2	42	47	2	0	2	10	0	103
2	43	47	2	0	2	10	0	104
2	44	47	2	0	2	10	0	105
2	45	47	2	0	2	10	0	106
2	46	47	2	0	2	10	0	107
2	47	47	2	0	2	10	0	108
2	48	47	2	0	2	10	0	109
2	49	47	2	0	2	10	0	110
2	50	47	2	0	2	10	0	111
2	51	47	2	0	2	10	0	112
2	52	47	2	0	2	10	0	113

2	53	47	2	0	2	10	0	114
2	54	47	2	0	2	10	0	115
2	55	47	2	0	2	10	0	116
2	56	47	2	0	2	10	0	117
2	57	47	2	0	2	10	0	118
2	58	47	2	0	2	10	0	119
2	59	47	2	0	2	10	0	120
2	60	47	2	0	2	10	0	121

Irrigation (1)

R_ID	NIRR	nirr_C	CRITDEF	critdef_C	IRRID	IRRYEARS	IRRSAME
2	1	0	-1	0	2	1	VERO
4	1	0	-1	0	4	1	VERO

Irrigation (2)

R_ID	2	4
IRRIG_no	1	1
AMIR	0.03	0.06
amir_C	2	2
CONCI	7000	1333.3
conci_C	2	2
IRRSTART	11	11
irrstart_c	2	2
IRREND	13	13
irrend_C	2	2
IRRDAY	46	336
irrdays_C	2	2
ZFINT	0.05	0.05
zfint_C	2	2
IRR_ID	337	452
IRRYEAR	1	1
IRRGROUP	1 2	1 2

Options

R_ID	2	4
AVERAGEX	2	2
AVERAGET	1	1

AVERAGEG	1	1
AVERAGED	1	1
ADDSIM	0	0
OUTFORN	0	0
INSTATE	0	0
OUTSTATE	0	0
DRIVPG	1	1
NITRATE	0	0
BOUNDARY	3	3
CHAPAR	0	0
COLLOID	0	0
CROP	2	2
DRIVING	0	0
EVAPORATE	1	1
HYDRAULIC	1	1
HYSTERES	1	1
IMMOBILE	1	1
INITIAL	2	2
IRRIGATE	1	1
LISALLV	2	2
MASSUNITS	3	3
METABOLIT	0	0
RAINFALL	2	2
SOLUTE	2	2
TILEDRAIN	1	1
VALIDPG	0	0
MANAGEMEN	0	0
CRUST	0	0
OPTID	47	49
KINETIC	1	0
UPSTREAM	0	0
SPECOUT	0	0
DEGKIN	1	0
TEMPINI	0	0
VARTEN	0	0

Physical parameters (the same for R_ID 2 and 4)

R_ID	2	2	2	2
Layer_no	1	2	3	4
XMPOR	53	50	49	46

xmpor_C	2	2	2	2
TPORV	53.63	50.86	49.19	46.1
tporv_C	3	3	3	3
WILT	26.21	35.04	34.21	31.57
wilt_C	3	3	3	3
GAMMA	1.17	1.26	1.31	1.4
gamma_C	0	0	0	0
RESID	0	0	0	0
resid_c	3	3	3	3
CTEN	10	10	20	20
cten_C	2	2	2	2
ZLAMB	1.177	1.111	1.076	1.076
zlamb_C	2	2	2	2
KSATMIN	26.9	8.8	8.2	9.4
ksatmin_C	2	2	2	2
KSM	0.029	0.1	0.098	0.12
ksm_C	2	2	2	2
ZN	3.5	3.5	3	2
zn_C	2	2	2	2
ZM	0.5	0.5	0.5	0.5
zm_C	0	0	0	0
ZP	0	0	0	0
zp_C	2	2	2	2
ZA	1	1	1	1
za_C	0	0	0	0
ASCALE	100	100	50	50
ascale_C	2	2	2	2
SCALEPSI	0.5	0.5	0.5	0
scalepsi_C	1	1	1	0
SCALEVG	0.030959	0.010347	0.010179	0.013242
scalevg_C	3	3	3	3
TRAP AIR	0	0	0	0
trap_air_c	0	0	0	0
PARID	1150	1151	1152	1156

Properties (the same for R_ID 2 and 4)

R_ID	2	2	2	2
Designat	A	Bg1	Bg2	BC
Thick	20	30	20	30
Sand	17	6	5	6

Silt	40	30	31	36
Clay	43	64	64	58
System				
Structur	moderate medium blocky	moderate medium blocky	moderate medium blocky	moderate medium blocky
Bulk	1.17	1.26	1.31	1.4
Orgc	2.9	1.2	0.8	0.4
macro1				
macro2				
texture	silty clay	clay	clay	clay
Ph	6.3	6.9	7	7.4
Nlayer	15	16	11	18
horiz_no	1	2	3	4
PROPID	280	281	282	286

Site (1) (the same for R_ID 2 and 4)

R_ID	2
ALBEDO	0.25
albedo_C	0
ANNAMP	7.55
annamp_C	2
ANNTAV	9.98
anntav_C	2
DRAINDEP	0.6
draindep_C	2
DWRL	4
dwrl_C	0
LAYERD	1
layerd_C	2
RAINCO	1
rainco_C	0
SPACE	10
space_C	2
PHI	52
phi_C	2
RGWFLOW	0
rgwflow_C	0
RINTEN	2

rinten_C	2
SNOWCO	1
snowco_C	0
SNOWMF	4.5
snowmf_C	0
ZMET	177
zmet_C	2
GAMMATILL	0.97
MACPTILL	53.53
MACDTILL	6
HALFRAIN	50
gamma_ch_c	0
macp_ch_c	0
macd_ch_c	0
halfrain_c	0
NTILL	1
HALFCRUS	50
CRUSTSTA	100
KSMTILLE	1
HALFCRUS_C	0
CRUSTSTA_C	0
KSMTILLE_C	0
DUMMY	0
DUMMY_C	0
SITEID	2
GAMMASEAL	0
KSMSEAL	0
ZNSEAL	0
XMPORSEAL	0
GAMMASEAL_C	0
XMPORSEAL_C	0
ZNSEAL_C	0
KSMSEAL_C	0

Site (2) (the same for R_ID 2 and 4)

TILL_DAY	1
TILL_INT	0.5
TILL_LAY	1
T_ASCALE	5
TILLCONS	50

R_ID	2
till_day_c	0
till_int_c	0
till_lay_c	0
t_ascale_c	0
tillcons_c	0
SITEID	2

Soil profile (the same for R_ID 2 and 4)

R_ID	Layer_no	Z	z_C	ID
2	1	0.3	1	61
2	2	0.4	1	62
2	3	0.6	1	63
2	4	0.7	1	64
2	5	1.64	1	65
2	6	1.64	1	66
2	7	1.64	1	67
2	8	1.64	1	68
2	9	1.64	1	69
2	10	1.64	1	70
2	11	1.64	1	71
2	12	1.63	1	72
2	13	1.63	1	73
2	14	1.63	1	74
2	15	1.63	1	75
2	16	1.88	1	76
2	17	1.88	1	77
2	18	1.88	1	78
2	19	1.88	1	79
2	20	1.88	1	80
2	21	1.88	1	81
2	22	1.88	1	82
2	23	1.88	1	83
2	24	1.87	1	84
2	25	1.87	1	85
2	26	1.87	1	86
2	27	1.87	1	87
2	28	1.87	1	88
2	29	1.87	1	89
2	30	1.87	1	90

2	31	1.87	1	91
2	32	1.82	1	92
2	33	1.82	1	93
2	34	1.82	1	94
2	35	1.82	1	95
2	36	1.82	1	96
2	37	1.82	1	97
2	38	1.82	1	98
2	39	1.82	1	99
2	40	1.82	1	100
2	41	1.81	1	101
2	42	1.81	1	102
2	43	1.67	1	103
2	44	1.67	1	104
2	45	1.67	1	105
2	46	1.67	1	106
2	47	1.67	1	107
2	48	1.67	1	108
2	49	1.67	1	109
2	50	1.67	1	110
2	51	1.67	1	111
2	52	1.67	1	112
2	53	1.67	1	113
2	54	1.67	1	114
2	55	1.66	1	115
2	56	1.66	1	116
2	57	1.66	1	117
2	58	1.66	1	118
2	59	1.66	1	119
2	60	1.66	1	120

Solute (1)

R_ID	2	4
DIFF	4.6E-10	4.6E-10
diff_C	0	0
DV	1	1
dv_C	0	0
PMAX	0.1	0.1
pmax_C	1	1
FSTAR	0	0

fstar_C	0	0
FRACMAC	0.01	0.01
fracmac_C	2	2
CANDEG	0.2	0.2
candeg_C	0	0
FEXT	0.01	0.01
fext_C	0	0
ZMIX	1	1
zmix_C	0	0
ZKDPC	1	1
zkdpc_C	1	1
CONC	0	0
conc_C	0	0
EXPB	0.001	0.001
expb_C	2	2
TRESP	0.001	0.001
tresp_C	2	2
TREF	20	20
tref_C	0	0
GENKD	5	5
genkd_C	1	1
FCONVERT	0.2	0.2
fconvert_C	1	1
PF1	2	2
pf1_C	1	1
PF2	3	3
pf2_C	1	1
FRACK	0.1	0.1
frack_C	0	0
FREUND		
freund_C		
VREF	50	50
vref_C	1	1
SETTLE	0.7	0.7
settle_C	1	1
FILTERMI	50	50
filtermi_C	1	1
REFILTER	5	5
refilter_C	1	1
REPLEN	1	1
replen_C	1	1

GRAVIT	0.003	0.003
gravit_C	1	1
SoluteID	2	4
SORP_RATE	1	1
sorp_rate_c	0	1
FRAC_EQ	0.5	0.5
frac_eq_c	0	1

Solute (2)

R_ID	2	2	2	2	4	4	4	4
Layer_no	1	2	3	4	1	2	3	4
ALPHA	1	1	1	1	1	1	1	1
alpha_C	0	0	0	0	0	0	0	0
ZKD	2.581	1.068	0.712	0.356	7.25	3	2	1
zkd_C	0	0	0	0	0	0	0	0
DEGMIL	0.1	0.0667	0.04	0.03	0.1	0.0667	0.04	0.03
degmil_C	0	0	0	0	0	0	0	0
DEGMAL	0.1	0.0667	0.04	0.03	0.1	0.0667	0.04	0.03
degmal_C	0	0	0	0	0	0	0	0
DEGMIS	0.1	0.0667	0.04	0.03	0.1	0.0667	0.04	0.03
degmis_C	0	0	0	0	0	0	0	0
DEGMAS	0.1	0.0667	0.04	0.03	0.1	0.0667	0.04	0.03
degmas_C	0	0	0	0	0	0	0	0
FMOBILE	0.5	0.5	0.5	0	0.5	0.5	0.5	0
fmobile_C	1	1	1	0	1	1	1	0
AEXC	0	0	0	0	0	0	0	0
aexc_C	0	0	0	0	0	0	0	0
PSEXC	10	10	10	0	10	10	10	0
psexc_C	1	1	1	0	1	1	1	0
SOLUTE ID	62	63	64	68	76	77	78	79
freund	0	0	0	0	0	0	0	0
freund_c	0	0	0	0	0	0	0	0

Appendix 5 – Temperature data series reconstruction

Data reconstruction was based, when possible, on the use of the data collected at the Experimental Field, which was used as a neighbouring station. In the next sections data sources and methodology used are presented.

A5.1 Data sources: temperature data

Air temperature data were obtained from the Radcliffe Meteorological Observatory in Oxford for a 13-year period (January 1996 to December 2008) (Paragraph 7.1.1). These temperature data were chosen as dataset for simulating flows and herbicide losses at the catchment outlet over the period October 2008 - March 2010. Therefore the data series needed to be completed for the missing period January 2009 to March 2010.

Temperature data monitored at the Experimental Field (period March 2009 - April 2010) can be considered, in absence of a better reference, a suitable station for the Oxford series reconstruction. Note that the Experimental Field is about 60 km North of Oxford.

A5.2 Methodology

Temperature data measured at Oxford were reconstructed as follows:

- The data missing in the period January 1996 - February 2009 (4.7% of the data records was missing) needed a synthetic imputation, since no neighbouring station data were available for this period. Given to the small amount of missing data, a fulfilment based on a synthetic data generation method (described below), was used;
- For the period March 2009 to March 2010: no data were available for the Oxford series and an estimation based on the reference station (Experimental Field) was performed.

Synthetic method

To obtain values having a good agreement with the series behaviour, in absence of a reference station data, the following method (Hayhoe, 2000) was adopted:

- 1) series decomposition (identification and removal of seasonal periodicity, spectral identification of higher frequency waves, first lag autocorrelation) and calculation of the series residuals (innovation component);
- 2) rearrangement of the series residuals in a year matrix format (one column per day of the year and a row per year of the series);
- 3) for each missing data, a value of the residual has been casually extracted from the year matrix picking from a sample of valid data available in the same part of the year (same day of the year ± 10 days);
- 4) backward composition starting from the so completed residuals series to the whole series (i.e. the same steps applied in decomposition are inverted and applied again in the reverse order).

Modified closest station method

For the period March 2009 to March 2010 an estimation of the missing values based on the reference station series (Experimental Field) was applied. After a first imputation where the data of the reference have been simply pasted in the Oxford series (closest station method: Xia *et al.*, 1999), a visual inspection of the run plot of the so completed series showed a lack of homogeneity along the series. To obtain values having a good agreement with the Oxford series behaviour, the following method was adopted.

So the data values of the reference series were paste on the Oxford series to fill the gaps. In order to complete the Oxford series obtaining the same behaviour of the original data and the imputed data, the reference neighbour data, before the imputation, were forced to take the same mean and variance of the series. Therefore, mean (m_o) and variance (s_o^2) of the Oxford series were computed; the same was done for the reference

series obtaining m_r and s_r^2 . The following operation was then applied to the reference data:

$$O_t = m_o + s_o \cdot \frac{(R_t - m_r)}{s_r} \quad (\text{A5.1})$$

where R_t are the original reference data (Experimental Field measurements), O_t are the values used for the imputation of the Oxford series, and t is the series time index (only time steps where the reference is present are considered).

It should be noted that, given the methodology used, the values generated for the missing data have the same features of the original series and maintains the same local behaviour. Therefore they can be considered a suitable estimate for the data series reconstruction in order to obtain appropriate and complete input for the model.

This piece of work is based on the following hypotheses:

- 1) mean and variance of the Oxford series where data are available are the same of those where data are missing, which is likely to be verified;
- 2) a linear relationship exists between reference series and Oxford series. Values from the two series (after the linear transformation) are not significantly different, apart from errors which do not affect the application of this method.